Cranfield University

Usama M. Attia

MICRO-INJECTION MOULDING OF THREE-DIMENSIONAL INTEGRATED MICROFLUIDIC DEVICES

SCHOOL OF APPLIED SCIENCES

PhD THESIS

Cranfield University

SCHOOL OF APPLIED SCIENCES

PhD THESIS

ACADEMIC YEAR 2009-2010

USAMA M. ATTIA

MICRO-INJECTION MOULDING OF THREE-DIMENSIONAL INTEGRATED MICROFLUIDIC DEVICES

Supervisor: Dr. J. R. Alcock

Academic Year 2009 to 2010

This thesis is submitted in partial fulfilment of the requirements for the degree of PhD

ABSTRACT

This thesis investigates the use of micro-injection moulding (μIM), as a high-volume process, for producing three-dimensional, integrated microfluidic devices. It started with literature reviews that covered three topics: μIM of thermoplastic microfluidics, designing for three-dimensional (3-D) microfluidics and functional integration in μIM. Research gaps were identified: Designing 3-D microfluidics within the limitations of μIM, process optimisation and the integration of functional elements. A process chain was presented to fabricate a three-dimensional microfluidic device for medical application by μIM. The thesis also investigated the effect of processing conditions on the quality of the replicated component. The design-of-experiments (DOE) approach is used to highlight the significant processing conditions that affect the part mass taking into consideration the change in part geometry. The approach was also used to evaluate the variability within the process and its effect on the replicability of the process. Part flatness was also evaluated with respect to post-filling process parameters. The thesis investigated the possibility of integrating functional elements within μIM to produce microfluidic devices with hybrid structures.

The literature reviews highlighted the importance of quality control in high-volume micromoulding and in-line functional integration in microfluidics. A taxonomy of process integration was also developed based on transformation functions. The experimental results showed that μIM can be used to fabricate microfluidic devices that have true three-dimensional structures by subsequent lamination. The DOE results showed a significant effect of individual process variables on the filling quality of the produced components and their flatness. The geometry of the replicated component was shown to have effect on influential parameters. Other variables, on the other hand, were shown to have a possible effect on process variability. Optimization statistical tools were used to improve multiple quality criteria. Thermoplastic elastomers (TPE) were processed with μIM to produce hybrid structures with functional elements.

Keywords:

Micro-injection moulding, three-dimensional, statistical quality control, design-of-experiments, functional integration

ACKNOWLEDGEMENTS

I would like to offer my sincerest gratitude to my supervisor, Dr Jeffrey Alcock, who has supported me throughout my thesis with his patience, knowledge and encouragement. Without him this thesis would not have been possible.

I am indebted to my colleagues at Cranfield Precision Centre. I owe my deepest gratitude to Dr Silvia Marson who offered help and guidance from the first day of my PhD. Special thanks to Dr Tan Jin for programming my mould designs to the micromilling machine. Many thanks to Mr John Hedge, a fine technician who operated the micromilling machine and was always ready to offer help and useful suggestions.

I would also like to thank Dr Heather Almond, the Subject Advisor, and Dr Iain James, the Independent Chairman, for their insightful comments and suggestions during my PhD review meetings. I would also like to thank Professor David Allen for his encouragement and advice throughout my PhD.

I am grateful to my project partners in the 3D-Mintegration group. Special thanks to Ms Maïwenn Kersaudy-Kerhoas from Heriot Watt University, Dr Xiangdong Xue from the University of Greenwich, Mr Daniel Smale form the University of Nottingham and Dr Alan Wilson from the National Physical Laboratory (NPL).

I also offer my regards to all of those who supported me in any respect during the completion of the project. Many thanks to Mr Andrea Battisti and Dr David Ayre for their help in polymer characterisation. Also many thanks to Mr Jim Hurley for helping me during the maintenance of the micro-moulding machine. Special thank to Dr Ahmed Al-Ashaab for his help with rapid prototyping.

I am grateful to Cranfield Innovative Manufacturing Research Centre (CIMRC) and the 3D-Mintegration Grand Challenge Project for supporting my research.

Last but of course not least, this work would not have been achieved without the support and understanding of my family. I am as ever indebted to my parents, Mr. Mohamed Attia and Ms. Asmaa Hasan for their love and support throughout my life. Many thanks to my sisters and my brother for their continuous encouragement.

TABLE OF CONTENTS

LIST OF FIGURES

LIST OF TABLES

LIST OF ABBREVIATIONS

2½-D	Two-and-a-half dimensional
2-D	Two-dimensional
3-D	Three-dimensional
AFM	Atomic force microscopy
AR	Aspect ratio
ASE	Advanced Silicon Etching
CAD	Computer-aided design
CAM	Computer-aided manufacturing
CE	Capillary electrophoresis
CNC	Computer numerical control
DLC	Diamond-like carbon
DOE	Design-of-Experiments
EDM	Electro discharge machining
EOF	Electro-osmotic flow
Err. %	Percent error
HSC	High-speed cutting
iDEP	Insulator-based dielectrophoresis
LIGA	Lithographie, Galvanoformung, Abformung (Lithography, Electro-plating, and Moulding)
LOC	Lab-on-a-chip
MEMS	Micro-electromechanical systems
MFI	Melt flow index
PCR	polymerase chain reaction
PDMS	Polydimethylsiloxane
PMMA	Polymethylmethacrylate
POC	Point-of-care
RBC	Red blood cells
RTP	Rapid thermal process
SD	Standard deviation
SEBS	Styrene-Ethylene-Butylene-Styrene
SEM	Scanning electron microscopy
sPROMs	Structurally programmable microfluidic system
TDB	Thermal diffusion bonding
Tg	Glass-transition temperature
T_m	Melt temperature
TPE(s)	Thermoplastic Elastomer(s)
TTP	Time to pressure
USM	Ultrasonic micromachining
μAIM	Micro-assembly injection moulding
μ-CMM	Micro-coordinate measurement machine
μ-EDM	Micro-electro discharge machining
μIM	Micro-injection moulding
μ-STL	Micro-stereolithography
μTAS	Micro-Total Analysis Systems

Abbreviations of polymeric materials are listed in Table 1-3

LIST OF SYMBOLS

c	Constant
C_{blood}	Concentrations of red blood cells in whole blood sample
C_{plasma}	Concentrations of red blood cells in plasma sample
D	Overall desirability
d_i	Individual desirability
F_e	Ejection force
L	Lower value in desirability functions
P_h	Holding pressure
$\dot{Q}$	Volume flow rate
r	Radius
R	Radius of the injection plunger
r_i	Desirability function weight
T	Target value in desirability functions
t_c	Cooling time
T_m	Melt temperature
T_p	Polymer melt temperature
U	Upper value in desirability functions
V_e	Ejection velocity
V_i	Injection velocity
W	Average mass
W_i	Response weight in desirability functions
x_i	Factor
β_i	Model-term coefficient
$\dot{\gamma}$	Shear rate
Δ	Difference between two averages of the response points for a particular factor.
σ	Plasma selectivity

PUBLICATIONS

Edited versions of the chapters have been published, presented, submitted or will be submitted as follows:

CHAPTER 1 Attia UM, Marson S, Alcock JR. Micro-injection moulding of polymer microfluidic devices. *Microfluidics and Nanofluidics*, 2009; 7(1): 1-28.

CHAPTER 2 Attia UM, Alcock JR. Integration of functionality into polymer-based microfluidic devices produced by high-volume micromoulding techniques. *The International Journal of Advanced Manufacturing Technology*. DOI: 10.1007/s00170-009-2345-8 (accepted)

CHAPTER 5 Marson S, Attia UM, Allen DM, Tipler P, Jin T, Hedge J, Alcock JR. Reconfigurable micro-mould for the manufacture of truly 3D polymer microfluidic device, *CIRP Design Conference 2009*, Cranfield, UK, 30-31 March 2009, pp. 343-346.

Attia UM, Alcock JR. Micro-injection moulding of three-dimensional microfluidic devices for a medical application, *Cranfield Multi-strand Conference (CMC)*, Cranfield, UK, 6-7 May 2008.

Kersaudy-Kerhoas M, Kaufmann J, Attia UM, Marson S, Allen DM, Douglas A, O'Neill W, Summersgill P, Ryan T, Desmulliez M. Evaluation of manufacturing techniques for a minifluidics demonstrator system, *4th International Conference on Responsive Manufacturing (ICRM 2007)*, Nottingham, UK, 17-19 September 2007.

CHAPTER 6 Attia UM, Alcock JR. An evaluation of process-parameter and part-geometry effects on the quality of filling in micro-injection moulding. *Microsystem Technologies,* 2009. (published online)

CHAPTER 7 Attia UM, Alcock JR. Evaluating process variability in micro-injection moulding. *Microsystem Technologies.* (submitted)

CHAPTER 8 Attia UM and Alcock JR. Optimizing process conditions for multiple quality criteria in micro-injection moulding. *The International Journal of Advanced Manufacturing Technology*. (submitted)

CHAPTER 10 Attia UM and Alcock JR. A process chain for integrating functional elements by micro-overmoulding of thermoplastic elastomers. *Journal of Micromechanics and Microengineering*. (to be submitted)

Introduction

Microsystem technologies have evolved over the past decades from pure-research fields to industrial applications. Since early starts within the semiconductor industry, the increasing number of microfabrication techniques has contributed to the production of various miniaturised products characterised by relatively light weight, low cost and energy efficiency.

Microfluidic systems are one area of micro-components where a lot of developments have been achieved in the recent years. Typical application areas cover a wide range of sectors including pharmaceutical, chemical, household, personal care and food sectors. A considerable amount of research has been done worldwide focusing on design, manufacturing, assembly and testing of microfluidics, and several companies currently produce relatively simple microfluidic systems on a commercial scale. The volume of microfluidic products was estimated to be approximately US$600 million in 2006, and the market was forecast to grow to US$1.9 billion by 2012 [1].

Due to the increasing demand for microfluidic systems that can perform relatively complex operations, more research has been directed to integrated systems. In such systems, also known as Lab-on-a-chip (LOC) devices or micro-Total Analysis Systems (μTAS), the microfluidic "chip" is capable of conducting a number of integrated tasks beyond simple fluid manipulation.

In spite of considerable developments, integrated microfluidics are still far from being fully commercialised, and most of the produced devices are limited to prototyping stages. A major reason for this is that the available manufacturing routes have not yet reached the maturity level required to mass-produce such complex systems without considerable investments. It was therefore predicted that future mass-market usage of microfluidic devices is dependent on finding methods which will allow their manufacture in large volumes and at low costs [2].

Another obstacle for commercialising integrated systems is that processing techniques had limitations in terms of possible manufacturable geometries, which were usually limited to flat, so-called 2½D, structures inherited from the silicon industry. Such geometrical limitations put extra constrains on the design, fabrication and packaging of the device.

Micro-injection moulding (μIM) is one of the most promising micro system technologies for high-volume manufacturing of micro-components. Dimensional accuracy, replication fidelity and potential for automation are some of the process characteristics associated with μIM. These capabilities, combined by the wide range of mechanical, thermal and optical properties of processable thermoplastic polymers, make μIM the main candidate for high-volume, low-cost microfabrication.

The advantages of μIM, in addition to the considerable process developments witnessed in the recent years and the inherited knowledge from conventional injection moulding, made it an ideal candidate for producing micro-components for a wide range of applications. Lenses, waveguides, micro-mechanical components, sensors, integrated microelectromechanical systems (MEMS), minifluidic devices are a few examples of micromoulded products used in applications, such as optical systems, chemical analysis and medical diagnostics.

This project aimed at investigating the use of micro-injection moulding for the production of three-dimensional integrated microfluidic devices. Three main issues were addressed throughout this thesis:

Firstly, it discussed the possibility of overcoming the geometrical limitations of μIM for producing truly 3D devices. This was addressed by laminating sections of the microfluidic systems into a truly 3D structure. Secondly, it presented a statistical approach for detecting and controlling processing parameters to improve replication quality and process stability within a mass-manufacturing process. This approach was selected to understand and predict the filling behaviour of polymers on the micro-scale, because the currently available simulation packages used for conventional injection moulding are not suitable on the micro-scale. Finally, the project investigated the possibility of integrating functional elements within the μIM process. Hybrid, multi-material, moulding was selected as an example for process integration.

A minifluidic demonstrator was used to illustrate the possibility of micro-moulding a truly 3D microfluidic device for blood-plasma separation for medical diagnostics. A design-of-experiments (DOE) approach was implemented to control the process parameters for increasing filling quality and decreasing process variability. Hybrid micro-injection moulding was presented as a possible technique for integrating functional elements in micro-fluidic devices by micro-moulding.

This thesis is divided into 12 chapters: The first three are the literature review which consists of three papers that collectively presents the state-of-the-art research in

μIM of 3D integrated microfluidics. They also present a taxonomy of microfluidic functionalities in relation to integration method, and they present an assessment approach of three-dimensional microfluidics produced by μIM. In Chapter 4, research gaps are identified, problems are selected and the corresponding research methodology is presented.

Chapter 5 presents the minifluidic demonstrator which is used as a case study for three-dimensional microfluidics. The chapter discusses the design-for-manufacturability approach used to turn the originally-designed 2½D device into a mouldable 3D device.

Chapter 6 investigates the effect of process parameters on the filling quality of micro-parts, and how they interact with the geometrical shape of the component.

Chapter 7 investigates the variability of μIM and its effect on the replicability of the moulding process. A statistical approach for process optimisation is implemented and validated.

Chapter 8 develops the quality control method used in previous chapters by presenting an optimisation technique for multiple responses, and how a compromise in process conditions would be necessary to meet multiple quality criteria.

Chapter 9 presents a statistical approach to evaluate flatness of micromoulded parts in relation to post-filling parameters.

Chapter 10 focuses on process integration, where micro-assembly injection moulding was used to integrate interconnect elements as an example for functionality integration within μIM.

The overall discussion of the project was summarised in Chapter 11, and main conclusions and contribution to knowledge were presented in Chapter 12 together with potential developments and future work.

1 Micro-Injection Moulding of Polymer Microfluidic Devices

Abstract

Microfluidic devices have several applications in different fields, such as chemistry, medicine and biotechnology. Many research activities are currently investigating the manufacturing of integrated microfluidic devices on a mass-production scale with relatively low costs. This is especially important for applications where disposable devices are used for medical analysis. Micromoulding of thermoplastic polymers is a developing process with great potential for producing low-cost microfluidic devices. Among different micromoulding techniques, micro-injection moulding is one of the most promising processes suitable for manufacturing polymeric disposable microfluidic devices. This review paper aims at presenting the main significant developments that have been achieved in different aspects of micro-injection moulding of microfluidic devices. Aspects covered include device design, machine capabilities, mould manufacturing, material selection and process parameters. Problems, challenges and potential areas for research are highlighted.

1.1 Introduction

Microfluidics is a rapidly growing domain with many applications and a strong potential for development. The volume of microfluidic products was estimated to be approximately US$600 million in 2006, and the market was forecast to grow to US$1.9 billion by 2012 [1]. Microfluidic devices are already used in a number of domains, including chemistry, biotechnology and medicine. Prototype Lab-on-a-chip (LOC) systems are developing rapidly in several areas.

However, future mass-market usage of microfluidic devices is dependent on finding methods which will allow their manufacture in large volumes and at low costs [2]. This is especially important for medical applications where, for safety considerations, devices should be disposable to avoid cross contamination. In addition, from an economical viewpoint, a disposable device would not require maintenance or recalibration. Disposability is also useful in situations where there

might not be access to human or technical resources to retest or recalibrate a microfluidic device for multiple usages, e.g. when devices are used in certain point-of-care situations or in developing countries.

For such mass-market applications, polymers possess several advantages over other materials, such as glass and silicon, which have previously been used in constructing microfluidic devices (advantages and limitations of polymers discussed later in section 1.1.4). They are obtainable at relatively low cost, require relatively simple processing techniques and can exhibit accurate repeatability in mass-production.

Several micromoulding techniques are available for the manufacturing of microfluidic devices from polymers. Of these, micro-injection moulding is one technique that offers mass-production capabilities with relatively low costs. Its other advantages include short-cycle times, the potential for full-automation, accurate replication and dimensional control as well as the existence of considerable know-how, transferable from conventional injection moulding.

The introductory section briefly summarises the relevant basic concepts of microfluidics, micromoulding and micro-injection moulding. Reviews of the micromoulding of thermoplastics [3,4], polymeric microfluidic devices [5] and fabrication of microfluidics and micro-Total Analysis Systems (μTAS) [6-8] can also be found in the literature.

Section 1.2 discusses the design of microfluidic structures that are mouldable by micro-injection moulding.

Sections 1.3 through 1.6 examine the challenges in mould and insert design, materials selection, moulding machine design and moulding process parameter optimisation for the micro-moulding of microfluidic components.

Section 1.7 discusses modelling and simulation of micro-injection moulding, and Section 1.8 presents the state of the art in post-ejection processes, which is particularly important for integrated systems. The outlook for micro-injection moulding of micro-fluidic devices is discussed followed by a conclusion.

1.1.1 Micromoulding

Micromoulding is the process of transferring the micron or even submicron precision of microstructured metallic moulds to moulded polymeric products [9,10].

Several micromoulding techniques are currently available for fabricating microfluidic devices. They include micro-injection moulding, reaction injection moulding [11], hot embossing [12] and thermoforming [13].

A precise definition for a micro-moulded part is usually controversial. Several authors [14-16,16-19] mention a set of criteria for what is to be classified as a micro-moulded part. Such a part has one or more of the following specifications:

- It is weighs less than 1 mg, or it is a fraction of a polymer pellet, where a pellet can be approximated to be spherical in shape with an average diameter of approximately 3 mm.
- It is a part with microstructured regions, or more specifically, with wall thicknesses less than 100 μm. Microfluidic devices usually fall in this category.
- It is a micro-precision part, which is a part that can have any dimensions, but has tolerances in the micrometre range, or more specifically, between 2-5 μm.

Due to the continuous developments, micro-moulded parts are soon expected to exceed the limits specified in these literature criteria. In fact, advances in micromoulding technology have already realized production of parts with masses of the order of micro-grammes [17].

1.1.2 Micro-injection moulding

Micro-injection moulding is the process of transferring a thermoplastic material in the form of granules from a hopper into a heated barrel so that it becomes molten and soft. The material is then forced under pressure inside a mould cavity where it is subjected to holding pressure for a specific time to compensate for material shrinkage. The material solidifies as the mould temperature is decreased below the glass-transition temperature of the polymer. After sufficient time, the material freezes into the mould shape and gets ejected, and the cycle is repeated. A typical cycle lasts between few seconds to few minutes. The process has a set of advantages that makes it commercially applicable with potential for further developments in the future. Advantages include the wide range of thermoplastics available and the potential for full-automation with short cycle times [10,20,21], cost-effectiveness for mass-production process, especially for disposable products [10,20,22-24], very accurate shape replication and good dimension control [20-22], low maintenance costs of capital equipment, when compared to lithographic methods, for example [21] and

applicability of the large amount of industrial information and 'know-how' available from conventional injection moulding. Within certain limitations, this may be scaled down to micro-injection moulding.

A comparison between micro-injection moulding and other techniques for microfluidic device manufacturing, such as hot-embossing and microelectromechanical systems casting, is available in the literature [25].

1.1.3 Applications for polymeric microfluidics

Due to the rapid development in micro-injection moulding, it has been used for producing parts suitable for a wide range of applications, which includes, for example:

- Micro-optical applications, such as gratings, waveguides and lenses [9,15,23,26-28].
- Micro-mechanical applications, such as micro-springs, gears and miniaturized switches [9,15,26,27].
- Sensors and actuators, such as sensors of flow-rates [23,27].

When it comes to microfluidics, micro-injection moulding is one of the main fabrication techniques to produce polymeric microfluidic devices for a number of applications, the majority of which are for medical diagnostics. Examples of polymeric microfluidics include components for micropumps, which are used for medical, chemical and environmental technology [9,10,15,26-28]. In industry, Bartels Microtechnik [29], for example, is specialized in micropumps for the delivery of small amount of fluids for different applications, such as point-of-care platforms or small fuel cells. The pumps are designed to be low in cost and disposable.

Reaction vessels and mixing structures are other commonly used microfluidic systems that are currently being produced by micro-injection moulding [26,30]. On a commercial basis, Thinxxs [31], for example, produces a lab-on-a-chip system for blood diagnostics. It includes functions such as sample absorption, separation, mixing with reagents, analysis and waste absorption. The "Snake" mixer slide is another commercially-available microfluidic system comprising of a plastic chip with meander-shaped mixers that can mix fluids possessing a range of viscosities and at different flow rates.

DNA analysis systems such as [10,23]bio-MEMS, μ-TAS and Integrated LOC, which are typically manufactured of glass, are currently being manufactured in polymers [10,23]. Such integrated systems usually combine an entire process chain, such as storage and waste vessels, transport channels, filters, mixing and separating structures, reaction chambers and detection points on a plastic substrate [10,15,27,30,32,33]. Mass-producing such integrated systems in polymers rather than glass would decrease their cost. Micralyne [34], for example, which is a company specialized in MEMS-based products, has decided to expand its manufacturing capabilities to include polymers as a lower-price alternative to glass [34].

Other producers, such as Abbott [35] and Microfludic ChipShop [36] produce polymeric microfluidic platforms for medical diagnostics and point-of-care applications.

Micro injection moulding was also reported in the literature to be used for microfluidic applications, such as capillary electrophoresis (CE) platforms [10,23,27,30,32], miniaturized heat-exchangers [26] and nanofilters [10].

Although several polymeric microfluidic systems have been made available commercially, it should be noted that due to process limitations, to be discussed in the following sections, the process is not fully implemented for relatively complex microfluidic systems. Integration of external elements, such as electrodes or micro-heaters, within a mass-production technique such as micro-injection moulding, still poses a major challenge for the technology. One of the major reasons for this limitation is the required price of the part compared with the costs of established techniques of insertion or encapsulation by injection moulding [2].

1.1.4 Using polymers for microfluidic applications

Several materials have been used for producing micro-featured parts, for example glass and silicon. Nevertheless, polymeric materials show superior properties over glass and silicon for a number of reasons.

Polymers are relatively low in cost, especially for high-production disposable devices [37,38]. In addition, costs are not greatly affected by the complexity of the design, as design complexity mostly impacts on mould design rather than on the moulding process itself [3,10,39-41]. More discussion about designing for micromoulding is detailed in section 1.2.

Polymers have a wide variety of characteristic material properties, such as mechanical strength, optical transparency, chemical stability and biocompatibility. They are therefore relatively easy to tailor to obtain required properties for processing and application [3,10,21,37,41-46].

Polymers have excellent replication fidelity, and if the optimum processing conditions are applied a typical polymer can completely fill and accurately replicate small features down to tens of nanometres. Due to the viscoelasticity of polymers, increasing the shear-rate and maintaining the polymer temperature above its T_g during the filling stage would usually ensure a low viscosity enough for the polymer to fill the smallest mould details. Therefore, the quality of the moulded surface features is almost completely dependent on the quality and precision of the mould [21]. Experiments have been reported on using injection moulding to successfully replicate, for example, sub-micron test features [47,48], sub-micron grating optical elements [22,49,50] and surfaces with nano-structured patterns [51,52] or nano-scale topography [53].

Polymers offer good electrical insulation compared to silicon. For example, the conductivity of silicon has proved problematic when applying high voltages necessary for the generation of electro-osmotic flow (EOF) [21,30].

On the other hand, polymers have some limitations related to their properties or processing techniques relative to glass. These include, for example, limited operation-temperature range, higher autofluorescence and limited well-established surface modification techniques. Table 1-1 presents a comparison between polymers and glass for manufacturing microfluidic devices, where information is compiled from the literature [5,21,30,34,43,54-57]. When it comes to processing, mass-production processing techniques impose limitations on the mouldable geometry of the microfluidic device. These geometrical limitations restrict the flexibility of integrating external functional elements within a mass-manufacturing technique.

	Polymers	Glass
Manufacturing costs	Low in cost relative to glass, especially for mass-production.	Higher in cost, especially for relatively large-area substrates. Higher costs are also associated with clean-room facilities.
Fabrication complexity	Fabrication steps are simpler than glass, and no wet chemistry is needed.	Time consuming and expensive, and wet chemistry is used.
Clean room facilities	Clean-room facilities are necessary for applications where avoiding contamination with dust is critical. In certain cases, particles may become pressed into the polymer during processing without having an effect on device functionality.	Clean-room facilities are needed to avoid contamination.
Properties	Wide selection of polymers, hence mechanical, optical, chemical and biological properties can be tailored.	Less variability in available properties relative to polymers.
Operation temperature	Limited for polymers because of relatively low T_g compared to glass.	Wider range of operation temperature relative to polymers.
Optical properties and fluorescence detection	Optical transparency is lower than glass. Except for special grades, polymers also have higher autofluorescence relative to glass.	Excellent optical properties; autoflourecence levels do not affect detection capabilities.
Bonding	Different bonding options are available, for example: adhesives, thermal fusion, ultrasonic welding and mechanical clamping.	Time consuming relative to polymers. Bonding options include thermal, adhesive and anodic bonding.
Surface treatment	Surface treatment methods are available for polymers, but routine, well-established derivatization techniques are not available.	Established chemical modification procedures for glass are available using organosilanes
Compatibility with organic solvents or strong acids	Except for some special grades, polymers are generally not compatible with most organic solvents and in some cases, strong bases or acids.	Good resistance to organic solvents and acids.
Joule heating	Subject to significant Joule heating because of low thermal conductivity.	More resistant to Joule heating relative to polymers.
Electro osmotic flow (EOF)	Smaller EOF produced relative to glass, because of lack of ionisable functional groups.	Higher EOF relative to polymers.
Geometrical flexibility	Polymer processing techniques offer more flexibility for geometrical designs, including for example different cross-section (curved, vertical or V-groove), high aspect ratio square channels, channels with a defined but arbitrary wall angle, or channels with different heights.	Limited to 2½-D designs. Due to the isotropic nature of the etching process, only shallow, low aspect ratio, mainly semicircular channel cross-sections are possible in glass substrates.
Permeability to gasses	Higher gas permeability relative to glass.	Glass does not have the gas permeability required for some biological applications, such as living mammalian cells.

Table 1-1 A comparison between polymers and glass properties with respect to their use for microfluidic applications

1.2 Designing Mouldable Microfluidic Structures

Designing for conventional injection moulding takes into consideration a number of manufacturability aspects, such as the part dimensions, the position and shape of the parting line, the existence of undercuts, mould-cavity features in addition to tolerances and surface finishing [58]. A number of studies have suggested techniques to evaluate the complexity of injection-moulded shapes with respect to replication and demoulding [59,60].

It should be noted that very little is mentioned in the literature about rigorous criteria for designing microfluidic devices for manufacturability by microinjection moulding. Most of design considerations focus on specific geometrical aspects such as achievable aspect ratios. This section will therefore focus on design criteria associated with the geometry of the moulded part rather than designing for functionality. The following subsections will highlight some generic design considerations for injection-moulding, which are also important for micro-scale moulding (section 1.2.1). Design elements specific to micromoulding, such as aspect ratios and mouldable micro-features will also be reviewed (section 1.2.2).

1.2.1 Shrinkage and shape stability in precision injection moulding

Different forms of shape change takes place due to the thermal history of the injection moulded part. Volume changes due to part shrinkage, and shape distortions such as warpage, are common examples.

Shrinkage occurs with the decrease in part volume due to the temperature change between the demoulding temperature and the ambient temperature. The contraction in part volume affects the demoulding of the part due to the stresses induced upon contraction. One of the techniques to improve demoulding is by controlling the processing parameters and, hence, the shrinkage performance. Geometrical changes can also improve demoulding as will be shown in the following section. Considering the feature placement, the further the features from the shrinking centre, the harder demoulding becomes [3].

Another factor that affects demoulding is the orientation of the polymer being injected, because this affects the direction at which shrinkage is most observed. Therefore, a design consideration for microfluidic substrates, should consider the path

of polymer injection inside the mould [3]. Examples of experiments investigating flow direction are presented in section 1.6.

In addition to demoulding and feature replication, shrinkage affects shape stability in the form of induced warpage. Warpage is produced due to the non-uniformity of the shrinkage because of the residual stresses induced by the complex thermal variation inside the mould [61]. Warpage, was investigated in parts incorporating micro features using a laser profilometer, and was reported to have an effect on micro-parts of the order of a few microns for a 3-mm length [61]. Warpage prediction is important for parts with relatively large area compared to its thickness, e.g. microfluidic chips. This is because the flatness of the chip is a demanding requirement for polymeric microfluidic chips, considering that optimum sealing of a polymer chip, with a quality level compared to glass, would not be achievable without a minimum flatness level. Otherwise, costly intermediate layers would be needed which compromises the economics of polymer mass-production. The flatness of the polymeric chip is affected by different factors including the flatness of the replicated mould [62], the processing parameters [61,63] and the ejection process. In comparison to its importance, flatness and its control have received little emphasis in the literature.

In injection moulding it is not always possible to design an ideal cooling system, because the position of the cooling channel is dependent on part geometry, cavity configuration and location of ejection mechanism. Thus, variation in temperature across the moulded part should be expected depending on the geometry [61]. Cooling the mould is not always required, especially when it is desired to keep the mould temperature above the T_g of the polymer to ensure complete filling of the mould cavity.

Different techniques have been suggested to decrease the effect of shrinkage. One method is to increase the amount of holding pressure, which, on the other hand, will also increase stresses inside the part [4]. Another technique is to have a long cooling time (i.e. to allow the part to thermally equilibrate inside the mould cavity). This allows the temperature to be approximately uniform. For precision moulding in particular, the part is likely to distort because of lack of homogeneity in shrinkage, which is likely to occur if the cycle is terminated before the thermal equilibrium is reached, i.e. the part is ejected before its temperature is reduced to the ambient

temperature [61]. Again, a trade-off of this technique would be an increased cycle time.

It should be noted that shrinkage is not identical throughout long runs. Therefore, moulded parts that need to be assembled in subsequent stages should be placed on the same mould [3].

In addition to shape-changes, demouldability of injection-moulded components is also affected by the geometrical structure of the component. Similar to conventional moulding, micromoulded parts should be designed to allow for part ejection from a two-half mould. Most microfluidic applications possess an undercut-free 2½-D geometry that is relatively simple to demould. For more complex 3D shapes (or shapes with integrated functional elements) injection moulding would not be applicable unless significant changes are made to the mould structure or subsequent assembly steps are integrated in the production process.

Another geometrical consideration for successful demoulding is the existence of draft angles. Draft angles and side-wall roughness need to be considered to ensure that the moulded plastic can be demoulded (Figure 1-1). A positive draft angle of greater than ¼° has been proposed for demoulding in plastic injection moulding [39].

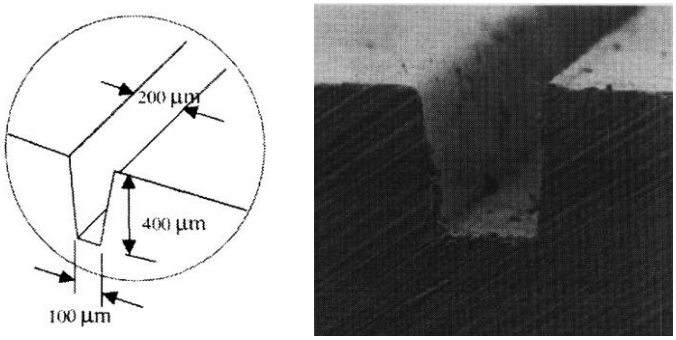

Figure 1-1 A micro-channel with a positive draft angle (nominal dimensions and actual channel) [39]

1.2.2 Minimum channel dimensions and maximum aspect ratios (AR) for microfluidics

Section 1.2.1 presented design-for-manufacturability criteria common for injection-moulding processes. This section focuses on geometry-related design criteria specific for injection-moulding microfluidic devices. Careful considerations should be given to the channel dimensions to ensure the complete filling of the mould

cavity. Polymeric melts can accurately fill microfeatures in the order of hundreds of nanometres. Therefore, the minimum mouldable dimensions will be determined by the tool-manufacturing capabilities. Because micromoulding is under continuous development, it is not possible to specify a size limit below which microfeatures can no longer be replicated successfully. Nevertheless, it has been reported in the literature that it is possible to replicate surfaces with a squares pattern having widths as small as 310 nm and heights of 220 nm [51]. In addition, optical grating elements of parallel walls having a thickness of 200 nm and depth of 1600 nm has also been fabricated [22].

The "hesitation effect" is a phenomenon that can occur during the filling of polymers, and is common when an injection-moulded part contains different thicknesses [20]. As shown in Figure 1-2, this effect takes place when high-aspect-ratio microstructures (usually larger than 2) are placed on a relatively thick substrate, which is the case for microfluidic devices.

The polymeric melt tends to flow more easily into mould cavities with relatively lower resistance areas, i.e. areas of greater cross section. Thus, the melt tends to fill the substrate completely before entering the micro-structured features (i.e. the flow stagnates at the entrance of micro-structures). This results in premature freezing because the filling time of the substrate is usually greater than the freezing time of the micro-feature.

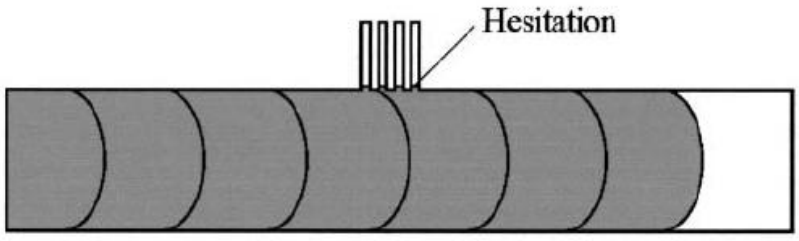

Figure 1-2 Hesitation effect in high-aspect-ratio micro-cavities [20]

Taking the hesitation effect into consideration, replication depends on the size and aspect ratios of the structural features as well as the size of the area covered with such structures and their density. The filling of the structures has to compete with the filling of the underlying thicker substrate [40]. This could be the explanation for why it was recommended in the literature that injection moulded parts with high-aspect-ratio microstructures should have a thickness of at least 2 mm [62] so that a quick

filling of the substrate can allow for filling the micro-cavities before solidification starts. It was recently reported, however, that micro-structures of aspect ratios of 5 carried on a 1.5-mm- thick disk substrate were successfully filled with poly lactic acid [64].

In addition, the effect of flow direction in either radial- and unidirectional injection was investigated in the literature [39], and it was shown that in unidirectional flow the depth of filling in microchannels is sensitive to the channel width, such that doubling the channel width from 200 μm to 400 μm causes the filling depth to increase from 150 μm to approximately 600 μm.

The concept of the so-called time to pressure (TTP) was introduced by researchers [65] to explain the fact that the degree of filling depends on the distance from the gate, which is the entrance of the polymer into the part cavity. Based on experimental measurements of the pressure drop vs. the injection speed at sections with different thicknesses, it was suggested that the shear stresses, and accordingly the pressure drop, required to fill the feature is in general much higher than that to fill the substrate.

Concerning achievable aspect ratios, it was suggested that there is a limitation regarding the achievable aspect ratio [3], which is a function of the geometry of the micro-features, its position on the sample, the polymer type and the process parameters. Thus, there is no simple rule to give the maximum aspect ratio which can be achieved in a particular case. Although it was not stated why these factors in particular affect the achievable aspect ratio, the experimental work presented throughout this section gives examples of how geometry and processing factors affect the aspect ratio.

With the recent developments in machine capabilities it has been reported that aspect ratios up to 20 can be filled [66,67]. Table 1-2 compares different experiments performed for different structural dimensions and materials. Information reported in this table is subject to change as more developments are continuously achieved in machining and processing. In the context of Table 1-2, it should be noted that the issue of dimensional tolerances is rarely addressed in the literature.

Polymer	Abbr.	AR	Min. structural thickness [µm]	Example of application	Ref.
Polymethyl methacrylate	PMMA	20	20	Optical fibre connector	[66]
Polycarbonate	PC	7	350	Cell container	[66]
		4 - 8	0.2 – 0.5	Optical element	[22]
Polyamide	PA	10	50	Micro gear wheels	[66]
Polyoxymethyleme	POM	5	50	Filter with defined pore diameters	[66]
		10	80	Micro-rods	[68]
Polysulfone	PSU	5	270	Housings for microfluidic devices	[66]
Polyetheretherketone	PEEK	5	270	Housing for micro-pumps	[66]
Liquid crystal polymers	LCP	5	270	Microelectronic devices	[66]
Polyethylene (High density)	HDPE	8	125	High aspect ratio squares	[69]
		10	225	Micro-wells	[20]
Cyclic Olefin Copolymer	COC	0.02 - 2	0.1 – 0.9	Microfluidic patterns	[47]
Conductively filled polyamide	PA 12-C	10	50	Housing for electrostatic micro valves	[66]

Table 1-2 Commonly used polymers for micro-injection moulding, maximum aspect ratios (AR), minimum structural thickness and applications

It has been suggested in the literature that the critical minimum dimensions which can be replicated successfully by injection moulding are mainly determined by the aspect ratio. Although this has not been presented in a rigorous numerical relation, experiments have shown that the sub-micrometer scale can be reached for aspect ratios less than 1, for example in CD and DVD fabrication. Polymeric materials with minimum wall thickness of 10 µm, structural details in the range of 0.2 µm, and surface roughness of about $R_z < 0.05$ µm have been manufactured [66].

A few attempts have been made to find the relation between part geometry and filling behaviour on the micro-scale by introducing standard micro-sized features for testing. As suggested in the literature [70], standard testing shapes can be helpful in comparing filling of structures with different wall thicknesses but the same aspect ratio. This will help in investigating the relation between wall thickness and flow path length and their limits. They can also be used for a wider range of polymers, since material properties affect flow behaviour. In both cases, using a statistical method (e.g. Design of Experiments) will be useful in optimizing the experimental procedure.

In one attempt [70] circle-shaped and wedged structures were used as testing shapes (Figure 1-3)

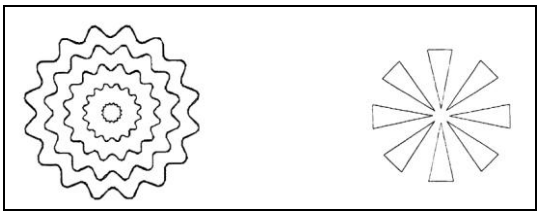

Figure 1-3 Circular and wedged insert-shapes for testing [70]

For the circle shapes, the wall thickness was varied in steps from 2.5 µm (inner circle) to 20 µm (outer circle) at a constant height of 50 µm, whereas for wedges, the tip radii were varied from 0.5 µm to 5 µm. POM was the material used for filling. The authors chose these two shapes based on earlier studies [71] in which different designs were compared, and guidelines were deduced for designing standardized testing shapes.

For the circular shape, all the circles were filled completely, but the inner one (2.5 µm) was deformed during demoulding. For the wedged shapes, the shape with radius 0.5 µm was partially filled, whereas larger radii were completely filled.

In another attempt to investigate dimensional and aspect ratio limits, different geometrical shapes with aspect ratios of 5 were tested for filling with Polylactic acid (Figure 1-4). It was shown that square shapes were easier to completely fill without premature freezing than cylindrical shapes.

The authors also reported that features that are farthest from the centrally located gate fill more than those closer to the gate. This is because the farther features have a lower thermal gradient and higher temperature that facilitates their filling. This was verified by numerical simulation, which showed that the polymer tends to fill the relatively thick substrate before completely filling the features, so the farthest features usually contain the hottest material and require less pressure during the holding stage to fill than the features closest to the gate [64].

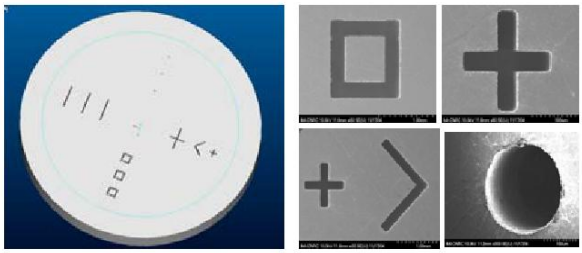

Figure 1-4 Micro-cavities with different geometries used for testing the filling behaviour of polymers [64]

The effect of geometric shape on demoulding quality has also been studied by comparing the quality of circular, meander, microfluidic and ray shapes (Figure 1-5) [72]. The ray shape proved to be optimum for demoulding conditions due to the shrinkage pattern it takes.

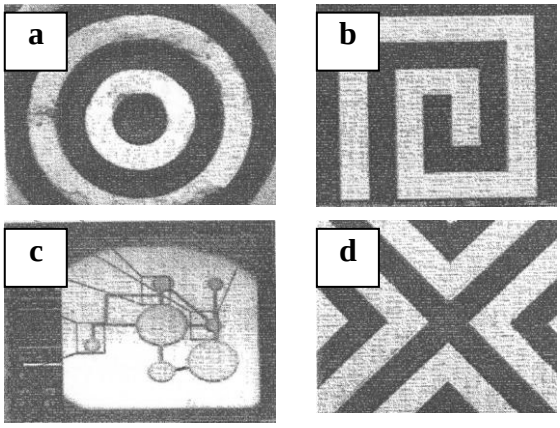

Figure 1-5 Testing shapes for demoulding. (a) Circular (b) Meander (c) Microfluidic (d) Ray [72]

1.3 Micro-Moulds & Inserts

1.3.1 Special features of moulds for micro-injection moulding

Moulds made for micro-injection moulding of microfluidic parts are in principle similar to moulds made for conventional injection moulding. They usually consist of a fixed part and one or more moving parts, depending on the design. Finished parts are demoulded with ejector pins that are usually controlled hydraulically and electrically. However, moulds made for microinjection moulding have special features [27,40].

For example, moulds can be controlled by the Variotherm process. This process permits heating rates of the order of several tens of Kelvins per second, and hence imposes no significant change in the process time compared to conventional injection moulding. The Variotherm process raises the mould temperature instantly above the polymer T_g during injection to prevent early freezing. During cooling, the mould temperature is decreased below the T_g to assist part solidification [27].

In addition to Variotherm, evacuation of the mould is done by air evacuation with evacuation rates that can reach up to 25 m^3/h in some systems [73]. Air evacuation is used rather than air vents used in conventional injection moulding. This is because the vents used in conventional injection moulding are larger in size than some of the cavity features in micro-injection moulding, i.e. they will simply be clogged with polymer melt. In addition, micro-cavities may form air pockets that cannot be released while the polymer is flowing in the mould, so the mould has to be evacuated just before injection [3].

Due to the size of the mould cavity and features, adapted mould sensors are used, because conventional sensors are not always suitable to micro-features. For example, pressure sensors with front diameters down to 1 mm and pressure range up to 2000 bar are currently available for measuring cavity pressures in micro-injection moulding [74].

Special ejector/withdrawal design is important, so that microfeatures are not deformed due to the induced friction between the mould and the part as discussed earlier in section 1.2.

1.3.2 Inserts for micro-injection moulding

For moulds used in micro-injection moulding, especially for microfluidic applications, micro-cavities are usually produced on an insert, which is then fitted in the main mould body. While the mould is made of steel, as in conventional injection moulding, inserts can be manufactured of other materials, depending on the technology used. This is because hardened steel, which is the commonly used material for mould-making, requires specialised, and hence expensive, tools for machining micro-sized channels and features.

The use of insert moulds also reduces the over-all cost of process set up where the finalised mould design is produced by a number of iterative steps in which parts are moulded and the mould design is then changed.

1.3.2.1 Special considerations about manufacturing inserts

Some considerations are recommended for manufacturing/processing inserts for micro-injection moulding [40]. An insert should exhibit extremely smooth side walls to avoid friction during demoulding. Although suggested wall roughness have not been reported in the literature, the inner walls of the insert should be smooth enough to prevent form-locking, i.e. the case where the part cannot be demoulded or the structures will be ripped or sheared off during demoulding [61]. A small inclination angle, preferably greater than ¼° [39], is also desirable, if this does no unduly impact on the functionality of the microstructures to be moulded.

In addition, the mould insert should ensure replication of the micro-features over many moulding cycles and withstand lateral and normal forces during injection and demoulding. In practice this is achieved by choosing a material that is hard and ductile enough for the mould insert.

The surface properties of the mould affect demoulding during micro-injection moulding. The effect of surface treatment has been investigated in the literature, where a tool coated with diamond-like carbon (DLC) was compared with an uncoated identical tool [75]. Measurements of demoulding forces showed that surface treatment significantly reduces demoulding forces.

1.3.2.2 Manufacturing inserts for micro-injection moulding

Several manufacturing techniques are used to produce inserts with micro-cavities. The choice of the technique depends on the dimension/geometry of the structure, the accuracy requirements and the fabrication costs. Manufacturing techniques include e-beam writing, lithography, electroforming processes (e.g. LIGA techniques, laser ablation) and precision engineering techniques (e.g. micromilling and electro discharge machining (EDM)) [26]. Other advanced processes include laser machining, ion machining and ultrasonic machining [18].

Some complex moulds require the combination of different processes in a modular way by combining components made by LIGA or laser ablation with components made by mechanical treatment [26].

1.3.2.3 Capabilities of manufacturing methods

Summaries of the capabilities of different manufacturing techniques are readily available in the literature [4,76]. Several comparison tables have been presented. For example, Rötting, et al, tabulated different processes in terms of choice of geometry, minimum feature size, height, total surface area, aspect ratio, life time, cost and availability [62]. High-speed cutting (HSC) milling, grinding, erosion and UV-LIGA have been compared in terms of reproducibility, minimum roughness, minimum groove width, minimum step width and maximum aspect ratio [40]. An extensive evaluation of the common manufacturing techniques, such as electroplating, EDM and the developing processes, such as laser technology is available [40]. The capabilities of precision manufacturing methods in terms of their geometric limitations (2½-D vs. 3-D structures) have been compared [77].

1.3.2.4 Challenges facing mould and insert manufacturing

It has been pointed out that the wide range of technologies available makes it practically impossible for any small or medium enterprise to have all technologies in house. It is therefore required to solve the problem of the availability of mould inserts on an industrial scale which includes comparatively short delivery times, a reproducibility in the manufacturing process and the guarantee of certain quality parameters of the mould insert [62].

Another challenge is the successful integration of pieces made with different insert-manufacturing technologies to create a micro-mould [18].

In a recent study, hybrid tooling was presented, in which tools are manufactured with combination of micro-machining techniques and tested by replication of several polymers. Comparison criteria were feature size, aspect ratios and surface finish [78].

Concerning mould manufacturing, one of the main challenges is to modify the mould design to allow for more complex processes versions of the micro-injection moulding process. New mould designs have been tested to allow for micro assembly injection moulding (μAIM), a process for combining two components in one process step [79-81]. The mould was designed such that the cavity holding the insert was interchangeable. This enabled some of the time-consuming steps of the moulding process (i.e. demoulding the part, positioning the integrated elements inside the cavity, heating the cavity) to be done out of the process cycle, while the other cavity was being injected. Some of the process steps were automated, such as the cavity

replacement process. This modification in the mould design enabled the process to produce micro-parts with joint-like movable components, fluidic hollow structures by lost-core technology and overmoulding of wires and optical fibres [82,83]

Some recent studies have focused on the problems caused by using ejector pins for demoulding the parts. Other alternatives are under investigation such as vacuum or ultrasonic ejection [72].

1.4 Material Selection for Polymeric Microfluidic Devices

Selecting the appropriate polymer to micro-inject microfluidic components is one of the most challenging tasks in process design for microfluidics, because several considerations have to be taken into account. These include the effect of polymer on achievable part tolerance, costs and the meeting of material property requirements.

1.4.1 Material requirements for microfluidics

In the case of parts with microfeatures, like microfluidic devices, material requirements have been discussed by several authors in the literature [10,21,27,30,45]. For example, the material should possess appropriate mechanical properties. Although microfluidic devices are not usually subject to severe mechanical stresses, mechanical properties could be of interest if the chip is to be stacked with other units or integrated within a larger cell. Thermal properties are also important, especially when the microfluidic device is subject to elevated temperatures while in service. In order to avoid softening of the device, and subsequent deformation in features, glass transition temperature T_g, melt temperature T_m and thermal expansion coefficient will be critical. In addition, the ability of the polymer to dissipate heat is important in order to avoid local high temperatures in the device when it is subject to high temperatures while in service. In addition to thermal properties, chemical resistance to certain solvents or strong acids can be required if chemical reactions are taking place in the microchannels. Chemical resistances of several micro-mouldable polymers to different chemical substances have been compared [30]. The authors adopted a qualitative poor-to-excellent scale in comparing the polymers.

During the processing of the polymer, dimensional stability and accuracy are key properties for microfluidic polymers. They include, for example, reproducibility, tendency to shrinkage and warpage.

If electrical connections are integrated with the microfluidic device, additional attention should be paid to the electrical properties of the polymer. It should possess good insulating properties, such that currents are allowed to pass only through the microfluidic substance moving in the channels.

Biological applications require the polymer to be biocompatible, and permeability could also be demanded if living cells are involved.

In addition to the previous conditions, optical properties might be significant if optical monitoring is involved. Amorphous polymers are usually used in such cases. For optical properties, charts comparing five common polymers (PMMA, COC, PC, MABS, SBS) in terms of transmittance and replication quality have been produced [47]. Transmittance was compared by the value of transmission percentage at a wavelength of 590 nm, whereas replication quality was compared by the depth of filling in nm.

Special microfluidic applications like micro-pumps require additional properties for the polymer. Such properties include hardness, surface charge, molecular adsorption and electro-osmotic flow mobility.

1.4.2 Material requirements for manufacturability

Micro-injection moulding is a process that involves severe operation conditions in terms of temperatures (up to few hundred degrees) and pressures (up to tens of mega-Pascals). In addition, being a viscoelastic material, polymeric melts experience shear-thinning, i.e. a decrease in viscosity with increase in shear rate. Thus, radical changes in the material properties are expected due to high shear-rates resulting from flow in to micro cavities. Therefore, the polymer selected should be appropriate for micro-injection moulding. Generally speaking, all standard thermoplastic materials suitable for conventional injection moulding can be used for micro-injection moulding [9], provided that some manufacturability conditions are met [28,42,84,85]. For example, the polymer should possess low viscosity and hence good flow properties. Therefore, most of the materials used today in micro-injection moulding are low-viscosity formulations of standard polymers.

High mechanical strength is also recommended in order for the moulded part to resist mechanical stresses associated with demoulding friction or ejector forces. This is especially important for high-aspect-ratio structures, where a larger surface of

contact between the mould and the polymer imposes higher frictional resistance while demoulding. Thus, small structures are often torn off at high-aspect ratios [42,86].

The polymer should be compatible with the mould material, as during processing, polymers may have different effects on the mould material. Also the material should not leave deposits in the mould. For example nickel mould inserts are not affected by moulding PC even after 10,000 moulding cycles [28]. On the other hands, it has been reported in the literature that polymers containing aggressive chemicals can lead to corrosion in the inserts. This causes rough mould surfaces leading to aggressive demoulding and damage to structural details in the sub-micrometer range [28]. No list of specifically aggressive chemicals was available in the literature covered in this review.

Taking into consideration the radical temperature changes in the Variotherm process, it is recommended that the polymer has a narrow temperature interval between free-flowing and solidification. Rapid solidification is thus required.

When it comes to the pellet size, The polymer pellets should be of size small enough to fit within the flights of the smaller conveying screws generally required for micromoulding, to ensure proper melting of the polymer [87]. In addition, if the polymer is filled, the size of the filler particles should be less than the size of the minimum microstructure; otherwise reproducibility will be affected.

1.4.3 Polymeric materials used in micro-injection moulding

A number of authors have reported on the mouldability of particular engineering plastics. Table 1-3 summarises polymers that have been reported as mouldable by the micro-injection moulding process. Most of the known engineering plastics appear on this list.

Among the listed materials, some have been specifically recommended for medical applications, because they comply with the approval criteria of the European regulatory agencies, such as POM, PPS, PBT and LCP [86].

Class	Polymer	Full name	References
Amorphous	PMMA (Acrylic)	Polymethylmethacrylate	[9,27,28,30,37,42,47,69,72,88,89]
	PC	Polycarbonate	[9,10,19,22,24,28,30,37,42,47,72,88-91]
	PSU	Polysulfon	[9,10,28,42,88]
	PS	Polystyrene	[9,19,37,42,92]
	COC	Cyclic Olefin Copolymer	[10,19,33,42,47,89,90]
	COP	Cyclic Olefin Polymer	[93]
	PPE (PPO)	Polyphenylene Oxide	[9,10,26,42]
	PEI	Polyetherimide	[9,10,26,42]
	PAI	Polyamide imide	[10,42]
	MABS	Methylmethacrylate Acrylonitrile-Butadiene-Styrene	[47]
	SAN	Styrene Acrylonitrile	[93]
	SBS	Styrene-Butadiene-Styrene	[47]
	ABS	Acrylonitrile-Butadiene-Styrene	[91,94,94]
Semicrystalline	LCP	Liquid Crystal Polymer	[9,10,42,87]
	PP	Polypropylene	[9,42,67,91,94,95]
	PE	Polyethylene	[9,19,20,42,69]
	POM (Acetal)	Polyoxymethylene	[9,10,19,26-28,42,67,68,70,72,84,88,94]
	POM-C	Polyoxymethylene (Carbon-filled)	[28]
	PBT (Polyester)	Polybutylene Terephthalate	[9,10,19,26,42]
	PBT-HI	Polybutylene Terephthalate (filled with 15% glass fibre)	[10]
	PA 6 (Nylon)	Polyamide 6	[42]
	PA 12	Polyamide 12	[9,10,28,88]
	PA 12 -C	Polyamide 12 (Carbon-filled)	[28]
	PVDF	Polyvinylidene Fluoride	[28,88]
	PFA (Teflon)	Perfluoroalkoxy	[88]
	PEEK	Polyetheretherketone	[9,10,26,28,42,87]
	PLA (Polyester)	Polylactic Acid (Polylactide)	[64]

Table 1-3 Polymers for micro-injection moulding

In addition to the listed materials, thermoplastic elastomers, such as polyurethanes, were recently reported to be injection mouldable with high-aspect-ratio features [96].

1.4.4 Comparing the performance of polymers in micro-injection moulding

Generally speaking, selecting the right polymeric material for micro-injection moulding microfluidic devices is an issue that is still under investigation. The available reported data have been collected through experiments done under different processing conditions with different types of machines and microfluidic feature

designs. Thus, it will be of great benefit to set a standard method by which polymer materials can be compared objectively for micro-injection moulding.

Several comparisons of the performance of different polymers in micro-injection moulding are now available in the literature. For example, commonly available polymers have been compared in terms of structure quality, filling properties and demoulding [28]. In this case, the authors adopted a qualitative approach in comparison, which was dependent on experience rather than reported measurements. Other authors have reported that the choice of materials can affect the quality of the produced parts in terms of dimensional stability, shrinkage, warpage and filling high aspect-ratios. For example, Weber, et al, tested six polymers for the manufacture of micro-sized features [26]. The experiments indicated that PBT and PEEK gave the best results for filling small V-grooves. This was represented in complete filling of the mould insert, minimum radius of curvature at the edges, and homogenous surface profile. With respect to shrinkage, LCP experienced the minimum percentage shrinkage of approximately 0.5%, whereas POM showed maximum percentage shrinkage of approximately 2%.

It has been reported [42] that the best filling results for micro-injection moulding were obtained with POM, PA and PBT for semicrystalline materials, and PC and PMMA for amorphous polymers. Numerical measurements, however, were not been reported by the authors.

In another filling experiment, it has been noted that PP and HDPE showed unusual flow behaviour in filling high-aspect-ratio structures. For PP, SEM micrographs of structures of aspect ratio 6 showed spherical or nipple-shaped protrusions on the flow fronts. For HDPE, the moulded micro-walls were tilted, and the surfaces at the base of the micro-walls were cambered [48].

Changing the processing parameters can affect the performance of the material. For example, one experiment has shown that changing the melt-zone temperature T_m, affects POM, but it does not affect other materials such as PP and ABS, from which it was deduced that some materials are more sensitive to temperature than others [67].

1.4.5 Ongoing developments in materials for micro-injection moulding

1.4.5.1 Developing new materials

The demand for developing special materials tailored for micro-injection moulding is increasing. However, although many developments have been achieved in micromoulding in terms of machine and processing capabilities, development of special polymers is lagging behind. The main reason for this is the small size of the part, which causes the demand for the material to be relatively low. If the size of a single part is between 0.001g and 1g, neglecting the weight of the sprue tree, the production of a million parts requires, at the most, 1 ton of starting material [27]. Under such low-material-demand conditions, it is sometimes difficult to find a supplier who is ready to deliver such small amounts of special polymers [28].

When parts with micro-structures are produced in larger quantities, the demand for special materials will increase. Material suppliers may find it more feasible to develop new materials when market consumption reaches several hundred tonnes per year [42,84].

1.4.5.2 Filled polymers for microfluidics

Fillers can enhance polymer properties in terms of, for example, mechanical properties, thermal properties and electrical properties. Filled polymers are currently being tested for micro-injection moulding of microfluidic applications. Carbon-filled POM and PA 12 have already being tested for microfluidics in addition to glass-fibre-filled PBT [28]. It is important that the filler size is smaller than the micro-structures of the part in order to maintain accurate reproducibility. New filler concepts are based on small-dimensioned fillers that provide the micro structure with high stiffness and strength while maintaining adequate reproduction fidelity compared with unfilled polymers [42].

Another developing area within the use of fillers is the introduction of nano-filled polymers. Filling polymers with nanoclay particles, for example, is a promising area in research, and the nano-composite market is expected to grow to over 25% a year to reach $250 million in 2008 [97]. Polymer nano-fillers, such as nanotalcs, carbon nanotubes and graphite platelets, are currently used to enhance properties of polymeric materials in applications such as food-packaging, automotive and electronics, where nano-fillers are currently used to enhance material properties

including lighter weight, added durability, dimensional stability, better temperature resistance, enhanced surface finish and surface aesthetics and easier processing [97]. The amount of improvement achieved is dependent on the application and the nano-filler used. It was not possible within the available literature covered in this review to find details as to how nano-fillers can enhance the properties of micromoulded microfluidic devices.

1.4.5.3 Two-component micro-injection moulding and hybrid microstructures for microfluidics

Multi-component micro-injection moulding is a developing method allowing for the possibility of connecting different materials within one part, thus combining different material properties. Possibilities include connecting conductive/insulating, hard/soft or magnetic/nonmagnetic combinations. For example, it has been reported in the literature [98] that it was possible to micro-injection mould insulating macro-structures over a conductive substrate. The part was then coated with a metal layer by electroforming, and the two-component thermoplastic part was separated afterwards.

Another research group introduced the process of micro assembly injection moulding (μAIM), which combines different materials by overmoulding. A set of articles was published detailing the methodology of this process in terms of the different materials combined, the investigation of the bonding strength and the potential applications for such a technology [79-83].

1.5 Micro-Injection Moulding Machines

1.5.1 Introduction

Micro-features have always been a challenge for injection machines, because of the requirement to completely fill cavities in the micro-range before the material starts to solidify. This is specifically critical for microfluidic devices where there is a large change in thickness between the substrate and the microfeatures. In fact, this challenge appeared before the spread of micro-injection mounding, when the same problem was to be solved for thin-wall injection moulding. At this stage it was required to completely fill 2-D thin-walled geometries before the frozen layers begin

to block the cavity. Such thin-walled parts were used in producing laptops and mobile phones. Conventional machines were able to overcome this problem by changing certain parameters such as injection pressure and speed [99]. Increasing the injection pressure forces the material to flow into the thin cavities when its resistance to flow increases due to premature freezing. This technique can, however, result in high stresses and sink marks in the part. Increasing the injection speed enhances the filling process because it decreases the viscosity of the polymer melt due to the shear-thinning effect associated with viscoelastic materials [99].

The same approach was adopted to allow conventional injection machines to produce 3-D micro-sized parts. Machines used for producing CDs proved to be qualified for producing low-aspect-ratio structures [99]. In addition, injection moulders produced large, but precise, sprues to achieve the necessary shot weights, because the minimum shot weights were larger than the part size [100].

Structures with higher aspect ratios required further modifications [69]:

1. Applying vacuum to ventilate the mould.
2. Increasing the mould temperature to the melt temperature of the polymer to avoid premature freezing.
3. Correctly timing the switchover between the injection pressure and holding pressure, so that the holding pressure is applied to compensate for part shrinkage before the materials is frozen.

Nevertheless, modifications in the machine design proved to be necessary, especially after the increase in market demand for products with microfeatures of complex design, higher aspect ratios (larger than 2) and sub-micron precision [26].

1.5.2 Modifications made for micro-injection moulding machines

Based on the set of problems discussed in the previous section, several technical modifications were necessary to manufacture injection machines capable of producing micro-parts:

1.5.2.1 Smaller injection (plastification) unit

In order to decrease the residence time to prevent material degradation, a smaller plastification unit was introduced to provide a shot size of 5 cc or less.

Because the most efficient operating range of most injection units is 20% to 80% of the allowable stroke, a typical injection unit size would be 30 cc or smaller [101].

Decreasing the size of the plastification unit requires the reduction of the screw size and also changes in its design parameters, such as residence time, length to diameter ratio (L/D ratio), root diameter, and compression ratio. Strength is the primary limitation to screw diameter, because the screw should withstand the torque required to convey the solid material through the transition zone. In addition, the standard pellet size imposes limits on the screw flight size. In micro-injection moulding, typical injection unit diameters are 14 and 18 mm with L/D ratios of 15 to 18.

In addition, decreasing the screw size makes it important to increase the linear injection speed in order to maintain the same filling rate. A target linear speed is larger than 200 mm/s for a screw diameter of 18 mm or less to achieve a fill time less than 0.2 seconds [101].

1.5.2.2 Lower tonnage

Injection moulding of small parts usually requires less projected area, which is the area of the mould surface occupied by the part cavity. Therefore a clamping unit with lower tonnage was required [102]. Both mechanical toggle systems and hydraulic clamp mechanisms are suitable for micro-injection moulding. The former system is less complicated, where as the latter is more accurate for small shot sizes [101].

1.5.2.3 Advanced control system

An accurate control system was necessary to meter smaller shot sizes. The accuracy depends on the control system response time and the resolution of the positional indicator [101]. In addition, accurate parameter-control is required for better reproducibility [10], especially in the changeover from injection to holding pressure [27].

1.5.2.4 Variotherm system (temperature variation program) [26]

In this system the mould is heated up to nearly the melt temperature, and when the mould is completely filled, it is cooled down rapidly using additional cooling lines inside the tool [10,23]. This system is a basic requirement to decrease the cycle time

for producing microfluidic parts with structural dimensions of several tens to several hundreds of micrometers, from aspect ratios of three to five, or extreme precision requirements of 1 μm [84].

The use of a rapid thermal process (RTP) has been investigated, in which the surface is heated with IR radiation using a high power halogen lamp [89].

1.5.2.5 Air evacuation

In order to avoid air vents that have sizes similar to some microstructures, the mould cavity has to be evacuated using an external evacuation system [23,26].

1.5.2.6 Handling and inspection

This should be integrated into the machine system for correct positioned removal of the part [27]. In addition, a robotized vacuum-suction system was integrated in some machines to demould the part, handle it and quality-inspect it against a video camera [19].

Several additional enhancements have been introduced to micro-injection machines, including turning-tables to optimize the cycle time. A clean-room environmental cell is sometimes added to create a controlled working environment. A detailed description of machine developments is provided in the literature [103].

Future enhancements for micro-injection moulding focuses on decreasing the sprue size and developing plastification units suitable for providing small amounts of melt using, for example, ultrasonic energy [104,105].

It should be noted that microfluidic devices can still be produced using conventional injection machines, provided that the optimum operational conditions are selected. In fact, several of the reported experiments used in this review are performed with conventional machines [48,51,106,107]. Conventional machines are usually used when a large-area mould is required. This is particularly important for the production of microfluidic devices with relatively large substrates, or where mass-production demands multi-cavity design. As mentioned in section 1.5.1, using conventional machines to produce microfluidic devices would require processing principles similar to those used for thin-wall moulding, such as increased injection pressure, increased melt temperature or high injection speed. Optimizing these parameters results in a decreased melt viscosity that allows the polymer to fill

relatively thin-walled, large-area cavities. Another option would be to implement Variothermal process for the mould by locally heating specific areas of the mould and maintaining the mould temperature above the T_g of the polymer during the injection process.

In the recent years there has been a trend towards the development of electric-hydraulic hybrid type machines or all-electrical machines [108]. It was reported in 2004 that all-electric machines hold a 75% share of the Japanese market and 30% of the US market [109]. Electric machines use servomotors to drive processes, such as injection, clamping and plasticating. The main advantages of electric machines vs. hydraulic machines are higher precision, clean environment without hydraulic oil, etc., low noise-level and energy efficiency [108-111]. A comparison between a number of injection moulding machines was reported in the literature. Four machines, two of which were electric, were compared in terms of performance factors, including process variation and energy consumption [111]. It was shown that electric machines are more reliable, in that they exhibit less variation over a number of process measurements, which was reflected in better repeatability. In addition, it was shown that hydraulic machines consume more power that electric machines by a factor of 3.6. On the other hand, electric machines are more expensive relative to hydraulic machines [109,111].

1.5.3 Micro-injection machine manufacturers

Several manufacturers began to produce injection machines tailored specifically for micro-parts. An example for this was a partnership project that was introduced to produce machines with specifications suitable for micro-injection moulding, including their design, styling and manufacture, as well as handling, testing and assembly [14]. The Austrian project group involved Battenfeld Kunststoffmaschinen GmbH, of Kottingbrunn, HB-Plastic GmbH, of Korneuburg, Inocon Technologie, of Attnang Puchheim and Zumtobel Staff GmbH of Dornbirn. In 1985 Battenfeld presented an injection unit for micro-parts with weights of 0.5 to 4 g: the Micromelt unit. With other partners, it could produce a unit capable of producing weights down to 0.1 g know as the Microsystem 50 [14]. Another example is the cooperation project between the Institute for Plastics Processing (IKV) at Aachen University of Technology (RWTH) and Ferromatik Milacron Maschinenbau GmbH in Germany.

They were able to produce a plastification unit with a shot weight of 0.1 to 1 g [100]. A detailed description of the Milacron machine is in the literature [102].

Comparison between different machine types available in the market and their capabilities are available in several references [4,84,112].

1.6 Optimization of Process Parameters

Common processing parameters usually include melt temperature, mould temperature, injection speed, injection pressure, holding pressure, injection profile controlled either by speed or pressure and cooling time, in addition to the possibility of changing the material type. The part quality can be measured in terms of complete filling, dimension stability, mechanical properties or any other parameter depending on the product.

1.6.1 Early experiments

In initial studies made to investigate process-parameter effects, the main method was by changing one parameter at a time and observing its effect on the part quality. This method was useful for injection moulders in making some basic conclusions about the role of each parameter by its own.

For example, low mould temperatures offer a short cycle time, but can cause premature freezing [69]. Thus, the injection rates have to be high enough to allow for complete filling before freezing. In addition, because of the viscoelasticity of polymeric melts, high temperatures allow for complete penetration without the need for high speeds. Thus, it was deduced that injection speed and melt temperature at various stages within the process are the most important parameters of the injection process.

In another experiment [22] the parts did not completely fill, except when the mould was heated up to a temperature above the T_g of the polymer, which illustrates that the mould temperature affected the filling depth of the polymer. This relation between the mould temperature and the filling depth was also shown in another experiment [20] where an attempt was made to overcome the hesitation effect caused by the viscoelastic nature of the polymer melt, which was preventing the filling of high-aspect-ratio cavities. It was concluded that the ideal situation will be reached when having a hot mould during injection stage and a cold mould during the cooling

stage. This concept has been adopted by several machine manufacturers in the form of a Variotherm system.

The effect of holding pressure was also investigated [21]. Birefringence was used to evaluate the effect of process parameters on the residual stresses in the moulded parts. Holding pressure was shown to provide better replication by eliminating material shrinkage, but at the expense of residual stresses. Recent experiments showed that mould temperature significantly improves optical properties of microstructured PC parts [113].

1.6.2 Design of Experiments (DOE) approach

The studies previously cited show that several parameters can affect the part quality. In fact, the interaction of more than one parameter may affect both the filling behaviour and the part quality. However, testing of all the possible combinations of the different parameters is not practical in terms of time and resources. Therefore, it was required to find a statistical method that has the capability of accounting for the interaction between different parameters and at the same time optimizing the experimental work so that only the important parameters were investigated. Hence, the Design of Experiment approach has become widely used in experiment assessments of micro-injection moulding.

Table 1-4 compares a number of designed experiments conducted by different research groups. The experiments presented indicate that many parameters can play a role in the part quality either independently or interactively. The table also shows that the main results of each set of experiments are different. This indicates that that the part quality is not only a factor of processing parameters. Other factors play a significant role such as the material used (rheological behaviour), the geometry of the mould, the selected response (quality parameter) and the surface finish of the mould. It is therefore advisable to run a designed experiment to optimize the process whenever an element is changed, such as the mould geometry or the polymeric material. Further study and investigation is required in this area.

Tested factors	Response	Materials	Main results	Ref.
Melt temp., injection pressure, holding pressure, injection speed and mould temp.	Filling quality of micro-featured channels	PC, SBS, MABS, COC and PMMA	Melt temp. and mould temp. are most significant parameters.	[47]
Injection time, injection pressure, injection temp. and mould temp.	3D numerical simulation of part filling.	PS, PC and PMMA	The mould temp. is the most important parameter. It must be higher than material T_g.	[114]
Injection speed, holding pressure time, metering size, melt temp. and mould temp.	Part weight and dimensions	PC and POM	Metering size and holding pressure are most significant. The interaction between both is also important	[115]
Injection speed, mould temp., melt temp. and holding pressure.	Complete filling of donut-shaped parts	PS and PC	Injection speed and holding pressure are the most influential, while melt temp. and mould temp. have less influence.	[116]
Melt temp., mould temp., injection speed, holding pressure, air evacuation and the size of features.	Complete filling of high-aspect-ratio rods.	PP, POM and ABS	Melt temp. and injection speed are key factors for PP and ABS. Mould temp. is also significant in case of POM.	[117]
Injection speed, shot size, vacuum, holding pressure, piston diameter	Micro-feature height.	PC	The diameter of the piston, shot size, injection speed and mould temperature are significant parameters.	[24]
Melt temp., mould temp., injection speed and distance between micro-features	Complete filling of micro-structures.	PP, POM and ABS	Injection speed and melt temp. are influential in case of POM and ABS with some side effects. Mould temp. improves filling for some shapes. Distance between micro-features is not influential.	[94]
Melt temp., mould temp., injection speed and surface finish	Flow length along a micro-channel into a flat cavity.	PP, ABS and PC	The high levels of all processing parameters result in better filling. Surface finish is related to level of turbulence in melt flow.	[91]
Melt temp., mould temp., injection speed and holding pressure	Weld-line formation	PS	Injection speed and mould temperature have the main effect on weld-line placement and orientation.	[118]
Injection pressure, melt temp., mould temp. And flow ratio	Flow length	PP	Melt temp. and injection pressure are the most significant factors.	[119]
Holding pressure, filling flow rate and mould temperature	Filled volume fraction of microfilters	COC	Flow rate found to be the most important processing parameter	[120]

Table 1-4 A summary of designed experiments to identify significant processing parameters

1.6.3 In process monitoring of process parameters

Multiple-sensors and data-acquisition systems have been used to monitor the change in processing parameters during the different stages of injection moulding. It was reported in a series of articles that several additional sensors could be used to monitor the change in, for example, injection pressure, cavity pressure, displacements and velocity of the injection pin, temperature in both halves of the mould and the injection force [16,121,122].

In addition, in-process rheometry has been used to monitor the change in the strain rates during processing [86].

Ultrasonic probes are currently used to evaluate the part quality in terms of filling incompletion, polymer degradation and melt flow speed [123,124].

1.6.4 Summary

From the previous discussion, it can be deduced that determining the most effective process parameters for micro-injection moulding is a topic that needs further investigation. Although several experiments have been done, even with the same type of machine, results are often different. This could be because studies were carried out under different experimental conditions (e.g. different polymers or test part structures were used) [94].

There is, however, a general agreement in the literature that the mould temperature should exceed the no-flow temperature of the polymer, but the most influential processing parameters are still a subject of debate.

This emphasises the idea that part quality is a factor of different parameters interacting with each other. Processing conditions, materials used, geometrical shapes and even the machine type are all significant in determining the quality of the final product. In addition, the most significant parameters can vary depending on which output parameter is chosen for evaluating the part quality. Output parameter may include, for example, a specific dimension, a weight or a tolerance. How these parameters interact together is an issue that needs further research.

It seems that the DOE approach is the most suitable strategy to deal with the considerable amount of variables available. However, the experiments need to be well planned, so that only the significant properties are identified without affecting the resolution of the results.

Running a DOE requires a mould to have been designed and built, such that it is ready for running the experiments. This is one limitation of the method, because the results obtained for specific geometrical shape are not necessarily valid for another shape. Thus, for design of moulds for microfluidic parts, it would be of great help if a simulation package were to be available, where it was possible to simulate the effect of changing processing parameters on the quality of parts of different geometrical designs. With the existence of such a package, it would also be possible to investigate post-ejection properties such as residual stresses, warpage, etc.

1.7 Modelling and Numerical Simulation

This section illustrates the areas in which numerical simulation can be useful in micromoulding of microfluidic devices, and it points out the simulation requirements specific to micro-scale processing. Some simulation experiments are also presented, in addition to the potential areas for improvement.

1.7.1 Applications of numerical simulation

The ability to numerically simulate micro-injection moulding would allow for the following major goals to be achieved [98,125,126]:

1. To visualize the flow and predict the last-filled sections of the mould. This is usually done by the short-shots method, where the mould is filled with different amounts of the material to see how the flow proceeds during injection. This is useful to identify defects that are usually associated with the last filled parts like incomplete filling, weld lines and voids.
2. To economically optimize the design of the mould. Because it usually expensive to manufacture injection-moulding moulds, it would be very useful to simulate different geometrical designs, sprue and gating systems, flow-paths to determine the optimum mould design before manufacturing.
3. To simulate the thermal conditions of the flow during filling and cooling which would be useful in estimating the cycle time and determine the processing bottlenecks.
4. To assist designed experiments in determining the most influential processing parameters on the part quality.
5. To identify post-processing properties, such as residual stresses, shrinkages and warpage.

1.7.2 Special considerations for simulating micro-injection moulding

Simulating injection moulding has always been a challenge even at the macro-scale processes. This is because many variables are involved in the process and also because of the non-Newtonian nature of polymers. Micro-injection moulding poses an extra challenge for simulation programs, because different physical concepts are

involved on the micro-scale, which makes it unfeasible just to scale down the macro-physics simulations [87].

Several factors affect the accuracy of modelling micro-injection moulding, which include [125,127]:

1. In conventional injection moulding, two-dimensional modelling is common, which neglects the effect of side and end surfaces. This is not accurate for micro-injection moulding because three-dimensional modelling becomes significant. This is because on the micro-scale it is not possible to approximate the flow shape to flow between two parallel plates. Thus, the Hele-Shaw approximation, which has been used several times to simulate micro-injection moulding, is not suitable for simulating micromoulding conditions such as fountain-flow and transverse pressure gradients. In addition, this approximation simplifies the modelling near corners, bifurcations and changes in the part thickness.
2. Some effects that are neglected in conventional injection moulding become significant in the micro-scale due to the increased surface-to-volume ratio, such as surface roughness, surface tension, heating of the melt by viscous friction and cooling of the melt front due to increased heat loss. In addition, models should account for the differences in dynamics of heat and mass transfer in the micro-scale. The heat transfer coefficient, for example, was shown to be significant on the micro-scale [107].
3. The viscoelastic nature of the polymeric melt becomes more significant at the micro scale because of the high shear rates involved in, for example, narrow gates. It has been mentioned in the literature that increasing the shear rate decreases the melt viscosity to values that are different from those that may be specified in data sheets. Experiments showed that reducing the gate sizes from 0.1651 to 0.0381 mm can decrease some physical properties by 5% to 7% [87].
4. Meshing elements should be chosen with particular care, because two-dimensional elements conventionally used on macro-scale, for example shell elements, give over-predicted filling.
5. Special processing conditions, such as the Variotherm processes, or evacuating the mould prior to filling, should be considered in modelling.

1.7.3 Examples of simulation experiments

Several attempts have been made to simulate micro-injection moulding using a variety of packages for different purposes. One of the earliest attempts [127] was undertaken using I-DEAS Master Series™ Thermoplastic Moulding version 1.3c to optimize the design of the mould, runner and gates, to define and optimize the process parameters and to predict problems associated with warpage and shrinkage during cooling. It was noticed that on the micro-scale, an increase in the significance of some factors appears which affects the accuracy of the software predictions. One factor, for example, is the large surface-to-volume ratios of micro parts, which make surface phenomena dominate the filling and cooling behaviour [127]. The Helle-Shaw approximation was used with shell elements. The simulation over-predicted the length of the short-shots. This was probably because of the two dimensional simplification of the geometry. In which all the surface effects were calculated only for the top and bottom of the mid-surface of the mesh element, whereas side and end effects were ignored.

In another experiment [39] 2-D simulation software C-MOLD ver. 2000 (Moldflow Corp.) was used to determine the most influential processing conditions. It was concluded that the injection speed, feature width and mould temperature were important for mould filling.

ABAQUS has been used to simulate the temperature distribution in the tool during the different steps of the cycle [66]. The filling was simulated by Moldflow. It was observed that it was possible to predict qualitative properties such as welding lines, but numerical values of filled volume, for example, could not be simulated as precisely as required [128]. It was proposed that the packages designed for macroscopic applications could not be relied for micro-scale processes, and it was pointed out that the development of software tools specifically tailored to micro-applications is one of the main future tasks.

The use of software such as C-MOLD to analyse the effect of different gate geometries and locations on the final part has been discussed. In the particular geometrical shape simulated, changing the size and position of the gate in addition to changing the material eliminated the knit line and flow hesitation [85].

Complex shapes and high-aspect-ratio micro-features have also been simulated. C-MOLD 2000 was used to simulate the filling of micro-gears [44]. A 2-D mid-plane

mesh structure was applied to represent a 3-D melt flow. The simulation was in agreement with the experimental design showing that the teeth of the gear were the last parts to be filled.

The effect of micro-scale phenomena on micro-injection moulding has been investigated [77]. These phenomena include size-dependent viscosity (i.e. the change in the fluid viscosity from the wall to the middle of the flow stream in microchannels), wall slip (i.e. the tendency of polymeric melts to slip over solid walls during flow in microchannels when the shear stress becomes higher than a critical value) and surface tension. Simulation was used to identify the most influential parameters in micro-injection moulding [114]. The Navier-Stokes equations were used for modelling the flow of PS, PC and PMMA, and the simulation showed that the mould temperature was the most effective parameter on part quality. A finite element code with a 3D solution approach was used[64] to simulate the filling of different shapes relative to their positions to the gate, and it was shown that the features far from the gate experienced more complete filling, because the material far from the gate required a smaller pressure drop in order to fill the features.

Several other simulation experiments were also reported in the literature [107,129-134].

1.7.4 Ongoing developments

As mentioned in section 1.7.3, it has been shown by different researchers that commercial simulation programs for conventional injection moulding have drawbacks when used in simulating micro-injection moulding. Some packages over-predict the filling of the cavity. Other packages give acceptable qualitative simulation results, but fail to give reliable quantitative values [46,90,98,125,126]. Therefore, two approaches are currently followed:

The first approach is to develop finite-element codes specifically for simulating micro-injection moulding, instead of using commercial packages. Attempts are made to add the special modifications associated with scaling down the physics from the macro-scale. For example, a finite element code was used to simulate three-dimensional non-Newtonian non-isothermal flow in micro-injection moulding. This was achieved by solving the momentum, mass and energy equations [125].

The second approach is to try and develop the currently available packages, so that they can simulate micro-injection moulding. An example of this is a combined project [135] in which a code was written that enables Moldflow system to accurately simulate the last place to fill in a micromoulded part. This replaces the method of using progressively short-shots of a real micro part in a real micromould.

1.8 Post-Ejection Processes for Microfluidic Parts

It is normally desired to obtain the final product with the least number of processing steps in order to limit time and error sources. Microfluidic devices, however, usually need extra processes before they are ready for use. Such processes may include, but are not limited to, sealing, coating, drilling holes and connecting inlets and outlets, depending on the application. Other logistic problems are also relevant to post-ejection processes, such as handling and inspection. Literature about these processes is currently scarce, either because such processes are still being researched or because they exist as in-house knowledge of commercial companies.

1.8.1 Handling the ejected parts

Given that the produced part can be very small in size, special care is required when handling, especially if other processes are still in line. Part handling is challenging given the sizes of micromoulded components. Micromoulders use different handling techniques depending on the product. Many micromoulders use edge-gated runners to carry parts from one location to another, and such runners are used as part of the automation process. In other cases customized end of arm tooling, vacuum systems, reel-to-reel take-up equipment and blister packs are used [18].

1.8.2 Inspection and metrology

The technique for evaluating the quality of the part varies depending on the parts' application. The quality parameter for microfluidic applications can be, for example, the micro-channel width, the tolerances or the filled aspect-ratio. Inspection can take place as a part of the process by using, for example, an in-line video camera.

However, in-line quality control may not be enough for some purposes, such as surface finish or material morphology within the component [16,136], and in this case further inspection has to be done with specialized equipment. Inspection techniques in measuring small micromoulded parts require customized vices, tweezers, and fixturing [112]. Moreover, there is limited availability of inspection equipment that is capable of measuring to sub-micron tolerances [18], and therefore most of the time functional tests were performed.

Quality assurance with regard to specific processing issues may require the use of specialized equipment. An example of this is the use of a laser profilometer to check warpage by measuring deviation in the flat surface of the part [26]. A 3D-measurement for the geometric dimensions of the part can be made by using a confocal microscope with suitable image-processing software [62]. In addition, Atomic Force Microscopy (AFM) has been used for surface inspection and characterization, and Scanning Electron Microscopy (SEM) for observing 3-D details and evaluating dimensions [16,136,137]. Although SEM is a standard imaging technique, it is not the best method for measurement of three-dimensional features. Contact-probe methods, such as micro-coordinate measurement machines (μ-CMM) have been commercially developed for three-dimensional dimensional metrology.

1.8.3 Measurement of mechanical properties

Due to the small sizes involved, conventional mechanical testing techniques such as tension and bending tests cannot be readily applied to micro-features of micro-fluidic parts. Nano-indentation can be used to investigate the mechanical properties such as the modulus of elasticity. For example, the relation between the processing conditions, the level of crystallization of the micromoulded part and the modulus measured has been investigated and reported in a set of articles [16,122,136,138,139].

1.8.4 Sealing the device

It is important to be able to seal the microfluidic device so that leakage is prevented. Different techniques are being developed to find applicable sealing techniques. Adhesives, different variants of welding or lamination are some examples.

MILDENDO GmbH introduced a method that does not involve a third material, which is useful for biocompatible applications [62].

Although sealing polymers is challenging, it is much easier than sealing silicon or glass to other substrates [30], because most polymers have T_g values between 120 and 180°C, so relatively low-temperature annealing could be used for assembly. Using the same technique for glass or quartz, the temperature would be raised to approximately 600°C [57]. A polymer with a lower T_g can be used to ensure that there is no deformation in the micro-channels during sealing process. Elastomeric polymers such as PDMS have excellent adhesion to a wide variety of substrate materials and can be used to enclose micro-channels with a non-permanent seal. In cases where permanent sealing is required, it can be performed by plasma oxidation of PDMS surfaces.

Different sealing techniques were tested for biological microfluidic devices [140]. For example, thermal diffusion bonding (TDB) results in low strength and moderate distortion, when the device is bonded below T_g. In this case TDB at or very near T_g results in increased bond strength but excessive deformation. Another example is solvent-assisted bonding, which allows low distortion, high strength bonding at low temperatures and pressures.

An economical approach to the sealing problem would be to find a method by which micro-injection moulding and sealing can take place in the same process. A method has been introduced in which it is possible to inject the microfluidic circuit and cover it at the same process, which is known as in-line covering. It was done by mounting both the microfluidic-substrate mould and the lid mould on a rotating table. After moulding the substrate it is not ejected, but the table rotates such that the lid is moulded and held at the fixed part of the mould. Finally, the table rotates again bringing the substrate opposite to the lid, and they are pressed together using temperature and ejected as one single part [40].

Most of the sealing techniques mentioned in the literature are associated with specific cases. The choice of the optimum sealing technique is therefore dependent on the application. Several questions have to be considered when attempting to seal a polymer microfluidic device:

- Is it possible to bond the lid to the substrate without using a third material? Examples include thermal-diffusion bonding [38,140-144], laser welding [5,145], ultrasonic welding [146] and mechanical clamping [106,147,148].

- If a layer of a bonding material is to be used, how would this affect the cross-sectional area of the micro-channel? Would excess bonding material flow into the micro-channel areas?
- If heating is involved in bonding, would this distort the micro-features on the substrate or affect the mechanical properties of the polymer chip?
- Is the bonding technique only applicable for joining two parts of the same polymeric material, or is it possible to use it with different polymers or a polymer and another material?
- Is the bond strength high enough to resist the pressure caused by injecting microfluids in the channels?
- Is the bonding material, if any, compatible with the microfluids biologically and chemically?
- Can the existence of bonding material affect the flow of the microfluid (for example by surface tension)?
- If bonding requires the use of solvents, are they compatible with the polymer of the device?
- Will the bonding interfere with other "add-ons", for example electrodes?

These are examples of questions that can pose a challenge in finding the right bonding technique. The answers will depend on the product itself and its technical requirements. Some sealing techniques for polymeric microfluidic devices are reviewed in the literature [145,149].

1.8.5 Additional processes

Additional post-ejection processes are sometimes required, which, in addition to inspection and sealing, are known as back-end processing. For example, holes can be used to connect the part to a macro-sized substrate, or they can be used as reservoirs. They can be drilled mechanically or by laser ablation, but problems may appear due to the formation of burrs by the drilling process, which prevents the bonding between the moulded part and the other piece. In addition to hole formation, dicing of individual devices out of a wafer can be done easily and quickly using, for example, a CO_2-laser. Mechanical sawing can also be used, but it is slower and may restrict the possible design. In some cases, additional activation of the polymer surface or

deposition of biologically active molecules on the polymer-surface might be needed [40].

1.9 Outlook for the micro-injection moulding of microfluidic devices

Significant developments have been recently combined to make micro-injection moulding a stable high-volume process for manufacturing disposable microfluidic devices. Several problems have been successfully overcome by improvements made to the process or to the equipment. Micro-injection moulding is currently used for commercial microfluidic applications. However, challenges remain which require further investigation and research, and for many of these challenges very little information is available in the literature. This is because most of the current research activities are driven by the needs of new products or specific applications, and, furthermore, some of the achievements obtained are not published for commercial reasons.

1.9.1 Design and geometry

Concerning the microfluidic circuit design and geometry, it was not possible from the covered literature to identify a standardized approach for designing a microfluidic circuit to be manufactured by micro-injection moulding. Most of the design aspects discussed in the literature are concerned with individual problems, such as gate-placing or "hesitation-effect" problems, or concerned with specific products.

General design recommendations used in conventional injection moulding can be useful in micro-injection moulding, such as uniform part thicknesses, gate and runner positioning, cooling system distribution and ejection points. In addition, the effect of shrinkage on part demoulding and shape stability becomes significant with higher aspect ratios.

Special design recommendations need to be identified for microfluidic circuits, such as the minimum channel dimensions, maximum aspect ratios, spacing between channels, surface roughness, flow direction and position of the ejection points.

A broader challenge would be to set standards for designing integrated microfluidic circuits, which more than one function is integrated into the chip. This will involve significant changes in the process to take account of the insert/capsulation technique.

Techniques for modifying the surface properties of polymeric microfluidic devices are not well-established as the case in glass. Special techniques for improving the surface properties of micro-featured polymer surfaces need to be investigated.

Micro-injection moulding of truly 3-D components is an open topic for research. Most microfluidic devices currently produced by micro-injection moulding are limited to 2½-D structures. This limits the design options of the system, and necessitates the use of post processing assembly.

1.9.2 Moulds and Inserts

Developments in precision engineering have allowed for several techniques to produce microfeatures. Laser ablation, LIGA and micro-machining are few examples of commonly used methods

Insert fabrication techniques have different limitations in terms of achievable minimum dimensions, fabrication time, economical feasibility, dimensional accuracy or finishing quality. It may be required to integrate several fabrication techniques, i.e. hybrid tooling, in order to overcome the limitations of each individual process. This requires choosing a suitable insert material and a cost-effective fabrication procedure.

Changing the mould design enables micro-injection moulding to produce more complex products. Micro-assembly injection moulding is an example for a process that can be used for integrating elements into the plastic chip. A proper mould design is required to allow for the assembly process to take place without significantly affecting the total cycle time.

1.9.3 Material selection

Generally speaking, most of the commonly known engineering plastics are already used in micro-injection moulding. Thermoplastic elastomers have also been used. Some challenges still exist with respect to polymer selection. Designed experiments show that a single polymer can have different filling quality for different part shapes or aspect ratios. In addition, for a specific geometrical shape, using

different polymers results in different part qualities in terms of filling and shrinkage. This interaction between the type of polymer moulded and the quality of the part produced makes it a challenging task to determine a specific material for a certain application without testing it under different conditions. Trial and error is usually the standard method used to select the optimum material.

No standardized methodology has been adopted to test the behaviour of different materials with respect to certain common microfluidic geometries, such as channels or reservoirs for example. Filled polymeric materials have not been widely tested for micro-injection moulding. Nano-clay particles, carbon nanotubes or metallic fillers may be of use to enhance specific properties in the microfluidic circuit. Considering the high shear rates involved in micro-injection moulding, problems such as particle distribution or migration in micro-moulded filled polymers should also be investigated.

1.9.4 Moulding Machines

Moulding Machines have been greatly developed during the past few years, and several manufacturers are currently offering machines for industrial-scale production. Screw-over-plunger design, small plastification units, advanced control, the Variotherm system and clean-room environments are some of the enhancements made specifically for micro-injection moulding. A major challenge would be the successful integration of additional elements to the microfluidic chip. This would allow the commercial use of microfluidic devices to cover more complex structures and applications.

1.9.5 Process parameters

Several experiments and approaches have been adapted to determine the most influential processing parameters, but the results are sometimes in conflict. There is common agreement that heating the mould temperature above the T_g of the material enhances the product quality considerably.

The interactions between the processing parameters, material properties and part geometry are still largely to be investigated. The Design of Experiment (DOE) approach seems to be the most appropriate strategy to investigate such complex interactions. Nevertheless, being a statistical method, the accuracy of the results

depends on the number of runs allowed and the tolerance ranges specified. In addition, a DOE is normally performed for certain circuit designs. Hence, the results obtained might not be applicable for other designs because of the change in, for example, surface properties or shear rates induced in the mould.

1.9.6 Post-Ejection processes

The function of the microfluidic device determines the number and type of post-ejection processes required before the device is ready for use. Some processes are common among most of the devices such as quality inspection, testing specific properties and sealing. Special processes may be needed such as drilling holes or metallization.

Sealing of microfluidic circuits is a factor of different interacting parameters. Preventing leakage and ensuring compatibility of the lid and seal with the material and the micro-fluid are some of the challenges that are subject to research. Integrating the sealing process within a mass-manufacturing process would be a major development in microfluidic manufacturing.

1.9.7 Integrated microfluidic devices

Integrating different components by micro-injection moulding is a potential area for development. Integrating external functional elements within a mass-production process like micro-injection moulding would allow for many complex microfluidic prototypes to be realized on a commercial scale. Two component micro-injection moulding is a developing field, and having it as an established process requires changing the design of the mould and machine parameters to allow for an automated process for series production. In addition, micro-assembly injection moulding is a promising technology for producing hybrid microstructures. Movable parts, hollow structures and overmoulded fibres are currently being developed. The technology has not yet been applied for microfluidic applications as far as the literature covered in this review is concerned, which makes it an open area for further investigation. A number of integrated microfluidic devices were produced by mass-manufacturing techniques, such as micro-injection moulding and hot-embossing, but this discussion is beyond the scope of this paper.

1.10 Conclusion

This review intended to present the state-of-the-art technology of micro-injection moulding for microfluidic devices and to present potential developments and research gaps. The recent decade has witnessed major developments in the technology that made it one of the most preferred high-volume techniques for fabricating microfluidics. The technology offers several advantages in terms of mass-manufacturability, variety of materials and accurate replication of micro-scaled features, and it is currently being used commercially for producing some types of microfluidic systems. Further technologies are being developed to allow for precise heating and metering of polymer for better control of the process.

A number of limitations, however, need to be overcome before the wide-scale fabrication of microfluidic devices can be realized by micro-injection moulding. The nature of end-shape processes puts limitations on the allowed geometrical designs to ensure smooth demouldability. In addition, polymers in general have limitations in terms of operation temperature and electrical properties that prevents them from replacing glass or silicon in specific applications. The optimization of the process parameters, especially for high aspect ratios, is essential for parts with acceptable quality. Finally, taking into consideration the complexity of integrated microfluidic systems, especially for applications like bio-MEMS, it is important to develop in-line integration techniques to allow the mass-fabrication of polymeric microfluidic devices that are economically feasible for commercial use.

2 Integration of functionality into polymer-based microfluidic devices produced by high-volume micromoulding techniques

Abstract

Microfluidic devices with integrated functional elements have gained increasing attention in the recent years. Many prototypes covering a wide range of applications have been fabricated and tested, especially in the fields of chemical and biomedical sciences. Nevertheless, integrated microfluidic devices are still far from being widely used as cost-efficient commercial products, often because they are produced by fabrication methods that are not suitable for mass production.

Several methods have been recently introduced for cost-efficient high-volume production of micro-featured plastic parts, such as micro-injection moulding and hot-embossing. These methods have been widely used for fabricating simple disposable microfluidic chips on a commercial scale, but have not yet been similarly applied for producing integrated microfluidic devices.

This review paper aims at presenting the state of the art in integrated microfluidic devices produced by cost-efficient high-volume replication processes. It takes micro-injection moulding and hot-embossing as its two process examples.

Several types of elements are classified according to their functions, defined relative to their physical inputs and outputs. Their level of integration is reviewed. In addition, elements are discussed from a manufacturing viewpoint, in terms of being readily produced by replication techniques or by back-end processes. Current and future challenges in integration are presented and discussed.

2.1 Introduction

Microfluidic systems have gained increasing interest in the past few years, especially in chemical and biomedical applications, because these systems have potential as easy-to-use, cost-efficient devices that can perform complex tasks. The

market volume of microfluidic systems is forecast to grow from approximately US$600 million in 2006 to US$1.9 billion by 2012 [1]. Considerable developments have been made in the manufacture of miniaturized microfluidic devices ranging from simple microfluidic chips up to multifunctional integrated systems, such as lab-on-a-chip (LOC) devices, also known as micro-Total Analysis Systems (μTAS).

Integrated microfluidic devices have been tested for a wide range of applications and have showed high potential for applications such as point-of-care (POC) diagnostics, where rapid clinical tests can be performed with relatively easy handling of samples and minimum volumes of reagents. Relatively simple microfluidic systems are currently being produced on a commercial scale using micromoulding techniques. ThinXXS [31], Micralyne [34], Bartels Microtechnik [29], Abbott [35] and Microfluidic ChipShop [36] are a few examples, and their products are mostly used for biomedical and POC applications. Integrated and relatively complex microfluidic systems, however, are not yet commercially used on a large scale, because the relatively high fabrication costs do not allow for an economical mass-production process. In addition, the complexity of some systems prevents them from being developed beyond lab-based prototyping to the stage where they become suitable for commercial use, especially by non-experts [56].

This review paper presents integration solutions proposed in the literature for microfluidic devices manufactured by high-volume polymer replication processes, namely micro-injection moulding and hot-embossing. The paper focuses on mass-production replication technologies, because they provide a potential for low-cost manufacturing solutions necessary for wider commercialization of integrated microfluidics. This would particularly help in producing low-cost disposable systems usually required in, for example, home health care, developing-country health care and medical analysis microfluidics in general, where cross-contamination should be avoided [38,150,151]. Thermoplastics offer a great potential for producing integrated microfluidics. They are already being processed commercially at low-cost and fewer manufacturing steps, relative to glass and silicon [5,37,142,143,152-154]. In addition, the large number of thermoplastics currently available offer a wide range of properties for different microfluidic applications [5,38,142,150,155]. Also, a number of integration

techniques have been successfully tested for replication processes at the micro scale including for example, overmoulding and insert moulding [156,157].

The structure of the paper is made to highlight the relation between the function of the integrated elements and the available integration/manufacturing techniques. The paper aims firstly to review the currently used device elements, categorized into a taxonomy based on their functions. Secondly, the paper aims to identify current potential challenges in developing integrated microfluidics, produced by cost-efficient processes that are directly transferable to industry.

This review concludes with an evaluation of the progress made in integrated microfluidic devices produced by polymer replication techniques in the light of the literature covered within this review. Possible research gaps and potential research areas will be highlighted.

Reviews of several areas, complimentary to the subject of this review paper, can be found in the literature. Gravesen et. al, presented an introductory review of the early stages of microfluidic developments with some examples of basic operations, such as microvalves and micro-pumps [158]. At this stage, integration and mass-production were still presented as potential developments. By the year 2000, polymers had shown great potential for microfluidics, and since then several reviews have covered the relation between polymer properties and microfluidic functions [5,45]. Microfabrication of polymers has also gained special interest in several reviews [30,159,160] including the microfabrication of polymeric microfluidics by micro-injection moulding [161]. More focus have also been directed towards integrated systems, such as lab-on-a-chip and micro Total Analysis Systems [6,159,162] and comparing different materials and production techniques [163,164]. In addition, the disposability of microfluidic devices has also been reviewed [8] with focus on minimally instrumented diagnostic devices [151]. Regarding applications of microfluidic devices, some reviews are available which discuss applications from a general perspective [54], whereas other reviews focus on specific applications of microfluidic devices, such as DNA analysis [165] and amplification [7].

2.1.1 Integrated microfluidic devices

Microfluidic devices can be identified as having one or more channels with at least one dimension less than 1 mm [37]. The flow conditions are mostly laminar and rarely turbulent [40]. Integrated microfluidic chips are often referred to as "lab-on-a-chip" (LOC) devices or micro Total Analysis System (μTAS), because they are designed to perform integrated functions of typical analysis labs. They usually perform standard operations, such as sample preparation, flow control, reaction/mixing, separation and detection [45]. The fluids used depend on the application, but they are usually related to biotechnological applications and hence examples include whole blood or blood components, bacterial cell suspensions and protein or antibody solutions.

A considerable number of microfluidic devices have been discussed in the literature in terms of design, fabrication and testing. However, the majority of such devices are simple in structure, i.e. containing single functions, and used for laboratory prototyping. There is an increasing need for more complex and integrated systems for a set of reasons:

1. To be able to perform a series of laboratory processes such as sample preparation, fluid handling, reaction, analysis and detection on a single device [166].
2. To achieve automation and high processing speed [38,152,167,168].
3. To be able to use the new technology within the physical limits of the existing lab equipment, for example standard holding frames and fluid-delivery systems [169].
4. To produce easy-to-use cost-efficient devices that can perform complex laboratory analyses. This is especially important for, for example, point-of-care applications, lab-on-a-chip and μTAS systems. Integration allows for rapid clinical diagnosis tests, easy usage without complex fluid handling, fewer costly reagents, smaller sample volumes, and shorter assay turnaround systems. In addition, such systems eliminate the often slow, complex and costly preparation techniques of conventional clinical laboratories, such as centrifugal techniques and membrane filtration [38,147,153,167,168,170-174].
5. To give the microfluidic device the ability to interact with electronic, magnetic, optic and chemical methods to have a chip with broad capabilities [170].
6. To connect microfluidic devices to the outer world by using micro-to-macro interfaces such that an efficient system is obtained [170].

7. To allow for the production of disposable and portable miniaturized devices with potentially low manufacturing costs [152,168,174].

Considerable progress has been achieved in mass-producing relatively simple microfluidic devices. However, similar progress has not yet been achieved for integrated systems, i.e. microfluidic systems that are a combination of the basic, fluid-handling elements of microfluidic chips with other functional units to perform more complex analytical tasks [170]. A number of reasons have been suggested for this lag in mass-production options for integration. For example, microfluidic devices are often made only for prototyping purposes; so many projects were intended solely for research, not taking into consideration the potentially high costs of commercializing the developed systems. [2,175]. In addition, there are relatively high additional costs for the currently established techniques of insertion of required functional elements and of device encapsulation [2,155]. It has also taken a longer time than estimated for new technologies to successfully compete with an existing, well-established, macro-scale technology [169].

2.1.2 Review methodology

This paper aims to review the literature from the perspective of progress achieved towards the manufacture of high volume, integrated microfluidic devices via cost-efficient processes. In this regard, micro-injection moulding and hot-embossing were chosen as the replication processes covered in this review. This is because they are commonly used, high-volume, cost-efficient processes. They both have relatively short cycle times, although it should be noted that the cycle time for hot embossing (few minutes to 10 minutes) is generally longer than that for micro-injection moulding (between seconds and minutes). In addition, both processes are similar in terms of polymeric materials used.

Within the context of manufacture by these potential high volume production routes, the review discusses the integration of elements of a microfluidic device. For the purposes of this review, these elements are classified according to their functions, where the selected definition of a "function" is any mechanism of transformation from one basic 'constituent,' to another, in response to environmental stimuli [176]. The three

basic ‘constituents’ are defined as, mass (M), energy (E), or information (I). In this definition, a function is neither the designed purpose of an element, nor the affect of the element on the environment. Instead it is a transformation mechanism [177]. The aim of using this classification system is allow comparison of the state of the art of integration at a fundamental level. This definition results in a set of 9 functions based on the type of input and output constituents as shown in Table 2-1:

		Outputs		
		M	E	I
Inputs	M	**To move:** e.g. motion of one gear causes another gear to move.	**To power:** e.g. burning fuel gives off energy.	**To activate:** e.g. closing a switch sends a signal.
	E	**To energize:** e.g. the volume of a heated fluid increases.	**To convert:** e.g. a wire carrying a current radiates heat	**To detect:** e.g. a photocell responds to light with a signal.
	I	**To actuate:** e.g. controller signal a robot to move.	**To regulate:** e.g. amplifier output is controlled by received signal.	**To transfer:** e.g. digital to analog conversion.

Table 2-1 Types of transformation functions [176]

For the purposes of this review, some of these classifications were considered too broad. For example, the “mass to mass” transformation function is described in Table 2-1 as a motion function “to move”, whereas mass-to-mass functions can take different forms such as “to store”, “to regulate”, “to mix”, etc. These forms are referred to here as “function descriptors” and are used as classifiers in the review.

As a second classification, functional elements in micro-fluidic devices are also classified in this review into integrated or non-integrated elements. Integrated elements are defined as elements manufactured as a part of the microfluidic chip, regardless of whether they are fabricated within the micromoulding process itself or added afterwards in a post-moulding process. Non-integrated elements are those external to the

microfluidic chip, and therefore generally are those which are, in practise, non-disposable and high in cost.

The complete classification scheme adopted in the review is tabulated in Table 2-2. The first four columns detail the classification scheme, showing transformation function, input, output and "function descriptor." The fifth column lists categories of microfluidic functional elements which have a particular transformation function. Columns six and seven describe the techniques, noted in the literature, by which these device elements can be integrated into microfluidic devices, either by micromoulding or hot embossing (column 6) or by post-processing (column 7). Columns 8 and 9 describe the techniques by which transformation functions are achieved by functional elements as yet not integrated onto microfluidic chips. Column 8 is allocated for elements associated with the input functions to the chip (e.g. fluid delivery), whereas column 9 is allocated for output functions (e.g. detection and analysis).

The remainder of this review follows the structure of Table 2-2. Techniques for achieving integrated transformation functions are reviewed in Section 2.2. Section 2.3 reviews the literature for non-integrated transformation functions of micromoulded devices.

Trans-formation Functions	Input	Output	Function Descriptor	Elements	How element are integrated		Non-integrated	
					Micromoulded (Injection or embossing)	Post-processed	Chip-input elements	Chip-output elements
M → M	fluid	fluid	to connect/ deliver	• Fluid connection elements	**Interconnects are moulded with the chip (2.2.1.1.1):** - Moulded ports. - Capillary features are replicated to deliver the fluid to the chip.	**Interconnects are added in post-moulding steps (2.2.1.1.2):** E.g. commercial ports, drilled holes with glued tubes, removable silicon adapters, etc.	-	-
			to move, to store, to mix to divide, to regulate, etc.	• Fluid manipulation elements	**Features are machined in the mould and replicated directly on a single chip (2.2.1.2.1):** - E.g. channels, reservoirs, mixers, dispensers, passive/capillary valves, etc.	**Post-processing is needed after replication (2.2.1.2.2):** E.g. stacked and bonded, fixed as a module on a standard frame,, etc.	-	-
			to contain	• Sealing elements	**Sealing takes place during moulding (2.2.1.3.1):** - E.g. "in-line" sealing.	**Sealing is done after moulding (2.2.1.3.2):** E.g. bonding, adhesives, etc.	-	-
M → E	-	-	-	-	-	-	-	-
M → I	-	-	-	-	-	-	-	-
E → M	Energy/ force	fluid	to move	• Fluid delivery elements.	-	**A miniaturized source of energy is added to the moulded chip (2.2.2.1):** - E.g. Pressurized-air pump, chemical propellant, gas mixture, etc.	**Fluid-delivery (2.3.1):** E.g. syringes or pipettes, pumps, high voltage, centrifugal forces, etc.	-
E → E	Electric current	Voltage/ Temp./ Magnetic field, etc.	to convert	• Energy- conversion elements (e.g. heaters, electrodes, electro-magnets, etc.)	**Elements are directly moulded on the chip (2.2.3.1):** E.g. overmoulding, insert moulding, micro-assembly moulding, embossing, etc.	**Post-processing a replicated chip (2.2.3.2):** E.g. Sputtering, pressing, mounting, etc.	**Connecting the chip to a power source (2.3.2):** E.g. Power supply, batteries, Peltier controller for temperature control, etc.	
E → I	Electric signal/ temp./ etc.	info.	to detect	• Data collection elements	-	**Detection device is mounted on the moulded chip:** - E.g. thermocouple, PCB, micro-ammeter, etc.	-	**Detection equipment (2.3.3):** E.g. optical detection instruments, fluorescence, etc.
I → M	-	-	-	-	-	-		-
I → E	-	-	-	-	-	-	-	-
I → I	Info.	Info.	to analyse	• Data analysis elements	-	-	-	- Analysis device/software

Table 2-2 Types and categories of functional elements currently applied in replicated microfluidic devices (relevant section numbers of the review in brackets)

2.2 Integrating Functional Elements in Micromoulded Microfluidics

Integration in polymer processing represents the ability to combine different functional elements on a polymer chip. This can directly be done during the fabrication of the chip, such as in the case of ducts and passive valves. Integration can also be carried out after the production of the plastic chip, particularly if it is difficult to achieve integration in-process, owing to limitations in the replication process. In this case, post processes, sometimes called back-end processes [40], are applied.

This section reviews the current situation of integrated elements for polymer-based, replicated microfluidic devices. Sections 2.2.1 to 2.2.4 present integrated elements currently reported in the literature. Following the sequence shown in the first column of Table 2-2, each section discusses one category of transformation function. For each functional category, sub-sections will compare integration by micromoulding or hot embossing to integration by post-processing. For ease of reference, in Table 2-2 the different categories of transformation function are marked with the corresponding section numbers of the review.

2.2.1 Integrated elements involving mass-to-mass transformation functions

Section 2.2.1 presents the main microfluidic components that perform mass-to-mass functions. They include fluid delivery and fluid manipulation elements, in addition to sealing.

2.2.1.1 Fluid connection elements

Delivering fluids to a microfluidic chip (or taking them out after processing) requires an interconnection system that allows for a secure and easy-to-plug input and output system. The interaction between the micro and macro world affects the efficiency of the microfluidic systems [170]. In fact, one of the main obstacles that prevents microfluidics from spreading further commercially is the lack of standard

interconnects for interfacing the macro-scale environment with the microfluidic channels within the chip [141].

Some requirements for an ideal interconnection system have been mentioned in the literature such as being leak-proof for fluids and gases, possessing minimal dead volume, ease of use, standard geometry to facilitate interfacing with commercially available devices, reversibility, reliability, lack of contamination and ease of fabrication [141,166].

As an alternative to conventional interconnection, capillary systems are also used in some applications to deliver the fluid sample to the device. The physical phenomena on which they depend are governed by a relationship between surface tension, fluid density, contact angle and the channel size. Therefore, they require the design of the inlet channels to the optimum dimensions in order to deliver the fluid inside the microfluidic chip. Examples are reviewed in the next section.

2.2.1.1.1 Fluid connection elements produced by micromoulding

Mounting interconnections by post-processing (discussed in the next section) is the commonly used method for most prototypes. There is, nevertheless, an increasing trend towards producing interconnection systems as an integrated part of the moulded chip. An example of micromoulded interconnections has been reported, where a micro-injection moulded chip was sealed by a plastic lid in which connection ports were integrated as one part [141] (Figure 1). The ports are made of a hollow boss with ANSI standard internal 6-32 threads located at each fluid entry point. The use of micro-injection moulding makes the cycle time almost independent of the number of ports. Tube fittings were fitted in a later stage.

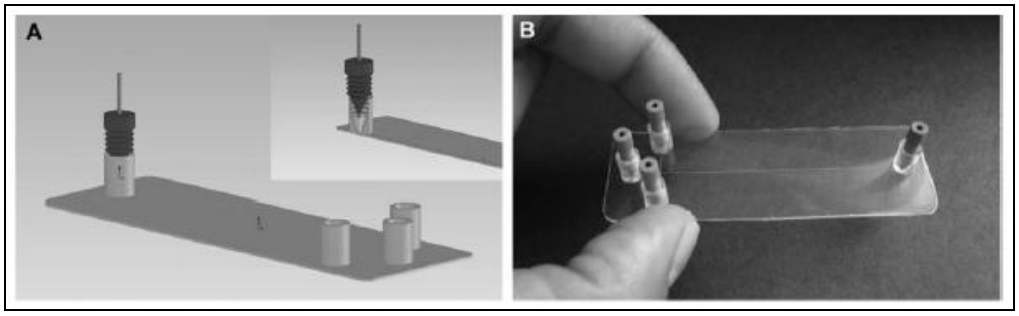

Figure 2-1 Concept of microfluidic chip featuring integrated ports (A) and a 4-port chip with commercial male fittings threaded integrated ports of an injection moulded chip (B) [141]

Moulded ports were also produced by injection moulding using moving mould-inserts that are shaped like pillars and can be adjusted in length to determine the final depth of the moulded connection port [178].

As mentioned earlier, capillary actions can be used as an alternative fluid-delivery system for interconnects. In an injection-moulded device for monitoring DNA migration, capillary action made the polymer fluid spread in the system, and the subsequent gentle centrifugation flushed the channels [148]. In a similar experiment, a hot-embossed microfluidic device for analysing human sweat applied a propulsion system in which the device was set to collect 600 µl of sweat from human body using capillary action. Afterwards, centrifugation was used to spin the sample out into an analytical container. The sample was finally collected by centrifugation in a standard bench-top swing-bucket centrifuge modified to accommodate the device [173].

2.2.1.1.2 Fluid connection elements produced by post-processing

Several post-processing connection techniques were mentioned in the literature. For example, access ports were used to connect modular chips together within a frame [170] (more details about modular designs in section 2.2.1.2.2). For connecting the chips to the outer world, Luer and Luer-Lok fittings were used, which have gluing edges allowing them to adhere on to the lid surface [169] (Figure 2-2):

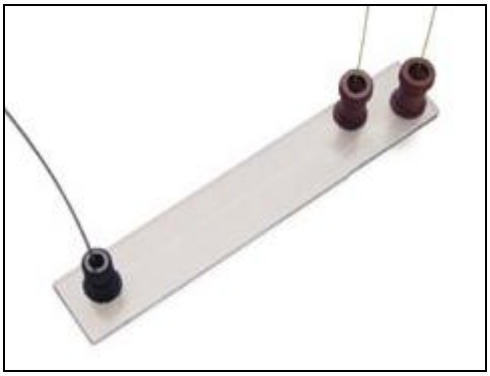

Figure 2-2 Nanoports used for fluid delivery [179]

In another modular device, where chips were laminated together, a special layer dedicated to connecting the system to the outside world was used. It had a standard format irrespective of the other layers, possessing interface connectors to liquids and electrical/electronics. It also formed the mechanical basis for alignment of the

subsequent layers [170]. Self-aligning microfluidic interconnects were also designed and tested for polymer microfluidics that are produced by micro-injection moulding or hot-embossing [180].

For some microfluidic devices, holes are manually drilled in the lid to fit the connection tubes, which are typically connected with glue [106,141,147,181]. In other devices, Luer-Lock syringes were used both as a fluid propulsion system and connection system [140]. Since most devices are produced for prototyping purposes, fluid delivery is usually achieved by manual delivery with syringes or pipettes or with syringe-pumps when flow-rate is an important consideration (section 2.3.1 for non-integrated methods). Removable silicon adapters were used to connect standard pipette tips into an injection moulded microfluidic chip [146].

Overmoulding was recently tested as a mass-production technique for both packaging and fluidic interconnection [156,182]. The method was applied as a generic interconnection system for microfluidic devices and also for post-packaging of a specific commercial pressure sensor module. This technique provides leak-proof connection between the chip and the fluid-delivery system. However, it requires an extra manufacturing steps in which a chip, with features already produced by a prior process step, is inserted in a special mould and overmoulded by the selected polymer.

2.2.1.2 Fluid manipulation elements

In medical diagnostics, as a common example for microfluidic applications, complex bodily fluids (e.g. blood) need to undergo a set of preparation steps before being suitable for analysis. Most of the currently demonstrated microfluidic device components pursue single functionality and use, for example, purified DNA as an input sample. Therefore, in the majority of the cases, sample preparation is still performed off-chip [172]. If real samples of bodily fluids are to be inserted directly to the device, e.g. in POC applications, the device has to perform several steps in a single integrated microfluidic system.

2.2.1.2.1 Micromoulded fluid manipulation elements

Mass-production of integrated subsystems by replication has the advantages of minimizing the cycle time, avoiding post-processing assembly, eliminating opportunities for fluid leakage between different microfluidic stages and reducing

fabrication costs. Nevertheless, this method does not have the flexibility of changing the microfluidic feature-shapes or sequences after manufacturing, because this requires the fabrication of a whole new insert. In addition, it is currently limited mostly to "flat", 2½-D geometries in order to facilitate part demouldability.

An example for fully integrated circuits is a microfluidic device used for blood typing (Figure 2-3) [33]. The disposable chip, which was micro-injection moulded of COC, comprised a number of fluid-manipulation steps, including flow splitting microchannels, chaotic micromixers, reaction microchambers and detection microfilters. The flow splitter divided the blood sample into four equal amounts, so that several agglutination tests could be performed in parallel, whereas the serpentine laminating micromixer was used to promote efficiency of reactions. The large reaction chambers were introduced to hold the reactant during the reaction time before filtering. Finally, the microfilters are used to effectively filter the reacted agglutinated red blood cells.

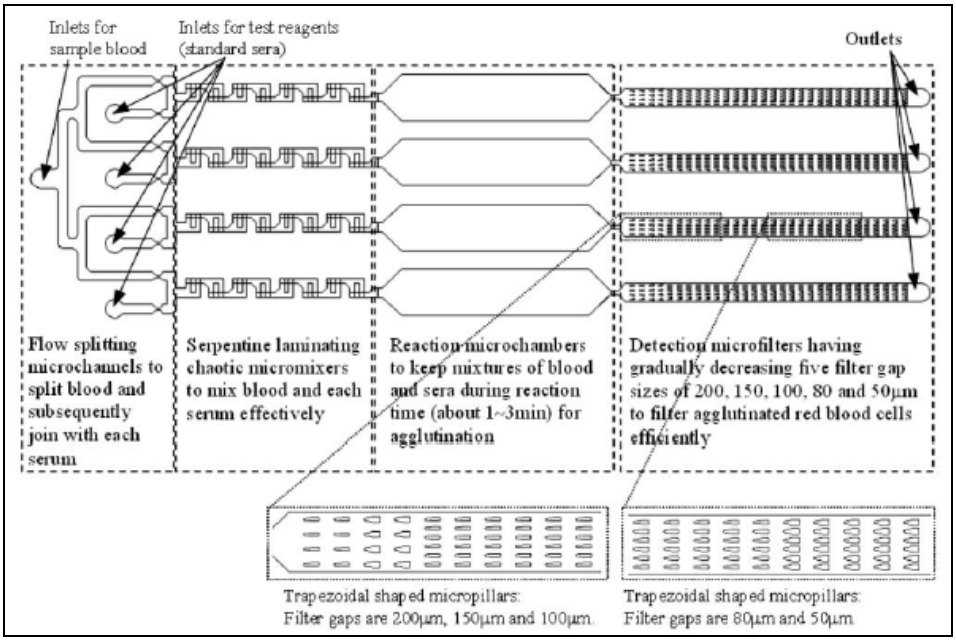

Figure 2-3 Schematic diagram of a blood-typing chip with integrated functional circuits [33]

Another attempt to integrate several circuits on a single plastic chip was presented in the form of a PMMA CD-like platform [155,183]. Functions integrated included flow sequencing, cascade micro-mixing, and capillary metering (Figure 2-4).

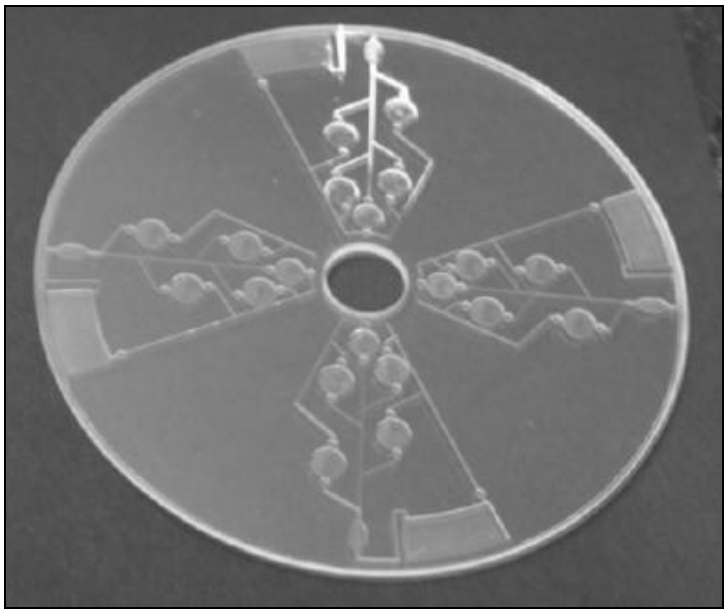

Figure 2-4 Integrated microfluidic CD platform [183]

In another example, an integrated microfluidic device was fabricated by hot-embossing polycyclic olefin. The device was for bacterial detection, and it integrated PCR, valving and electrophoresis on a single plastic chip (Figure 2-3) [174]. Also, a microfluidic device containing a cross-junction channel was used to produce micro-sized beads of Calcium Alginate [106]. The CD-like device was produced by injection moulding PC, and by changing the flow rates of the inputs, the cross-junction was used to produce beads of 20-50 μm in diameter with narrow size distribution (<10% variation in diameter). Micro-injection moulding was also used to produce an integrated disposable microfluidic device for detection of agglutination. The device which was moulded of COC included micro-wells, passive micro-valves and a serpentine micro-mixer [184]. All features were replicated from a nickel mould insert and the device layers were thermally bonded.

Flow control elements, such as valves and dispensers, are usually an essential fluid manipulation element in microfluidic systems. Two main fluid control systems are usually available for microfluidic applications: passive and active. Passive valves operate without the need for physical actuation, by utilizing energy from the flow and are typically used as check valves [185,186]. Active valves require more sophisticated control systems involving, for example, actuation, which means that multiple inputs, namely mass and information/energy, are involved.

More attention has been recently directed towards passive fluid control systems, such as passive valves, mixers, diffusion-based extractors, passive filters and membranes. Passive systems have several advantages, including the need for no external power requirement (mass-to-mass function), ease of integration, continuity in substrate material, low cost and, by definition, possibility of use without active control. Nevertheless, some challenges still face passive systems. They are usually application specific and cannot be easily reconfigured. They are strongly dependent on variances in the fabrication process (as will be shown next section) and not suitable for several fluidic mediums [171].

Several types of passive vales have been fabricated and tested. Mechanical valves, such as flap or membrane check valves, and non-mechanical valves, such as capillary valves, have been used for microfluidic devices [187].

The advantages of the passive control systems make them a preferable system for flow control, especially for plastic chips produced by replication techniques, because no back-end processes are needed. For example, in the microfluidic CD platform presented earlier, which was produced by both injection-moulding and hot-embossing [183], a passive capillary-valve that relies on the capillary force to stop the flow in micro-channels, was used [155]. The principle of operation was based on a "pressure barrier" that develops when the cross-section of the capillary expands abruptly. The fluid moves through this valve when the capillary forces are overcome by the centrifugation forces (Figure 2-5). As shown in Figure 2-5, the sequence of the fluid flow initiation from each chamber was planned to go in the order of calibrant 1, wash 1, calibrant 2, wash 2 and the sample.

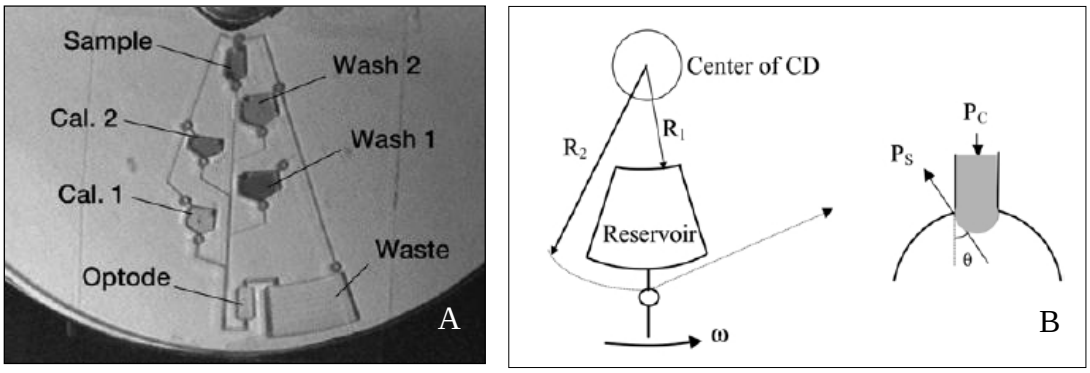

Figure 2-5 (A) Passive capillary valve system. (B) A schematic illustration of fluid propulsion [155]

Passive valving was also applied in a microfluidic device for point-of-care clinical diagnostics [171]. In this device, a special sequence of flow was required in the microchannels, so the flow was controlled using a so-called "structurally programmable" microfluidic system (sPROMs). sPROMs technology allows fluids to move through a set of valves in designed stages with only an on-chip pressure source. It consists of passive valves and flow conduits, which have different pressure drops depending on the structure and surface properties of the fluidic path [188] (Figure 2-6).

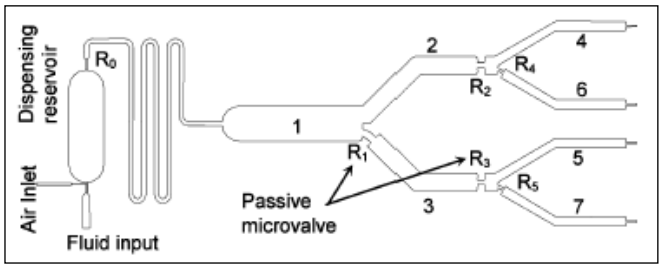

Figure 2-6 sPROMs system [188]

Other types of passive systems can also be found in a variety of fluid handling applications. Capillary metering, for example, is used for delivering precisely metered fluids from one reservoir to another in a controlled sequence. Bubble snap-off is one technique that has been presented in the literature for sample metering [155]. Here, a gas bubble in the liquid-gas flow passes through a constriction and breaks up into a number of equally-spaced small bubbles (Figure 2-7). Although metering is not a valving technique, it is still a passive flow-manipulation technique that is dependent on the same principles of geometry change and fluid-surface interaction.

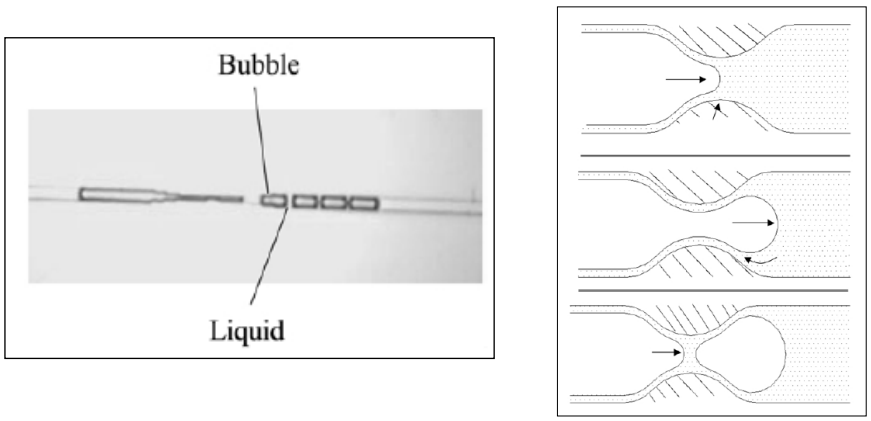

Figure 2-7 A micro-channel design for bubble snap-off [155]

This mechanism can be used in sample metering of microfluidic systems, because a fixed amount of liquid is trapped between two bubbles that are snapped off.

Other fluid control elements have also been tested, such as micro-dispensers in which sample fluid volumes were loaded into a fixed volume micro-dispenser, which in turn dispensed an exact volume of liquid for further biochemical analysis. This was done by designing the geometry of the chamber to contain a specific volume of the liquid between inlet and outlet valves. When the pressure source is released, the metered volume is pushed through the outlet passive valve [171].

As shown in the previous examples, passive fluid-control systems, including valves and dispensers, are a promising technique for fluid manipulation in microfluidic devices. Considering that such systems do not need external actuation or feedback, and that they are readily manufactured as an integrated feature of the substrate, this makes them practical solutions for on-line fluid control systems. The operation principles of the systems are similar, in that they depend on the geometry of the valve (hydrodynamic radius), the fluid properties (viscosity) and the interaction between the fluid and the surface (contact angle and surface tension). Their relative simplicity of principles of operation makes them easy to integrate into devices produced by high-volume replication techniques, as their operation depends primarily on the existence of abrupt change in the geometry of a channel. As the market demand increases for cost-efficient complex systems, more attention is expected to be directed towards passive control systems.

A recently introduced concept of passive fluid control systems is the so-called "lotus surfaces", where sub-µm structures were directly replicated into microfluidic surfaces by hot-embossing [189]. The replicated surfaces had structural gradient that generated driving forces to move liquids in microfluidic channels.

2.2.1.2.2 Post-processed fluid-manipulation elements

Connecting separate subsystems has been widely used in prototyping microfluidic devices. This is due to the flexibility this allows for modifying of the overall device design. Furthermore, separate chips can be integrated in standard laboratory equipment, or they allow, by stacking 2.5-D chips for example, for 3-D designs to be realized.

Several connection techniques have been described in the literature. Stacking, for example, is one well-known technique. In a published experiment, a modular design concept with standard interfaces between each functional module was introduced to present a chemiluminescence experiment [170]. Each module was a discrete microfluidic chip fabricated by hot-embossing for dedicated tasks such as sample preparation, mixing, analysis, etc. Consequently, any new microfluidic design could be incorporated into the system for a specific function as long as some fundamental design rules were adhered to. Elastic averaging, which involves the constraints of the layers using dowel pins, was used to align the different chips together (Figure 2-8).

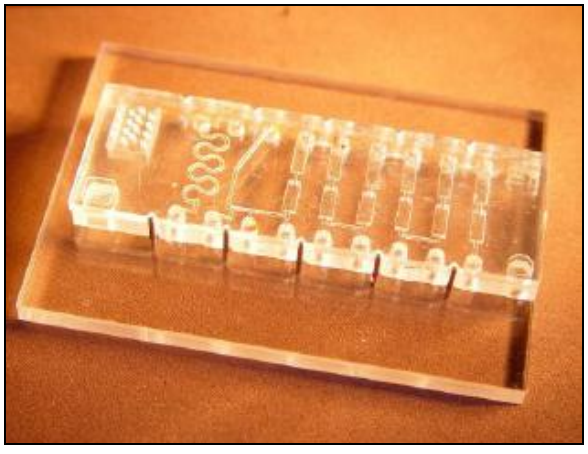

Figure 2-8 Two stacked chips aligned using elastic averaging with V-grooves and dowel pins [170]

The elastic properties of the material and the constraint structure cause deformations in each individual contact feature to average out over the sum of contact

features throughout the solid body. The alignment offset measured was between 10 to 20 µm. Better accuracy (10 µm or less) was required for this method [170].

A second example of post-processed integrated subsystems connected from separate chips was a lab-on-a-chip for POC clinical diagnostics, namely a micro biosensor [171,190]. The device was designed for detecting and identifying three metabolic parameters: Partial pressure of oxygen, lactate concentration, and glucose concentration in human blood. The chips were produced by injection moulding using a replaceable insert with micro-features [191], and they were stacked and laminated together using thermal fusion (Figure 2-9). The same lamination approach was used to integrate injection moulded layers of an integrated microfluidic device for magnetic immunoassay [192].

The integrated functions included chambers and buffer reservoirs, multiplexing channels and a dispenser. Valves and other functional elements were also integrated, and they will be mentioned in more details in the corresponding sections.

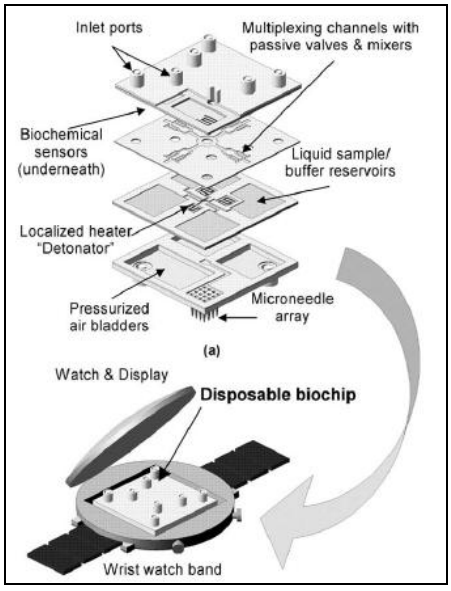

Figure 2-9 Multilayer disposable plastic biochip consisting of laminated microfluidic chips [171]

Stacking was also used to fabricate a pneumatically actuated microfluidic device for bio-analytical applications [193] (Figure 2-10).

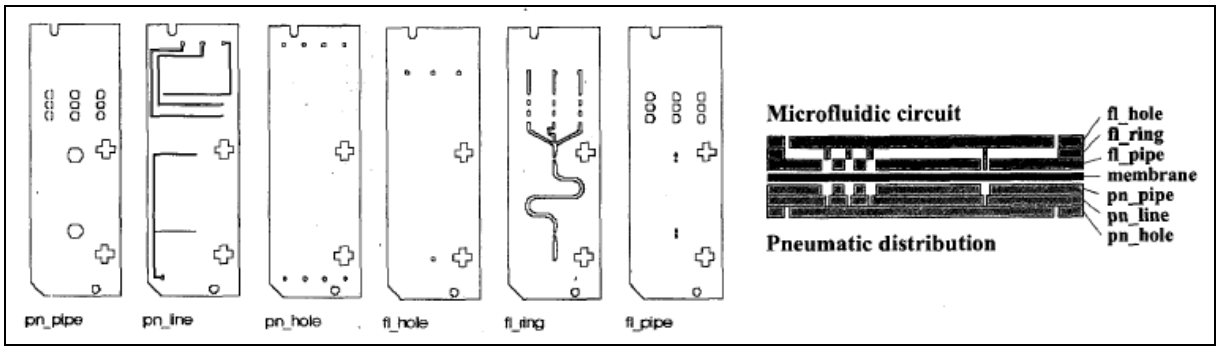

Figure 2-10 Pneumatically actuated microfluidic device [193]

Modular structures have been proposed as an alternative method for stacking as a method for both integration and standardization. A microfluidic construction kit was presented, based on modern plastic production technology such as micro-injection moulding and hot-embossing [166]. Chips of different microfluidic functions could be fabricated to the size of a standard microscope slide and connected in a standard frame, used for e.g. POC diagnostics (Figure 2-11). Modular designs with integrated interconnects were also produced by micro-injection moulding for continuous PCR [194].

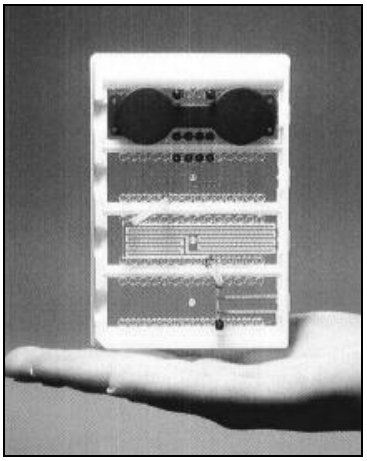

Figure 2-11 Modular microfluidic construction kit [166]

LOC devices integrated modularly can join several laboratory processes, such as sample preparation, fluid handling, reaction, analysis and detection. Since miniaturized systems are likely to be used in parallel with standard laboratory equipment, a modular

standard kit has been produced as a method for standardizing microfluidic chips with laboratory equipment [169].

A microfluidic system for DNA sequencing was also reported in the literature in which a set of functional circuits was integrated with micro-fabricated connects. The functional chips were manufactured by hot-embossing PMMA and PC chips. They performed the following functions: PCR amplification of DNA, purification of the PCR products, cycle sequencing using dye-terminator chemistry, purification of sequencing products, solid-phase reversible immobilization and DNA electrophoresis [167]. COC was also injection moulded to produce a laminate-type microfluidic device for PCR application [144].

Both micro-injection moulding and hot-embossing were used to produce an integrated chip for protein analysis [195]. Micro-injection moulding was used to fabricate the COC substrate with micro-channels, while hot-embossing was used to fabricate a polymeric piezoelectric micro-diaphragm. The two parts were bonded together using UV adhesive bonding in a subsequent step.

When it comes to valving, some integrated solutions were presented for micromoulding. Pinch valves, for example, have been recently used as disposable on-chip fluid control elements. A number of designs have been successfully tested for micromoulded integrated chips applied for point-of-care testing of metabolic parameters [196] and PCR analysis [144].

2.2.1.3 Sealing elements for microfluidic devices

Due to the constraints imposed by the replication processes on the geometrical design of the part, microfluidic devices are replicated as open channels that need to be closed to prevent leakage. From a functional point of view, sealing can be considered as a mass-to-mass function, where the functional descriptor would be to “contain” the fluid. Sealing takes place, either, during fabrication as an integrated step in the processing, or, by post-processing sealing techniques. Section 2.2.1.3.1 reviews sealing by micromoulding, whereas post-processing sealing techniques will be presented in section 2.2.1.3.2.

2.2.1.3.1 Sealing by micromoulding

In the literature covered within this review, a single experiment was reported in which sealing took place as an integrated fabrication step [40]. In this experiment the covering step was integrated as part of the injection moulding process known as in-line covering. Both the substrate and the cover are injected at the same time with the same material, such that the cover part is attached to the nozzle side of the mould, while the micro-structured substrate is attached to the ejector side. The index plate carrying the cover rotates 180° causing the two parts to be aligned, and the surfaces of the two parts are warmed up, and after renewed closing of the mould the covering process follows. When the mould is opened, the covered part falls finished from the machine after 40 seconds.

2.2.1.3.2 Sealing by post-processing

Bonding lids to microfluidic substrates is the commonly used post-processing method to close microfluidic channels. The major challenges for bonding are to join the lid to the substrate without clogging the channels, changing their physical parameters or altering their dimensions [5,145]. Several techniques have been developed to seal polymeric microfluidic devices, and they can be grouped into three major categories: Sealing with the use of intermediate material, sealing with the use of energy and mechanical sealing.

Sealing with the use of *intermediate material* is commonly used for post-processing micromoulded microfluidic systems. Adhesives, for example, have been reported in the literature as intermediate sealing agents for micromoulded microfluidic systems, such as conventional glues [5,38], UV-curable adhesives [153], thermally activated adhesives [168] and copolymer adhesives [152]. In addition to adhesives, polymeric foils, such as PET, have also been tested as intermediate materials to laminate microfluidic substrates together [5]. Solvent-assisted bonding is another technique where microfluidic substrates are wetted with, for example, mixed organic solvents [154] or acetyl acetone [197] and joined permanently under pressure [140,198].

Sealing with energy is based on using one or more types of energy to join the micromoulded devices without the use of an intermediate material. The literature reports a few examples of micromoulded microfluidic devices that were bonded using energy, such as induction heating [145], laser welding [5,145] and thermal-diffusion bonding

[38,140-144]. Ultrasonic welding and UV-bonding are other available energy-based techniques for bonding polymers, but very little is mentioned in the literature about using them for microfluidics.

Mechanical sealing is commonly used as a sealing technique, especially for prototyping purposes. A number of examples were mentioned in the literature, where screws [106,147,148] or snap-fit systems [173] were used to seal polymeric microfluidic devices. A polyethylene/thermoplastic elastomers (PE/TPA) film was used to seal and injection moulded CE chip made of PMMA and PC [178].

Selecting an appropriate packaging technique for polymeric microfluidic devices depends on a number of factors, such as the substrate material, the temperatures involved, compatibility with fluids used and channel size. In addition, the cost of the process is significant to the feasibility of the process for mass-production. A more detailed comparison between packaging techniques for disposable microfluidics is available in the literature [193,199]. A recent review has also been published addressing bonding of thermoplastic polymer microfluidics [200].

2.2.2 Integrated elements involving energy-to-mass transformation functions

A propulsion force, such as mechanical pressure or centrifugal force is needed to pump fluids throughout the microfluidic channels. Generating forces is usually done by interaction between on-chip elements, e.g. pressure reservoir or capillary channels, and off-chip elements, such as a motor for rotation or a pressure pump. Fluid propulsion systems can, therefore, be considered as "interfacial" integration tools, in the sense that they connect on-chip micro-components to off-chip macro-components.

The amount of energy needed to pump liquids in microfluidic channels vary depending on application. For example, a microfluidic device for chemical analysis was made in which deionised water was pumped at a rate of 730 nl/min with a fixed power of 500 mW [201]. In another application, a microfluidic chip was designed to have a power supply from a commercially available 12V-type MN21 battery [202]. The power consumed for transferring a liquid across the chip ranged between 145 mW initially down to 71 mW after 40 cycles of operation, because the battery was unable to maintain

the supply voltage above 75% of the initial output. The experiment revealed, however, that only 8% of the power consumed was consumed in the chip, while the rest was consumed by the electric converter and control circuitry.

Several techniques have been developed for fluid propulsion. In the literature, three main propulsion methods were discussed: mechanical, electrical and thermal [155].

For mechanical propulsion systems, a mechanical pump is often used to provide the driving pressure. It can be as simple as a roller in the blister pouch design, or as complicated as a miniaturized syringe or acoustic pump [155].

For electrically-driven systems, electro-kinetic techniques such as electro-osmosis or electrophoresis, electrodynamics and electrowetting have the advantage that they scale favourably for miniaturization. In electro-osmosis or electrophoresis, the driving forces for flow are generated by the interaction of applied electric fields with ionic species in the fluids. In electrodynamics, the flow is generated by the interaction of electric fields with induced electric charges in the fluids. Electrowetting is based on the principle that the contact angle between a liquid and a solid surface can be changed through the application of an electrical potential. This change may result in capillary forces that provide a driving pressure in small flow channel.

For thermally driven propulsion, it is possible to manipulate the contact angle between a liquid and a solid surface by changing the local fluid temperature. The resulting capillary force is used to drive the fluid as in electro-wetting [155].

2.2.2.1 Post-processed fluid propulsion elements

The recent trend towards further integration has resulted in the development of techniques in which the off-chip assistance is minimized. One example is a microinjection moulded device used for medical diagnostics applications, which had an integrated air-bursting detonator as a fluid-driving source. This eliminated costly, non-disposable, active microfluidic pumps. As soon as the membrane is broken, the pressurized gas is released pushing the fluid samples into the microchannel through the ruptured membrane [171,190] (Figure 2-12). The detonator was powered by a 40 mW pulse to power the microheater for 700 ms, which resulted in the release of 650 μJ of stored pneumatic energy to drive a 500 nl sample through microchannels [203]. This

technique allows for a relatively higher degree of integrity, since the pressure pump is a cheap and disposable part of the microfluidic device.

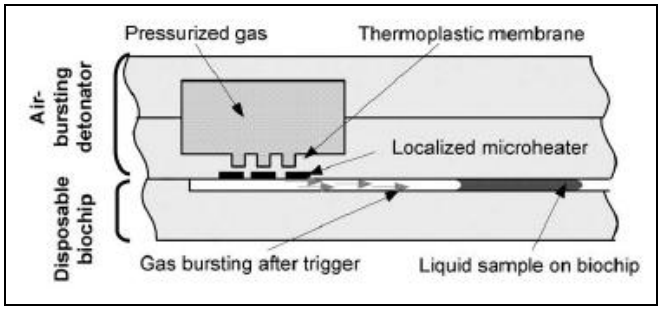

Figure 2-12 Air-bursting detonator [171]

On-chip propulsion was also achieved using a chemical propellant, where azobisisobutyronitrile (AIBN) was used as an actuator that releases N_2 gas. The gas pressure can then be controlled to accurately control the fluid flow [196].

In another application, a microfluidic system was designed for medical diagnosis, and fluid propulsion takes place using a hydrogen-oxygen gas mixture generated by a sodium polyacrylate-based hydrogel. The gas is created by applying an electric voltage to the water in the hydrogel stored on the chip [204].

Developing integrated energy-to-mass elements will greatly affect the production of integrated microfluidic devices. They have the advantages of mass-to-mass delivery systems in the sense that they are integrated as on-chip, power-source elements. At the same time they have the potential of supplying relatively large amounts of power comparable to what is offered by non-integrated elements, such as syringe pumps and pipettes.

2.2.3 Integrated elements involving energy-to-energy transformation functions

Several applications of energy conversion have been used in microfluidic devices, such as microheaters and electromagnets.

Electrically conducting structures such as wires and electrodes are the most commonly used elements, especially for applications such as resistive or capacitive

sensing, electrophoresis, integrated heaters and electro-hydrodynamic pumping [205]. Magnetic, optical or thermal elements may also be used depending on the application.

The majority of devices with elements performing energy-to-energy transformation functions reported in the literature have external elements that are added by post-processing by, for example, ink-printing or sputtering. Very few devices have been reported having functional elements integrated within the same micromoulding process of the plastic substrate, because integrating such elements requires an additional step of placing them in the mould or the insert. This additional step elongates the cycle time unless a design modification is made in the machine or the mould to integrate and automate the process.

The following sections review integrated elements fabricated by micromoulding and post-processing.

2.2.3.1 Energy-conversion functional elements fabricated by micromoulding

One of the advantages of micromoulding is the possibility of embedding elements into the plastic during moulding [206]. Conduction paths have been integrated into device structures by hot-embossing a composite polymer/metal material. Paths were first applied to the unstructured substrate and then pressed into the polymer layer during hot embossing so that embedded conduction paths are obtained following the embossed topology [142]. A hybrid structure was also manufactured by integrating a metal insert inside a polymer matrix by hot embossing [157]. In a recent application, conductive polymer electrodes coated with metal were integrated by micro-injection moulding into a polystyrene substrate using over moulding [206]. A similar technique was used to directly emboss a gold nanoelectrode ensemble film into a PMMA based microchip for CE [207]. Hot-embossing was also used to fabricate electro-fluidic polymer microchips [205]. In this application, electrical wires were integrated by a single-step method into an embossed polymeric microfluidic chip. Using this method, wires could be placed in contact with the flowing fluid or embedded in close proximity to the fluid channels.

For micro-injection moulding, a developing approach for integrating energy-to-energy elements is micro-assembly injection moulding. This process is suitable for producing hybrid micro-structures by injection moulding, such as movable joints, hollow structures and overmoulding wires and optical fibres [79,80,82,208,209]. In this

process, electronic connections or optical fibres can be overmoulded within the injection moulding cycle (Figure 2-13).

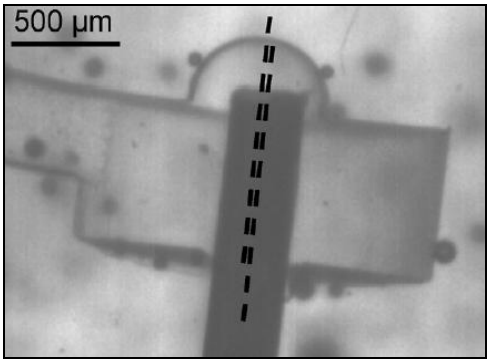

Figure 2-13 Overmoulded optical fibre [80]

In order not to affect the cycle time, the micro-structured cavity is allowed to be exchanged during the machine cycle such that the process steps of demoulding, positioning of insert and heating the cavity for Variothermal processing can be done at an external station. In other words, an external cycle is allowed to take place parallel to the main cycle of the machine.

In order to ensure dimensional stability, the behaviour of different materials for both the insert and the polymer in the injection process should be considered. Additionally, the influence of the flow direction of the polymer is also significant for dimensional stability.

2.2.3.2 Energy-conversion functional elements fabricated by post-processing

2.2.3.2.1 Electrodes

Electrodes are commonly used in microfluidic applications, either for electrical measurements or for voltage application. They are particularly important for microfluidic applications that use electroosmotic flow or electrochemical detection [186]. Electrodes are classified as energy-to-energy elements, since they are used to generate voltages in applications such as electrophoresis.

Several post-processing techniques have been used for integrating electrodes onto replicated polymer-based microfluidic devices. Conventional deposition methods such as sputtering and thermal or electron beam evaporation can be used [210]. However,

there is limitation on the electrode dimension due to the shadow mask used, which restricts the electrode width to 40 μm and above. Alternatively, laser ablated microchannels can be filled with a conducting ink and act as electrodes [5,174,211,212]. It should be noted that not all metals are equally easily applied to polymer materials, as some problems might appear such as formation of metal clusters instead of uniform films and formation of micro-cracks in the metal film [186].

For an injection-moulded device used for insulator-based dielectrophoresis (iDEP), platinum-wire electrodes were inserted directly into the syringes used for fluid delivery. A programmable high-voltage sequencer was used to apply voltage [213]. In another micro-injection moulded device for monitoring DNA migration, four holes were drilled in the lid, and platinum electrodes were inserted in the chambers afterwards and fixed in narrow slits [148]. Sputtering by using adapted shadow masks was used to generate electric thin-film electrodes of gold in an injection-moulded electrophoresis separation device [198]. Furthermore, in an injection-moulded device for DNA separation, electrodes of 76-μm-diameter wire were routed to each of the four reservoirs available and terminated at one edge of the chip with a four-prong 2.54-mm-pitch electric header [168]. Gold electrodes were also patterned over a hot-embossed polymeric diaphragm as a part of an integrated microfluidic device for protein analysis [195].

An example for the use of conductive ink printing is a hot-embossed microfluidic device for bacteria detection. Electrodes, with contact pads, function as capillary-electrophoresis driving electrodes. They were integrated by connecting them to high voltage via “pogo” pins. They were manufactured by screen-printing silver/graphite inks onto the polycyclic olefin support film. After being cured at 95°C for 2 hours, the ink pattern on its supporting film was aligned and thermally laminated onto the cover film of the device [174].

2.2.3.2.2 Microheaters

A common application for energy conversion is microheaters, where localized elevated temperatures are needed in specific places on the microfluidic chip, such as in the case of polymerase chain reaction (PCR) devices. In these devices, thermal cycles consist typically of two steps: a “denaturing” step at 95˚C and an “anneal/extend” step at 60˚C [211].

Installing a microheater on a microfluidic chip is currently done by post processing techniques, since it is technically difficult to integrate microheaters into micromoulding processes. This is because insert-moulding a microheater requires accurate alignment in each cycle, and there is possibility of malfunction in the microheater due to the high pressures associated with micromoulding.

Two examples were reported in the literature. The first example is the microheater used in the air-bursting detonator discussed in the previous section (Figure 2-12 above), where electric pulses were applied to heat the thermoplastic membrane causing it to melt and release pressurized gas [171].

The second example for using microheaters is PCR devices, where integrating thermal elements is essential for the function of the device. Heaters were integrated in PCR microfluidic devices produced by hot embossing by mounting electrical resistance heaters to the chip (Figure 2-14) [181,214].

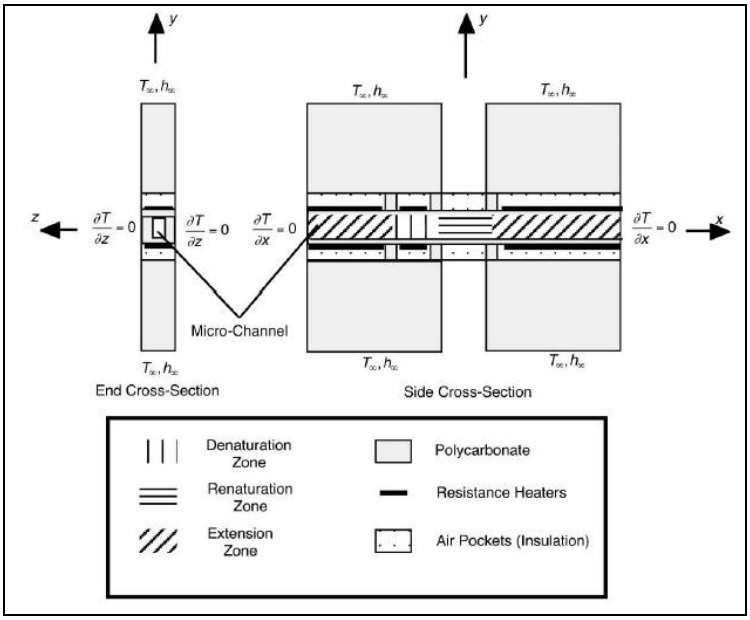

Figure 2-14 A schematic diagram of a microfluidic system with resistance heaters [214]

2.2.3.2.3 Electromagnets and optical fibres

Examples of integrating functional elements other than electrical parts also appear in the literature. For example, in a magnetic bead-separation device, an external electromagnet was integrated to produce the magnetic fields required for separation.

The magnetic forces acting on the beads were different depending on the bead size. For example, for a bead diameter in the order of tens of microns, the magnetic forces were in the order of thousands of pico-Newtons. Magnetic beads in the size of 2-9 μm could be separated from an aqueous solution at the flow rate of 3-7 μl/min [215].

Post-processed elements may also include optical fibres used for fluorescence excitation light. The optical fibre inserted was coupled to a laser fibre that was connected to a diode laser. The laser produced approximately 2.5 mW of power at a wave length of 750 nm.

Integrating detection fibres was used for a hot-embossed DNA separation device, where a dual fibre detector was inserted into the assembled device. The fibres were etched and sealed with epoxy [152]. Optical fibres were also integrated into a hot embossed microfluidic device for CE [216,217].

2.2.4 Integrated elements involving energy-to-information transformation functions

Few examples for integrated detection and measurement systems are presented in the literature. Thermocouples, for example, can be used to monitor the temperature variation on the microfluidic chip for PCR applications [181,214]. Micro-ammeters, of resolution down to 0.1 μA, were also reported to be used for current monitoring in micro-injection moulded devices for DNA separation [168]. However, the complexity of the detection process requires interaction between on-chip sensing elements, e.g. a thermocouple, and external, non-integrated, devices for recording and analysis. Therefore, energy-to-information elements should probably by identified as "interfacial" elements between what can be integrated on-chip and what is external to the system. More about non-integrated elements is discussed in the following section.

2.3 Non-integrated Functional Elements

This part of the review is concerned with presenting functional elements that are commonly used with microfluidic devices, yet not integrated on the chip. Non-integrated elements, often expensive and non-disposable, are connected to microfluidic

chips to perform relatively complex functions. Such functions are usually related to the input or output elements of the microfluidic system. Input elements, in turn, are usually associated with delivering the fluidic sample to the chip, and include inlet tubes and relevant connections. These input elements are tabulated in column 8 of Table 2. Output elements are associated with the outcome of the microfluidic system, such as detection and data analysis. These input elements are tabulated in column 9 of Table 2. A few non-integrated elements are used for both inputs and outputs, such as a power supply.

These types of elements are usually a source of the high costs often currently associated with microfluidic applications, a fact that limits many microfluidic devices to lab prototyping experiments rather than high-volume commercial purposes. The following sections present some of the commonly used elements.

2.3.1 Non-integrated elements involving energy-to-mass transformation functions

These elements are usually used for fluid propulsion systems, especially when energy is required for the fluid to either be able to balance capillary forces or to flow into different chambers in a specific sequence.

Several integrated devices covered within this literature review depend on external mechanical pumping equipment, e.g. syringes or pipettes. For example, a hot-embossed microfluidic device for magnetic bead separation was equipped with a syringe pump to deliver the beads in the form of an aqueous solution containing magnetic beads of three different sizes [215]. The same system was applied for an injection-moulded integrated microfluidic device for blood-typing, where the blood and the serum streams were pumped with two separate syringe-pumps to allow for different flow rates [33] (Figure 2-15).

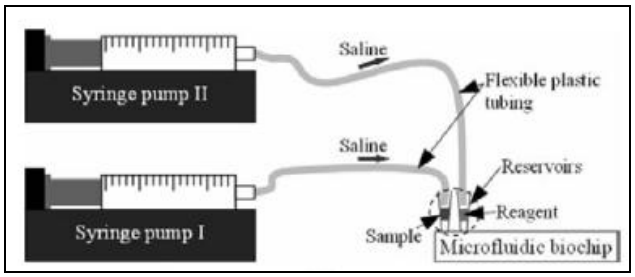

Figure 2-15 Schematic diagram for fluid propulsion system using syringe pumps [33]

In an injection-moulded device, syringe pumps were also used to control flow inlets in a microfluidic cross-junction to produce beads [106]. Computer-controlled syringe pumps were also used to control the flow of the sample in a micromoulded chip for monitoring of microarray hybridizations [146].

Vacuum pumping was also pointed out in the literature as a possible mechanical fluid propulsion system, where a vacuum-driven system was used in a modularly integrated hot-embossed device [170]. In another hot-embossed device for bacteria detection, vacuum was used to move the sample throughout the device [174]. In addition, vacuum pumping was used for moving blood cells across micro-channels in a micro-injection moulded device used for monitoring DNA fragments [148].

Centrifugation is a developing method for fluid propulsion, where reagents are preloaded in the chip, and centrifugal forces are used to trigger the fluid flow throughout the channels. In centrifugal pumping, fluid propulsion is achieved through rotationally induced hydrostatic pressure. It uses a single low-cost motor, and is capable of fine flow control through proper design of the location, dimensions and geometry of channels and reservoirs based on fluid properties. A device works by spinning a CD-format chip such that the centrifugal forces overcome the capillary forces and the fluid is pumped throughout the channels [155]. However, it should be noted that centrifugation is not only dependent on energy, because the design of the channels themselves play a role in the propulsion of the fluid. The usually-radial configuration of the channels (see Figure 2-4) in addition to the sizes of the different channels/reservoirs determines how the fluid will proceed.

An electric field has been applied through integrated electrodes in order to control voltage changes leading to particle separation by electrophoresis [153,218] or electro-osmotic flow [167].

2.3.2 Non-integrated elements involving energy-to-energy transformation functions

Power supply sources are commonly used to deliver electrical power to different functional elements on the chip. As mentioned previously, with integrated elements for energy-to-energy transformation (section 2.2.3), an external power source is needed to supply high voltages or to operate heaters. Electrophoresis microfluidic devices reviewed in this paper needed a source of high voltage either from lab-scale power supplies [148,150,152,154,168,174,219] or a voltage-control unit adjusted by an accompanying software [143]. Electric field values can be in the order of few tens up to few hundreds of volts depending on the application [220,221].

Power supply is also associated with temperature control, where microfluidic systems are required to operate under constant temperature. This can be done by a Peltier controller, for example [146].

2.3.3 Non-integrated elements involving energy-to-information transformation functions

Device elements performing energy-to-information transformation functions are usually associated with detection and inspection. As an example of a relatively advanced detection element, a detection system was designed in which a circuit converted the output signal from the biosensors to a voltage signal, which in turn was amplified, and the peak value detected and displayed [171] (Figure 2-16).

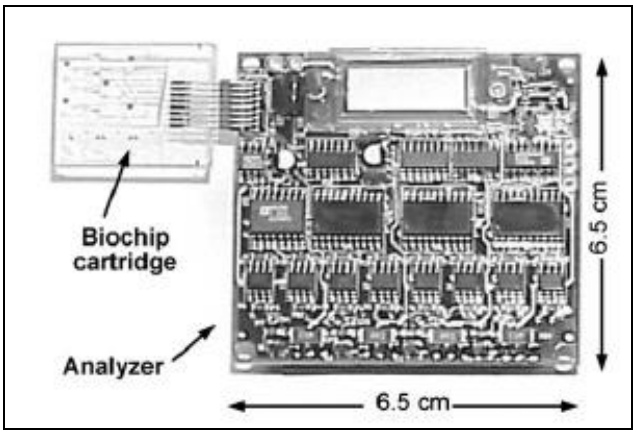

Figure 2-16 Biochip cartridge inserted into analyzer module for multi-parameter detection [171]

Inspection is essential for the majority of microfluidic applications, because it is usually required to observe the micro-scale motion of the fluid or to count specific particles.

Conventional microscopes are used to optically observe specific processes inside the microchannels. They can be used, for example, for monitoring cell movements [148]. CCD cameras were also used for monitoring sample movement in channels [154].

In other applications, especially in DNA separation processes, fluorescence is the most popular optical detection method for microfluidics due to its excellent sensitivity down to measuring single molecules [186]. A sensitive technique is often required because of the small sample volumes involved [8,173]. Off-chip fluorescence detection is typically accomplished through the use of lasers for the excitation of fluorescent molecules and CCD cameras or photomultiplier tubes for detection of the emitted fluorescent light [8]. Usually confocal microscopes are used for this purpose [148,150,181,219]. Laser induced confocal microscopes have been used in several microfluidic experiments mentioned in the literature [143,153,154,174,222]. Contactless conductivity detection was also proposed as a detection technique that overcomes some of florescence limitations. It was used within an injection-moulded system for measuring small ions in foodstuff [210].

2.4 Discussion

2.4.1 An overview of the current state of integrated micro-moulded microfluidics:

In this review paper, the current state of research was presented for integrated polymeric microfluidic devices produced by two micro-moulding techniques, namely micro-injection moulding and hot-embossing.

The classification system used in this review was intended to link the functional aspects of microfluidic devices together with the degree of integration allowed by current device fabrication techniques. It allowed the review of integrated microfluidic devices from a taxonomical perspective, by combining a physical functional

perspective, represented in the nine types of "transformation functions", with a manufacturing perspective, represented in integration technologies. This approach was summarised in Table 2-2.

The approach used in this paper gave an indication of the level of difficulty involved in integrating each of these generic components and the relationship of this to the elements' transformation function. For example, Table 2-2 showed that elements of relatively "simple" transformation function, e.g. mass-to-mass, are likely to be directly micro-mouldable (column 6), whereas other transformation functions appear to be currently not-integrated (columns 8 and 9). Most of the elements used for moving or storing masses of liquids, essentially the fluidic subsystem, are able to be incorporated into the chip as part of the operation of micro-moulding, though manifold designs for connection of the devices to the outer world still generally require off-chip integration.

It can be noticed that the majority of non-integrated elements are associated with energy-driven elements (fluid propulsion, for example) and with data collection and analysis. When energy or information are involved as inputs or outputs, the system becomes more complex in structure, because the current level of technology does not easily allow elements involving energy or information transformations to be incorporated into polymer-based chips. Therefore, non-integrated, non-disposable elements are usually needed to ensure the successful overall performance of the chip, with consequences in higher manufacturing complexity and higher costs. This is one of the major reasons why much of the current state of art of microfluidic chips is mainly confined to prototypes that are not easily mass-manufacturable.

Table 2-2 offered an overall summary of the *current* state of integrated, replicated, microfluidic devices based on thermoplastic high-volume processes. Hence, the blanks in Table 2-2 represent examples of one of two possibilities: either research gaps, or applications that are not yet needed. It is possible to separate the two by noting whether the application is currently achieved by non-integrated means. An example of the former is the mass-production of a fluid-propulsion system (energy-to-mass) that is fully integrated in a microfluidic system. This requirement is currently met only by non-integrated syringe pumps and centrifugal forces. An example of the latter is the mass-production of a mass-to-energy system, where there is no indication in the literature of a non-integrated system having been developed.

In this regard, several transformation functions were not discussed in the review as no integrated or non-integrated examples were found in the literature. These are highlighted by the blank rows in Table 2-2. These were mass-to-energy (as noted above), mass-to-information, information-to-mass, information-to-energy and information-to-information.

The classification method was limited to the transformation from *one* basic element to another. Therefore, elements that have multiple inputs or outputs were not presented in Table 2-2. Very few examples of multiple input and output functions exist in the literature. However, those that do exist are worth highlighting, because of their relatively level of sophistication. The main example is that of active micro-valves.

The classification method, represented in Table 2-2, was mainly directed to the viewpoint of a "designer" wishing to design a microfluidic system consisting of a set of integrated functions, which, at the same time, would be producible by high-volume polymer replication processes. However, for a manufacturer, the focus might be mainly on the integration technique, i.e. *how* to integrate an external element by high-volume processes.

To attempt to satisfy such a requirement, Table 2-3 tabulates the literature using integration techniques rather than integrated functions as the basis of tabulation. (It therefore, does not include the literature on non-integrated techniques.)

If the volume of literature references can be taken as a guide, then post-processing appears to dominate integration techniques. On-machine assembly is relatively common, followed by direct integration, with modular integration represented by a small portion of the literature.

However, it should also be noted that some integration methods that are used as established techniques for conventional injection moulding have not yet been developed for micro-moulding. Three-component moulding, for example, is used on the conventional scale to integrate a number of elements in a single moulding cycle using a special mould system fitted with a robotic system [223].

Integration Technique	Applications	Ref.
• Direct integration of fluid-manipulation functions within the mould design	Integrating microfluidic systems, CD-like designs, passive valves and moulded interconnections.	[33,155,171,174,183]
	Passive valves	[155,171]
	Moulded interconnects	[141]
• Modular integration	Integrating microfluidic systems by lamination or modular kits	[166,170,171,193]
• On-the-machine assembly [157]:		
- Micro-assembly injection moulding	Integrating movable joints, hollow structures	[79,80,82]
- In-line sealing	Sealing the microfluidic system directly during micro-moulding	[40]
- Micro-overmoulding	Integrating fibres and wires or integrating interconnects.	[80,156,157,182,206]
• Post processing	Sealing the microfluidic device	[5,38,106,145,152,154,168,198]
	Interconnections by ports or drilled holes	[106,140,169,170,179,181]
	Adding external functional elements, such as electrodes, micro-heaters, magnets and optical fibres.	[148,152,168,174,181,198,213-215]

Table 2-3 An example of a classification method based on integration technique

2.4.2 Potential developments from a low cost, mass manufacturing viewpoint:

As has been shown in this review, micro-moulding techniques have gained increasing interest as low cost manufacturing solutions for integrated microfluidics. Figure 2-17 shows a schematic diagram of the degree of integration in micromoulded microfluidics based on the reviewed literature. The figure, which presents Table 2-2 from another viewpoint, shows that micromoulding technologies are still far from realizing fully integrated microfluidic systems capable of covering the required range of transformation functions. This is due to a number of challenges that are discussed below.

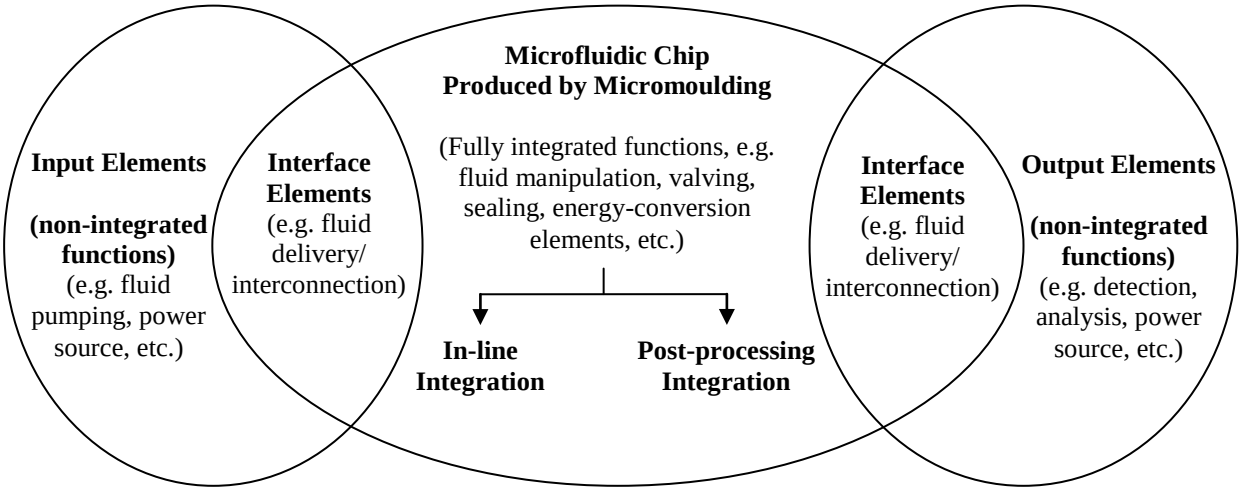

Figure 2-17 A schematic diagram showing current state of technology regarding the production of integrated elements within micromoulded microfluidic devices

2.4.2.1 Geometrical constraints for microfluidic subsystems

Micromoulding has become an established technique for producing microfluidic chips with generally passive integrated functions, such as channels, passive valves and dispensers. However, it is noted from the reported examples discussed in this review that almost all the devices are based on a 2½-D design, which is the simplest geometry producible by injection moulding or hot embossing. This is due to the conventional parallel-movement design of the two platens typical for net-shape manufacturing techniques, which limits the complexity of the manufacturable geometry. In order to produce true three-dimensional geometries with cavities or undercuts, modular lamination is the currently used method. Despite of the number of advantages that such "modular" designs might offer, such systems require additional fabrication steps for bonding or connection. Accurate alignment of different stacked layers can also be challenging. In addition, there is an added cost arising from using frame systems and inter-layer connections.

2.4.2.2 Energy-conversion functional elements

Post-processing is currently the dominant technique for integrating such elements, but this is time consuming and a considerable bottleneck in mass-production. In addition, they are main sources of raised manufacturing costs, knowing that back-end

processing steps can make up to 80% of the device manufacturing cost [160]. In order for microfluidic devices to perform more sophisticated processes, more functional elements will need to be integrated in an efficient manufacturing process. Micro-overmoulding and micro- insert-moulding are solutions currently under investigation. However, these techniques would require considerable automation to place, accurately, the inserted element in the mould each cycle.

2.4.2.3 Sealing micro-fluidic devices

Sealing is usually attempted by face-to-face bonding or by adhesives. Several techniques are being established for connecting polymers to similar or dissimilar polymers or to other materials. Nevertheless, sealing is also a process bottleneck from an industrial perspective, because of the time consumed in sealing individual devices and the difficulty encountered in bonding polymers.

In-line sealing has been described, very briefly, within the literature for micro-injection moulding, and remains a challenge for further research. The main advantage of this technique is that it integrates the sealing process in the fabrication cycle making the manufacturing cycle time of the whole device acceptable. The automation of the process can result in accurate alignment and control over bonding parameters such as time and force. In addition the process eliminates the use of external adhesives or back-end processes.

Nevertheless, this technique uses special machine designs and setups in order to undertake the covering process. Furthermore, in cases where it is desired to have the substrate and the lid from different materials, the process will be more complex: two different injection units will be required. This is perhaps the reason why this technology has not yet seen wider adoption.

2.4.2.4 Fluid delivery to the device

Most of the available interconnection solutions are either not suitable for mass-production, for example drilling and gluing, or too expensive, for example self-adhesive ports. Fluid delivery can be improved by designing a fitting system that can be moulded together with the device substrate (or lid) to allow standard tubes to be attached more easily and securely. However, it is relatively challenging to replicate ports with internal or external threads via plastic replication techniques because of geometrical complexity

associated with undercuts and because of the elongated cycle time. Overmoulding is currently being tested as an interconnection technology, and it has the potential of producing a microfluidic substrate where tubes are inserted in the mould and the polymer is injected over them, sealing in place by overmoulding.

2.4.2.5 Fluid propulsion

Fluid pumping is generally still performed by off-chip sources or at least with the interaction of external elements, because energy-to-mass functions currently require external sources of energy. Pre-installing the required reagents and using capillary motion are suggested alternatives, unless a continuous-flow system is required for specific applications. In mass-production environment, a fluid propulsion element could be manufactured externally, such as air-pressure pumps, and then integrated as an insert within a moulding process.

2.4.2.6 Fluid control

With regard to fluid regulation, many valving options have been developed for fluid control in microfluidic devices. Active valves form the majority of types and mechanisms, but very little is available in the literature about using active valves within micro-injection moulding or hot-embossing techniques. Passive valves are more promising in terms of manufacturing integration and cost, since several types of them can readily be produced by micromoulding. Passive valves, nevertheless, are not suitable for all applications, and they need further development for applications where more complex flow patterns are required.

2.4.2.7 Data collection and analysis

Some innovations have been achieved in detection techniques for POC applications [224]. However, detection and analysis systems are likely to remain as non-disposable elements, for the near future, because of the cost and manufacturing complexity associated with them within the currently available technology.

A current trend to overcome this limitation is to integrate relatively-cheap disposable chips with non-disposable, but portable, analysis elements. Several research groups are currently testing the use of a “cartridge” approach, where a disposable chip,

either micromoulded or glass-etched, is inserted and operated within a non-disposable, but portable, analysis system [171,225].

The "wristwatch" example is a step forward in this direction. In this system, a disposable chip is inserted and accessed by a portable watch-like analysis device (see Figure 9). The disposable chip is designed to be inserted into the analyser unit where the microfluidic sequencing is initiated by a trigger signal from the electronic controller. The electrochemical detection circuitry on the analyser is used to determine the concentration of different analytes [171]. The same principle has been recently developed for testing metabolic parameters in human blood with a micromoulded disposable chip and a portable analyser [196].

This approach to integration, despite being a practical solution within the currently available technology, has some limitations. It makes use of the disposability and low-cost offered by micromoulding, but it still requires the availability of relatively costly equipment to analyse the collected data. Moreover, very precise positioning and alignment is required between the chip and the analyser system in order to ensure robust contact between their interactive elements, such as electrical components and valves. As suggested in the literature, having the microfluidic chip as just a small part of system in which sample introduction and detection are much more complicated than the chip's operation may be appropriate in some circumstances, but does detract from the potential advantages of microfluidic devices [56].

2.4.2.8 Power Sources

Some examples of power source solutions were presented in sections 2.2.2 and 2.3.2. The majority of the review literature presented conventional sources of power, either main power-supply or batteries. Some examples have been shown where air-pressure or chemical reaction can be used as powers source for fluid propulsion, but even these systems require the existence of an external power source, like a battery, to trigger the release of air or chemical reagents. Power generation is, therefore, likely to remain a non-integrated functional element until more convenient integrable solutions are developed.

2.5 Conclusion

This paper aimed to critically review the state-of-the-art of technology for producing integrated polymeric microfluidic chips by high-volume micromoulding techniques. In this regard, micro-injection moulding and hot-embossing were chosen as the replication processes covered in this review.

The current state-of-the-art of integration of functional elements into moulded polymer microfluidic devices was assessed. Levels of integration were classified by two methods. Firstly, by "transformation function" of the element, i.e. transformations between mass, energy and information. Secondly, by the current level of integration of these elements into microfluidic devices, whether integrated via moulding, by post-processing or, as yet, not integrated. The review gave detailed examples of elements used to perform the transformation functions and their current level of integration.

The review showed considerable differences between the level of integration of elements, dependant on the elements' transformation function. In particular, non-integration was found for elements with either energy-driven, or data collection and analysis transformation functions. At the present time, analysis systems with disposable microfluidic cartridges, represent the state of the art for the latter. Certain transformation functions, for example mass-to-energy showed no elements currently under development.

The review also assessed the options for integration of elements by such high volume processes. Post-processing appeared relatively common, followed by on-machine assembly, direct integration and then modular integration.

Potential developments in several key areas were assessed. Overmoulding, insert-moulding and in-line sealing all have potential for improving the direct integration of elements.

3 Micro-injection moulding: A review of process capabilities and limitations as a three-dimensional microfabrication technique

3.1 Introduction

Since its early development more than a decade ago, micro-injection moulding (μIM) has evolved to be one of the most promising 3-D microfabrication technologies. High-volume capacity, dimensional accuracy and replication fidelity are some of the process advantages. In addition, the wide range of mechanical, chemical and optical properties of polymers provide extra opportunities for industries working in different applications (Please refer to section 1.1 and subsections for more details).

The ability of the process to produce 3-D features and structures is particularly important as it adds more potential to the process as a technique for mass-producing disposable micro-scaled or micro-featured components with relatively complex geometries.

Three-dimensionality, in particular, is a significant aspect for microfabrication for a number of reasons:

- Three-dimensional features offer a higher degree of design flexibility beyond the limited conventional 2-½D structures. Free-form shapes for example are possible to produce, unlike, for example, lithographic techniques.
- Three-dimensional structures increase the interface area between the component and the outer world. For microfluidics, for example, 3-D structures have more flexibility in terms of interconnection with surrounding equipment.
- Three-dimensional structures optimise the use of space to integrate more functionality or increase throughput. This is evident in, for example, microfluidics, where transforming conventional 2½-D designs into truly 3-D devices could render higher throughput within a constrained volume [226].

This paper aims at assessing the capabilities of μIM as a microfabrication technique for producing 3-D features and structures. The paper reviews the two basic stages of the process chain: mould fabrication and polymer replication.

Section 3.2 aims at addressing design and manufacturing consideration for 3-D micro-structured moulds. The concept of 2½-D versus 3-D structures is discussed, and the essential requirements for designing micro-structured mould inserts in presented.

Section 3.3 focuses the scope of 3-D manufacturing on injection moulding as a well-established, net-shape manufacturing technique. Designing for µIM is addressed, where the main differences between micro- and conventional injection moulding are highlighted. The discussion covers design guidelines for both 3-D features and structures on the micro-scale.

3.2 Mould design and manufacturing for µIM

Injection moulding belongs to a category of processes known as net-shape manufacturing (NSM), where the geometry of the part is produced by setting a specific volume of material to replicate the shape of a die. Similar to other NSM techniques, the manufacturing chain of µIM starts with fabricating the mould. The capability of µIM to produce 3-D features is dependent on introducing these features into the mould using a 3-D microfabrication method. The following sections address critical issues for designing and manufacturing moulds for µIM of 3-D components.

3.2.1 Microfabrication of three-dimensional features

3.2.1.1 Background

In the literature that deals with microsystems technology, it is not uncommon to find authors describing their designs or manufacturing techniques as "three-dimensional". This is usually mentioned in the context of highlighting a development in a design or technology beyond the conventional "flat", also called 2½-D, systems rooted to the silicon industry. However, what three-dimensional manufacturing in general actually indicates is rarely discussed, as is whether it refers to specific "features" or a whole component. *Features* were defined in different ways, which can be accessed in the literature [227-229]. In this context, they refer to prototypical shapes with some engineering significance or meaning [229]. A *structure* or a *component* refers rather to a combination of features that constructs a whole, self-contained system.

In dictionary definitions, two-dimensionality refers to flatness [230] or the state of lacking the illusion of depth [231]. Three-dimensionality refers to the state of having length, depth and height [230] or generally having three dimensions [231]. Two-and-a-half dimensionality (2½-D) is a term that was introduced in the machining field to help in classifying shapes and cutting processes as discussed in the following sections.

The term "2½-D" originated in the machining industry to refer to what was apparently the simplest geometrical shape to be fabricated with basic machining capabilities in terms of the number of motion axes and the shape of cutting tools. In spite of the fact that the term has been used by a number of researchers to define the geometric domain of the parts, its precise definition is not complete [232] and the available definitions are sometimes unclear [233].

The increasing interest in computer-aided manufacturing (CAM) demanded more rigorous criteria for classifying geometrical shapes into 2½-D and 3-D, so that computer codes can be generated for machining steps and sequences [232].

3.2.1.2 Geometrical classification of conventional, "macro" features

Machined parts are sometimes classified as rotational or prismatic [232]. The latter type are parts machinable on milling type machine tools, and they can be further classified as 2½-D or 3-D, based on geometrical complexity and the machining requirements of the part [232].

An early definition of 2½-D parts was published describing them in general terms as "a class of components which have planar and cylindrical faces as orthogonal sets, such that features are a product of a 2-D profile swept through a linear distance along an axis normal to their plane" [234]. Despite appearing detailed enough to cover all classes of 2½-D geometries, this definition did not specify issues such as whether, for example, a multi-faced part will be defined as 2½-D.

A more elaborate classification highlighted that fact that the characteristics of 2½-D components are related to the *approach direction* of the cutting tool, which needs to be determined early enough to select the setup of the component. This implied that specifying whether a specific component is 2½-D or true 3-D is a factor of its orientation [233].

Later literature sources attempted to specify a more rigorous definition of 2½-D components, which can be used as a base for knowledge-based systems (KBS) used in computer-aided engineering applications. A proposed classification specified 2½-D components as "components that can be produced on a 3-axis NC milling machine using three pairs of orthogonal tool approach directions. Such components consist only of planar and cylindrical faces in orthogonal sets such that all machining features are a product of a 2-D profile swept along the tool approach direction. It is possible to extend the definition to cover components comprising of a number of 2½-D facets, i.e. "multi-faced 2½-D" [235].

This definition sets four conditions for 2½-D geometries. Hence, if any of them is violated, the component is a true 3-D one. Violations can be one or more of the following:

- Any sloping faces to the approach direction. The approach direction is the direction in which the tool approaches the part (usually –z direction in CNC machines). The component must consist of only planar faces either perpendicular or parallel to the approach direction.
- Any cylindrical faces with their axes not parallel to the approach direction. Inclined cylindrical faces are not possible to for a machine with three orthogonal axes.
- Any other non-planar faces. This means that free-form faces, for example, are not allowed.
- Any blind horizontal faces. Blind faces refer to undercuts or overhanging features, and the horizontal face in this context is the face perpendicular to the approach direction (undercuts are discussed in more detail in section 3.2.2).

The above 4 conditions implied that, firstly, multi-faced 2½-D components are *not* considered as 3-D components (Figure 3-1 [a] and [b]). Secondly, the shape of the cutting tool does not affect the classification of the component as a 2½-D component, so slope-faced components produced by the shape of the cutting tool still belong to the 2½-D category. Thirdly, true 3-D components can be realized by assembling different 2½-D components. Finally, 2½-D shapes are based on rotational cutting tools, so internal sharp corners parallel to the approach direction of the tool violates this condition (Figure 3-1 [c] and [d]).

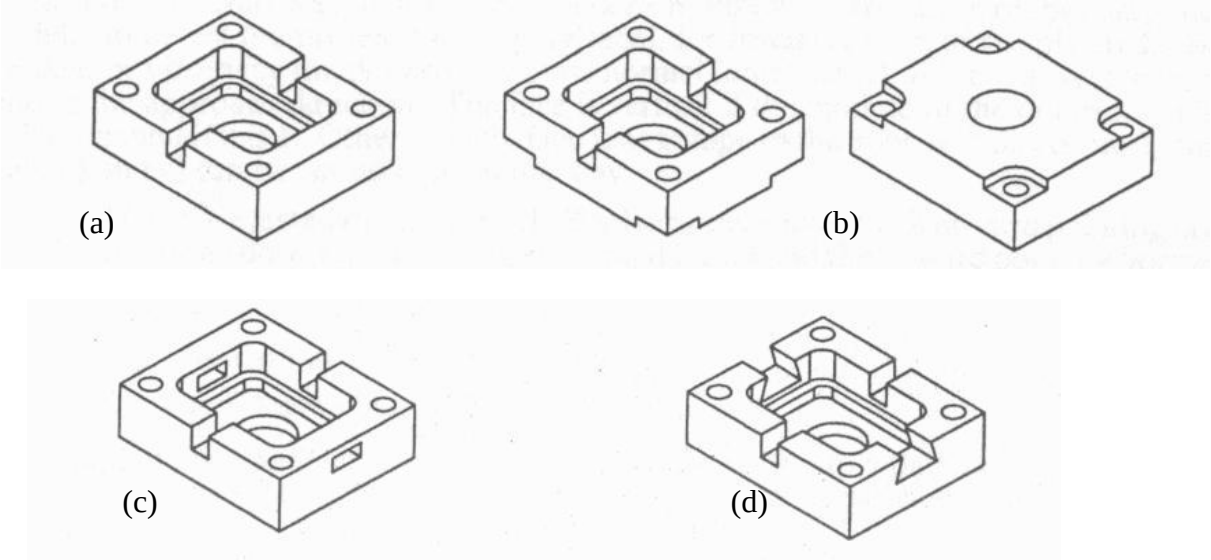

Figure 3-1 (a) One-sided 2½-D component. b) Double-sided 2½-D component. (c) A true 3-D component due to the two side sharp-cornered "windows". (d) A true 3-D component due to the sharp corners of the two inclines slots. [235]

A more recent definition of a 2½-D component was developed for automatic shape recognition [232]. It specified 2½-D parts as "a range of objects that can be machined on a three-axis CNC milling machine from a maximum of three mutually orthogonal tool approach directions and their opposites (also called aspect vectors), and by using standard flat-bottomed end-milling cutters and standard clamping devices such as vice-clamp, a strap clamp and a bolt clamp" [232]. The definition, in principle, is similar to the previous one except that it excludes the inclined faces produced by the tool shape from the 2½-D category.

3.2.1.3 Geometrical classification of microfabricated features

Classifying geometries on the micro scale is, in some aspects, different from conventional components. Geometrical classification of conventional "macro" components originated essentially from three-axis machining. For micro-components, on the other hand, classification was based on microfabrication methods widely used in the silicon industry, where lithographic techniques were used for fabricating semiconductors. Such microfabrication techniques resulted in "flat", chip-like components, which are essentially two-dimensional planar features extruded over a certain thickness in a direction normal to the plan.

Unlike conventional manufacturing methods, microfabrication techniques are not necessarily based on rotating cutting tools for material removal. Instead, other chemical and thermal principles are widely applied. This makes defining 2½-D microfabrication processes rather flexible relative to conventional machining. For example, such processes are sometimes defined as ones capable of producing any 2D structure that has a finite depth [236].

Based on this understanding of 2½-D structures, any process that can overcome the limitations of semiconductor-rooted techniques, by producing free-form or contoured surface features for example, is a three-dimensional process [237]. Figure 3-2 shows an example of a microfluidic device carrying both 2½-D (prismatic) and true 3-D (pyramidal) features.

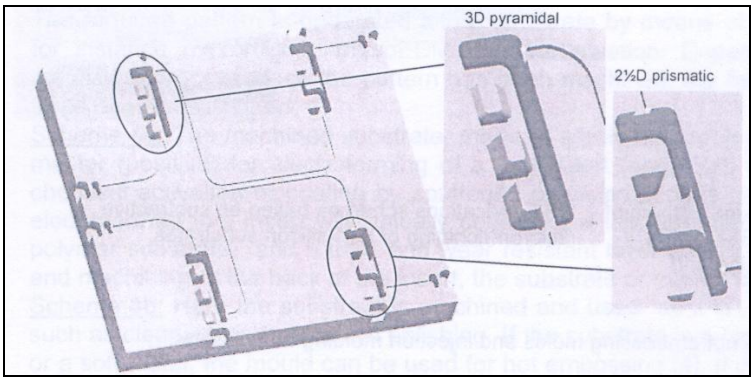

Figure 3-2 A microfluidic device with 2½-D and 3-D microfeatures [76]

Micro-scaled 3-D structures were realised when processes from the precision engineering domain where introduced [238]. The variety of energy sources involved in removal or addition of materials include [239] mechanical, chemical, thermal, electrochemical and electrothermal sources, a range that resulted in various microfabrication methods with different geometrical capabilities. For example, 2½-D processes, such as photolithography, etching and electro-disposition are limited to producing flat, straight-walled structures. 3-D processes, on the other hand, such as laser machining, micro-electrodischarge machining (μ-EDM), micromilling and micro-grinding [76,240] produce relatively more complex geometries. Table 3-1 [76,239,241,242] compares the capabilities of common micro-manufacturing techniques with respect to the type of geometries they can produce and common materials.

Process	Geometry	Typical material
Micromilling	3-D	Metals, polymers
Diamond turning	3-D	Aluminium, copper, gold and silver
Ultrasonic micromachining (USM)	2½-D	Fragile and porous, e.g. silicon and glass
Laser micromachining	2½-D	Metals, polymers, ceramics and glass
Ion and electron beam	2½-D	Polycrystalline Silicon
Micro-stereolithography (μ-STL)	3-D	Specialised polymer resins
Micro Electrodischarge machining (μ-EDM)	3-D	Hard and brittle materials for tool making
Chemical forming (deposition)	2½-D	Silicon and copper
LIGA	2½-D	Nickel, gold and ceramic
Photoresist	2½-D	SU-8, polyimide
Advanced Silicon Etching (ASE)	2½-D	Silicon

Table 3-1 A comparison between common microfabrication techniques in terms of geometry

It should be noted that the geometrical classification in Table 3-1 is based on the common, well-established capabilities of the processes. Some of the 2½-D processes are under development to produce 3-D features, for example LIGA and electron-beam lithography [243], but the process is not yet established for this purpose. Hybrid tooling [78], i.e. the combination of more than one microfabrication method, is another approach for producing 3-D features making use of the advantages provided by individual microfabrication techniques. Reviews of three-dimensional microfabrication processes could be found in the literature [239,242,244].

3.2.2 Ejection considerations in mould design for μIM

Ejection or demouldability refers to the separation of the plastic part from the mould. It is a basic design challenge in injection moulding, since it affects the design of both the plastic part and the mould. Fundamental examples of such design considerations include the location of the parting line of the mould relative to the mould-opening direction, tapering of vertical surfaces that need to be separated from a core and possible undercuts that might prevent the separation of the part from the mould [245].

A number of references and handbooks offers design guidelines for part ejection of conventional injection moulding [245-247]. The same design principles are usually applicable for μIM. For example, draft angles of ¼° were suggested as a method to facilitate demoulding of micro-structured channels [39]. Another recommendation for demouldability in μIM is the development of extremely smooth side walls to avoid

friction of form-locking (shearing or ripping of the part) during demoulding [61]. It should be noted, however, that introducing draft angles requires either a three dimensional process or a cutting tool that is shaped to the required inclination.

In addition to draft angles, recent research has started focusing on the effect of surface properties on ejection in μIM. For example, the effect of process parameters on ejection forces in μIM under different surface-treatment conditions was investigated [75]. The surface properties of micro-moulds affects not only the ejection forces but also the flow behaviour of the polymer during the injection process, as will be discussed in the next section.

Recent developments have been achieved in designing an ejection system for μIM that are based on ultrasonic vibrations [248]. The new system is claimed to overcome the limitation of conventional ejection pins, such as limited spacing and surface markings. In addition, a number of techniques were developed for demoulding in μIM, such as guided retraction, vacuum assisted and ultrasonic assisted demoulding [249].

A critical aspect of demouldability is the existence of undercuts (also referred to as overhangs or blind faces). Undercuts are defined as elements that prevent either the core mould half from being extracted after the component has been formed, or the component from being ejected out of the cavity. Undercuts are either external, i.e. surfaces of the component project onto one another, or internal, i.e. surface of one half of the mould project onto one another. Undercuts can either be simple or compound (Figure 3-3) [60].

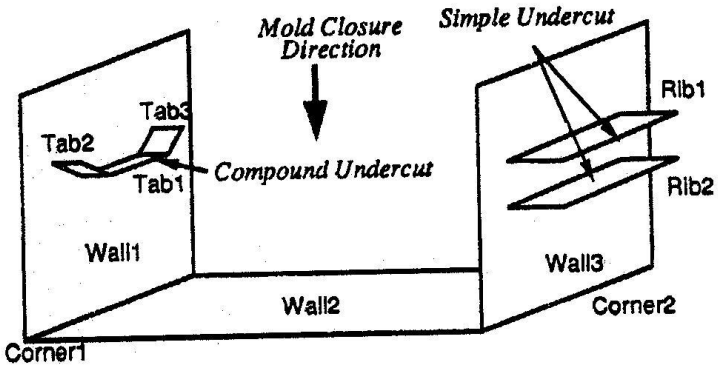

Figure 3-3 Simple and compound undercuts [60]

For conventional moulding, the use of sliding cores or complex parting surfaces, for example, is a common practise for moulding shapes with undercuts. With special design and material considerations, undercuts might be introduces into moulds and be overcome by the demoulding forces of the ejection system [246].

On the micro-scale, such approaches are not yet developed as established methods, and will significantly add extra costs to the manufacturing process. A few experiments were reported on micro-moulding complex 3-D shapes using, for example, lost-core technology [79,80], but this method is still in its early stages.

3.2.3 Mould surface properties in μIM

A basic difference between conventional and micro-injection moulding lies in the principles governing the filling of the mould cavity during processing. While the general viscoelastic polymer-melt behaviour is similar in both cases, more surface-related factors appear to interfere with flow behaviour on the micro-scale.

Surface roughness, for example, started to receive more attention in the literature as a factor for better mould filling. The effect of surface roughness on cavity filling during μIM was investigated [250]. It was shown that increasing the mould roughness whiles keeping the process parameters constant reduces cavity filling. In addition, increasing the mould temperature resulted in decreasing the effect of surface finish.

In another experiment, the effect of mould surface finish on melt flow in μIM was investigated for PP, ABS and PC [91]. It was shown that the flow length for PP was less susceptible to tool surface quality than PC and ABC. It was also shown that suface finish affects the turbulence of flow for all the materials.

Numerical simulation attempts were also made to investigate the effect of surface roughness on mould filling in μIM [251]. It was shown that cavity roughness does resist polymer melt flow during the filling process, but the significance of roughness is dependent on other parameters, such as mould and melt temperatures, cavity thickness and injection velocity.

The effect of other surface-related properties, such as surface tension [252] in μIM was also investigated. Although relatively little information is currently available in the literature about surface properties in μIM, it is gaining more research interest.

3.2.4 Dimensions, tolerances and aspect ratios

Producing moulds with microfeatures requires careful investigations of the required geometry in terms of dimensions, tolerances and aspect ratios. The selection of a microfabrication technique affects not only the type of the geometry (in terms of being 2½-D or 3-D), but it also limits the selection of dimensions and aspect ratios.

Table 3-2 presents a comparison of common microfabrication techniques compiles from different sources [76,239,244].

Process	Feature Accuracy [µm]		Min. channel width [µm]	Max. channel depth [µm]	Max. Aspect ratio	Roughness Ra (µm)
	X-Y	Z				
Photoresist processes	2	1-5	5	200	20	-
ASE	5	1-5	10	500	10	-
Micromilling	Depends on material and feature	3-10	20-200	Depends on the tool diameter	7.5 for holes and pins; 10-15 for channels	0.3
Laser micromachining	1-20	3-10	20-200	-	7.5	0.1
Micro-EDM	1-3	-	50-150	-	10-50	0.4-0.5
LIGA	1	-	-	100 up to 1 cm	100	0.02
Electrochemical milling	2	-	0.2-10	-	10	-

Table 3-2 A comparison of microfabrication techniques in terms of dimensional properties

When it comes to tolerances, designing the mould dimensions should take into consideration possible changes in shape due to e.g. shrinkage.

3.3 Part design for µIM

Injection moulding of both macro- and micro-components, similar to other net-shape processes, replicates the features made into the mould, which include 2½-D and 3-D features. It is classified as a 3-D process in the sense that it can replicate 3-D features of a mould, such as free-form shapes, which are usually fabricated by one or more of the fabrication processes listed in Table 3-1. Figure 3-4 shows an example of injection moulded 2½-D and 3-D models for a self-locking orthopaedic fastener [253].

The 2½-D design consisted of the 2-D shape extruded over a vertical distance, whereas the 3-D design has inclined walls and possible internal undercuts.

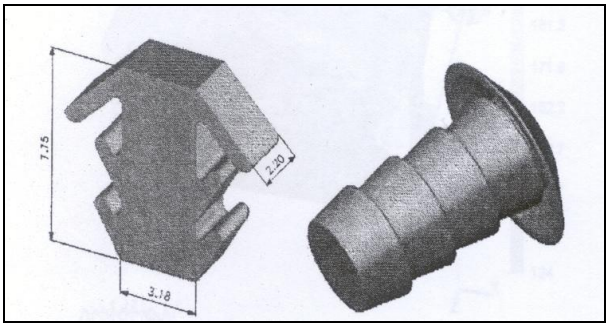

Figure 3-4 2½-D and 3-D models for a self-locking fastener produced by conventional injection moulding [253]

3.3.1 µIM of 3-D features: designing for manufacturability

Being a variant of conventional injection moulding, µIM follows similar design rules to the conventional process. As discussed earlier for moulds, design issues related to part demouldability, such as parting-line location and undercuts are essentially common on both scales. Some design aspects are, however, specific to µIM due to the manufacturing scale of the component. The following sections discuss part-design element specific to µIM.

3.3.1.1 Flow behaviour

The essential difference lies in the principles governing the filling of the mould cavity during processing. While the general viscoelastic polymer-melt behaviour is similar in both cases, more factors appear to interfere with flow behaviour on the micro-scale. Surface tension [252], mould surface roughness [91], high shear rate in micro-scale cavities [87] and wall-slip [77] are examples of physical parameters that become of more significance to flow on the micro-scale [254]. For this reason commercial simulation packages developed for conventional moulding lack accuracy when describing the filling behaviour on micro-scale [107,125,127]. These differences in filling behaviour between conventional and micro-moulding also affect the morphological structure of the produced parts [255].

3.3.1.2 Minimum dimensions and maximum aspect ratios

Section 3.2.4 discussed the limitations of microfabrication techniques in terms of dimensions and aspect ratios. The same issue is important when considering replications of such features, because μIM has limitations in terms of the filling of micro-scaled features. In addition to the actual dimensions and aspect ratios of the mould, factors such as the process parameters and material type play a significant role in the filling process. Section 1.2.2 presented a detailed discussion about the capabilities of μIM in terms of minimum dimensions and maximum aspect ratios.

3.3.1.3 Shrinkage and shape stability

Sources of shape changes, such as shrinkage and warpage, are due to the thermal history of the moulded part. They affect the part dimensions and, hence, could influence the tolerances of feature dimensions. Shrinkage not only affects the part dimensions but also the demoulding of the part due to stresses induced upon contraction [3]. Some experiments focused on minimising shrinkage in micro-moulding by, for example, increasing holding pressure [4] or increasing cooling time.

Warpage, on the other hand, results from non-uniform shrinkage of the component due to residual stresses induced by the cooling of the polymer [61]. For components with large substrates relative to features, such as microfluidics, warpage becomes an important consideration to ensure part flatness, for example for subsequent sealing. The flatness is usually affected by, for example, the flatness of the replicated mould itself [62] and the processing parameters [61,63].

3.3.2 μIM of 3-D structures: overcoming process limitations

The previous discussion about three-dimensionality was mainly focused on "features". Increasing demand for complex micro-components, however, puts requirements on 3-D "structures" rather than just features, where truly 3-D structures or devices can be made by μIM containing, for example, integrated functional elements or a number of 3-D features, such as hollow cavities or complex channel networks.

For such requirements, extra integration processes would be required beyond the conventional replication. μIM would be useful in terms of its high-volume and

dimensional accuracy capabilities to produce “building blocks” of a 3-D structure. Subsequent assembly processes would be needed to join the replicated process into full 3-D structures.

A number of examples of such a 3-D assembly approach were reported in the literature, focusing basically on lamination of replicated layers to construct true 3-D microfluidic structures out of 3-D or 2½-D featured layers. This multi-layer approach was adopted not only for micro-injection moulded polymeric devices but for 3-D devices of different materials and via different processing technologies. 3-D microfluidic laminates were constructed out of, for example, paper and tape [256], laser-cut thin-film plastics [257], by soft-lithography of elastomers [258] and as multi-material layered microfluidics [259,260].

When it comes to μIM, a few 3-D laminate structures have been tested for different applications. For example, a lab-on-a-chip (LOC) device was designed for detecting metabolic parameters [171,190], where layers of micro-moulded thermoplastics were fabricated and joined by thermal fusion (Figure 3-5). A number of design considerations for 3-D multilayered polymer structures were discussed in the literature [199].

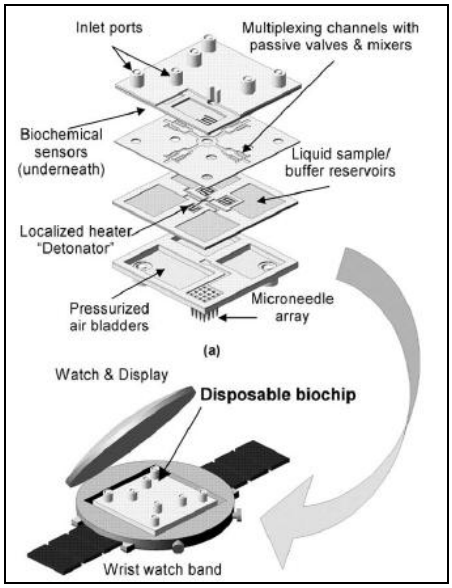

Figure 3-5 Multilayer disposable plastic biochip consisting of laminated microfluidic chips [171]

Lamination has proved to be an effective approach to overcome the geometrical limitations of μIM. As mentioned in section 3.2.2, new approaches have been developed to realise 3-D structures, such as hybrid micro-moulding and lost-core techniques, but such technologies are still in their early stages.

3.4 Discussion

Micro-injection moulding has the capability of producing 3-D features and structures at mass-production scale. The similarity between conventional and micro-injection moulding makes it possible to generalise most of the design principles on both scales. Some design aspects are as yet specific to μIM due to the physical effects that interact with the moulding process at the micro-scale.

Being a relatively new microfabrication process, μIM is continuously developing in both areas of tool making and replication. Rigorous design rules for moulding 3-D micro-components have not been developed yet. Most of the design recommendations available in the literature are specific to particular case studies, and they focus on individual aspects of design rather than presenting generic design-for-manufacturing rules.

The following discussion will focus on developing basic design guidelines for μIM of 3-D components. The guidelines are presented in the form of a flowchart, which aims at assessing the feasibility of producing a specific 3-D component by μIM. The outcome of the chart would be to decide whether the component is directly manufacturable by μIM, the component can be manufactured by μIM but will require considerable post-processing or an alternative process should be sought.

As discussed in sections 3.2 and 3.3, assessing the manufacturability of a 3-D component involves two main "checkpoints":

- A conventional two- or three-plate mould can be made for the component.
- The component is replicable by μIM.

The proposed flow chart aims at ensuring that the two conditions are fulfilled. If both are fulfilled, the component is directly manufacturable by μIM. If one or both

requirements are not fulfilled, modifications on mould design and/or part design are necessary.

Modifications in mould design could be on the feature level, such as changing dimensions and aspect ratios, or they could be on the mould mechanism level, such as introducing cores or moving parts. Modifications related to the replication process involve, for example, changing dimensions, aspect ratios, optimising process parameters or changing the material.

If the geometry of the component is too complex to mould in spite of suggested modifications, it might be necessary to consider producing the component as an assembly of relatively simple mouldable constituents. This would require considerable post-processing, which should add extra time and cost to the production process.

Figure 3-6 presents a flowchart that could be used as a guideline for assessing the manufacturability of a specific 3-D component by μIM.

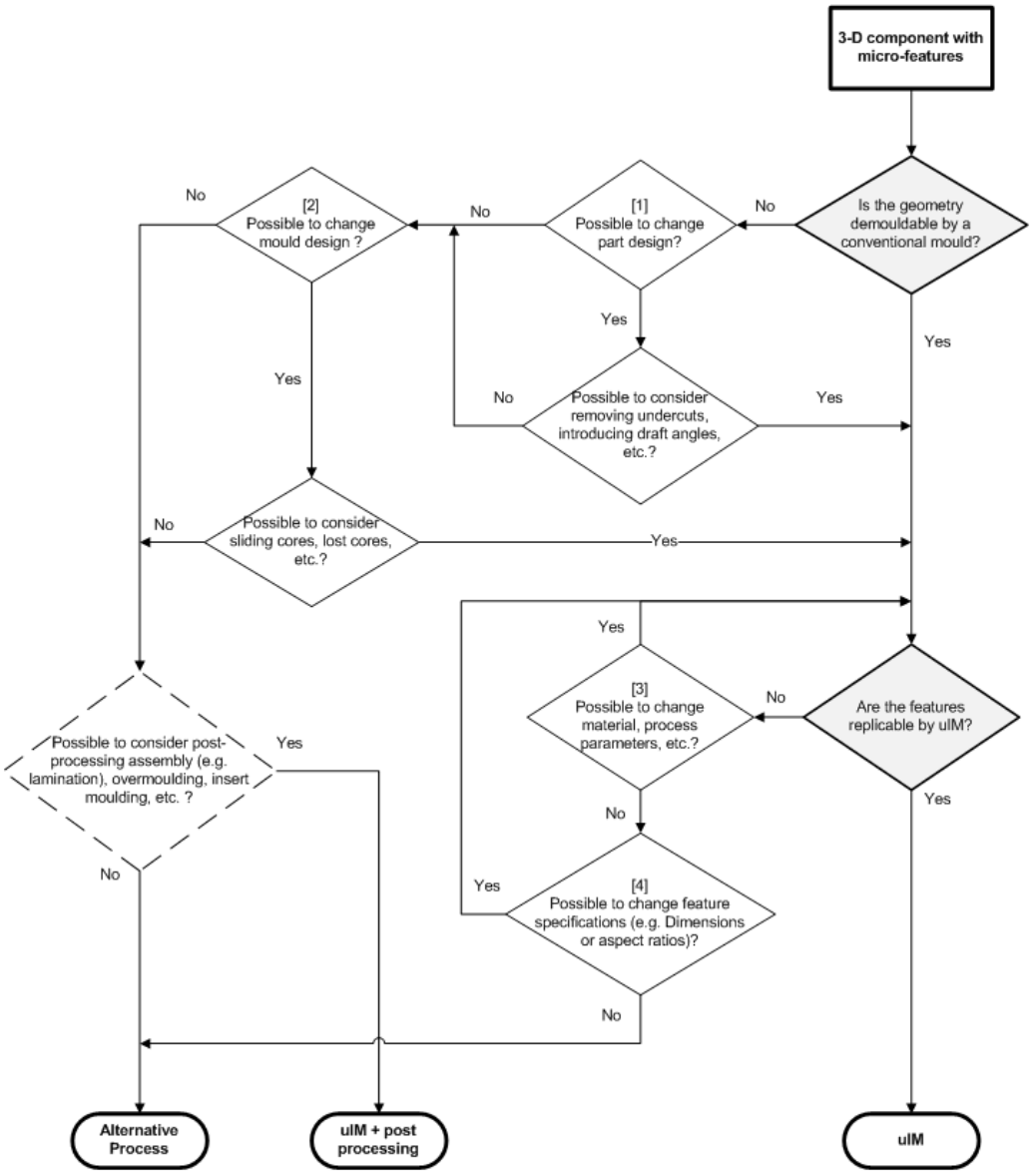

Figure 3-6 A flowchart for design considerations for µIM of 3-D components

The chart starts with at the top right corner, where a 3-D component is under consideration for manufacturing by µIM. The assessment result should decide whether the component is directly manufacturable by µIM, is manufacturable by µIM with considerable post processing or is not manufacturable by µIM. The assessment process is based on two basic criteria: demouldability and replicability by µIM. These two criteria are shown in the grey diamonds of Figure 3-6. If both are satisfied, the component can be directly manufactured by µIM. If one or more conditions are not met,

the decision process is based on modification “loops” that suggest possible changes to fulfil the requirements.

If the challenge is in demouldability, the alternative loops are either to change the geometry of the component (diamond [1]) or to change the mould mechanism (diamond [2]). If none is possible, the alternative would be to simplify the geometry by dividing it into relatively simple, components (dashed diamond). These components could either be joined during the moulding process by, for example, overmould, or they could be assembled by post-processing. This approach will overcome the demoulding complications but will need considerable post-processing, which is the available alternative to direct μIM. If this approach is not applicable, then another processing route should be considered for this particular component.

If the challenge is in replication, the alternative options would be to change the processing conditions or the material to achieve better replication (diamond [3]). If this is not possible or not sufficient, it would be necessary to modify the features that causes filling problems (diamond [4]). If none of the options are possible, then another processing route should be considered.

A number of issues should be noted about this chart:

- The chart focuses on manufacturability aspects and does not take cost or time into consideration. In mass-production environments, these are decisive factors that could influence the decision about the use of μIM.
- That chart is generic in the sense that it presents a bird’s-eye view of the process without going into details. In a more detailed chart, some decision “diamonds” could be replaced by minor flow charts of their own.
- Designing the component and the mould are dependent on each other, which implies that changes introduced in one will affect the other. Therefore, it might be necessary to go through the whole chart again after each introduced modification to recheck that all requirements are fulfilled.

3.5 Conclusion

This chapter addressed the issue of designing for micro-moulded 3-D components. It presented the main design consideration for both the mould and the replicated part.

For the mould, geometrical classification approaches for micro-fabricating three-dimensional features were presented. Design consideration for mould-making included demouldability, dimensions and surface properties.

For the replication stage, design considerations and guidelines specific to μIM were discussed for manufacturing both 3-D features and structures. These included flow behaviour, dimensions and shape stability.

A flowchart was proposed as a generic guideline of assessing the manufacturability of a 3-D component by μIM. The chart investigates the component based on evaluating both mould-making and cavity-filling requirements.

4 Research Gap and Methodology

Chapters 1, 2 and 3 aimed at critically reviewing the state-of-the-art technology in μIM of integrated 3-D microfluidic devices. Chapter 1 reviewed the process itself in terms of its advantages and limitations, design and manufacturing aspects, quality control and potential areas of development. Chapter 2 focused on integration of functionalities within high-volume micro-replication techniques. Both μIM and hot-embossing were reviewed because of the similarity in the process principles and design aspects. Integrated elements were classified in terms of their functionalities and integration technique. Chapter 3 discussed the manufacturability of three-dimensional micro-components by μIM. It aimed at identifying the concept of three-dimensionality in micro-manufacturing with special focus on μIM. Design-for-manufacturing guidelines were proposed in a chart format for how 3-D features and structures should be assessed for μIM.

Based on these reviews, potential research gaps were identified, and a number of research questions were selected to be the focus of this thesis. The following sections present the selected research problems and the methodology used to investigate them throughout the chapters of this thesis.

4.1 Problem Definition:

The aim of this thesis was to assess the feasibility of high-volume manufacturing of three-dimensional, disposable and integrated microfluidic devices using μIM. These requirements can be identified into the following specific goals:

- Mass manufacturability: High-volume, low-cost processes are of particular importance to applications, where disposable components are produced to, for example, prevent cross-contamination in medical diagnostics or to avoid the need for maintenance or device-recalibration facilities in resource-limited areas. The research aimed at demonstrating a method to predict the performance of the μIM process and to evaluate and control the quality of the produced parts in terms of accuracy and repeatability required for miniaturised components.

- Three-dimensionality: More research interest is currently directed towards geometrically complex 3-D microfluidics, where higher throughput and volume optimisation could be achieved. It was required to demonstrate the ability of μIM to produce components with relatively complex, truly 3-D geometries, and to investigate design requirements in light of the process possibilities and limitations.
- Integration of functionality: Microfluidic devices are required to perform more demanding tasks than simple fluid-manipulation. In the fields of medical analysis and diagnostics, for example, relatively complex operations are required within the limited size of the device. This requires integrating functionalities within the microfluidic device, either during the fabrication process or by post-processing. It is required to demonstrate the ability of μIM to integrate functionalities without significantly compromising the cost or manufacturing time of the device.

4.2 Research strategy

Tackling the research problems was conducted through a number of stages, starting with the literature review presented in the previous three chapters. The second stage was to identify research areas that covered the main requirements of the research problem definition, namely three-dimensionality, quality-controlled mass-manufacturability and potential for integration. A step-by-step approach was applied, where each problem was dealt with independently.

4.2.1 Micro-moulding of three dimensional structures

It was evident from Chapter 3 that research work in microfabrication of 3-D structures in general was at its early stages. Specifically for replication techniques, very little was presented about how to use high-volume processes to generate relatively complex geometries, or how conventional 2½-D "chips" might be transferred into "true" 3-D structures.

To investigate this issue, a case study of a 2½-D microfluidic device for medical application was selected, where it was required to redesign and fabricate it in 3-D to increase the device throughput. Chapter 5 covers the whole process chain starting from conceptual design up to assembly and testing.

The purpose of this step was to present a novel method of designing and producing 3-D microfluidic devices by a high volume process, in light of the design considerations stated in Chapter 3, and to demonstrate a practical example of how a design could be adapted such that the fabrication technology could produce products beyond its usual capabilities.

4.2.2 Statistical quality control and process optimisation of μIM

The second step was to investigate and control the process parameters that affect the replication quality. Numerical simulation would usually be the first approach to predict the effect of process parameters on the quality of the parts. However, it was shown from the review in Chapter 1 that conventional simulation packages were not valid on the micro-scale due to the change in physical principles that govern polymer flow behaviour on this scale. An alternative method was to use statistical quality control, where the relation between process factors and part quality can be quantified from measured samples. The results could then be used to predict filling behaviour for other process parameters combination.

The moulded components of the 3-D microfluidic device were used as test samples for quality-controlling and optimising the micro-moulding process itself. Chapters 6, 7, 8 and 9 investigated controlling quality parameters such as part mass, process variability, and multi-response optimisation. A design-of-experiments (DOE) approach was applied to explore the relationship between the process parameters, part geometry and the quality criteria of interest. The analysis results were used to aid in optimising the process such that desired quality criteria were met.

4.2.3 In-line integration of functional elements

The third research gap investigated in this thesis was the potential for integrating functional elements within μIM, which was presented in Chapter 10. The minifluidic demonstrator was used as a test sample for two-material hybrid micro-moulding. The purpose of this work was to apply micro-injection moulding to directly integrate interconnects to the outlets of the microfluidic device.

A novel interconnection approach was used by overmoulding a thermoplastic elastomer over the PMMA substrate, making use of the elastic properties of the elastomer to seal the connection tubes.

After addressing the three research questions, the main results and contribution to knowledge were summarised, followed by potential developments and future work. Figure 4-1 shows a schematic structure of the research problems and corresponding thesis structure.

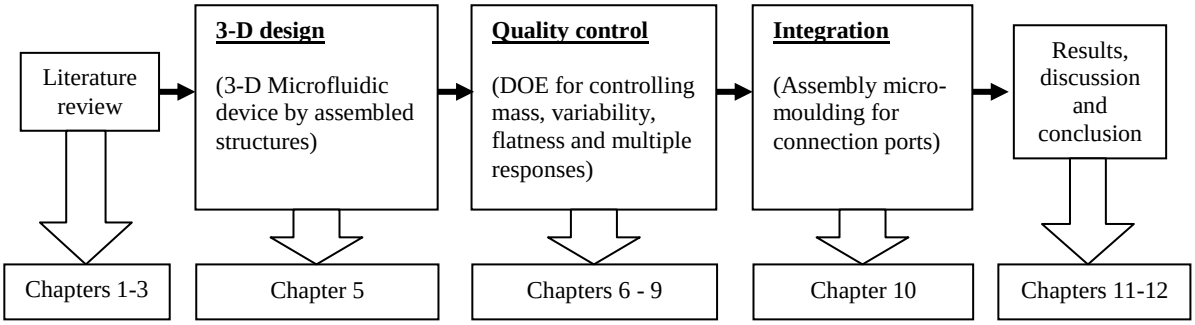

Figure 4-1 Research plan of the thesis

5 A process chain for high-volume manufacturing of three-dimensional microfluidic devices for medical applications by micro-injection moulding

5.1 Introduction

The demand for low cost, high quality miniature parts in the medical technology sector is rapidly growing. The ability of introducing new micro-parts into the market is dependent on finding methods for the manufacture of parts in high-volume and at low cost albeit ensuring high product reliability. These characteristics are particularly important for those medical products where devices should be disposable for safety considerations.

Micro-injection moulding (µIM) is a micro-replication technique that offers mass-production capabilities of polymer parts at relatively low cost, short-cycle times (a few seconds), and the potential for full-automation, accurate replication and dimensional control. Hence, micro-injection moulding is currently commercially used for the production of a number of biomedical miniaturised devices. Similar to conventional injection moulding, µIM is a technology in which a thermoplastic material is fed in the form of granules into the plasticating unit and then injected at high pressure into a mould, which is the inverse of the desired shape. The molten polymer freezes into the mould becoming a solid part and is then released from the mould by opening the mould and ejecting the plastic part with a set of ejection pins. The whole process is normally very fast with production cycles of a few seconds.

In µIM, the mould cavities contain features in the micrometre range which need to be completely filled by the polymer melt. In many cases this requires the process to be adapted by removing the air entrapped in the small features and by using additional heating elements to account for the very fast cooling of the injected melt into the small, cold mould micro-features. Moreover, in order to ensure proper cavity filling, high injection speeds and pressures are required. The machines for performing microinjection moulding need to possess the following characteristics:

- Small plasticating units to avoid prolonged residence of the polymer melt which could result in material degradation.
- Precise and repeatable shot volume control to carefully meter the volume of material required. No material cushion resides in the injection unit to ensure material uniformity.
- Adjustable injection speed and pressure.
- Precise mould alignment and gentle open/close mould movements to avoid deformation of the small mould features.

In order to achieve these characteristics, recent designs of micro-injection moulding machines have featured separate plasticating, metering and injection units. These functions were typically performed by a single screw in conventional injection moulding. Separating these functions allows for accurate dosing of the material and control over injection speeds. Figure 5-1 presents a typical structure of such a dedicated micro-injection moulding unit:

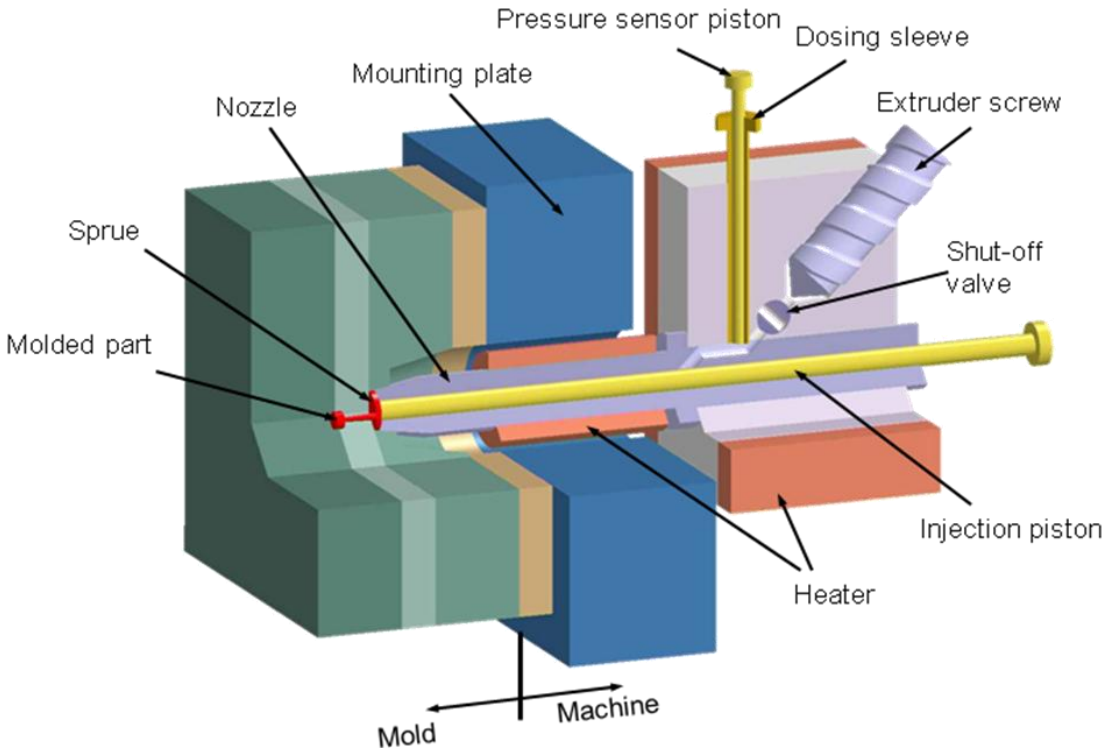

Figure 5-1 Micro-injection moulding unit (Image courtesy of Battenfed SMS Group)

One of the focal points of the work currently ongoing within the Precision Engineering Centre at Cranfield University is the investigation of μIM as a potential technology for high-volume manufacture of a specific category of biomedical devices, commonly called microfluidic devices or lab-on-a-chip (LOC) devices. LOC is a term for devices that integrate multiple laboratory functions on a single chip of only millimeters to a few square centimeters in size. The devices are capable of handling extremely small fluid volumes, down to less than pico-liters. This category of products is being widely investigated at a prototype level. However the examples of integrated polymer microfluidic devices successfully introduced in the market are very few.

Since the introduction of LOC devices in the early 1990s, glass has been the dominant substrate material for their fabrication [261] because of its material properties and because the fabrication methods were well established by the semiconductor industry. However, the cost of producing systems in glass is driving commercial producers to seek other materials. Commercial manufacturers of microfluidic devices see many benefits in employing plastics. Polymers are, in fact, a group of materials showing several advantages over other conventional materials such as glass, silicon or various metals [30]. The wide varieties of properties which are tuneable, the relatively low costs, relative simplicity of processing and accurate repeatability in high-volume production are some of their attractive characteristics (Please refer to Chapter 1 for advantages and limitations of μIM).

As part of the EPSRC-funded project 3D-Mintegration (EP/C534212/1) [262] a multidisciplinary team based at Cranfield University and Herriot Watt University has identified and designed a versatile, generic module for use in the preparation of blood samples necessary for a number of LOC diagnostic devices based on blood analysis.

The element under consideration is a blood/plasma separator aimed at producing high-speed and high-efficiency plasma separation in the simplest designs to compete with conventional plasma extraction such as centrifugation, blood filtration or CD-like platforms [263]. Different biomechanical separation principles such as Fahraeus and Zweifach-Fung effects are combined to produce a separation between blood cells and plasma within microchannels without the help of external forces aside from pressure on the fluid. No filtration is used at any stage of the process which results in a clog-free

system. The method benefits from the natural plasma skimming effect in microchannels of dimensions below 300 µm [264-266].

This paper describes the design and the manufacturing process chain for producing a three-dimensionally structured microfluidic device for blood/plasma separation.

5.2 Microfluidic device design

5.2.1 Device functionality and conceptual design

The device is an integrated diagnostic system for detecting foetal genetic disorders in samples of a mother's blood. This novel approach to prenatal diagnosis was designed to replace the currently used invasive methods, which have the risk of harming the foetus in a way that might lead to miscarriage or growth abnormalities.

The device functional design, which was developed at Heriot-Watt University, consists of a number of analysis stages starting with blood-sample delivery and ending with analysis output results. Figure 5-2 presents a simplified schematic diagram of the device structure.

The device was planned to be designed and manufactured in a modular format, such that each major "box" in Figure 5-2 is developed and tested as a separate module. Afterwards, the developed modules would be put together as an integrated diagnostics system.

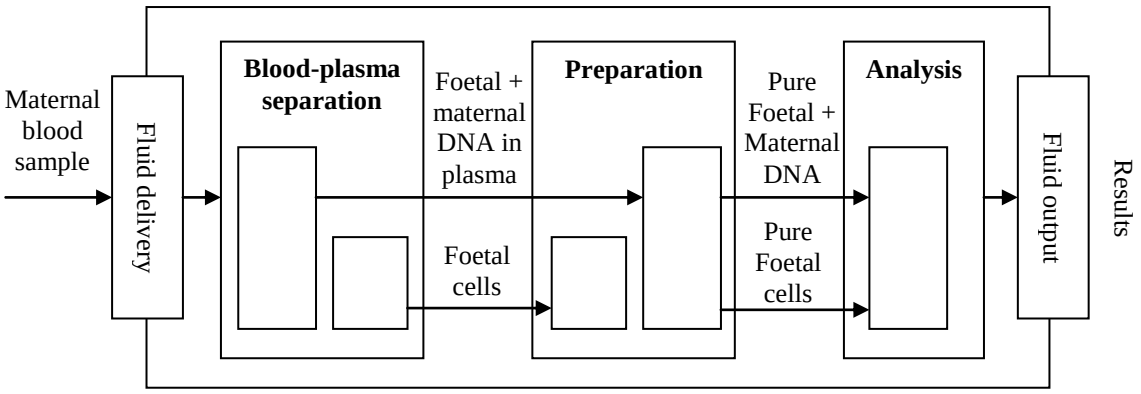

Figure 5-2 Schematic diagram of a diagnostic microfluidic system

5.2.2 Three-dimensional blood-plasma separator

The demonstrator resented in this paper focuses on the first major stage, or module, of operation, which is blood-plasma separation. The initial design proposed by Heriot Watt [267] was based on a 2½-D structure (Figure 5-3) characterised by a 25 µm constriction in the whole blood inlet channel, followed by several bifurcating plasma sub-channels 20µm wide and deep.

The separation of the whole blood (which in first approximation can be seen as a suspension of red blood cells (RBC) in plasma) into its basic components, red blood cells and plasma, is made possible in the micro-channel structure by the presence of biomechanical effects. When passing through the bifurcation region, the RBS tend to flow with the main-stream channel, which has the largest cross section, whilst the plasma tends to flow into the side junctions with the smallest cross section.

The separation yield is mainly dependent on the ratio of the cross sections of the main channel and the side channels. The performances of the systems are believed to be governed by the channel width ratios and the constrictions' lengths; however there is currently no definite design rule for determining the exact channels dimensions required for achieving efficient separation.

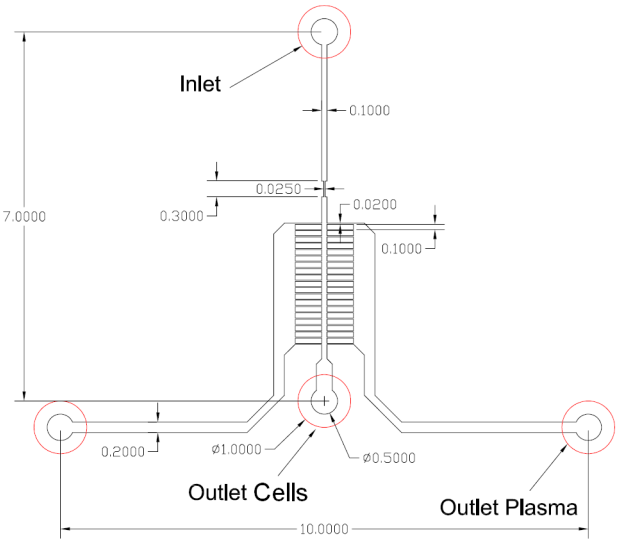

Figure 5-3 Design of a 2½-D microfluidic device for plasma/blood separation (All dimensions in mm. Image courtesy of Maïwenn Kersaudy-Kerhoas, Heriot-Watt University)

The initial 2½-D design concept was reconsidered and a new 3-D design was proposed. The 3-D conceptual design was developed by revolving the set of separation channels around the main inlet channel. This approach rendered an axial design, where the central 2½-D RBC channel became a 3-D tube, and the side 2½-D plasma channels became 3-D discs. Separation in this case would take place across surfaces rather than channels. A drawing of the 3-D device half-cross section is shown in Figure 5-4.

The initial dimensions as proposed by the designers in the 2½-D model were modified considering the available micro-moulds manufacturing processes and the relative lack of clear design guidelines for what concerns the absolute dimensions of the microchannels. The dimensions of the 3-D system took into consideration both mould manufacturability by micro-milling, in addition to dimensional requirements for separation. Initial numerical simulation tests were made at Greenwich University to evaluate the separation efficiency of the 3-D design, and additional simulation experiments are currently under investigation. The new proposed critical dimensions were as depicted in Figure 5-4.

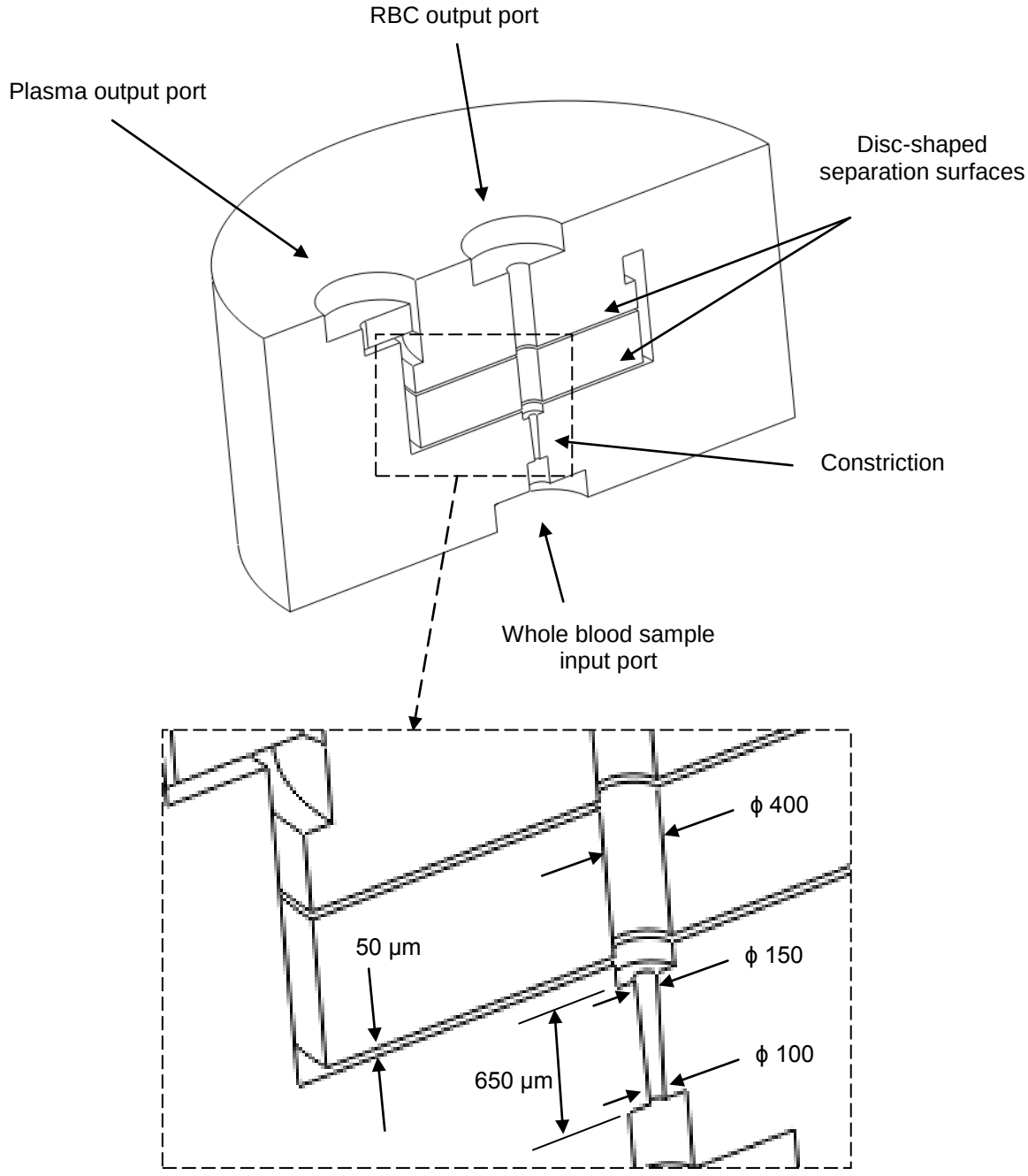

Figure 5-4 Half-cross sectional image of a 3-D microfluidic device for plasma/blood separation obtained by revolving the 2½-D device around the main blood channel

5.2.3 Designing for manufacturability by μIM

The design shown in Figure 5-4, in spite of its apparent simplicity, poses serious challenges for manufacturability by μIM. As discussed in Chapter 3, the 3-D geometry of the structure, considering its complex hollow cavities, would not be producible by

μIM as a single part. It would be necessary to adapt the design to the geometry-limitation of the process, and the approach followed in this case was to produce the device as a number of parts that could be assembled in subsequent assembly process.

The device was redesigned as a laminate of mouldable layers, which is a common approach in producing 3-D microstructures (Please refer to examples in Section 3.3.2). The 3-D structure of Figure 5-5 was achieved by lamination of 5 mouldable PMMA discs, all of which had the same external dimensions (10 mm in diameter and 1 mm in thickness). The parts are labelled from A to E for convenience. For dimensioned drawings please refer to Appendix A1.

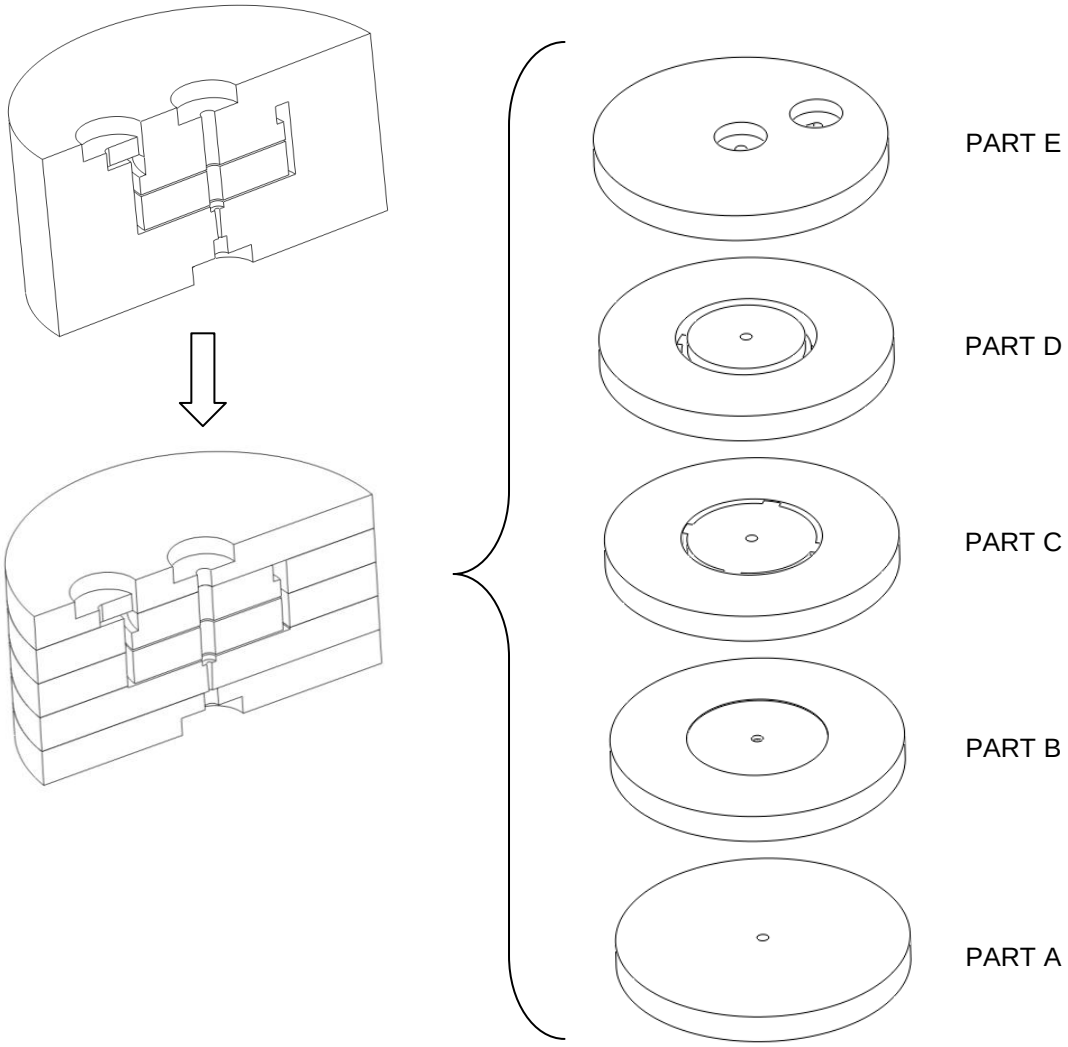

Figure 5-5 Laminated structure of the 3-D microfluidic device

In the design shown in Figure 5-5, layers A and E are interconnection interfaces for fixing tubes that connect the device to the surrounding environment. Layer B carries the 100-150 μm-constriction responsible for the flow-focusing effect, in addition to the first plasma separation circular 50 μm-depression. Layer C is a dedicated separation element with a circular depression similar to B. Layer E is a collection layer to combine the flow of the separated plasma into a single outlet.

Layer C was designed as an independent separation layer such that stacking a number of its replicates would add extra separation layers and, hence, increase the efficiency of separation. Adding more layers of C would be analogous to adding extra separation channels in the 2½-D design in Figure 5-3. Figure 5-6 shows a half-cross sectioned, front view of a device with 5 layers of C.

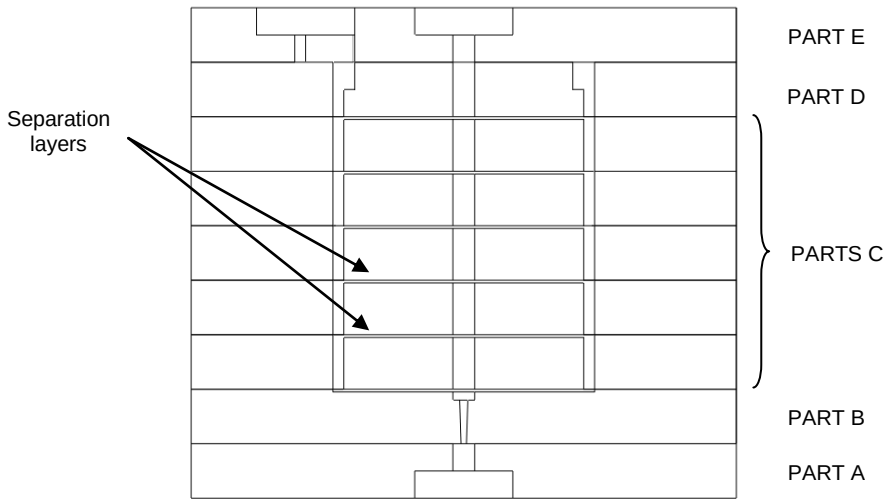

Figure 5-6 An expanded version of the 3-D blood/plasma separator

5.2.4 Designing for assembly

The 3-D device was designed such that joining the layers could take place using ultrasonic welding. This was taken into consideration by the following design elements:

- All the layers were designed with axially symmetric features, such that no specific axial orientation was required between adjacent layers.
- The diameter of the layers was increased beyond the features required for separation to allow for enough area for ultrasonic welding to take place.

- The outer diameter of the layers was selected as the alignment edge, when the parts would be stacked for welding. The most critical part for alignment is the 100 µm constriction. However, this was designed so that it lies completely on one side of layer B and does overlap with a much larger feature (the large inlet channel which has a diameter of 400 µm in layer A).
- As will be shown in more details when discussing mould-manufacturing, all the five layers were produced from a single polymer shot, such that 1 complete set was produced per machine cycle (Figure 5-7). This would ensure that possible dimensional changes, particularly shrinkage, produced by the process parameters would be induced in all the layers, such that possible differences between the diameters of the five discs that construct a single device would be minimised.

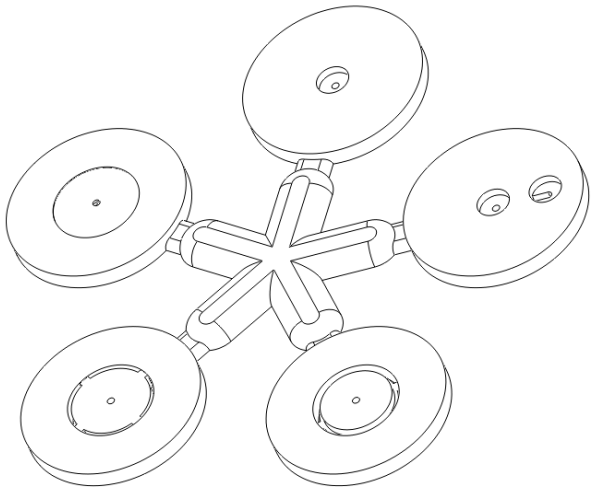

Figure 5-7 A CAD model of the micro-moulded 5 layers attached to their gate and runner system

5.3 Micromould manufacture

The mould insert was designed as a set of 5 interchangeable elements. Figure 5-8 shows a top view of the assembled mould (Engineering drawings of the mould constituents are available in Appendix A2). The 5 micro-structured inserts, the carrying holder and the mould housing all fit together within tight tolerances.

This reconfigurable structure was selected to allow for the flexibility of changing the design and/or re-machining the features when deemed necessary. The time and cost involved in machining moulds, especially with micro-features, makes it a high risk to

machine the whole mould as a single piece. This manufacturing path was selected as an alternative approach for prototyping purposes.

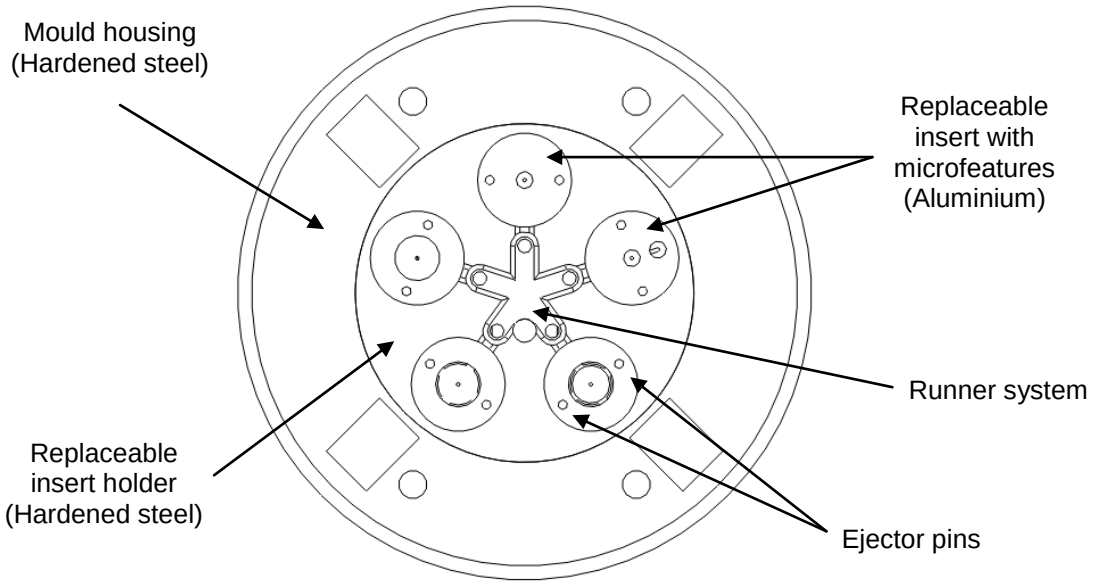

Figure 5-8 Top view of the assembled micro-mould structure

While the insert-holder was fabricated in hardened steel, the micro-structured inserts were fabricated in Alumold 1-500 (Alcan). From a functional point of view, this type of aluminium was selected because it is commonly used in injection-moulds. From a machining point of view, Alumold 1-500 was selected because it is a highly machinable type of Aluminium and is suitable for micromilling, polishing and, if required, for subsequent diamond turning processes.

All the five inserts were fabricated by micromilling with a Kern micromilling centre (Figure 5-9) using a CAD/CAM software, Cimatron E7.1. This software package supports the micromilling functions, and produces optimal tool paths and the CNC programme for making the precise mould inserts.

Figure 5-9 A KERN, 5-axis micromilling machine (Image courtesy of Rianford Precision Machines)

Figure 5-10 (a) and (b) shows a photo of the disassembled and assembled mould structures, respectively.

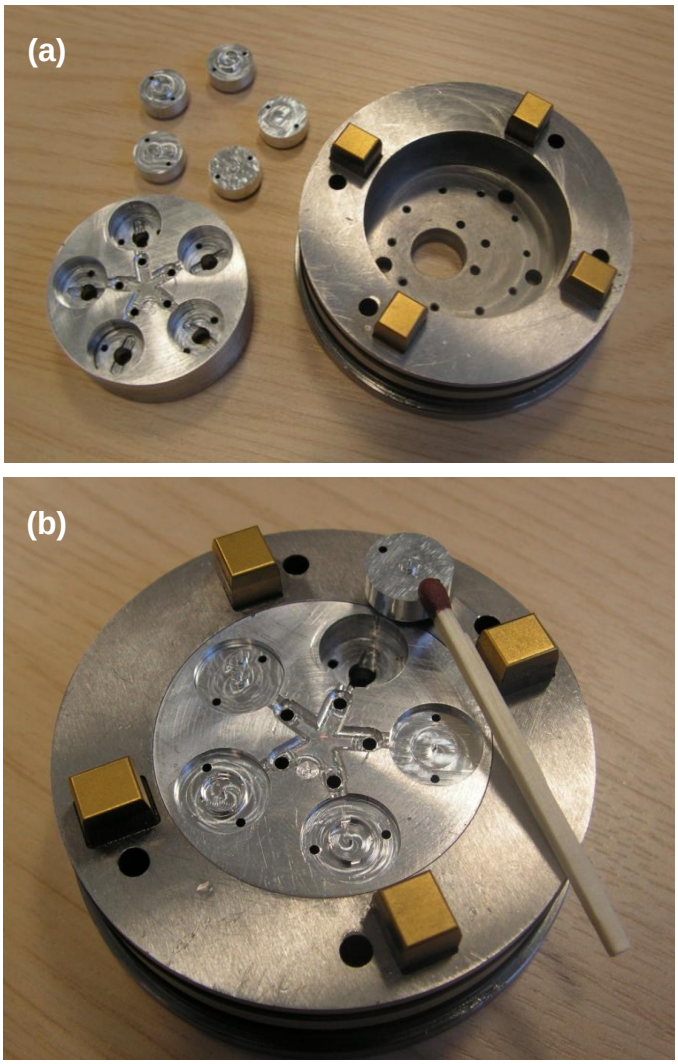

Figure 5-10 Reconfigurable micro-injection mould (a) disassembled and (b) assembled

The cutting strategy for each insert consisted of a roughing step and a subsequent finishing step to remove the top 0.1 mm layer. Both roughing and finishing steps were performed using tungsten carbide flat-end milling cutters. For insert A, due to its full rotational symmetry, an additional finishing step by diamond turning was used. Figure 5-11 shows SEM micrographs of the five inserts.

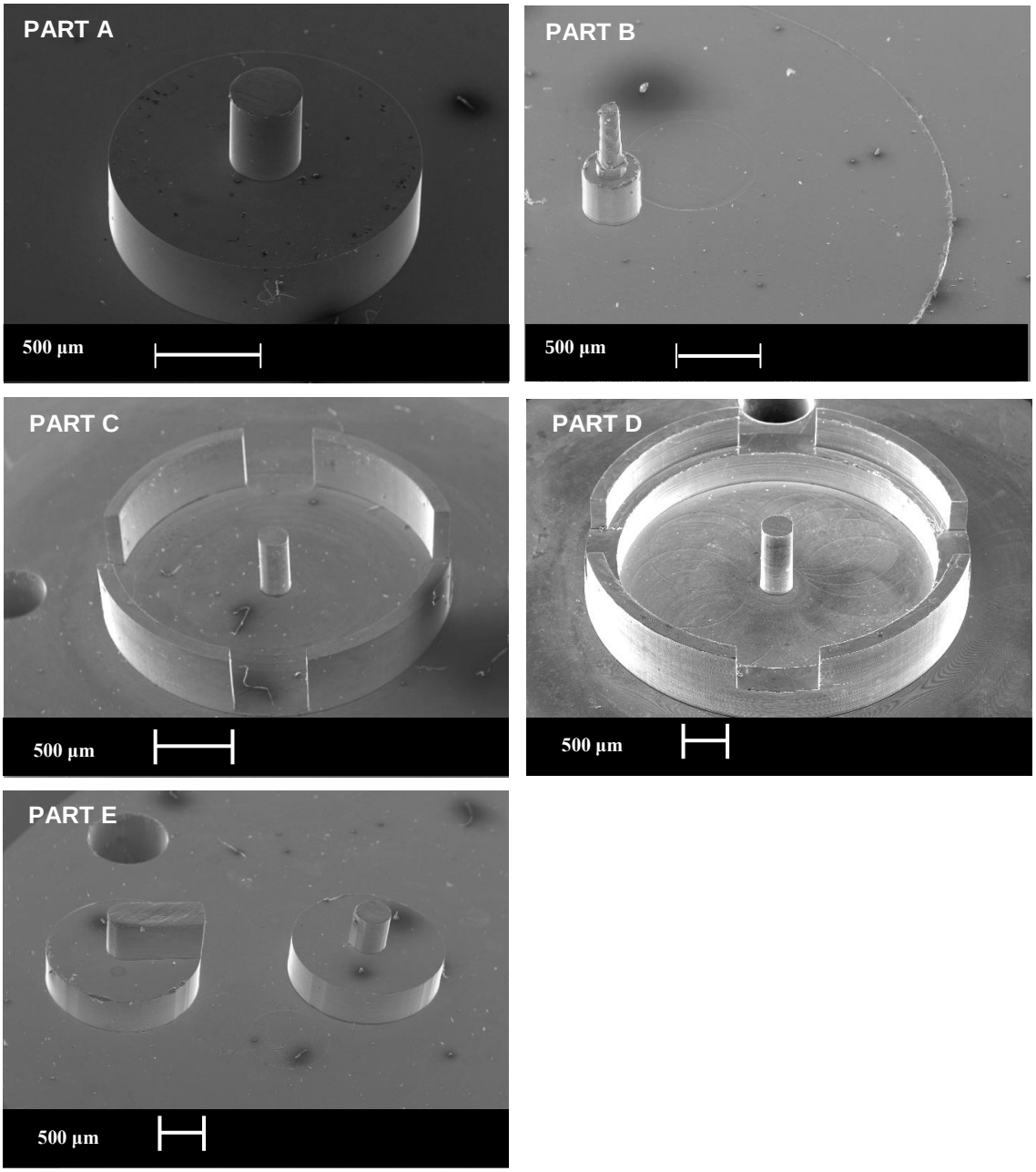

Figure 5-11 SEM micrographs of the five aluminium micro-structured mould inserts

Table 5-1 presents typical micromilling parameters for machining the inserts:

	Roughing		Finishing	
Tool diameter (mm)	Feed rate (mm/s)	Rotational speed (rpm)	Feed rate (mm/s)	Rotational speed (rpm)
2	200	5000	/	/
1.5	200	8000	150	8000
1 (4 slots)	200	8000	200	8000

Table 5-1 Micro-milling process parameters

The holes visible in the mould inserts for Parts C, D and E (Figure 5-11) were machined for the ejection system. Once completed the inserts outside diameter was machined to fit the insert holder with a H7/h6 sliding fit (clearance of approximately 15 μm).

5.4 Replication with μIM

The polymer layers were moulded with a Battenfeld Microsystems 50 μIM machine (Figure 5-12). The material used was Polymethylmethacrylate (PMMA) of the grade Altuglas® VS-UVT. The grade was selected for its ease of flow (MFI = 24 g/10 min), optical transparency (light transmittance 92%) and compatibility with medical applications involving blood.

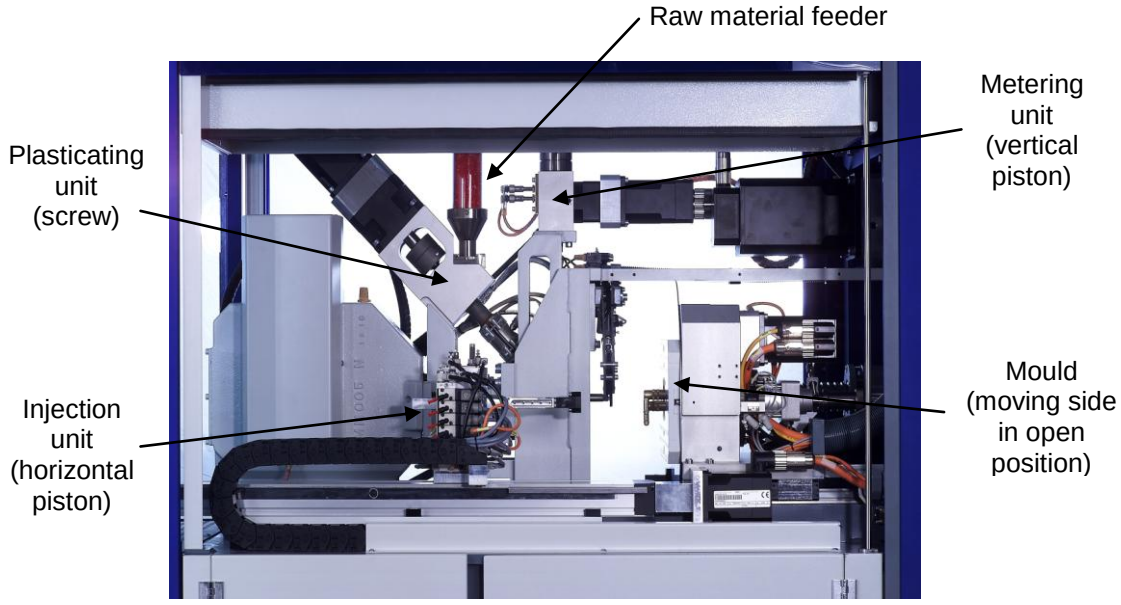

Figure 5-12 Micro-injection moulding machine (Image courtesy of Battenfeld, SMS Group)

The main restrictions posed by the replication process were taken into consideration during the design phase: firstly, the maximum shot volume of the machine was 1.1 cm^3. Secondly, all the features were put on one side of the mould platen, since in the available two-plate mould the injection side would not be available for machining. Finally, the overall allowable area for features was about 25x25 mm^2. The process conditions were selected as shown in Table 5-2, and the cycle time for the one moulding operation was approximately 5 seconds.

Parameter	**T_p [°C]**	**T_m [°C]**	**V_i [mm/s]**	**P_h [bar]**	**t_c [s]**
Value	250	84	200	300	3

Table 5-2 Processing parameters for a five-part micro-moulded component

Figure 5-13 shows a photo of the moulded parts, while Figure 5-14 shows SEM micrographs of the parts features.

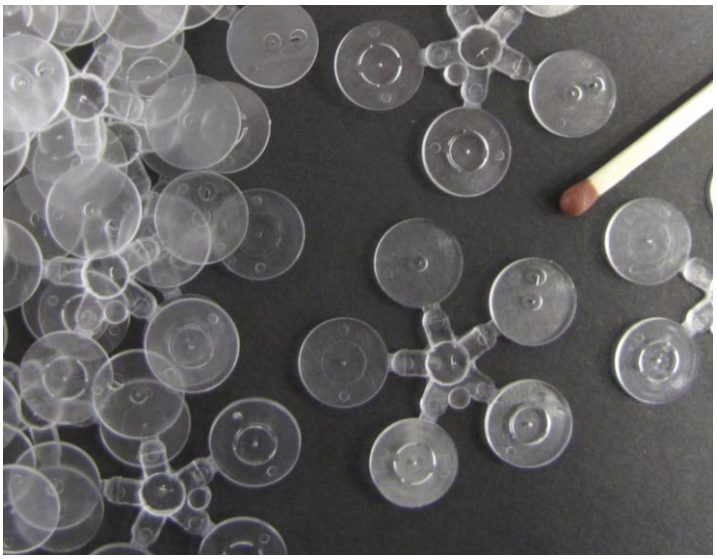

Figure 5-13 Micro-injection moulded plastic components

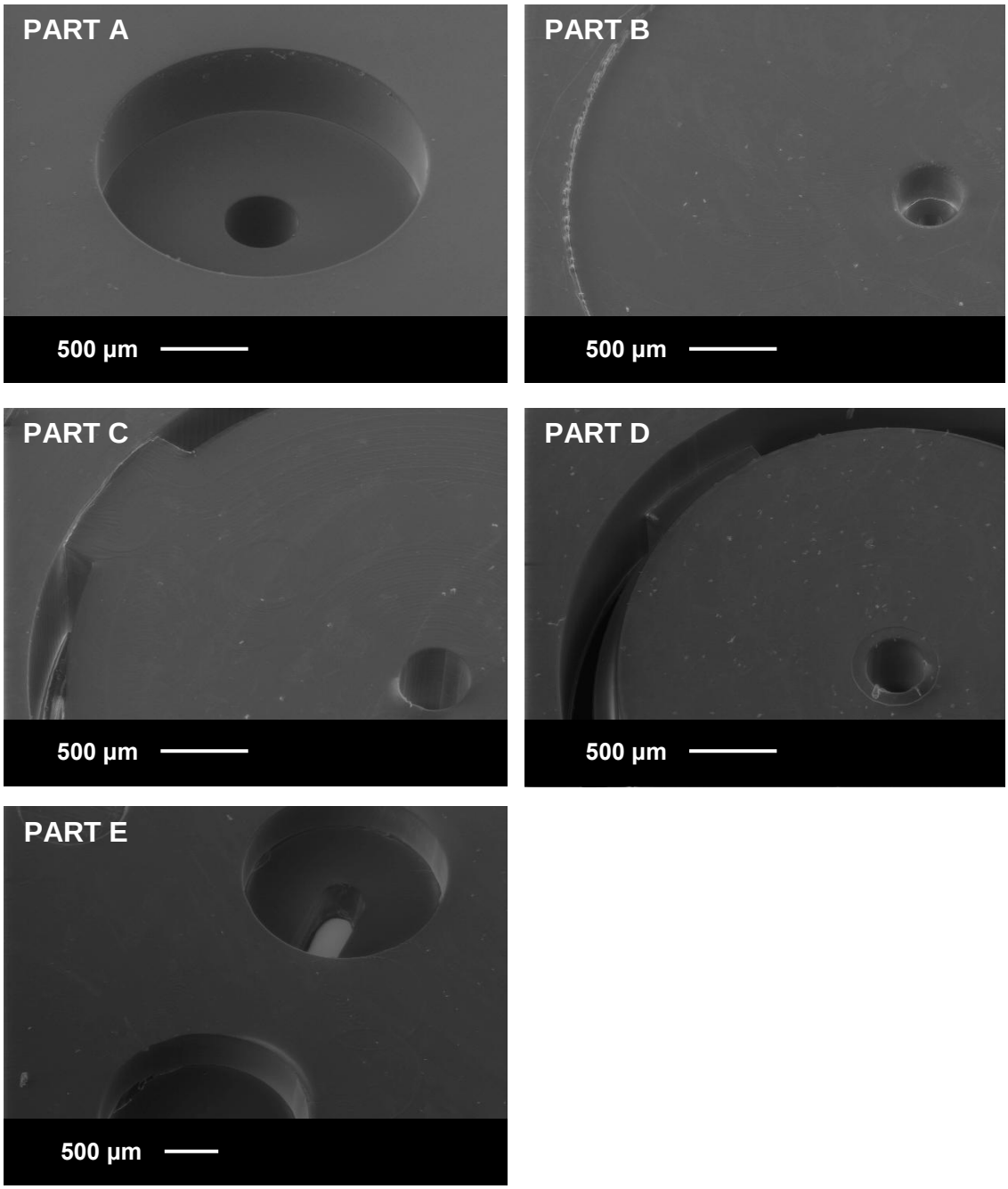

Figure 5-14 SEM micrographs of PMMA micro-moulded components

5.5 Metrology and quality control

As a first approach to characterise the filling quality, the dimensions of the part were measured using SEM and compared to the ones of the insert. The initial

measurement attempts showed that SEM did not produce repeatable measurement data, and hence, a relatively large standard deviation (SD) was recorded for each set of measurements.

As a second approach, the parts were measured with a micro-coordinate measurement machine (µ-CMM) available at the National Physical Laboratory (NPL). The Carl Zeiss F25 system was used to obtain measurements using a touch probe of 300-µm in diameter within an uncertainty of 250 nm (Figure 5-15).

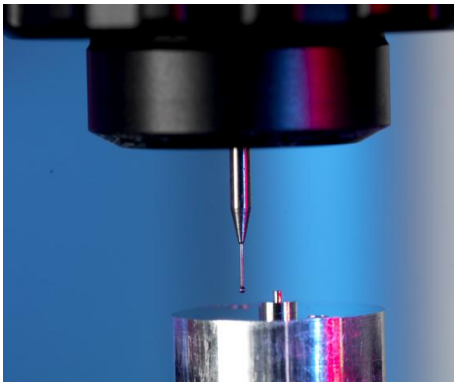

Figure 5-15 Part A being measured with µ-CMM using a 300-µm touch probe (Image courtesy of Alan Wilson, NPL)

The recorded data showed much better repeatability relative to SEM. To illustrate this difference, Figure 5-16 shows the dimensions that were assessed for Part A. Table 5-3 compares the dimensions measured of insert A using both SEM and µ-CMM. The standard deviation values were based on 5 repeated measurements for each feature.

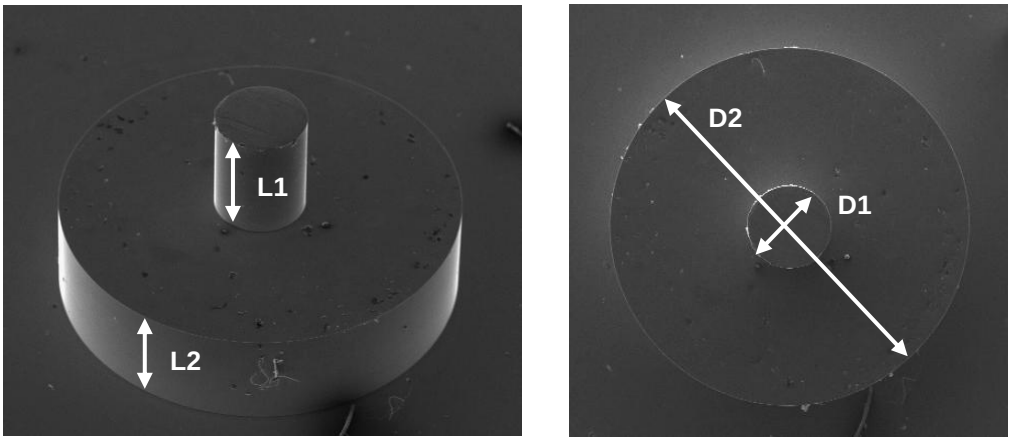

Figure 5-16 Measured dimensions in Part A

	Designed [µm]	SEM [µm]	Err. %	SD	µ-CMM [µm]	Err. %	SD
D1	**400**	392	2.0	14.8	410.7	10.7	1.2
D2	**1800**	1730	3.9	42.4	1803.3	3.3	0.02
L1	**500**	450	10.0	68.4	496.5	0.7	0.05
L2	**500**	492	1.6	17.5	500.7	0.1	1.64

Table 5-3 Measurements of micro-milled Insert A by SEM and µCMM

In spite of the high accuracy and repeatability of µ-CMM, it was not suitable for the type of experiments needed in this research for a number of reasons. Firstly, measuring internal features (channels and holes) was limited by the diameter of the probe (probe diameter was 300 µm while some holes were 100 µm or less). Secondly, the statistical approach used in this research requires measuring a large number of samples, which it was not possible to do at NPL within the available time and resources.

As an alternative approach to evaluating the complete filling of the mould, part mass was adopted as a quality parameter rather than dimensions. Quality control tests conducted using control charts showed that it was possible to control the mass of the injection moulded part within an average standard deviation of 0.2 mg. The inspected samples under the microscope showed that part mass could be used to represent the filling of the microfeatures in the replicated parts.

In order to control and optimise processing conditions for filling quality of all the five inserts, a design-of-experiments (DOE) approach was used to investigate the effect of processing conditions on filling quality. The detailed description of the technique and its outcome is discussed in Chapter 6.

5.6 Assembly and testing

The device was designed to be assembled using ultrasonic welding. The microassembly group at the University of Nottingham are in the process of developing a welding technique using a commercial plastics assembly system (private communication). The equipment used is a Sonics 40 kHz ElectoPress™ machine that has a stepper motor drive that produce weld depths with tolerances of 0.008 mm. Figure 5-17 shows initial successful welding attempts of 2 layers.

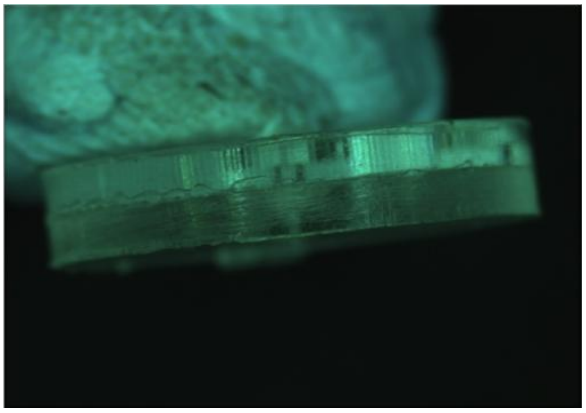

Figure 5-17 Two PMMA layers welded by ultrasonic welding (Image courtesy of Daniel Smale, University of Nottingham)

A preliminary assembly attempt was performed at Cranfield University using a commercial PMMA-compatible adhesive. The layers were assembled using an assembly fixture (Figure 5-18). The assembled device is then immersed in a resin to ensure complete sealing of the system. Figure 5-19 presents an image of an assembled device while being tested with water.

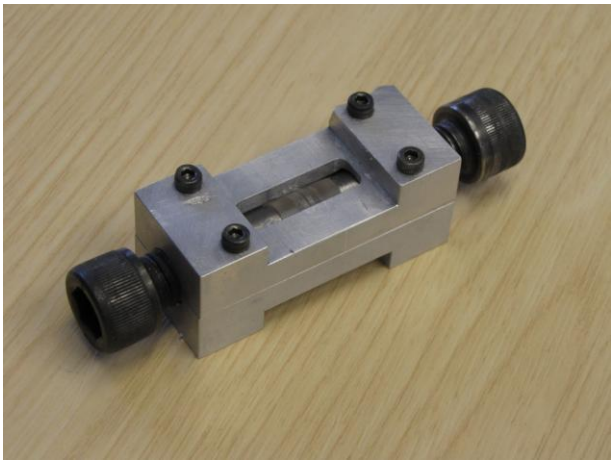

Figure 5-18 An assembly fixture for assembling device layers

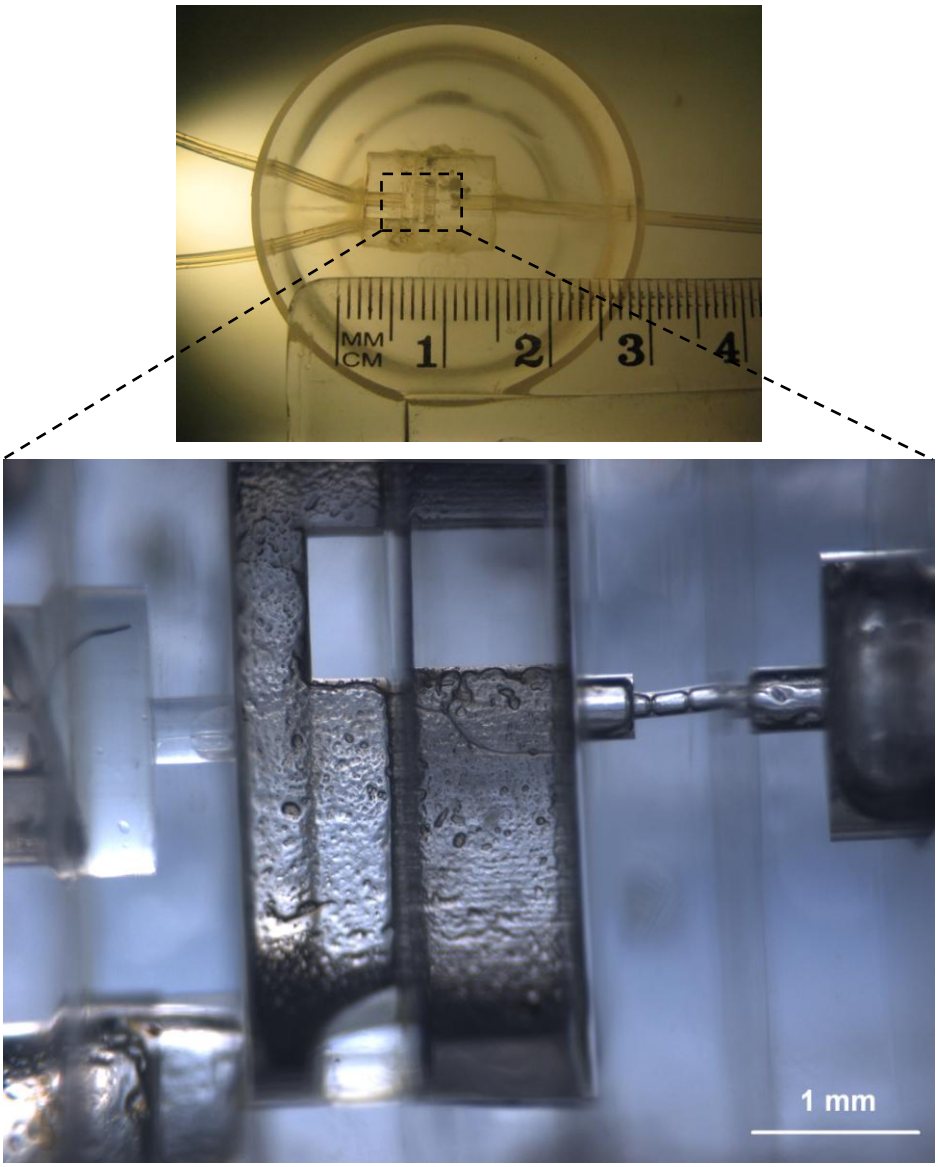

Figure 5-19 An assembled device being tested with water

After testing the device with water to ensure a leak-proof system, horse blood was used to test the functionality of the device (Figure 5-20).

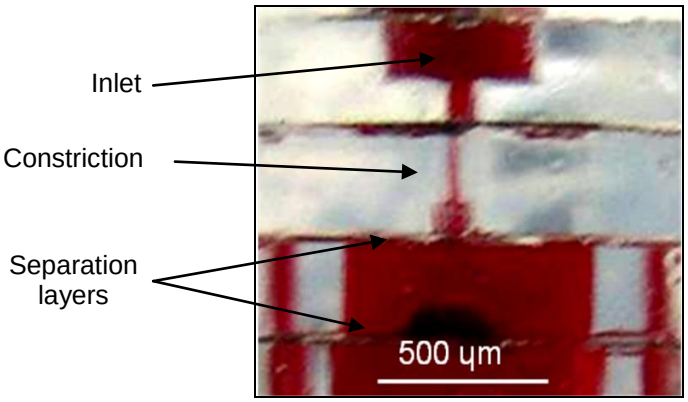

Figure 5-20 Blood flow throw an assembled separator

Diluted samples of horse blood were pumped into the device at a rate of 0.35 ml/min to avoid clogging. Separation was achieved through the device, which contained 3 separation layers. Separation efficiency was characterised by plasma selectivity (σ) defined as:

$$\sigma = 100\left(1 - \frac{C_{plasma}}{C_{input}}\right)\% \quad \text{..... (Equation 5-1)}$$

In Equation 5-1 C_{plasma} and C_{input} are the concentrations of RBC in the sample collected at the plasma outlet and in the whole blood sample, respectively. A plasma selectivity of 100% implies that the plasma is completely free of red blood cells. The selectivity measured for this particular experiment was 79.9%.

5.7 Discussion

The process chain presented in this chapter aimed at utilising high-volume micro-fabrication methods to manufacture microfluidic systems with 3-D structures. The process chain is shown in Figure 5-21.

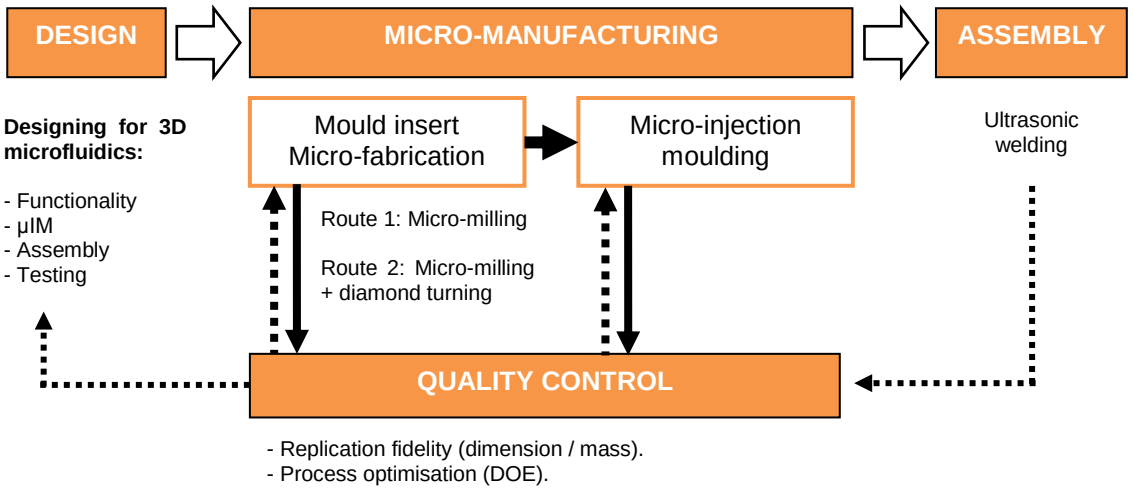

Figure 5-21 A process chain for manufacturing 3-D microfluidic devices

The work presented in this chapter has shown that this process chain functions as a feasible fabrication route for 3-D microfluidics. It is suitable for industrial high-volume fabrication since all the equipment used was commercially available. The following sections discuss the different design and manufacturing stages and assess the feasibility of the process chain.

5.7.1 Designing for manufacturability

The blood separator demonstrator was used as a case study for designing 3-D micro-components for manufacturing by µIM. The device was adapted for manufacturability by laminating microstructured layers, which is an approach that was previously demonstrated in µIM for LOC applications (please refer to section 3.3.2 in Chapter 3 for a review of such applications). This separator design is different in the sense that previous injection-moulded systems were based on laminating layers with independent 2½-D microfluidic structures, while the separator system presented here consists of a truly 3-D microfluidic structure built across all the layers. The conceptual 3-D design had a number of benefits compared to the 2½-D:

- Overall size optimisation which allows a more compact product.
- Use of 2 of the functional layers, namely A and E, to act as a top and bottom lid for the device; therefore no need for manufacturing the lid in a separate process.

- Optimisation of the area involved in the separation (small channels in the 2½-D design which become thin discs in the 3-D).
- Possibility of adding units, namely of Part C, in the module to incorporate extra separation channels if required.
- Potential for integration of other modular units in series with the blood separation module (for example, mixing units, detection etc).

On the other hand, the 3-D design posed a number of challenges in terms of manufacturability:

- The assembling approach was necessary to produce such a complex shape by μIM. The high-volume capabilities of the process allowed for replicating a complete device set every 5 seconds. However, the subsequent assembly steps add extra time to the overall time of the process chain. Automated handling and assembly systems would be necessary to minimise post-processing time.
- As presented earlier, assembling micro-devices requires accurate alignment and leak-proof joining methods. In this research, simple alignment and joining methods were enough for the tolerances required for this particular application. For more complex applications, where tight tolerances are typical for micro-structures, more accurate alignment techniques would be necessary, which might add to the cost and time of the process chain.

In spite of the manufacturability and assembly challenges, the 3-D concept demonstrated was capable of yielding separation during the preliminary experiments with animal blood. This shows a great potential for improvements in the 3-D design concept, taking into consideration the possibility of integrating automated, high-precision handling and assembly systems within the process chain.

Another issue that would enhance the capabilities of μIM for producing 3-D structures is the development of process variants, similar to conventional injection moulding. Multi-material micro-moulding and micro-lost-core techniques would open the way for improvement and design innovations for 3-D microstructures. Developments in the mould design would also be necessary for realising relatively complex structures. The use of 3-plate micro-moulds, for example, offer alternative design options in terms of feature design, flow direction and part ejection.

5.7.2 Mould manufacturing

A mould configuration based on replaceable inserts such as the one proposed here has potentially a number of advantages, particularly during the prototyping and pre-production stages. It allows for more design flexibility of the microfluidic device. This is crucial in particular for blood microfluidic devices where the support from simulations or modelling is relatively limited because of the lack of practical data on the blood rheology in microchannels and because of the difficulties in simulating complex fluids such as blood.

A similar issue also exists for the simulation of the polymer flow behaviour in microstructured inserts. Flow simulation software programs have proved very successful with conventional mouldings and allow for investigating the feasibility of a micromoulding process for component manufacture without a costly R&D moulding trial. However these software packages cannot generally be applied to micro moulding as they lose predictive accuracy when considering micro-scale flows [268]. (Please refer to Chapter 1 Section 1.7 for detailed discussion about simulation of μIM).

To overcome these limitations micromoulders typically rely on the feedback from the moulders to optimise the mould tools. This requires measuring the properties of the first runs of polymer parts and checking them against predictions. Because of the complexity of the manufacturing processes and the dimension of the cavity it is normally impossible to modify an existing micromould. This means that it typically takes more than one micromould to obtain a plastic part manufactured according to the required specifications.

Developing a mould in which the cavities are replaceable is therefore highly desirable, especially in the prototyping stages. On the other hand, this poses new challenges during the micromould manufacture because of the tight tolerances required between the inserts and the insert-holder to prevent polymer flash, which may occur because of the high pressure, high speed conditions of the μIM process. Also the ejection system needs to travel a more complex path through the various parts. This creates new requirements during the micro-mould manufacturing and assembly steps to ensure a smooth ejection process.

In a normal industrial environment, reconfigurable systems could be used for prototyping purposes until all the process parameters are determined throughout the

process chain. Afterwards, a "production" mould would preferably be micro-manufactured directly into the mould body to avoid misalignments and also the use of mould materials with different thermal properties.

In the set of experiments discussed here, micromilling was used as the main tool fabrication method, and diamond-turning was used as a finishing step for one of the inserts. Micromilling offered good capabilities in terms of three-dimensional machining and the relative speed of the process. On the other hand, some cutting tests were needed to determine the appropriate cutting parameters. For some of the machined inserts, the software was unable to determine cutting paths to produce perfectly cylindrical shapes. In addition, the surface finish of the micro-milled parts was not uniform in general, so diamond turning was used for one of the parts to obtain a uniform surface finish and accurate dimensions. Figure 5-22 shows an example of two inserts machined by micromilling with and without finishing by diamond turning.

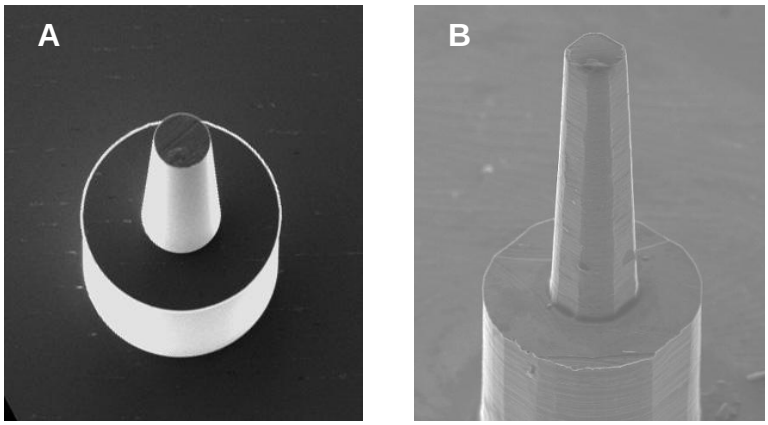

Figure 5-22 A micrograph of Part B machined by micromilling (A) finished by diamond turning, and (B) without diamond turning

Diamond turning was not available on regular basis, so it was not used as standard part of the process chain, and all replicated inserts, except for Part A, were machined used micro-milling only.

5.7.3 Replication by µIM

The device was successfully replicated by µIM using PMMA at a cycle time of 5 seconds. Initial replication trials produced some defects such as incomplete filling and void marks.

Initial measurements of the machined and replicated parts showed that SEM was not suitable for dimensional quality control due to its relatively low repeatability. This was because measurements depended on magnification scale, screen resolution and human interaction in determining the measured distances. These factors posed a combination of error-sources that increased the amount of uncertainty in the measured data. Another limitation of SEM is the difficulty in measuring in the z-direction perpendicular to the imaging plane. This required tilting or reorienting the part, which contributed to the measurement error sources.

µ-CMM proved to be a much reliable measurement system because it is a contact-based technique with high resolution relative to SEM. It also has the capability to measure in three-dimensions. µ-CMM was not available at Cranfield University as a standard measurement system, so another quality parameter was necessary to reflect the filling of the moulded part.

Part mass was proposed as an alternative quality parameter rather than dimensions. Process control charts showed that µIM can produce parts in a continuous process within an average standard deviation of 0.2 mg (Please refer to Appendix A3 for mass measurement technique). Therefore, changes in process conditions that produce changes in part mass beyond this range could be detected. Changes in part mass were usually associated with incomplete filling and voids.

Designed experiments were used to correlate process conditions to part mass and to optimise the processing conditions for complete filling, at the parameters set shown in Table 5-2. Chapter 6 presents a detailed discussion about optimising process conditions taking the geometrical differences of the mould into consideration. Subsequent chapters present changes in part mass due to process replicability.

5.8 Chapter conclusions

This paper concerns the design and manufacture process chain of a micromould for the manufacture of a polymer 3D microfluidic device. The 3D polymer device was designed for functioning as a blood/plasma separator for a lab-on-a-chip diagnostic device and was obtained by lamination of 5 layers.

The micromould was designed as a set of replaceable inserts to allow for adaptations in the microfluidic design during the prototyping stage. The mould cavities were manufactured using a micromilling centre by adapting a two plate mould designed to fit onto a Battenfeld Microsystem 50 micro-injection moulding machine.

The concept of replaceable inserts for micro-mould fabrication can be applied for the manufacture of all those polymer devices that still require a degree of design optimisation which can be only achieved by a trial and error process.

The designed layers were replicated by μIM of PMMA, and designed experiments were used to optimise processing condition for complete filling. Part mass, rather than feature dimension, was selected as the quality parameter to present degree of filling.

Initial separation tests of diluted animal blood samples were done using manually assembled devices. These showed successfully separation of red blood cells and plasma to a 79.9% efficiency.

6 An evaluation of process-parameter and part-geometry effects on the quality of filling in micro-injection moulding

Abstract

This paper addresses the use of micro-injection moulding for the fabrication of polymeric parts with microfeatures. Five separate parts with different micro-feature designs are moulded of Polymethylmethacrylate. The design-of-experiments approach is applied to correlate the quality of the parts to the processing parameters. Five processing parameters are investigated using a screening half-factorial experimentation plan to determine their possible effect on the filling quality of the moulded parts. The part mass is used as an output parameter to reflect the filling of the parts. The experiments showed that the holding pressure is the most significant processing parameter for all the different shapes. In addition, the experiments showed that the geometry of the parts plays a role in determining the significant processing parameters. For a more complex part, injection speed and mould temperature became statistically significant. A desirability function approach was successfully used to improve the filling quality of each part.

6.1 Introduction

Micro-injection moulding (μIM) is a polymer replication process of high potential for the mass-production of polymeric parts with microfeatures. Mass-production capabilities, high replication fidelity and the ability to process polymers of a wide range of properties are some of the advantages associated with μIM.

For some time the main approach to identify influential processing parameters in μIM was by changing one parameter at a time while keeping the others constant and then observing the effect of this parameter [20-22]. This approach was inherited from conventional injection moulding, as it was useful in drawing basic conclusions about how each parameter affects the filling quality of the moulded part.

This approach, however, has two main limitations [269]: the first limitation is that it is relatively time consuming when many parameters are being investigated. The

second drawback is that it does not take into consideration the effect of the interaction between two or more parameters, which is a relevant consideration in complex processes such as micromoulding.

The design-of-experiments (DOE) approach was introduced into this research domain as a useful alternative to this conventional method. A number of research groups have used a variety of DOE experimentation plans to investigate the relation between processing parameters and part-filling quality. A summary of the main DOE experiments is available in the literature [161].

The responses chosen for the experiments have included, filling quality of micro-sized channels [47], part dimensions [24,94,115-117], flow length [91,119], weld-line formation [118], demoulding forces [75] and filled volume fraction [120]. This is a reflection of the main research challenge in micro-moulding, which is the filling of small cavities. The choice of response is informed by such considerations as: is a specific dimension (or dimensions) critical for the part functionality, e.g. the depth of a channel or the diameter of a hole?, or is the order of magnitude of the part mass suitable for measurement?, e.g. variations in the part mass may be too small to be separated from experimental noise. DOE has also been used to minimise injection time, pressure and temperature distribution using a three-dimensional simulation package [114].

Results presented in the literature show that different DOE designs yield different outputs. For example, there is disagreement about the importance of holding pressure and injection speed. Furthermore, certain experiments have highlighted interactions between processing parameters which have not been seen in other work. These differences in experimental results may be due to the different geometrical shapes, polymers and experimental set-ups used in each experiment. It would, therefore, seem reasonable to claim that, at present, significant processing parameters in μIM are indentified on case-by-case basis and cannot be generalized for all situations.

This paper addresses the effect of processing parameters on the filling quality of μIM through a design-of-experiments (DOE) approach. In order to focus on the issue of general applicability highlighted above, the most influential processing parameters of five differently micro-structured parts were each investigated. The parts were of high enough mass to allow part mass to be used as the response. The polymer type (Polymethylmethacrylate (PMMA)) and grade were kept constant over the five micro-

parts. Optimized processing conditions were calculated and tested for each of the five parts. They were then compared, so that the effect of the part geometry on the filling behaviour of the polymer could be discussed.

It is worth noting in more detail the prior work which is closest to that of this present study. Whilst some DOE-based experimental data are available, in which part geometries have been deliberately varied within a single moulding [117], no prior work exists which assesses geometrically-different whole micro-moulded parts produced using a particular polymer. In the literature [44,115], part mass was used as the response for two different micro-parts, but the moulding polymer was also varied: a polyoxymethylene (POM) micro-gear and a polycarbonate (PC) lens array. The micro-gear consisted of a gear-and-shaft arrangement, where the gear diameter was 2.5 mm and the shaft length was 5 mm. It was produced with a three-plate mould with a gate diameter of 0.6 mm. The lens component had overall dimensions of 12x3x2 mm carrying lens surfaces of radii 0.35 and 0.5 mm with a gate diameter of 0.3 mm. Five processing parameters were evaluated, namely mould temperature, melt temperature, injection speed, metering size, hold pressure time and cooling time. For the gear structure, the holding pressure time and metering size were highlighted as significant parameters. For the lens array, metering size, injection speed and mould temperature were identified as most significant parameters.

6.2 Experiment

6.2.1 Methodology and equipment

In this experiment, five parts (*a* to *e*) with micro-scaled features were investigated. The parts, which were components of a microfluidic device, were designed to have the same external dimensions but different sets of features, both on the surface of, and through the component. Different definitions of micromoulding are in the literature [161], so the scope of micromoulding in this experiment was “macro” components with micro-structured regions.

The polymer chosen for this study was Polymethylmethacrylate (PMMA) (VS-UVT, Altuglas®). The grade was selected for its ease of flow (MFI = 24 g/10 min) and its optical transparency (light transmittance 92%). The micro-injection moulding machine was a Battenfeld Microsystems 50.

Five processing parameters were investigated as input factors: polymer-melt temperature (T_p), mould temperature (T_m), injection speed (V_i), holding pressure (P_h) and cooling time (t_c). The response (quality parameter) in all experiments was the part mass (W).

The experimental programme was conducted in three stages following the protocol laid out in Eriksson et al.: familiarization, screening, and optimization [269]. These are detailed in Section 6.2.4. Weighing of the moulded parts was done using a sensitive scale with a readability of 0.01 mg. Experimental data were processed and analysed using Minitab® 15 [270].

6.2.2 Part Geometry

The five moulded parts used in this study were all disc-shaped with a diameter of 10 mm and a thickness of 1 mm. The parts were designed to be building elements in a microfluidic device for a medical application. Each of the five components has a different set of micro-features, the majority of which are in place in order to form through-hole features in the final device. Figure 6-1 presents a schematic half-cross-section diagram of the five part designs (denoted by letters from *a* to *e*) with some of their critical dimensions.

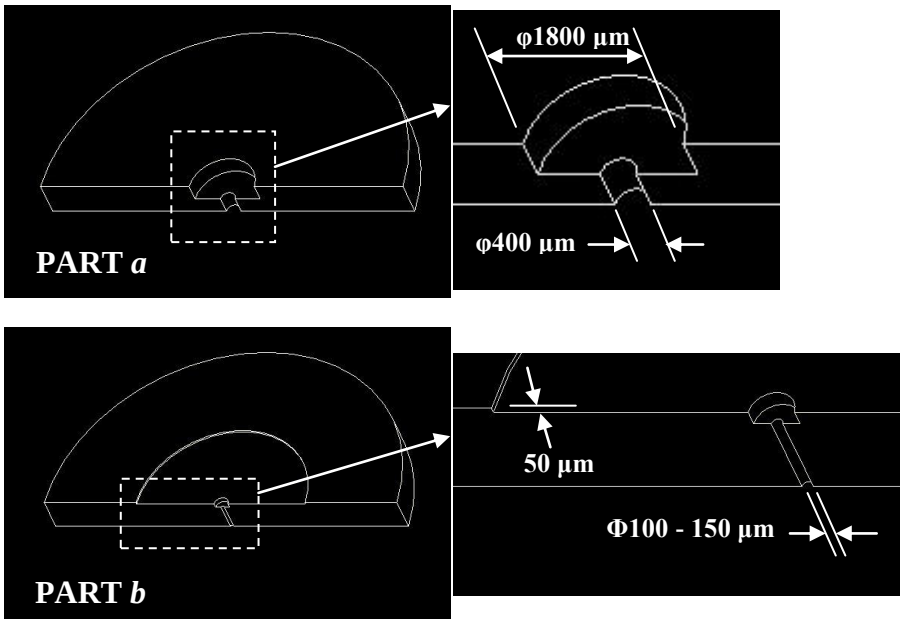

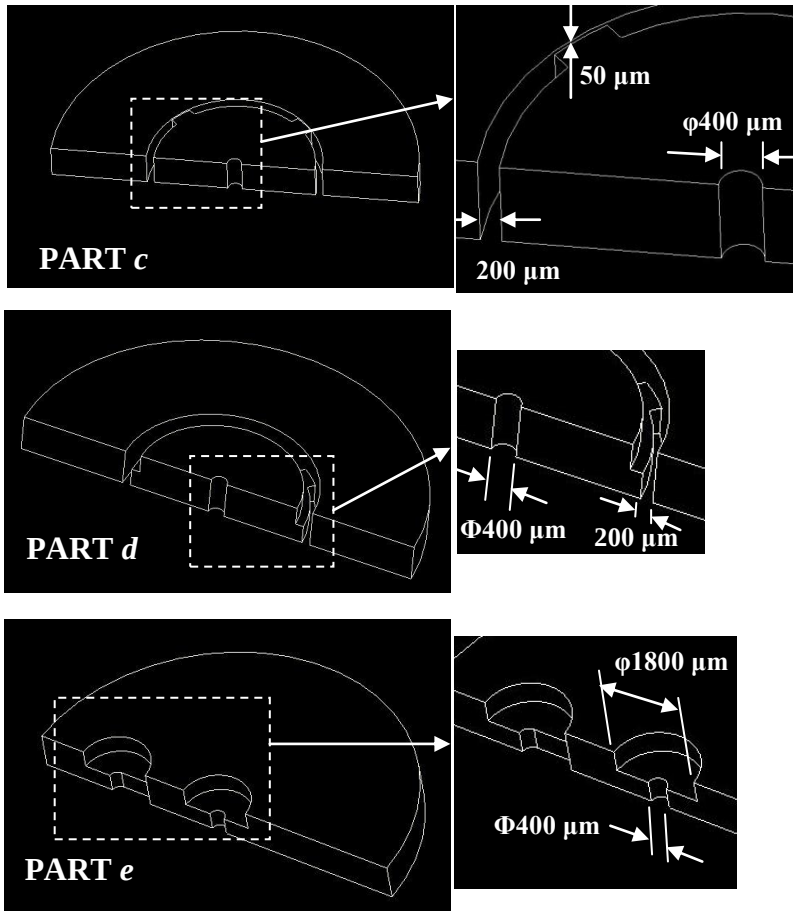

Figure 6-1 Half-cross-section diagrams of the five parts a to e with some of the main dimensions highlighted

6.2.3 Mould manufacturing

Each part was moulded by an individual aluminium mould that was housed within a main steel micro-mould body. A detailed description of the mould design and machining process for the mould inserts can be found elsewhere [271]. Figure 6-2 shows SEM images of two of the mould-inserts.

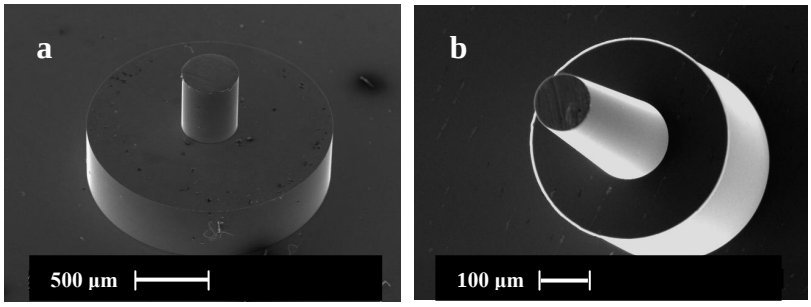

Figure 6-2 SEM micrographs of the micro-features of mould inserts

6.2.4 Experimentation stages

6.2.4.1 Familiarization stage

In the familiarization stage, a set of experiments were conducted in which the selected input parameters were assessed in order to determine the most extreme levels at which the experiment successfully yielded a response. This process window of parameters was then translated to become the high and low levels of the input parameters used in the screening experiments. The metering volumes of the parts were determined experimentally. The volume of each part was selected such that the polymer amount is enough to fill the cavity space without applying any holding pressure. The metering volumes are then kept constant throughout the experiments.

The sampling range was also determined, i.e. the number of moulding cycles after which the process is considered to become stable. Stability was defined as having been achieved when each of the moulded parts possess the same mass within a given tolerance.

The sampling range of the moulding process was determined using statistical control charts. The average mass of the produced parts become stable within the upper and lower limits of the chart after 30 to 40 continuous cycles depending on the mould insert used. As a standard practice, for each set of experimental conditions, samples were randomly collected after 50 cycles.

Table 6-1 shows the criteria used for selecting the upper and lower values for each parameter.

Factor	Selection criteria	
	Lower level	**Higher level**
T_p [°C]	The minimum value for this level was the recommendation of the material supplier (around 200°C). Based on experimentation, relatively higher temperatures were selected, such that the injection process ran continuously.	This was selected by experimentation as a safe high limit, above which signs of degradation appeared.
T_m [°C]	The minimum temperature was selected as the temperature recommended by the material supplier.	The high level was selected close to, but below, the Tg of the polymer (approx. 86°C).
P_h [bar]	The minimum holding pressure value was obtained from the literature [245].	The higher holding pressure value was selected not to cause the material to flash.
V_i [mm/s]	This value was selected based on experimentation.	This value was selected based on experimentation.
t_c [s]	The minimum value was calculated as the no-flow time, which is the time by which the gate was actually frozen.	The maximum was selected as approximately twice the minimum.

Table 6-1 Criteria for selecting the upper and lower levels of the experiment

Table 6-2 shows the upper and lower parameter levels selected for each of the five parts in addition to the metering volume selected for each part (including the runner system):

Part	Meter. Volume [mm^3]	T_p [°C]		T_m [°C]		V_i [mm/s]		P_h [bar]		t_c [s]	
		Low level (-)	High level (+)	Low level (-)	High level (+)	Low level (-)	High level (+)	Low level (-)	High level (+)	Low level (-)	High level (+)
a	179	240	255	70	81	200	300	250	500	4	7
b	178	230	250	72	80	200	300	100	300	4	7
c	177	230	250	72	84	200	300	100	300	3	6
d	177	230	250	72	84	200	300	100	300	3	6
e	177	230	250	70	84	150	300	100	300	3	6

Table 6-2 Higher and lower levels for the five tested parameters for the five parts

6.2.4.2 Screening stage

The screening stage consisted of the execution of the set of designed experiments. The number of samples and the levels of the input variables were obtained from the familiarization stage. Statistical software and regression models

were used to analyse the data. Significant processing parameters and interactions were determined.

The data obtained from the familiarization stage were used in the selected experimentation design. The DOE scheme used was a two-level, half-factorial 16-run (2^{5-1}) design.

This design was selected because it is a resolution-V design, which offers two advantages. Firstly, the number of experimental runs required is half that of a full factorial design. Secondly, this reduction in runs does not affect the results significantly. This is because the main effects are not confounded with other main effects or with second-order interactions and the second-order interactions are not confounded with each other.

The levels of the experimental runs are tabulated in Table 6-3. For each set of experiments, the order in which the experimental runs were conducted was randomized using a built-in randomization function in Minitab.

Standard Order	T_p [°C]	T_m [°C]	P_h [bar]	V_i [mm/s]	t_c [s]
1	-	-	-	-	+
2	+	-	-	-	-
3	-	+	-	-	-
4	+	+	-	-	+
5	-	-	+	-	-
6	+	-	+	-	+
7	-	+	+	-	+
8	+	+	+	-	-
9	-	-	-	+	-
10	+	-	-	+	+
11	-	+	-	+	+
12	+	+	-	+	-
13	-	-	+	+	+
14	+	-	+	+	-
15	-	+	+	+	-
16	+	+	+	+	+

Table 6-3 A half-factorial, two level 16-run (2^{5-1}) experimentation design

After stabilisation, ten samples were randomly collected for each run. The average mass of the samples was recorded as the experiment response. The experimental data collected was processed with Minitab® 15 and main-effects plots and Pareto charts were plotted.

One technique for correlating the factors to the response is by regression models. Similar to conventional regression models used to correlate two variables, a regression model can be used to fit the obtained responses to the input factors. The model can be linear, interaction, quadratic or even cubic, depending on the number of experiments conducted [269]. In this particular screening design, an interaction model was selected since it takes into consideration the effect of possible interactions on the response value. The selected regression model takes the following format:

$$y = c + \beta_1 x_1 + \beta_2 x_2 + \beta_3 x_3 + \beta_4 x_4 + \beta_5 x_5 + \beta_{12} x_1 x_2 + \beta_{13} x_1 x_3 + \beta_{14} x_1 x_4 + \ldots \quad (6\text{-}1)$$

In equation (6-1): y is the response, c is a constant, β values are the model-term coefficients and x_1 to x_5 are factors. The values and signs of the regression coefficients, β, represent the magnitude and the relation of each model term, respectively. Once the coefficients of equation (6-1) are determined, the response y of any set of given factors can be calculated.

The accuracy of the fit was evaluated by comparing the values of responses calculated from the model, based on the obtained coefficients, to the corresponding actual experimental values.

6.2.4.3 Determining optimum processing conditions

One approach to optimize the data obtained from the screening stage is to run another round of full factorial designs involving the influential parameters obtained during the screening stage. This approach is usually used when there are a number of influential factors with relatively close effects. A full factorial design would be implemented in this case to optimize the factors with a design that has no confounding factors. In this set of experiments, however, only one or two significant parameters are already identified from the screening stage, so optimization will basically focus on obtaining a suggested set of processing parameters that gives a required value of the response within specified limits.

Optimization was carried out using the desirability function approach to calculate optimum values of the input parameters [272,273]. This approach searches for a combination of values for input factors to satisfy a requirement for an output response (or multiple responses). The pre-set requirement of the function would be either to hit a target value within an upper and lower limit, to minimize the response value or to maximize the response value. Another pre-set value of the function is the

weight *r*, which specifies the function shape and emphasises (or deemphasises) the target value relative to the limit values.

In case of one response being optimized, the individual desirability can be represented by the equation [270]:

$$d_i = f_i(y)^{Wi} \qquad (6\text{-}2)$$

In equation (6-2), *Wi* is the weight of the response, in this case equal to 1, and the function *fi(y)* depends on whether the purpose of the optimisation is to hit a target, minimize or maximize. In this case, the function is desired to hit a target value *T* within upper and lower limits, so it can be represented by the following equation, where *U* and *L* are the upper and lower limits, respectively [273]:

$$f_i(y) = \begin{cases} 0 & y \prec L \\ \left(\dfrac{y-L}{T-L}\right) & L \le y \le T \\ \left(\dfrac{U-y}{U-T}\right) & T \le y \le U \\ 0 & y \succ U \end{cases} \qquad (6\text{-}3)$$

The function in equation (6-3) is linear because the weight *r* is set to 1. Otherwise, the bracket terms would have been raised to the power r_1 and r_2 that define the weights of the lower and upper limits, respectively.

For each of the five parts investigated in this set of experiments, the target, upper and lower values were selected based on the filling quality of the produced samples. This was undertaken as follows. For each part, after each set of experiments, samples of the 16 runs were inspected under the microscope to check their filling quality. Although each run had a different average mass, one or more runs (i.e. one or more combinations of factors) could have produced completely-filled samples. All the completely filled samples were weighed and an average mass was calculated. The filled samples that had the smallest and the largest masses were also identified. The average mass calculated from all of the filled samples was set as the target weight for the desirability function. The masses of the filled samples with smallest and largest mass values were used as the pre-set lower and upper limits of the desirability function, respectively.

6.3 Results

6.3.1 Responses from the screening experiments

Table 6-4 shows the average masses in milligrams of the 10 samples collected for each of the five parts:

Standard Order	T_p	T_m	P_h	V_i	t_c	Mass [mg] averaged from 10 samples				
						a	***b***	***c***	***d***	***e***
1	-	-	-	-	+	91.0	86.4	84.8	88.3	86.9
2	+	-	-	-	-	91.2	87.3	85.2	88.5	88.0
3	-	+	-	-	-	91.9	87.8	84.9	88.6	87.5
4	+	+	-	-	+	91.2	87.4	85.3	88.8	89.6
5	-	-	+	-	-	92.5	88.4	87.0	90.0	91.6
6	+	-	+	-	+	93.4	87.9	86.7	89.8	91.6
7	-	+	+	-	+	93.6	88.3	87.2	89.9	91.6
8	+	+	+	-	-	93.8	88.7	87.2	90.5	92.1
9	-	-	-	+	-	90.6	86.6	84.8	87.4	89.3
10	+	-	-	+	+	90.4	86.7	85.0	87.7	88.1
11	-	+	-	+	+	90.7	86.5	85.2	87.8	88.1
12	+	+	-	+	-	91.3	87.3	85.8	88.4	90.7
13	-	-	+	+	+	92.8	88.2	86.5	89.4	90.6
14	+	-	+	+	-	93.2	88.2	87.1	89.6	92.2
15	-	+	+	+	-	93.2	88.0	87.1	89.8	91.0
16	+	+	+	+	+	93.0	88.3	87.3	89.8	92.5

Table 6-4 Average masses in mg for each of the five parts

Figure 6-3 shows a number of SEM micrographs of the replicated plastic parts.

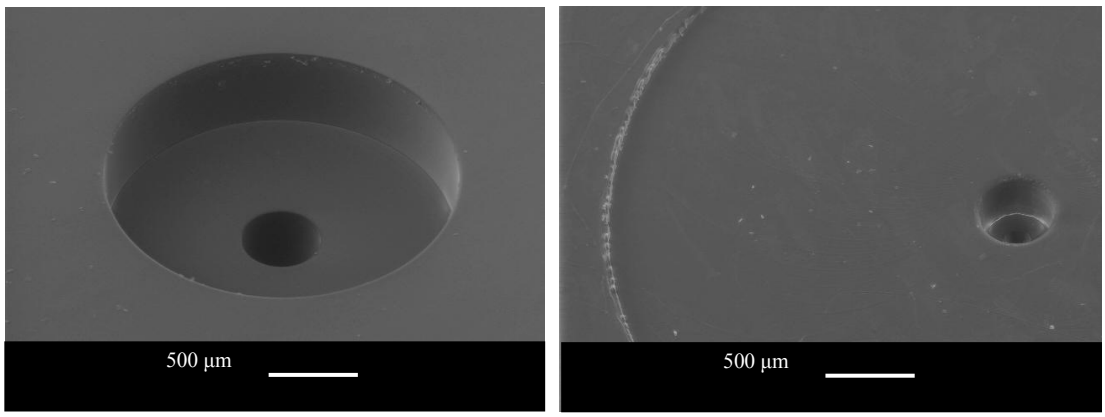

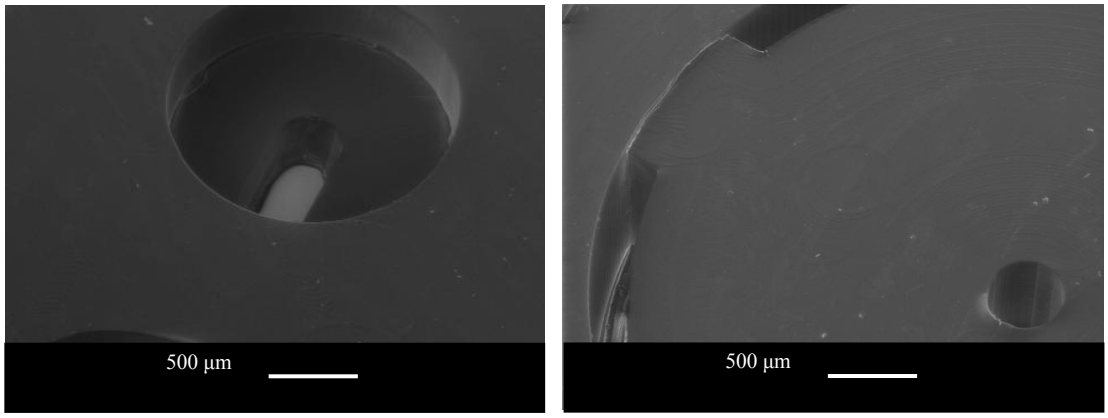

Figure 6-3 SEM images of some of the replicated plastic parts

Figures 6-4 to 6-8 show the Main-effects plots and Pareto charts of standardized effects plotted for the five moulded parts. A main-effect plot for a particular factor is a plot of the average of the data points at the low factor setting and the average of the data points at the high factor setting. The larger the slope of the line that connects the two averages, the more important the effect is. A Pareto chart is a bar chart where bars are ordered in decreasing magnitude. The greater the bar magnitude, the more effect its corresponding factor (or interaction) has on the response. In the Pareto chart the following symbol set is used: polymer-melt temperature (A), mould temperature (B), holding pressure (C), injection speed (D) and cooling time (E).

In figure 6-4 (a) main effect are plotted for each of the input parameters, with mass as the output parameter. Hence, for example, the first graph of figure 4a is a plot of mass against melt temperature (A).

In figure 6-4 (b) factor effects are plotted as a bar chart, which are related to the averages of the main-effect plots. Briefly, if Δ is the difference between the two averages of the response points for a particular factor, i.e. the difference between the two points connected by the sloped line, then the effect bar corresponding to that particular factor is the absolute value of half the effect, i.e. $|\Delta/2|$ [272].

Figure 6-4 (b) plots both the main input parameters, for example, C the holding pressure, and the interactions between input parameters, for example, BE, the interaction between the mould temperature and the cooling time. The vertical line on the figure corresponds to the threshold beyond which factors become statistically significant at the significance level determined by the value of alpha. This value is determined from the *t*-distribution, where *t* is the 1-(alpha/2) quantile of the

distribution [270]. The significance of the effect can be found by the relationship of the histogram value to this line. The alpha value, also referred to as the level of significance, is a measurement of risk in detecting effects, and is expressed as a probability between 0 and 1. An alpha value of 0.05 indicates that the chance of finding an effect that does not exist is only 5% (a confidence limit of 95%).

Figures 6-5 to 6-8, representing the screening experiment data for parts *b* to *e*, are plotted using the same approach.

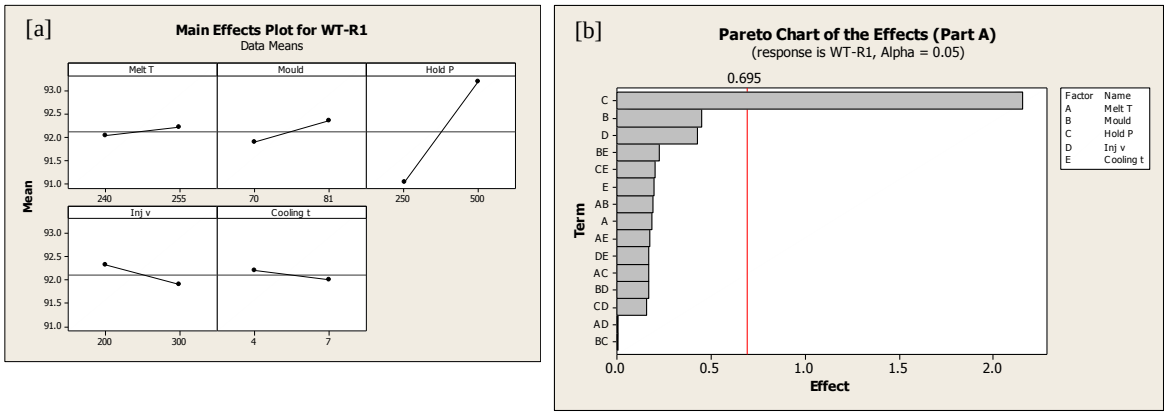

Figure 6-4 Screening results for part *a*: [a] Main effects plot, and [b] Pareto chart

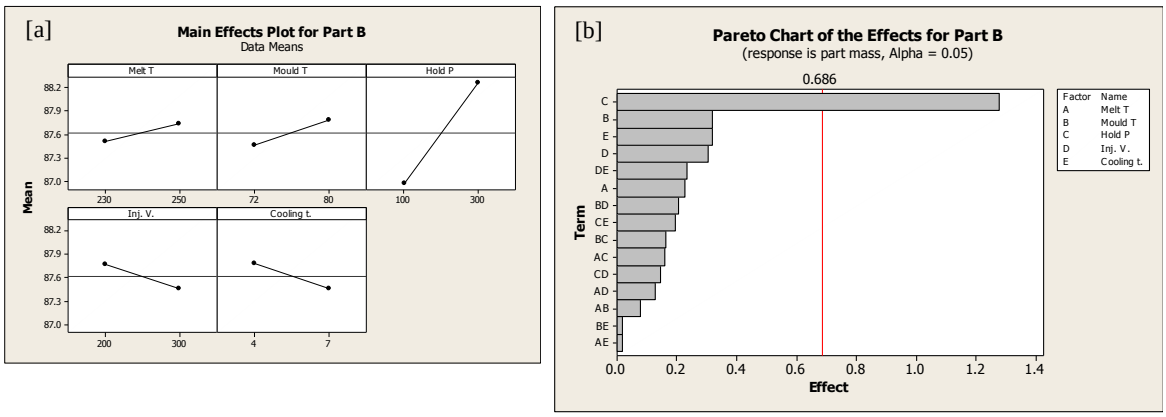

Figure 6-5 Screening results for part *b*: [a] Main effects plot, and [b] Pareto chart

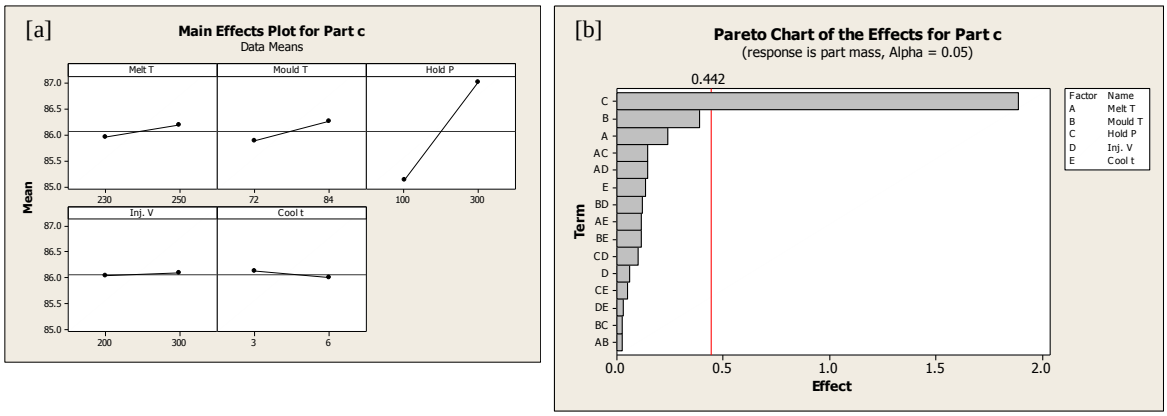

Figure 6-6 Screening results for part *c*: [a] Main effects plot, and [b] Pareto chart

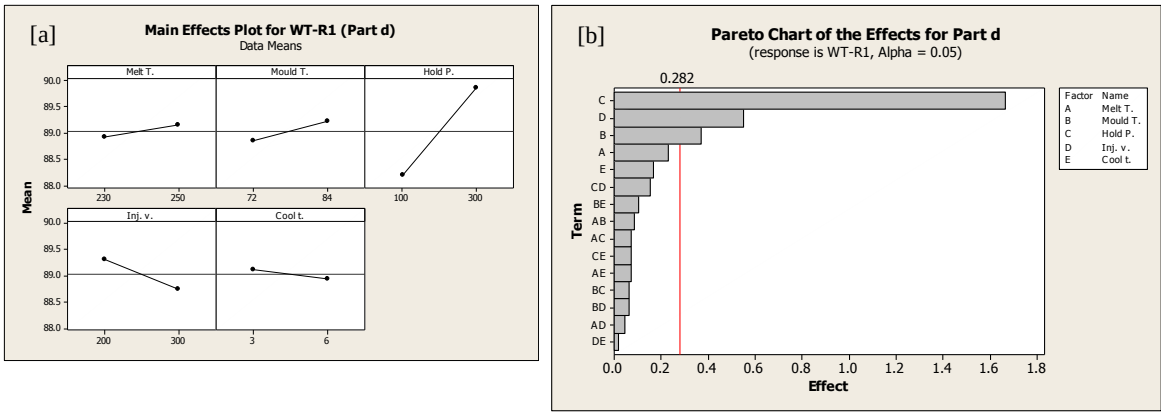

Figure 6-7 Screening results for part *d*: [a] Main effects plot, and [b] Pareto chart

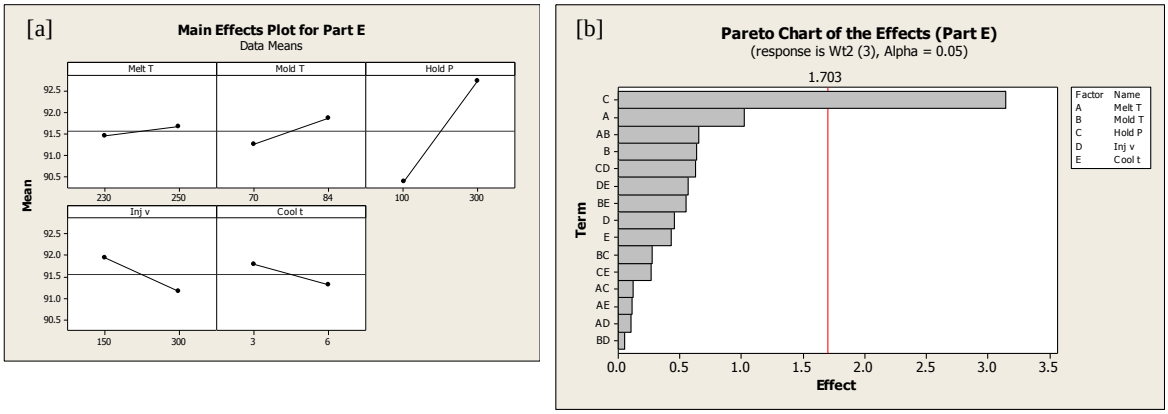

Figure 6-8 Screening results for part *e*: [a] Main effects plot, and [b] Pareto chart

6.3.2 Desirability function processing conditions

Table 6-5 tabulates desired part mass, the calculated optimum values of the process parameters to achieve these mass values and actual part mass obtained experimentally at these processing conditions.

The desired part masses were derived from the screening experiments. The moulded samples are inspected, and the completely filled samples are identified and weighed. The average mass of the complete samples is used as the "target" mass for the desirability function. The minimum and maximum masses of the completely filled samples are input as the lower and upper limits for the target mass, respectively. They are tabulated in Table 6-5 as the target mass and a minimum and maximum acceptable mass value.

The experimental conditions, i.e. the levels of the input parameters, predicted to achieve those masses are outputs of the desirability function. These are tabulated in table 6-5 for each of the five input variables (denoted as "required levels").

In Table 6-5, the "experimental mass" is the average mass of ten samples collected randomly after the moulding machine had reached stability. The minimum and maximum values are the mass of the samples with lowest and highest mass magnitude within the ten samples, respectively.

Part	**Desired mass [mg]**			**Required levels of process parameters**					**Experimental mass [mg]**		
	Target	Min.	Max.	T_p [°C]	T_m [°C]	V_i [mm/s]	P_h [bar]	t_c [sec]	Avg.	Min.	Max.
a	93.1	92.6	93.6	250	81	200	416	4	93.1	92.9	93.3
b	88.6	88.2	89.0	250	80	200	300	4	88.7	88.4	88.9
c	86.5	86.0	87.0	250	81	300	170	3	86.7	86.2	86.9
d	90.0	89.6	90.4	250	84	200	300	3	90.1	89.9	90.3
e	92.5	92.0	93.0	243	84	300	300	3	92.0	91.8	92.2

Table 6-5 Required masses and limits, calculated optimum parameters and corresponding experimental results

6.4 Discussion

6.4.1 Screening stage

Figures 6-4 to 6-8 show a significant effect of holding pressure for all the five parts, with four parts, *a*, *b*, *c* and *e*, showing it as the only significant effect. This substantial effect was also visible during the experiments, as all samples that were produced at a lower level of holding pressure exhibited evidence of incomplete filling, regardless of the levels of the other four parameters. In contrast, cooling time had no effect for any of the parts.

For Part *d*, three significant effects were observed: holding pressure, injection velocity and mould temperature. However, aside from Part *d*, mould temperature and injection velocity had no apparent effect on the mass of other parts.

The importance of holding pressure lies in the fact that it overcomes the tendency of the polymer melt to prematurely freeze before the injection process is complete. Premature freezing is likely to be exacerbated by the relatively high rate of heat transfer between the polymer and the mould walls for parts with micro-scaled dimensions. In prior work [44,115], metering volume and holding pressure time were used as factors. In this work, metering size was kept constant, as it was determined from the familiarization stage (Section 6.2.4.1), and the holding pressure value was used rather than the holding pressure time. It is possible that both the holding pressure magnitude and time (or their interaction) would be significant if they are used together as factors in a more extended DOE plan.

The lack of significance of cooling time is consistent with previous work [44,115]. This is because the effect of cooling in injection moulding is usually associated with changes in the component geometry (e.g. shrinkage, warpage) [245], but the cooling scheme does not have the same effect on the part weight as its effect takes place after the cavity is already filled.

The lack of significance of mould temperature may lie in the selection of the two levels at values below the T_g of the polymer. This is consistent with the data presented in [114] where increasing the mould temperature improved the filling quality, although all the experiments were performed while the mould temperature was below the T_g of the PMMA. It is less consistent with the numerical simulation

data of [115] which predicted short shots unless the mould temperature was raised above the T_g of the PMMA.

The general tendency found here of the lack of significance of melt temperature was also found in prior work. For small part volumes, like those found in micro-moulding, the melt temperature decreases at a very high rate once the polymer contacts the cavity walls, as long as the mould temperature is kept below the melt temperature of the polymer [254]. In the work presented here, both the high and low levels of the mould temperature were kept below T_g. Hence, by the time the polymer filled the part cavity it would have seen a significant reduction in its temperature.

The lack of significance of the injection velocity as a parameter may lie in the relatively small change of shear rate associated with changing between the two levels of injection velocity. The relation between shear rate and injection velocity can be approximated by [245]:

$$\dot{\gamma} = \frac{4\dot{Q}}{\pi r^3} \qquad (6\text{-}4)$$

In equation (6-4), $\dot{Q}$ is the volume flow rate, and r is the radius of the flow path cross section (in this case the part gate). The flow rate is a function of the injection speed V_i, so equation (6-4) can be rewritten as:

$$\dot{\gamma} = \frac{4V_i R^2}{r^3} \qquad (6\text{-}5)$$

In equation (6-5), R is the radius of the injection plunger.

Since the gates have a rectangular cross section (1x0.5 mm), the equivalent hydraulic diameter may be used in equation (6-5) to estimate the value of r. The calculated shear rates based on low-level and high-level value for injection velocity both have an order of magnitude of 10^5 s^{-1}. Shear rate vs. viscosity data for the PMMA grade used indicates that these shear rates correspond to viscosities in the order of 10^1 Pa.s at 230°C at which no significant shear-thinning behaviour would be observed.

6.4.2 Desirability function processing conditions

Table 6-5 presented the suggested processing parameters for improved filling, which are obtained by meeting the conditions listed in equation (6-3). It should be noted that the desirability function cannot recommend parameter values outside the

lower and high levels of the factors. Whilst certain parameter values in Table 6-5 lie between the high and low levels, the majority lie either at the high level or the low level. This is indicates that the desirability function might have recommended an even higher or lower level of the parameter, had the original levels been more widely spread.

Table 6-5 shows also that the average masses of the parts produced under the conditions predicted by the desirability function lie within 0.5% of the specified target values. All the produced parts were within the mass upper limit pre-set in the function, but for Parts *b* and *e*, some of the produced samples were under the lower limit by approximately 0.2 mg.

Figure 6-9 shows an example of how the desirability function improved the filling quality of the parts. Figure 6-9 (a) shows a view of a sample of Part *d* from the screening stage (run 5) where some areas of the edges that are close to the last filled point are incomplete. Voids can also be seen on the surface around the cylindrical hole. Figure 6-9 (b) shows the same part after application of the desirability function, where the edges are completely filled and voids are no longer apparent on the part surface.

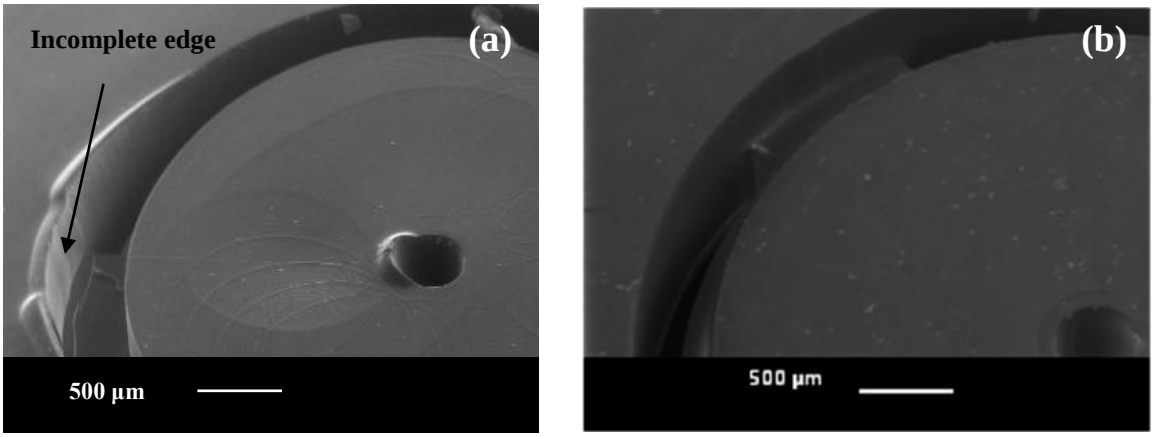

Figure 6-9 SEM micrograph of samples of Part *d*. 4(a) an example before applying the desirability function (T_p = 230°C, T_m =72°C, V_i = 300 mm/s, P_h = 100 bar and t_c = 3 s); 4(b) after applying the desirability function (T_p = 250°C, T_m =84°C, V_i = 200 mm/s, P_h = 300 bar and t_c = 3)

Table 6-5 shows the data from applying the desirability function independently to each part. However, an individual-part desirability function approach is difficult to extend to a prediction of any compromise parameters which would be result in

relatively high filling quality for all the five parts if they were produced by a single mould in one shot.

One method to achieve such a compromise might be to discern if there were general trends that could be observed when comparing the desirability function to the screening parameters, and then apply these trends in required process parameters to establish compromise conditions. In effect, this means comparing the required levels of process parameters in Table 6-5 with the envelope of parameter high and low levels of Table 6-2. Such a comparison does show that general trends are present, independent of the part shape. The desirability function predicts that setting the melt temperature, mould temperature and holding pressure to their high levels would generally result in better filling, as does, with a few exceptions, setting the injection velocity and cooling temperature to their low levels.

Table 6-6 shows a set of compromise processing conditions constructed following these general trends in desirable process parameters. To test this prediction, the micro-mould was reconfigured such that all the five parts are injected through a common runner system, and parts processed using the conditions of Table 6-6.

Parameter	**T_p [°C]**	**T_m [°C]**	**V_i [mm/s]**	**P_h [bar]**	**t_c [s]**
Value	250	84	200	300	3

Table 6-6 Processing parameters for a five-part micro-moulded component

The produced part is shown in Figure 6-10, where all the parts were checked under the microscope to be completely filled.

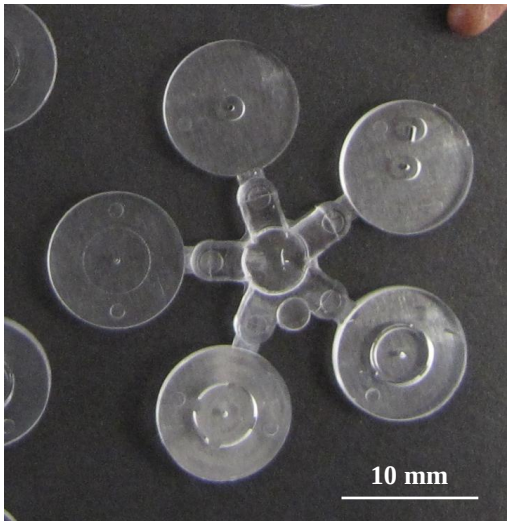

Figure 6-10 A photograph of a completely filled, five-part plastic component produced under compromise conditions

6.4.3 Effect of part geometry

The results shown in Figures 6-4 to 6-8 provide some information on the effect of the mould geometry on the filling quality of the part.

As noted in section 6.4.1, for Part *d*, other effects, in addition to the holding pressure, were of significance in filling quality. It seems likely that this is owing to the relatively high geometrical complexity of this part in comparison to the other parts. This complexity is generated from the four micro-scaled flow paths that exist in Part *d*, which represent a rapid change in part thickness that imposes 'extra resistance' on the flow of the material to completely fill the cavity. Figure 6-11 presents photographs of mouldings of Parts *a* and *d*, as being at the two extremes of geometrical complexity amongst the five moulded parts. The mouldings are 'short shots' produced to visualise the difference in filling sequence between the two parts.

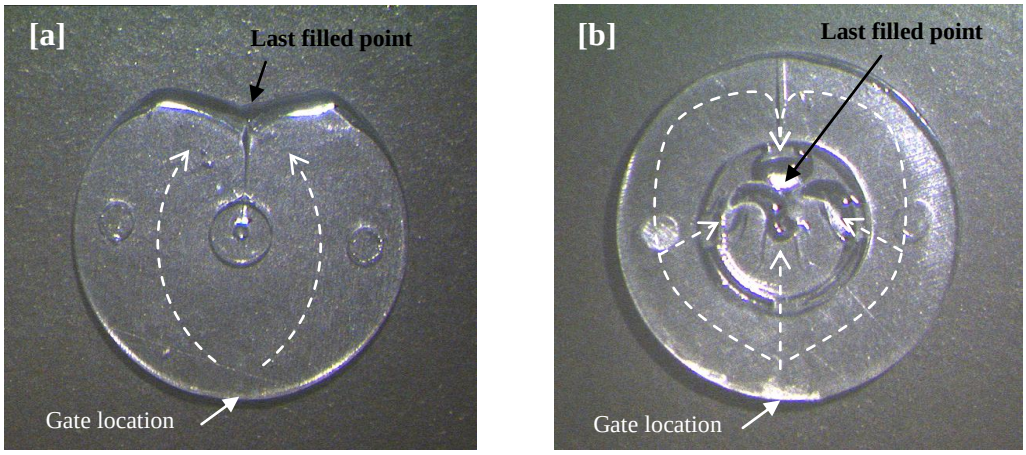

Figure 6-11 (a) Short shot of Part *a*. (b) Short shot of Part *d*

In Part *a* the last filled point is located at the far end of the flow path, whereas in Part *d* the last filled point is located close to the centre. Such differences are expected as a consequence of the 'hesitation effect' commonly seen in polymer flow, where, in cavities with varying thickness values, polymer melts tend to fill areas with larger thickness before they flow into smaller thicknesses. In Part *a*, where the part thickness is uniform, the polymer fills the cavity gradually as the flow path is divided at the central "pin" of the mould and then rejoins afterwards forming a weld line. In Part *d*, the rapid change in thickness causes the polymer flow to experience hesitation during the filling process, and a higher injection pressure will be required for the polymer to flow through these features. Larger flow-path cross-sections, for example the

perimeter of the shape in Part *d*, are filled before the polymer starts to pass through the four "openings" at the centre area of the part (see Figure 6-1 Part *d*).

Owing to the relatively small dimensions of each of the four openings (500 x 600 μm) a high possibility of premature freezing would be expected at these locations. Similarly to conventional injection moulding, the cooling time of the polymer during micromoulding is dependent, among other factors, on the part thickness squared [254]. This indicates that the cooling process in Part *d*, where, in the four opening areas, the minimum thickness is 500 μm, is much faster than, for example, Parts *a* and *b*, where the minimum thickness is 950 μm to 1 mm.

The rapid decrease in thickness does not only affect the freezing process, but it also influences other parameters. As suggested in the literature [254], as the part thickness decreases to fractions of a millimetre, a drastic increase is observed in the injection pressure required to fill the cavity, and a higher possibility of incomplete filling is expected. This is particularly observed for cold-mould filling, i.e. when mould temperature is lower than the melt temperature, as is the case in this work. This explains why mould temperature becomes significant at such rapid changes in thickness as seen in Part *d*. Part thickness also affects the role of injection speed on the required filling pressure. As the thickness decreases, the variation in injection speed becomes more significant in affecting the injection pressure required to fill the mould cavity [254].

6.5 Conclusions

In order to investigate the effect of part geometry on moulding parameters, this paper investigated the moulding parameters of five different micro-parts using mass as an experiment response. Parts differed in the through-hole and surface geometries, but had a constant outer radius and similar thicknesses. The same polymer, a PMMA grade, was used throughout the experiments.

A three-stage design of experiments approach consisting of feasibility, screening and desirability function, was undertaken to evaluate the filling quality in micro-injection moulding and correlate it to the processing parameters. It was shown that holding pressure was the main influential processing parameter for all of the part geometries.

A comparison of desirable moulding parameters for different part geometries, showed the influence of geometry on processing conditions. Sharp changes in thickness within a part correlated with an increase in the number of significant moulding parameters. For a complex part, injection speed and mould temperature became statistically significant.

For each part, a desirability function was used to specify a combination of processing conditions that would improve filling quality. The produced parts had average masses that were within 0.5% of the target values.

Comparing the desirability function predictions with the high and low parameter values of the screening stage showed, with some exceptions, that regardless of part geometry, desirability function predictions for a particular process parameter exhibited clustering behaviour. These trends in clustering behaviour were used to produce a set of compromise moulding conditions to micromould a multi-part component. Multi-part components moulded using these parameters exhibited complete filling in each of the five parts.

7 Evaluating and controlling process variability in micro-injection moulding

Abstract

An important quality aspect of micro-injection moulding is to ensure the consistency of replicated components by minimising process variability. This paper implemented a design-of-experiments approach, where five process parameters were investigated for possible effects on the process variability of two components. The variability was represented by the standard deviation of the replicated part mass. It was found that melt temperature was a significant source of variability in part mass for one of the components. Optimisations tools such as response surfaces and desirability functions were implemented to minimize mass variability by more than 40%.

7.1 Introduction

Micro-injection moulding, a key technology in high-volume micro-manufacturing, requires accurate control of quality parameters to ensure the replication fidelity and consistency of produced components.

The design-of-experiments (DOE) approach has been used in the recent years to evaluate and control the effect of processing parameters on the replication quality of micro-injection moulding (μIM) [161]. DOE allows the correlation of process inputs and outputs whilst using less experiments compared to the conventional approach of changing one parameter at a time. It is also used to detect interactions between input factors.

Typical processing parameters (factors) include polymer-melt temperature, mould temperature, holding pressure, cooling time, injection velocity and metering volume. Quality parameters (responses) are usually associated with evaluating the replication fidelity of the processes associate with the complete filling of the mould cavity. Typical responses include filling quality of micro-sized channels [47], feature dimension [24,94,116,117], part mass [44,115,274], flow length [91,119], filling volume fraction

[120], weld-line formation [118], demoulding forces [75] and minimising injection time, pressure and temperature distribution using a three-dimensional simulation package [114].

However, a processing aspect that is rarely addressed in the literature is the possible influence of process parameters on the variability of the response in micro-injection moulding.

Variation occurs normally in industrial processes, which means that measuring a specific output value from the process will reveal differences in measurements between experimental runs even if the processing conditions are kept the same [275]. However, an important element of understanding the effect of processing conditions on the process output is to be able to distinguish between variations that are attributed to changes in factors and those that result from other causes. The former variations are usually referred to as the *signal* [276], or *systematic variability* [269], which is the change of response that the experimenter is seeking to detect. The latter is usually referred to as the *noise*, *scatter* or *unsystematic variability* of the response that occurs during standard operation conditions. Hence, a fairly high signal-to-noise ration, for example from 4 to 10 [275], is favourable, because it indicates that the effect of changing the factors can be distinguished from experimental noise.

A concept relevant to experimental signal and noise is the difference between *replicates* and *repeats*. *Replication* is the process of conducting experimental trials in a random order, such that factor combination is kept the same, while each experimental trial is done independently [273,275,276]. *Repetition*, on the other hand, is the process of running experimental trials under the same setup of machine parameters. Replicates are useful for improving the chance of detecting statistically significant factors (signals) from within the natural process variation (noise). The more replicates undertaken, the higher are the chances of accurately identifying signals from process noise.

This paper investigates controlling process variability in micro-injection moulding. It compares the "natural" process variation to variations attributed to specific factors. Two micro-moulded Polymethyl Methacrylate (PMMA) components were experimentally tested to determine process variability and its effect on the produced part mass. Optimisation tools such as response curves and desirability functions are applied to minimize process variation.

7.2 Experiment

7.2.1 Component geometries

The two components, denoted as Part 1 and Part 2, were assembly elements of a microfluidic device. (A description of the device functionality and process chain is available in the literature [271]). The components were of the same radial dimension and both contained through-section holes. However, the shape complexity and the dimensions of the micro-features varied between components. Part 1 consisted of simple cylindrical features with a relatively large surrounding space for polymer melt to freely fill the cavity. Part 2, on the other hand, contained more complex features that would pose relatively "challenging" flow paths for polymer flow. Figure 7-1 shows SEM micrographs of the mould inserts and corresponding PMMA replicates for both components.

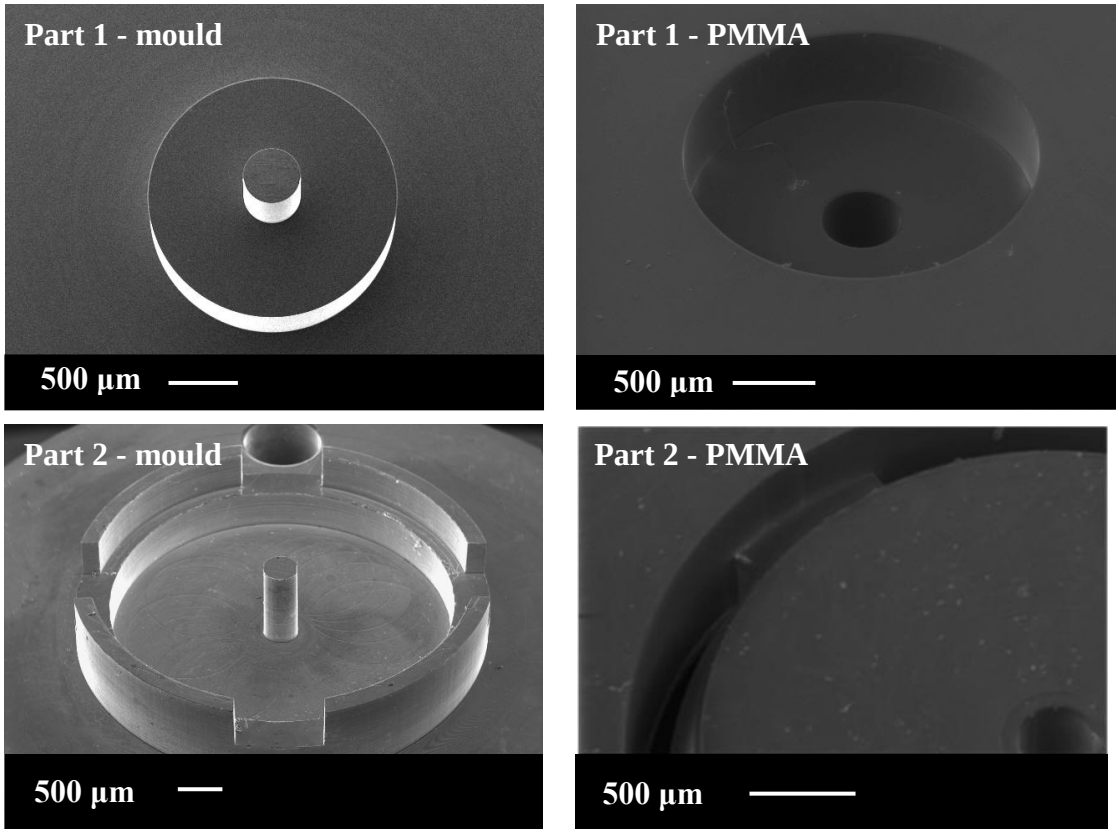

Figure 7-1 SEM micrographs of mould-inserts and replicated PMMA parts of the two tested components

7.2.2 Methodology and equipment

Five processing parameters were investigated: Polymer-melt temperature (T_p), mould temperature (T_m), holding pressure (P_h), Injection velocity (V_i) and cooling time (t_c). The data collected was the component mass (W).

A 2-level, half-factorial design of Resolution-V (2^{5-1}) was selected for this application. In this design the main effects are not confounded with other main effects or with second-order interactions, and the second-order interactions are not confounded with each other. This allowed for a relatively small number of experiments to be undertaken without significantly compromising the accuracy of the results.

The micro moulding machine used is a Battenfeld Microsystems 50. The PMMA grade was VS-UVT from Altuglas®. This particular grade was selected for its ease of flow (MFI = 24 g/10 min) and its optical transparency (light transmittance 92%). A sensitive weighing scale with a readability of 0.01 mg was used to weigh the parts. Data analysis and optimization was conducted with Minitab® 15 [270].

7.2.3 Experimentation design and procedure

The low and high levels of the factors were determined by several different methods. For T_p and T_m, the levels were determined by polymer supplier recommendations. For the P_h, the levels were determined from the literature [245]. Injection velocity and cooling time levels were selected based on initial experimental tests. Table 7-1 presents the levels of the five factors for the tested components.

Part	Metering Volume [mm^3]	T_p [°C]		T_m [°C]		V_i [mm/s]		P_h [bar]		t_c [s]	
		Low level (-)	High level (+)	Low level (-)	High level (+)	Low level (-)	High level (+)	Low level (-)	High level (+)	Low level (-)	High level (+)
1	179	240	255	70	81	200	300	250	500	4	7
2	177	230	250	72	84	200	300	100	300	3	6

Table 7-1 Higher and lower levels for the five factors for Part 1 and Part 2

Table 7-2 presents the half-factorial design in its standard order. All runs were randomised using a built-in randomisation function in Minitab. For each run, the moulder was left to operate for 50 cycles to ensure process stability, and then 10 parts

are collected to represent the samples of the process "repeats" for that particular run. An average mass (W) was obtained from 10 samples for each run. Each set of designed experiments was repeated 3 times, R1 to R3, where runs are conducted in a random order in each replicate, such that 3 "replicates" are obtained for each experimental run.

Standard Order	T_p [°C]	T_m [°C]	P_h [bar]	V_i [mm/s]	t_c [s]
1	-	-	-	-	+
2	+	-	-	-	-
3	-	+	-	-	-
4	+	+	-	-	+
5	-	-	+	-	-
6	+	-	+	-	+
7	-	+	+	-	+
8	+	+	+	-	-
9	-	-	-	+	-
10	+	-	-	+	+
11	-	+	-	+	+
12	+	+	-	+	-
13	-	-	+	+	+
14	+	-	+	+	-
15	-	+	+	+	-
16	+	+	+	+	+

Table 7-2 A half-factorial, two level 16-run (2^{5-1}) experimentation design

The purpose of the experiment was to detect potential influential process parameters that affect the *variability* in part mass rather than the mass of the part itself. Therefore, the response of the experiment design was required to be a parameter that reflects variability in mass rather than the mass magnitude. Standard deviation (SD) of the process replicates would be such a measure. However, as SD does not follow a normal distribution, an assumption in DOE, it could not be used as a direct response to the experiments. Hence, the natural logarithm of the SD was used as the experimental response [273,276]. Specifically, the response of the factorial design was set as ln (SD) of the 3 replicates. The possible influences of the processing parameters on the response were detected and analysed.

The experimental data is presented below in a series of Pareto charts, where the magnitude of each bar was calculated from the half the difference, i.e. $|\Delta/2|$, of the responses obtained for the average masses measured at the low and high levels of a specific factor (or interaction). Alpha represented a measurement of risk, the value of 0.05 indicating a confidence limit of 95%. The vertical line on each Pareto chart corresponded to the threshold beyond which factors become statistically significant, where the significance threshold was determined by the chosen value of alpha. The value of the line was determined from the *t*-distribution, where *t* is the 1-(alpha/2) quantile of the distribution [270].

7.2.4 Minimising process variability

As noted above, if the DOE design revealed no significant effect of any factor on the process variability, this would indicate that variation in part mass could be attributed to the "natural" noise of the process, and that none of the chosen input factors had played a role in this variation. If, on the other hand, one or more factors were shown to be statistically significant in process variation, this would indicate that a certain "signal" was detectable from particular factor(s). In this latter case there would be a possibility to minimize or at least decrease this variability using an optimization tool.

In this paper, two methods were used to provide guidance on minimising detected variability. Firstly, surface plots were used to visualise and minimize the effect of influential factors. Secondly, a desirability-function tool was also implemented to predict a combination of factor values that would render a target *T*, where that target was to minimise the response beyond a pre-set upper limit *U*.

For the example of one response being optimized, the individual desirability can be represented by the equation [273]:

$$f_i(y) = \begin{cases} 1 & y \prec L \\ \left(\dfrac{U-y}{U-T}\right)^r & T \le y \le U \\ 0 & y \succ U \end{cases} \qquad (7\text{-}1)$$

The response, *y*, varies over a range between 0 and 1, where 1 corresponds to achieving the target and 0 where the function is outside the pre-set limits. In Equation

(7-1), the function weight, *r*, determines the shape of the function, which was set to be linear in this set of experiments, the simplest use of the function.

7.3 Results

7.3.1 Part mass data

Table 7-3 shows the measurements of mass obtained from the produced parts. R1 to R3 represent the three "replicates" of each experimental run. Each mass reported in the table was the average mass of 10 repeats. The table also presents the average of part mass for the 3 replicates of each run, W_1 and W_2 respectively, the standard deviation of the replicate masses and the ln (SD) of the replicate masses.

	T_p	T_m	P_h	V_i	t_c	Part 1					Part 2				
						Average masses of replicates [mg]			W_1 [mg]	ln (SD)	Average masses of replicates [mg]			W_2 [mg]	ln (SD)
						R1	R2	R3			R1	R2	R3		
1	-	-	-	-	+	91.1	91.2	91.3	91.2	-2.61	88.3	88.1	88.9	88.4	-0.78
2	+	-	-	-	-	91.3	91.8	92.7	91.9	-0.33	88.5	88.8	88.6	88.6	-2.76
3	-	+	-	-	-	92.0	92.2	92.4	92.2	-1.59	88.6	89.4	89.3	89.1	-1.68
4	+	+	-	-	+	91.2	92.0	92.8	92.0	-0.24	88.8	89.1	89.1	89.0	-2.49
5	-	-	+	-	-	92.6	94.1	95.2	93.9	0.28	90.0	90.8	90.2	90.3	-1.67
6	+	-	+	-	+	93.5	93.4	94.9	94.0	-0.16	89.8	90.2	89.9	90.0	-2.53
7	-	+	+	-	+	93.7	94.2	95.2	94.4	-0.31	89.9	90.3	90.5	90.2	-2.11
8	+	+	+	-	-	93.9	94.1	94.5	94.2	-1.20	90.5	90.8	90.8	90.7	-2.62
9	-	-	-	+	-	90.7	91.6	92.2	91.5	-0.26	87.4	87.9	87.9	87.7	-2.02
10	+	-	-	+	+	90.5	90.7	91.1	90.8	-1.24	87.7	87.8	88.0	87.8	-2.71
11	-	+	-	+	+	90.8	91.5	91.3	91.2	-0.97	87.8	87.9	88.3	88.0	-2.11
12	+	+	-	+	-	91.4	91.6	92.6	91.9	-0.46	88.4	88.2	88.2	88.3	-2.83
13	-	-	+	+	+	92.9	94.3	93.6	93.6	-0.38	89.4	90.0	90.0	89.8	-1.86
14	+	-	+	+	-	93.4	93.5	95.0	93.9	-0.10	89.6	90.2	90.1	89.9	-2.06
15	-	+	+	+	-	93.3	94.1	95.2	94.2	-0.08	89.8	90.4	90.0	90.1	-2.05
16	+	+	+	+	+	93.1	93.6	94.0	93.6	-0.82	89.8	90.2	90.1	90.0	-2.29

Table 7-3 Average masses of measured repeats for each of the three replicates (R1 to R3)

Figures 7-2 and 7-3 plot graphically the data of Table 7-3 for Part 1 and Part 2, respectively. The points represent the ten-part average part-mass data for each of the three replicates. The vertical lines represent the standard deviations of the corresponding 10 repeats.

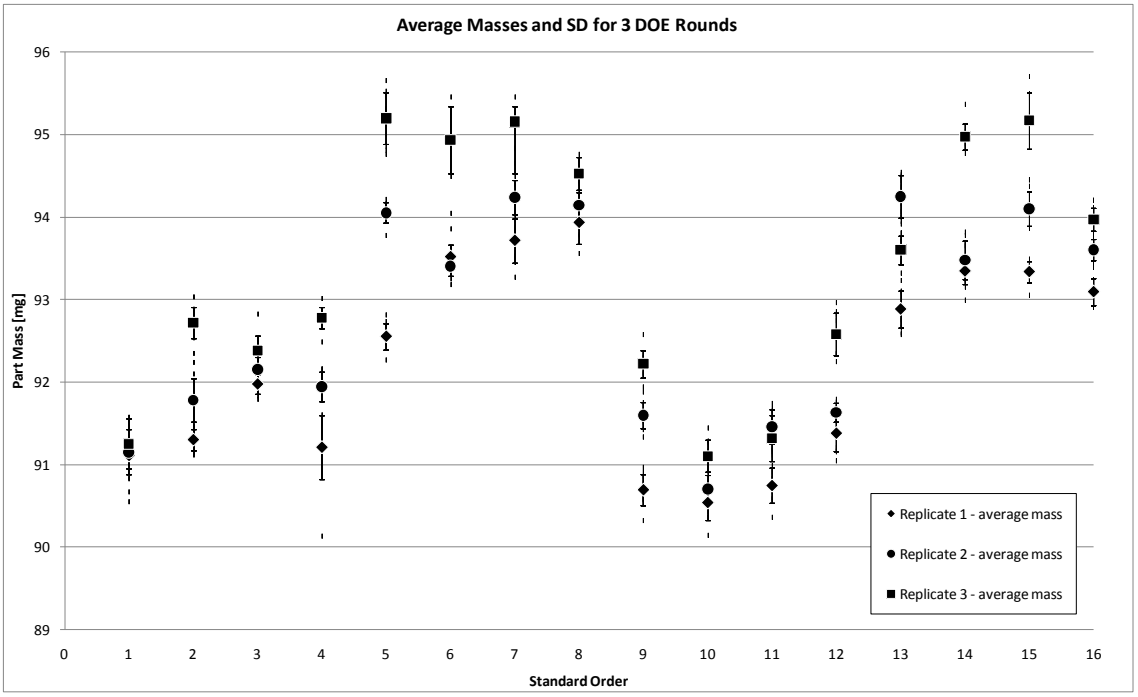

Figure 7-2 Part 1: Average masses of three replicates and their corresponding standard deviations

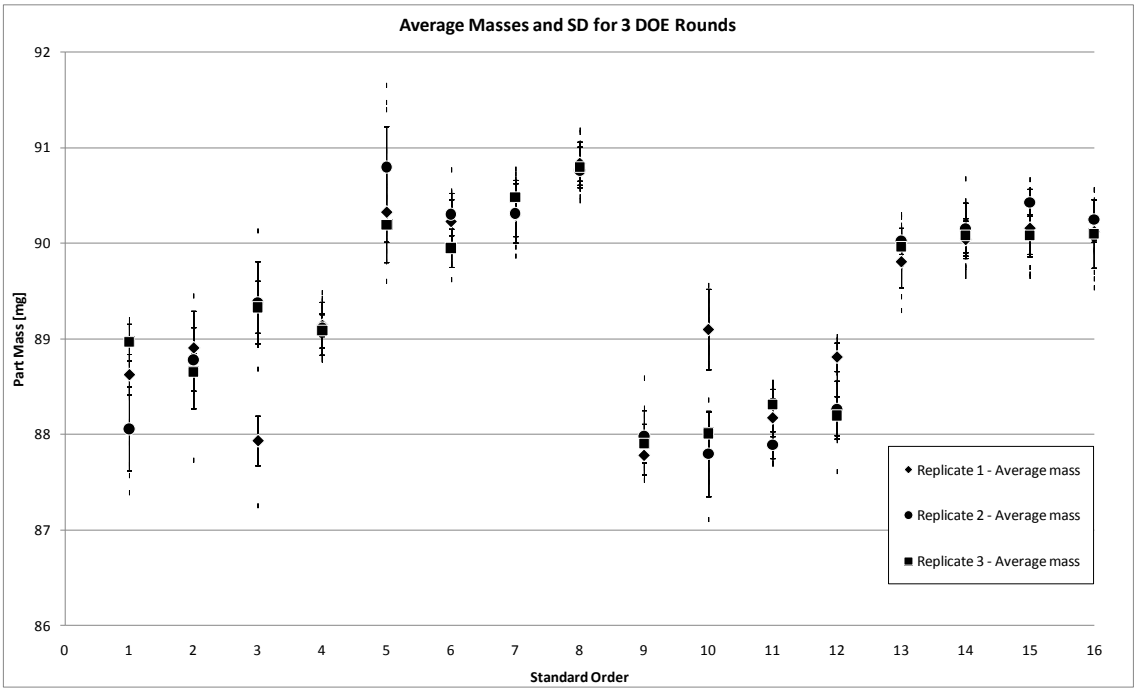

Figure 7-3 Part 2: Average masses of three replicates and their corresponding standard deviations

7.3.2 DOE analysis and results

7.3.2.1 Part 1

Figure 7-4 is a set of Pareto charts of the magnitude of the effect of a specific experimental factor, or of the interactions of such factors, on the output response, ln(SD). The factors were: polymer-melt temperature (A), mould temperature (B), holding pressure (C), injection speed (D) and cooling time (E). In Figure 7-4, plots (a), (b) and (c) correspond to individual experimental responses of R1, R2 and R3 respectively. Figure 7-5 presents a Pareto chart for the average weight of the three replicates (W_1).

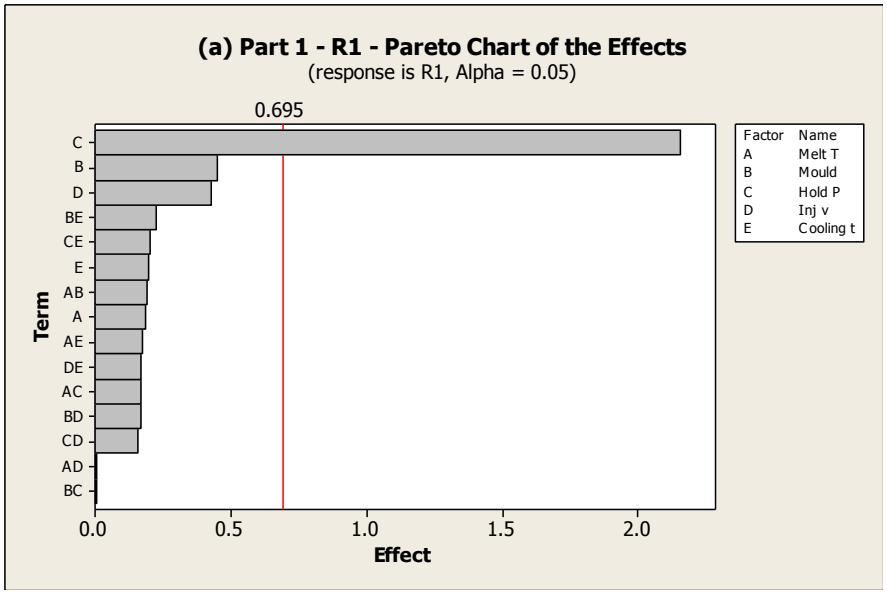

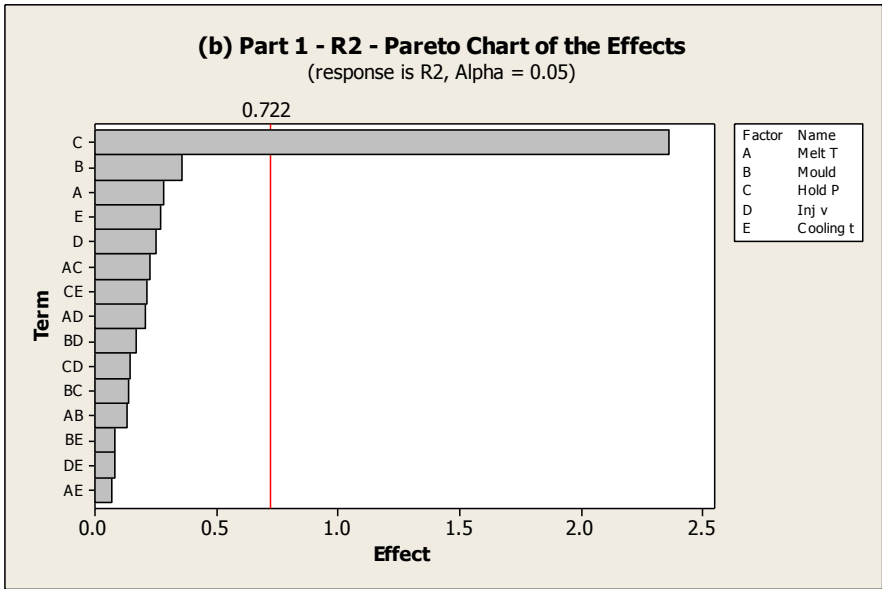

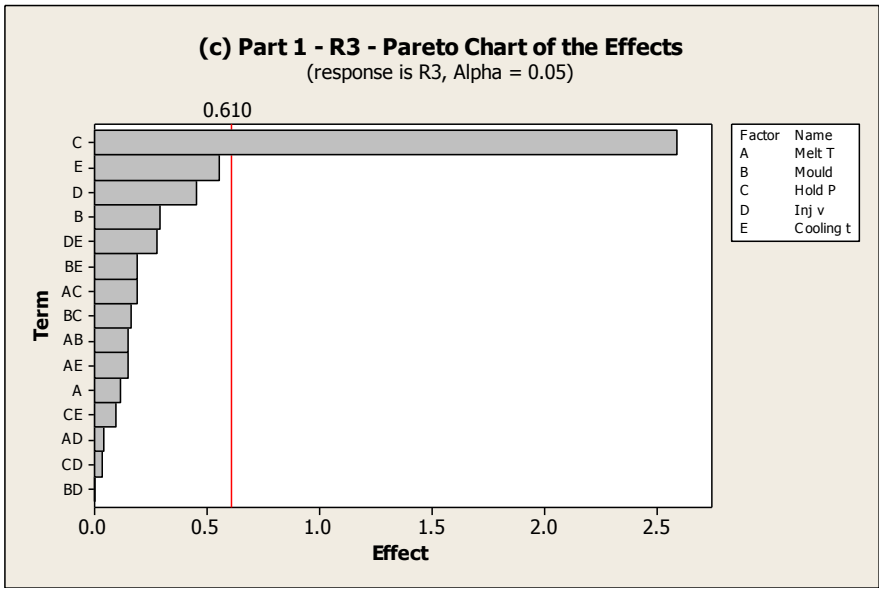

Figure 7-4 Pareto charts of effects for Part 1 of (a) Replicate 1, (b) Replicate 2 and (c) Replicate 3

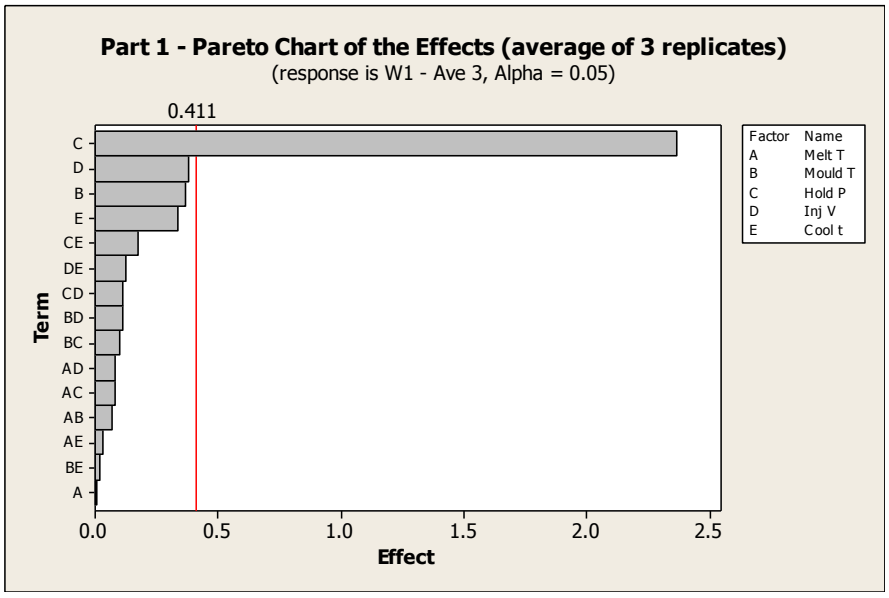

Figure 7-5 Pareto chart of effects for Part 1, where response is average mass W1

Figure 7-6 present the Pareto chart for variability in the mass of Part 1, where the response used to assess variability is ln (SD).

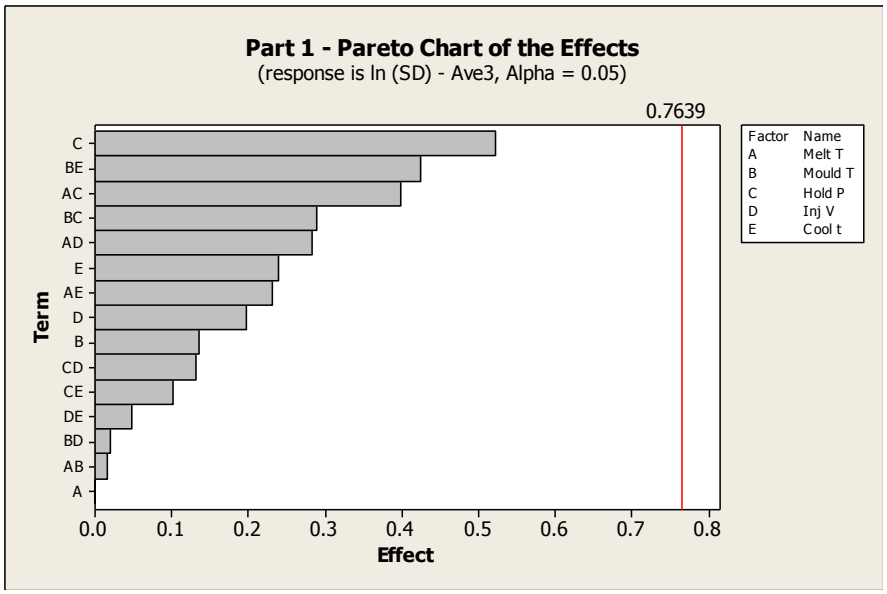

Figure 7-6 Pareto chart of effects for variability in mass for Part 1, where Response is ln (SD)

7.3.2.2 Part 2

Figure 7-7 presents the Pareto chart for part mass, where the three replicated experiments are analysed individually. As with Part 1, the factors were: polymer-melt temperature (A), mould temperature (B), holding pressure (C), injection speed (D) and cooling time (E).

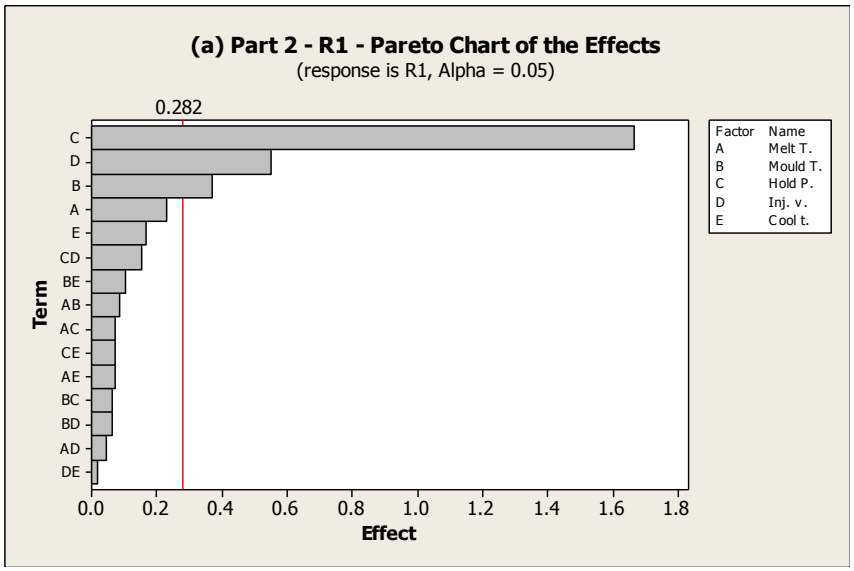

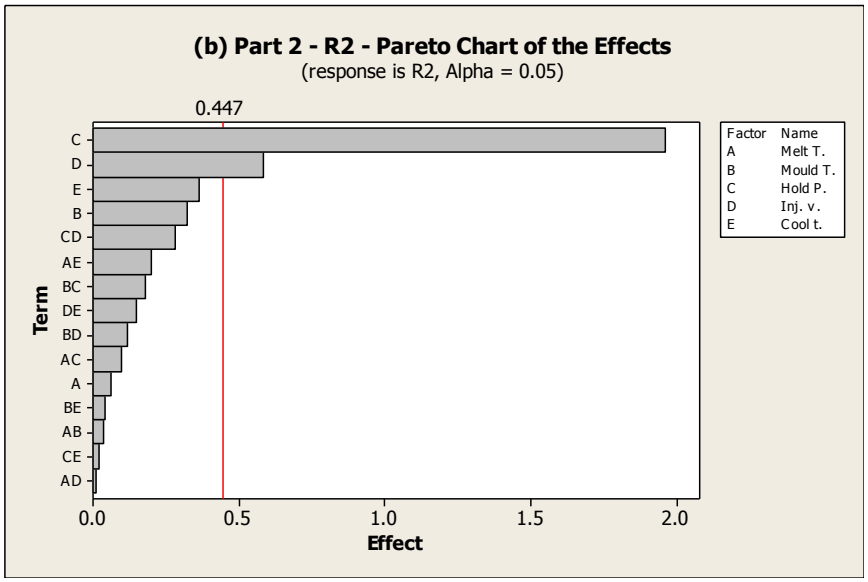

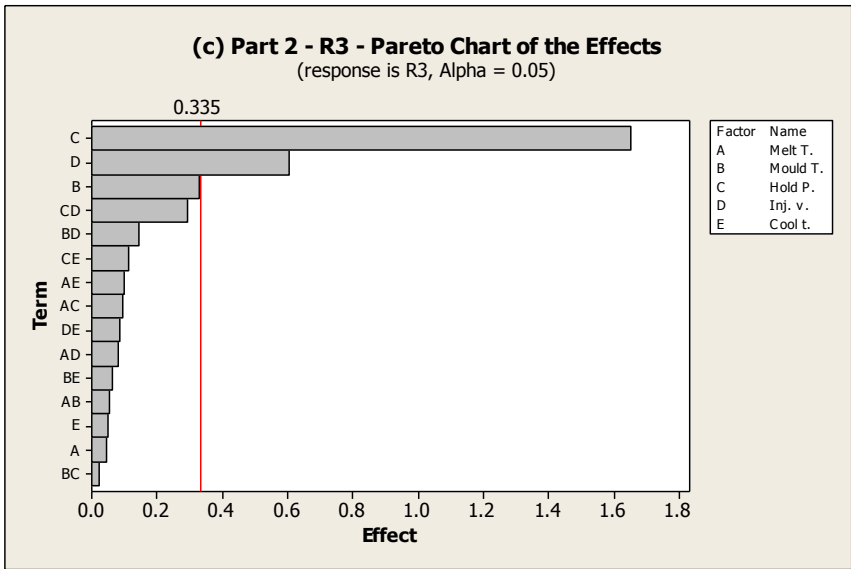

Figure 7-7 Pareto charts of effects for Part 2 of (a) Replicate 1, (b) Replicate 2 and (c) Replicate 3

Figure 7-8 presents the chart corresponding to the overall average of part masses (W_2) listed in Table 7-3.

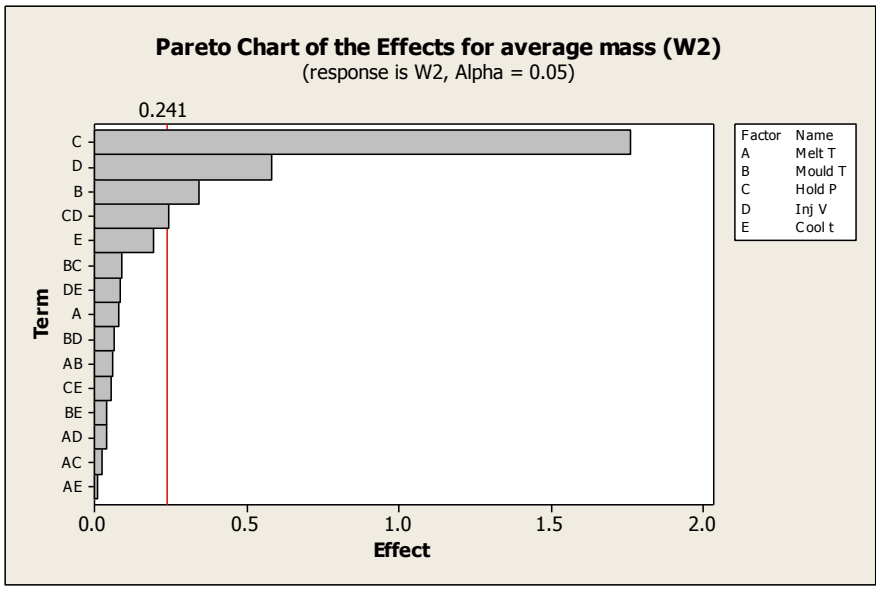

Figure 7-8 Pareto chart of effects for Part 2, where response is average mass W2

Figure 7-9 presents the Pareto chart for mass variability in Part 2.

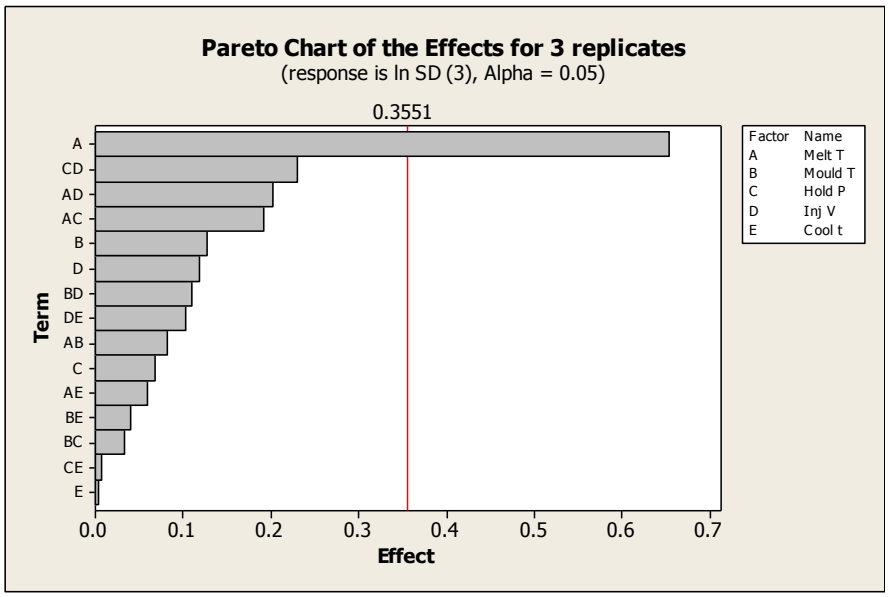

Figure 7-9 Pareto Chart for ln (SD) for average part mass of three replicates

7.4 Discussion

7.4.1 Replication

Figure 7-4 presents the three Pareto plots corresponding to R1, R2 and R3 as responses. The plots show that in each case holding pressure was identified as the most influential parameter on the mass of the part. The magnitude of the bar reveals that its effect is considerably larger than any other factor (or interaction between factors).

The order and magnitude of other factors differ from one plot to another, but they are not statistically significant, and their variation can be attributed to process noise. The similarity between the three plots of Figure 7-4 indicates that process replicability does not affect the mass, and hence the filling quality, of Part 1. The half-factorial DOE design is also shown to be sufficient for rendering reproducible results. Figure 7-5, the Pareto chart of the average mass for Part 1 (W_1), shows that, again, holding pressure is the only statistically significant process parameter for part mass.

Figure 7-7 shows the effects of the individual replicates of Part 2. Where average masses in replicates R1 or R3 were the responses, the most influential parameters were, in order, holding pressure, injection velocity and mould temperature. However, when R2 was used as a response, holding pressure followed by injection velocity were influential parameters, whereas other factors were evaluated to be statistically insignificant. This discrepancy suggested that process variability was high enough that it affected the replication of the part.

The Pareto chart of the average mass (W_2) is plotted in Figure 7-8. Similar to the individual plots of R1 and R3 of Figure 7-7, holding pressure, injection velocity and mould temperature are highlighted as the main effects influencing part mass. However, a borderline effect of interaction between holding pressure and injection velocity is also detected. This "disturbance" in effects for the average-mass plot arises from the inconsistency in results for the individual replicates.

7.4.2 Evaluating parameters that influence variability

Figures 7-4 and 7-5 showed similar results for analysing individual replicated data and average data. This similarity suggests that the process replicability was not

influenced by specific factors). The three plots of Figure 7-4 were similar in showing that holding pressure is a statistically significant factor. On the other hand, they showed discrepancies in the position of the threshold line and the significance and order of other factors and interactions. These variations may be attributed to the noise of the process that made the three replicates slightly different, without affecting the overall main output of the analysis. Hence, Figure 7-5, which combined the data points of all the three replicates, revealed the same significant factor.

In order to confirm the lack of influence of a specific factor on variability, process variability was investigated as the experimental response, represented by ln (SD). Figure 7-6 showed the Pareto chart for variability of Part 1. The main effects and interactions lie below the threshold of statistically significant effects. Changes between process replicates could not be attributed to any particular factor or interaction.

In contrast Figures 7-7 and 7-8 indicated process variability was high enough that it affected the replication of Part 2. Figure 7-9 showed the Pareto chart for variability of Part 2. It shows that melt temperature was the statistically significant source of variation between the three replicates.

The results in Figure 7-9 show an example of how DOE may be used to detect a specific source of variation in micro-injection moulding. They further show that the factor (or factors) that are significant for process variation may not necessarily the same as those that affect the part quality parameters. For Part 2, for example, *variation* in part mass was affected by melt temperature, whereas *part mass* itself was affected by holding pressure and injection velocity, as shown in Figures 7-7 and 7-8.

7.4.3 Minimizing variability

Detecting a particular source of variability makes it possible to control it, and hence minimise it, by studying the relation between the factor and the response.

Figure 7-10 comprises surface plots illustrating the behaviour of variability versus melt temperature and the other factors.

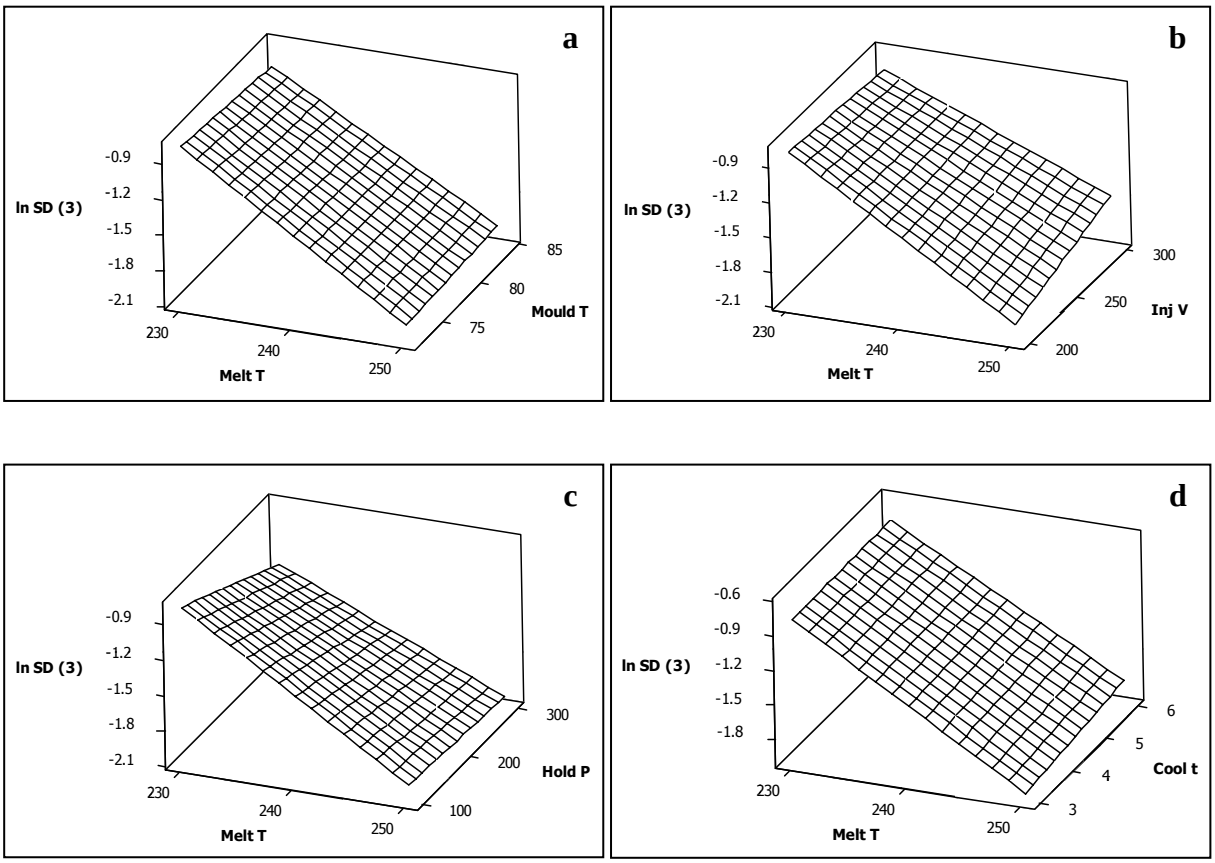

Figure 7-10 Surface plot of ln (SD) for three replicates versus melt temperature combined with (a) injection velocity (b) mould temperature (c) holding pressure and (d) cooling time

The four surface plots in Figure 7-10 show that decreasing the process variability would be achieved by increasing melt temperature. It should be noted that the surfaces are linear in shape, because of the preset assumption in the applied 2-level design that the relation between the factors and the responses followed a linear model. On average the plots in Figure 7-10 indicate that setting the melt temperature to its high level (250°C) would decrease ln (SD) to approximately -1.9, a standard deviation of approximately 0.15.

A more quantitative approach to control the relation between the standard deviation and process factors was applied by using a desirability function that, by iterating over Equation 7-1, suggested a combination of factor values to reach a pre-set target. The pre-set condition of the desirability function was to minimize ln (SD) with a maximum acceptable value of -1.9, as noted from Figure 7-10.

Table 7-4 lists the set of processing conditions suggested by the desirability function and the predicted value of the response.

Factors	Melt T [°C]	250
	Mould T [°C]	84
	Hold P [bar]	300
	Inj. V [mm/s]	200
	Cool t [°C]	3
Response	ln (SD)	-2.05

Table 7-4 Processing conditions and predicted response values by desirability function

The values shown in Table 7-4 agree, in general, with the trends shown in Figure 10, where the statistically significant factor, melt temperature, is maximized to its upper level, and the other factors, although not statistically significant, are set to minimize the response following the trends calculated from the DOE analysis and presented in the plots of Figure 7-10. The predicted response of -2.05 corresponds to a standard deviation of 0.13.

A set of experiments was conducted to attempt to validate the recommendations of the desirability function. The process conditions in Table 7-4 were applied to produce parts for three replicates. The standard deviation of the three replicates was calculated and compared to the value of 0.13 predicted by the desirability function. The experimental value of ln (SD) following the setup recommended by the desirability function was -1.90 (SD of 0.15).

It should be noted, however, that the recommended factor values listed in Table 7-4 are limited by the original setup of the experimental design, which sets the upper limit of the melt temperature to 250°C. The trends shown in Figure 7-10 suggest that increasing the melt temperature beyond the upper limit of 250°C would render lower values of ln (SD) and, hence, less variability. Hence, the same set of experiments was repeated while increasing the melt temperature from 255°C to 270°C by increments of 5 degrees.

Figure 7-11 presents the standard deviation of the replicates at each value of melt temperature (where the datum at 250°C is from the conditions described in Table 7-4).

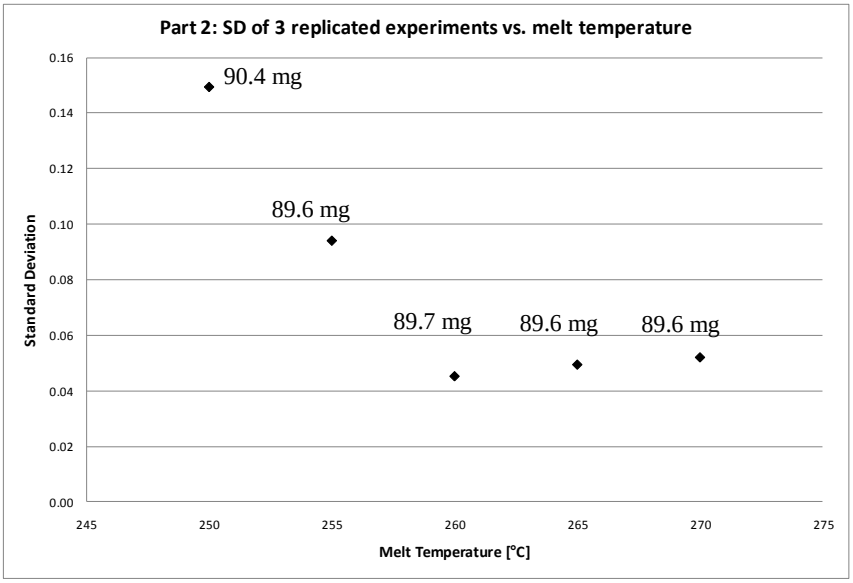

Figure 7-11 Standard deviation vs. melt temperature at recommended setup (mould T of 84°C, injection V of 200 mm/s, holding P of 300 bars and cooling t of 3 sec). Average mass noted for each data point

Figure 7-11 shows that increasing the melt temperature resulted in a significant decrease in standard deviation of the replicated runs from approximately 0.09 at 255°C down to approximately 0.04 at 260°C – a decrease in variability by approximately 44%. Above 260°C, increasing the melt temperature had little effect on the variation of the process. In addition, Figure 7-11 shows that altering the factors to decrease variability induced no significant change in average part mass, and hence filling quality.

It has been shown above that DOE can be used as an effective tool not just to quantify the influence of factors on part quality in micro-moulding, but to quantify the influence of factors on part reproducibility. Furthermore, with the addition of response surfaces and the use of a desirability function it has been shown that DOE can be used as a tool to minimise process variability in micro-moulding.

However, DOE cannot give information on causal mechanisms, i.e. why melt temperature affects process variability. In this respect, it can be noted that Parts 1 and 2 showed different responses to process variability, although the same experimental design, machine setup and material were used. This suggests a possibility that the complexity of the geometry plays a role in process variability in micro-injection moulding. The flow behaviour of molten polymer is highly influenced by the material viscosity, which changes with temperature. The variability observed in Part 2 could be

associated with the flow resistance posed by the relatively complex cavity geometry. Increasing melt temperature may result in better flow behaviour and, hence, consistency in replicated parts.

7.5 Conclusion

This paper aimed at investigating possible effects of processing parameters on process variability in micro-injection moulding. The design of experiments (DOE) approach was shown to be an effective tool to quantify the influence of factors on part reproducibility. DOE was used to analyse the effect of five processing parameters on the variability of part mass for two components. In one component no factor was identified as a source of variability, whilst for the other component melt temperature was identified as a statistically significant factor affecting the replicability of the process.

It was shown that a combination of DOE with response surfaces and a desirability function could be used as a tool to minimise process variability in micro-moulding. Response surfaces were used to illustrate the inverse relationship between standard deviation of part mass and melt temperature. Desirability functions were used to calculate a possible combination of factors that minimized standard deviation within the preset limits of the experimental design. The reduction in variation achieved experimentally displayed a close match with the prediction of the function

It was shown that increasing the melt temperature beyond the limits of the experimental design decreased standard deviation by more than 40%. These results suggested that the complexity of the moulded geometry may be related to the variability of the process.

8 Optimizing process conditions for multiple quality criteria in micro-injection moulding

Abstract

This paper presents a statistical technique to optimise process conditions for multiple quality requirements in micro-injection moulding. A sample hierarchical component with micro-features was replicated, where it was required to improve the process conditions for both complete mould filling and variability in mass. A design-of-experiments approach was used to investigate the effect of five processing parameters on both responses. It was found that holding pressure, melt temperature and injection velocity were statistically significant for part mass, whereas injection velocity alone was significant for mass variation. Desirability functions were used to predict processing conditions that improved both requirements within pre-set conditions. The technique was validated by experiment and it was shown to be applicable for process parameters for multiple responses.

8.1 Introduction

Micro-injection moulding (μIM) is a key technology in mass-producing micro-scaled components. High-volume production, replication fidelity and high precision are some of the features that promote the use of μIM for applications such as medical diagnostics and chemical analysis.

Quality parameters (responses) in μIM are usually associated with the ability to completely fill the micro-size cavities in the mould cavity during processing. For example, experimental responses include filling quality of micro-sized channels [47], feature dimension [24,94,116,117], part mass [44,115,274], flow length [91,119], filling volume fraction [120], weld-line formation [118], demoulding forces [75] and optimisation of part-filling 3D simulation [114].

The work summarised above has focused on using design-of-experiment (DOE) approach to study the effect of a set of process parameters on a single response.

However, micro-manufacturing processes such as μIM may often require a number of quality criteria to be met simultaneously. These could be, for example, a specific feature dimension and a maximum acceptable variability in part mass. In such cases, an optimisation process would be required to attempt to meet both requirements within the "process window" that was available.

Process variability, in this context, refers to variations that occur normally in industrial processes. Such variations are usually attributed to changes in process parameters (factors), i.e. those which can be varied in a controlled manner, and/or changes that result from other causes, which have not been or cannot be controlled. In experimental terms, the former variations are usually referred to as the *signal* [276], or *systematic variability* [269], which is the change of response that the experimenter is seeking to detect. The latter is usually referred to as the *noise*, *scatter* or *unsystematic variability* of the response that occurs during standard operation conditions.

This paper presents an example of a micro-injection moulded part, where DOE was used to investigate the effect of processing parameters on two responses, namely complete mould filling, as represented by part mass and variability in part mass in replicated experiments. A desirability function approach was then used to attempt to optimise process conditions for both responses.

8.2 Experiments

8.2.1 Overview of statistical methodology

The aspect of variability that was investigated in this paper was that of replicability. Replication, in this context, is the process of running experimental trials in a random order, such that resetting is done after each experimental trial [275,276]. Hence, investigating variability using DOE requires that each set of DOE experiments is replicated as part of the experimental methodology. This is in contrast with repetition, which is the process of running experimental trials under the same combination of machine parameters during a single machine run [276].

DOE assumes that responses follow a normal probability distribution, which is not the case for standard deviation. Hence, variability was represented here using the natural

logarithm of the standard deviation, ln (SD), which transforms the data closer to a normal distribution [273,276].

To improve both replicability and part quality a statistical tool was required to optimise factors for multiple responses [272,273]. Here, desirability functions were used to predict a combination of processing parameters that fulfilled the two requirements. Each response y_i is individually converted into a desirability function di that ranges between 0 and 1, where d_i=1 represents being at the target and d_i=0 lies outside the target range. The factors are calculated to maximise the overall desirability, D, where D = $(d_1.d_2. \ldots .d_m)^{1/m}$, and m is the number of responses.

Objectives of the desirability functions can be either to meet a target within specified range, to minimize or to maximize responses. In this paper, the target *T* was to produce parts within a specific mass range and to minimize variability in part mass. The individual functions for meeting a target and minimising the response are represented in Equations (8-1) and (8-2), respectively.

$$d_1 = \begin{cases} 0 & y \prec L \\ \left(\dfrac{y-L}{T-L}\right)^{r_1} & L \le y \le T \\ \left(\dfrac{U-y}{U-T}\right)^{r_2} & T \le y \le U \\ 0 & y \succ U \end{cases} \qquad (8\text{-}1)$$

$$d_2 = \begin{cases} 1 & y \prec T \\ \left(\dfrac{U-y}{U-T}\right)^{r} & T \le y \le U \\ 0 & y \succ U \end{cases} \qquad (8\text{-}2)$$

In both equations *U* and *L* are the upper and lower limits, respectively, and *r*-values are the function weight (liner or non-liner), which in this case are all set to be equal to 1.

For Equation (8-1) the target, upper and lower values were selected based on the filling quality of the produced samples. Briefly, after each set of experiments, samples of the 16 runs were inspected under the microscope to check their filling quality. The

completely filled parts were weighed and their average mass was calculated and set as the "target" mass for the desirability function. The filled samples that had the smallest and the largest masses were also identified, and their weights were selected as the lower and upper limits, respectively.

A similar approach was followed for Equation (8-2), except that no lower limit existed, since the purpose of the function was to minimise the response (variability).

8.2.2 Component geometry

The component chosen for this study was a Polymethyl Methacrylate (PMMA) assembly element of a microfluidic device for use in medical diagnostics. More details about the manufacturing process-chain and device design are available in the literature [271]. The component possessed several micro-scale geometries, including a central, conically shaped through-hole that was 100 um to 150 μm in diameter, and a disk impression on the component surface, which had a depth of 50 μm. Figure 8-1 shows SEM micrographs of the mould insert and an example of a replicated PMMA part from a fully-filled moulding.

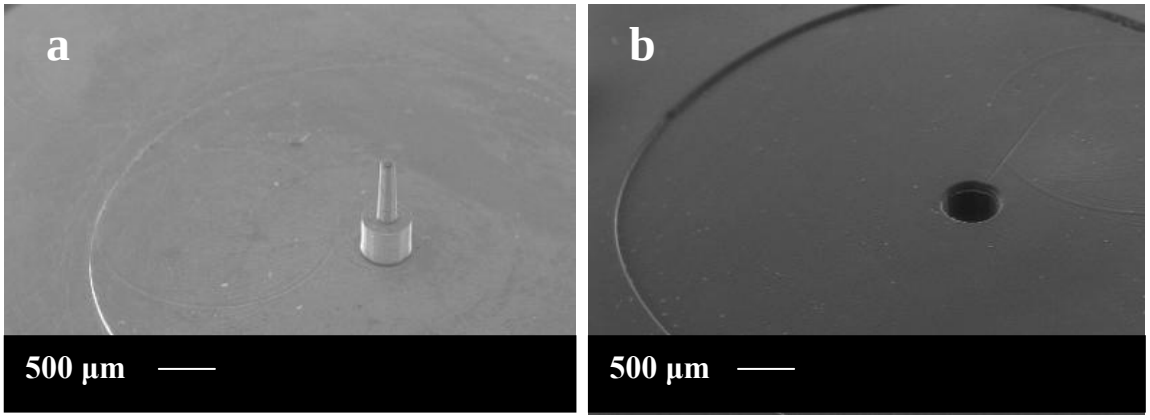

Figure 8-1 SEM micrographs of (a) mould insert and (b) replicated PMMA part

8.2.3 Equipment and process parameters

Five process parameters (factors) were investigated: Polymer-melt temperature (T_p), mould temperature (T_m), holding pressure (P_h), Injection velocity (V_i) and cooling time (t_c).

The micro moulding machine used was a Battenfeld Microsystems 50. The PMMA material was VS-UVT from Altuglas®. This particular grade was selected for its

ease of flow (MFI = 24 g/10 min) and its optical transparency (light transmittance 92%). A sensitive weighing scale with a readability of 0.01 mg was used to weigh the parts. Data analysis and optimization was conducted with Minitab® 15 [270].

8.2.4 Experimental design and procedure

A two-level, half-factorial (2^{5-1}) design was used to test the effect of process parameters on the two selected responses. The resolution-V design decreases the number of required experiments to half of that of a full-factorial one (16 runs per experiment instead of 32). In addition, in this particular design main effects are not confounded with second-order interactions, and second-order interactions are not confounded with each other. This allowed for fewer experimental runs without compromising the accuracy of the results.

Table 8-1 presents the levels of the five factors tested in the experimental design.

Metering Volume [mm^3]	T_p [°C]		T_m [°C]		V_i [mm/s]		P_h [bar]		t_c [s]	
	Low level (-)	High level (+)	Low level (-)	High level (+)	Low level (-)	High level (+)	Low level (-)	High level (+)	Low level (-)	High level (+)
178	230	250	72	80	200	300	100	300	4	7

Table 8-1 Higher and lower levels for the five factors

Table 8-2 presents the half-factorial design in its standard order. The experiments were performed following a randomised order of the runs using a built-in randomisation function in Minitab. For each run, the machine was left to finish 50 continuous cycles (repeats) and then 10 parts were collected for inspection. This was done to ensure that the process reached stability before sample collection. The experimentation setup shown in Table 8-2 was replicated three times in randomised run sequences.

Standard Order	T_p [°C]	T_m [°C]	P_h [bar]	V_i [mm/s]	t_c [s]
1	-	-	-	-	+
2	+	-	-	-	-
3	-	+	-	-	-
4	+	+	-	-	+
5	-	-	+	-	-
6	+	-	+	-	+
7	-	+	+	-	+
8	+	+	+	-	-
9	-	-	-	+	-
10	+	-	-	+	+
11	-	+	-	+	+
12	+	+	-	+	-
13	-	-	+	+	+
14	+	-	+	+	-
15	-	+	+	+	-
16	+	+	+	+	+

Table 8-2 A half-factorial, two level 16-run (2^{5-1}) experimentation design

Two outputs (responses) were evaluated: filling quality and process variability. The former response was represented by the average mass calculated from the three replicates (W), where producing a part that has a mass within a specific tolerance indicates that it is completely filled. Inspecting the replicated parts under the microscope showed that completely filled parts had average mass of 88.6 mg within a range of approximately ±0.5%. The latter response was represented by ln (SD), calculated from the standard deviation of the three replicates.

As outlined above, desirability functions were used to optimise factors for part mass and variability. The filled part mass tolerance was used to pre-set the conditions used in the desirability function to a target mass of 88.6 mg, a lower limit of 88.4 mg and an upper limit of 89 mg, based on the 0.5 percentage point limits. The target for process variability was set to minimise the value of ln (SD), such that its maximum value would not exceed -1.9, corresponding to SD of 0.15. This set the upper limit not to exceed the average of the SD found from the previous 16 runs of the DOE.

Table 8-3 presents the combination of factors calculated from Equations 8-1 and 8-2 to meet both these requirements. The responses show the expected values for both mass and variability. The values of d_1 and d_2 represent the individual desirabilities of each response from Equations (8-1) and (8-2). *D* represents the combined desirability, which is a measure of how the factors combination recommended by the function was able to meet both response requirements.

Factors	
Melt T [°C]	250
Mould T [°C]	80
Hold [bar]	300
Inj. V [mm/s]	285
Cool t [sec]	4
Responses	
Part mass [mg]	88.5
d_1	0.72
ln (SD)	-2.0
d_2	0.97
D	0.83

Table 8-3 Factors combination suggested by desirability function for multiple responses

8.3 Results

Table 8-4 lists the measured masses of the replicated parts for the three replicated experimental sets R1, R2 and R3. The average mass (W) of the three replicates and ln (SD) are listed as the first and second response of the DOE, respectively.

	T_p	T_m	P_h	V_i	t_c	Average mass [mg]			W [mg]	SD	ln (SD)
						R1	R2	R3			
1	-	-	-	-	+	87.7	86.5	86.2	86.8	0.77	-0.26
2	+	-	-	-	-	88.5	87.4	87.6	87.8	0.54	-0.61
3	-	+	-	-	-	88.6	87.9	87.4	88.0	0.58	-0.54
4	+	+	-	-	+	88.0	87.5	87.5	87.7	0.31	-1.18
5	-	-	+	-	-	88.9	88.5	88.0	88.5	0.44	-0.81
6	+	-	+	-	+	89.0	88.4	88.2	88.5	0.38	-0.98
7	-	+	+	-	+	88.8	88.4	87.9	88.4	0.49	-0.71
8	+	+	+	-	-	89.3	88.8	88.9	89.0	0.26	-1.34
9	-	-	-	+	-	86.7	86.7	86.4	86.6	0.17	-1.77
10	+	-	-	+	+	87.1	86.8	86.9	87.0	0.14	-1.94
11	-	+	-	+	+	86.6	86.6	86.4	86.5	0.09	-2.39
12	+	+	-	+	-	87.9	87.7	87.5	87.7	0.23	-1.47
13	-	-	+	+	+	87.8	88.3	88.0	88.0	0.24	-1.41
14	+	-	+	+	-	88.6	88.3	88.5	88.4	0.13	-2.04
15	-	+	+	+	-	88.8	88.1	88.3	88.4	0.35	-1.04
16	+	+	+	+	+	89.1	88.7	88.1	88.6	0.48	-0.74

Table 8-4 Average masses of measured repeats for each of the three replicates (R1 to R3)

Figure 8-2 plots the average masses listed in Table 8-4 in addition to interval lines that represent the standard deviation of the repeated cycles for each of the 16 runs. The interval lines represent the *repeatability* of the process whilst the three average-mass points represent the *replicability* of the process.

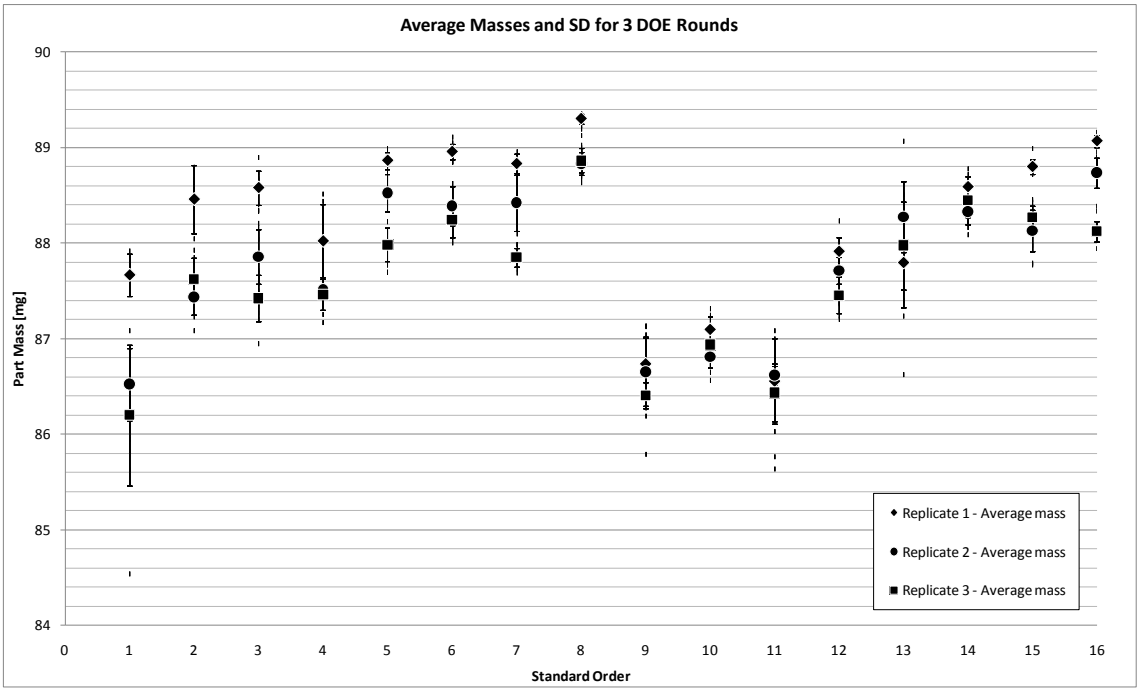

Figure 8-2 Average masses of three replicates and corresponding SD interval lines

The results of the experimental design are presented in the form of main-effect charts and Pareto Charts. The former correlates the factors to the response by taking the average response values for each factor at its high and low levels. The difference, denoted as Δ, is then plotted as a line (linear for 2-level designs) for each factor, where the slope represents the significance of the factor effect. The bars of the Pareto charts represent a factor, or interaction between factors, with the bar length reflecting its effect on the response. The effects are calculated by taking the absolute value of half the difference between averages, i.e. |Δ/2|.

Figures 8-3 and 8-4 show the main-effect charts and the Pareto Charts for mass and variability, respectively. The five tested factors are denoted by letters: polymer-melt temperature (A), mould temperature (B), holding pressure (C), injection speed (D) and cooling time (E).

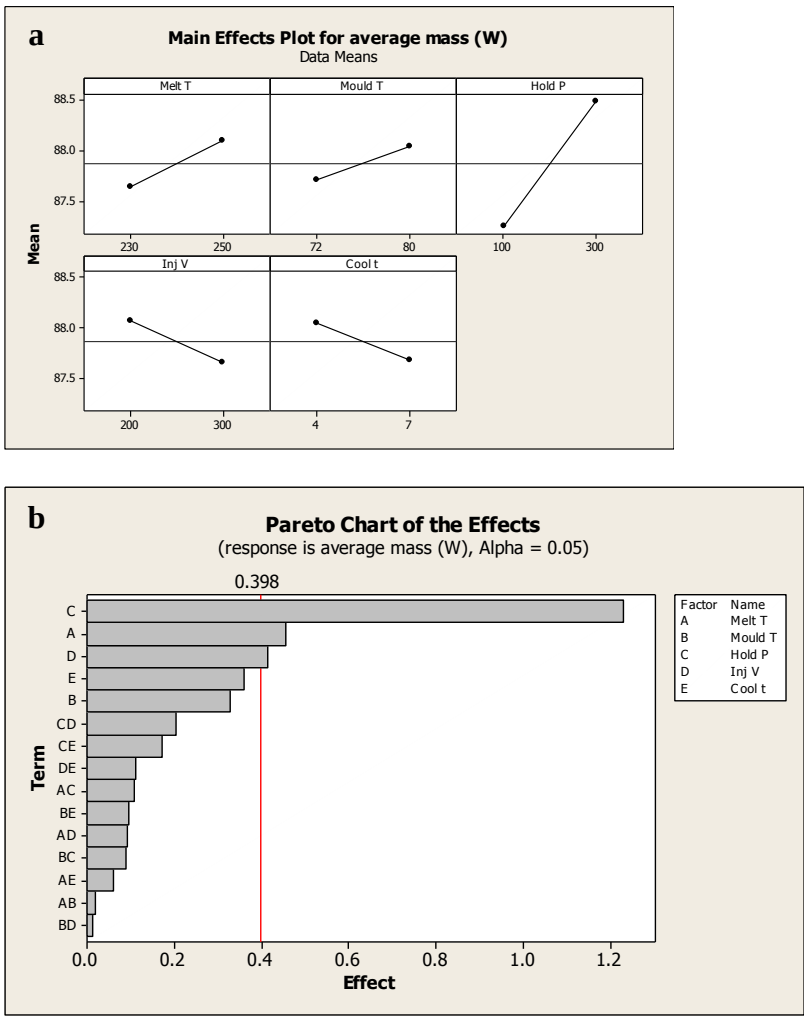

Figure 8-3 Analysis result for average part mass (W) (a) Main effect chart and (b) Pareto chart

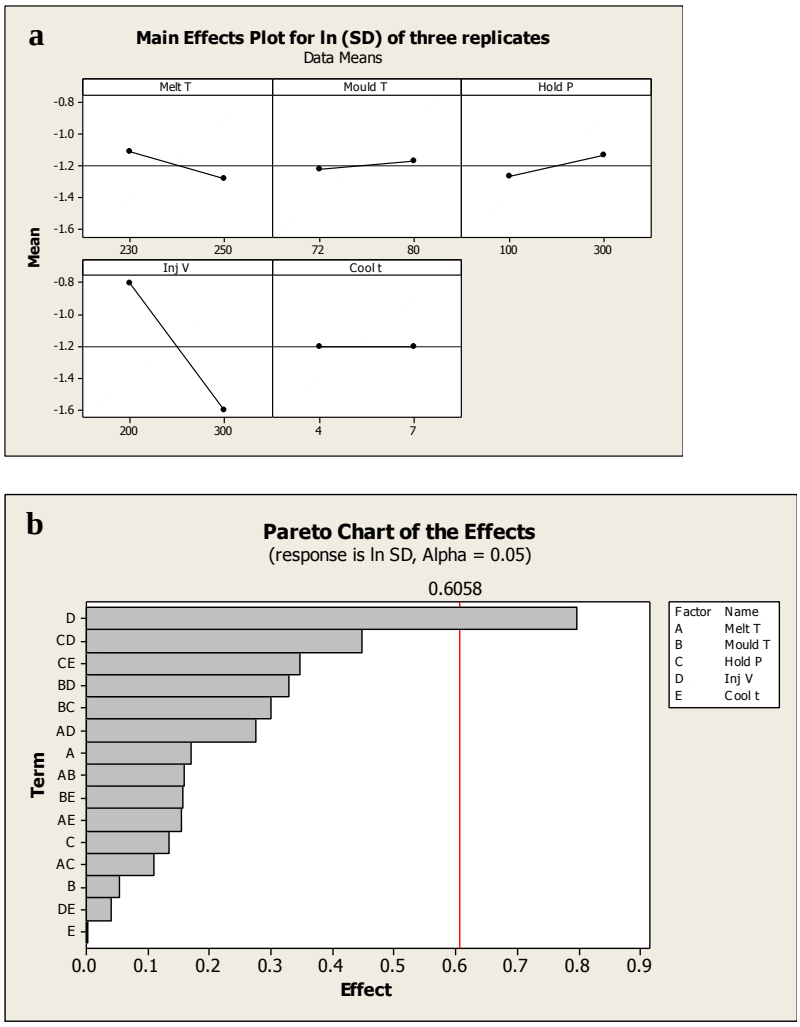

Figure 8-4 Analysis result for variability (ln SD) (a) Main effect chart and (b) Pareto chart

In Figures 8-3 (b) and 8-4 (b) the alpha value represents the risk of finding an effect that does not actually exists, where an alpha value of 0.05 means confidence limit of 95%. The vertical lines represent the threshold value beyond which the effect becomes statistically significant within the pre-set confidence limit of alpha. The position of the line is determined from the *t*-distribution, where *t* is the 1-(alpha/2) quantile of the distribution [270].

Polymer parts were replicated following the factor values shown in Table 8-3. Table 8-5 presents the data for the replicated experiments. Each replicated value (R_1, R_2 and R_3) represents the average from 10 repeats. The standard deviation is calculated for the three replicates.

Part mass [mg]			Average [mg]	SD	Ln (SD)
R1	R2	R3			
88.9	89.0	88.8	88.9	0.10	-2.33

Table 8-5 Results of validation experiments for the desirability function

8.4 Discussion

The plots in Figure 8-3 showed that three influential parameters affect the *magnitude* of the part mass, namely holding pressure followed by melt temperature and injection velocity. No significant interactions were detected

Concerning part-mass *variability*, Figure 8-4 indicated that a single experimental factor was a significant source of mass variation in replicated parts, in this case the injection velocity. Hence, the main significant factor that affected the mass *magnitude* (holding pressure) was not the same as the one that affected mass *variation* (injection velocity).

Figure 8-4 (a) indicated that increasing injection velocity, the identified significant effect, leads to a decrease in ln (SD), i.e. a decrease in process *variation*. On the other hand, Figure 8-3 (a) showed that increasing injection velocity led to a decrease in part mass. This indicates that if a combination of factors is to be found to fulfil both response requirements, i.e. a decrease in variability and an increase in part mass, a compromise would be necessary for the value of injection velocity.

The values shown in Table 8-3 indicate how the desirability function took into consideration the trends discussed above. The holding pressure and melt temperature were set to their upper limits to satisfy the part-mass requirement. For the injection velocity, the selected value was at a point closer to the upper limit (to satisfy variability requirement) but not at the upper limit in order not to violate the velocity requirement for part mass.

This compromise in injection velocity affected the predicted responses, as shown in Table 8-3. The predicted part mass was 88.5 which was slightly lower than the target mass of 88.6 but still within the pre-set tolerance of ±0.4 mg. The predicted ln (SD) was -2.0 (corresponding to SD of 0.14) which was lower than the upper limit set to -1.9.

Since a compromise had to be made between two responses, the individual desirability d_1 and d_2 of mass and mass-variability, respectively, are less than 1. The overall desirability, D, is therefore calculated to be 0.83.

Table 8-5 presents the results of the validation experiments, where average mass was 88.9 mg and SD was shown to be 0.10. Hence, the average part mass was higher than predicted by approximately 0.3%, although it still lay within the pre-set tolerance of ±0.4 mg, whereas the standard deviation obtained was lower than predicted by the desirability function. Comparing the obtained SD of 0.1 to the original run standard deviations listed in Table 8-4 shows that it was possible to achieve variability, when optimising for both mass magnitude and mass variability, which fell within the lowest quarter of the original experimental data.

8.5 Conclusion

This paper aimed at presenting a methodology for optimising process conditions for multiple quality requirements in μIM. Five processing parameters were investigated for their effect on part mass and mass variation. It was found that holding pressure followed by melt temperature and velocity were significant for part mass, whilst injection velocity alone was significant for mass variation. Hence the main significant effect differed between part mass and mass variation. Further, injection velocity was found to be a parameter of a different effect on the two responses, its effect proportional to mass variation but inversely related to part mass. Hence, for some micro-moulded components, attempting process optimization for part quality alone may lead to an unintended consequence of increases in mass variation.

Desirability functions were used to find a combination of factors to meet a specific mass requirement and to minimise variability simultaneously. The function produced a set of values that took into consideration the contradicting effect of injection velocity on both responses. The suggested conditions were tested, where the average mass deviated by only 0.3% and the variability was better than what was predicted by the functions. Both responses were within the pre-set requirements and the method was shown to be useful in optimising multiple responses.

9 Improving surface flatness of micro-injection moulded substrates

9.1 Introduction

Micro-injection moulding (μIM) has developed to be one of main technologies for producing microfluidic devices. The advantages of the process include high-volume manufacturing, replication fidelity and a wide variety of mouldable materials.

A basic step in fabricating microfluidics is to seal the open channels by attaching a lid over the replicated substrate. This can be achieved by several different polymer joining techniques, the advantages and limitations of which are compared in the literature [193,199,200].

For most bonding techniques, the flatness of the mating surfaces is an essential requirement to achieve efficient and leak-proof sealing [277]. The flatness of the polymeric chip is affected by different factors, such as the flatness of the replicated mould [62], the processing parameters [61] and the ejection process. Flatness and its control have, however, received little attention in the literature. In one previous experiment, a microfluidic device for clinical diagnostics was replicated by micro-injection moulding. It was possible to replicate a PMMA, disc-shaped substrate, which had a diameter of 300 mm. The produced flatness was 100 μm edge to edge [278].

This paper addresses one possible contribution to the flatness of substrates: the effect of post-filling process conditions. As an example, the flatness of micro-injected discs was investigated. A design-of-experiment approach was used to investigate the effect of process conditions on part flatness. Three post-filling parameters were investigated: cooling time (t_c), ejection force (F_e) and ejection velocity (V_e). A 2-level, full factorial design was selected for this application.

The results are then validated with a set of extra experiments at conditions designed to improve the flatness.

9.2 Experimental Method

9.2.1 Parts and part geometry

The investigated part was a disc-shaped PMMA substrate, which was designed to form a layer in a laminated microfluidic device, which would be ultrasonically welded to a mating layer of the same external dimensions. The welding would take place across a ring-shaped area close to the circumference of the parts.

An example of the polymer substrate is shown in Figure 9-1. The disc was 10 mm in diameter and 1 mm in thickness. The substrate carried simple micro-scaled features at the centre of the geometry. Further details of the functionality of the complete microfluidic device and its fabrication process chain are available in the literature [271].

The substrates were produced using a Battenfeld Microsystems 50 micro-injection moulding machine. The PMMA grade was VS-UVT from Altuglas®. Optimised process conditions for completely filling the part cavity, have been derived in previous experiments [279]. These were used to form the initial experimental process conditions for the substrate, which are given in Table 9-1

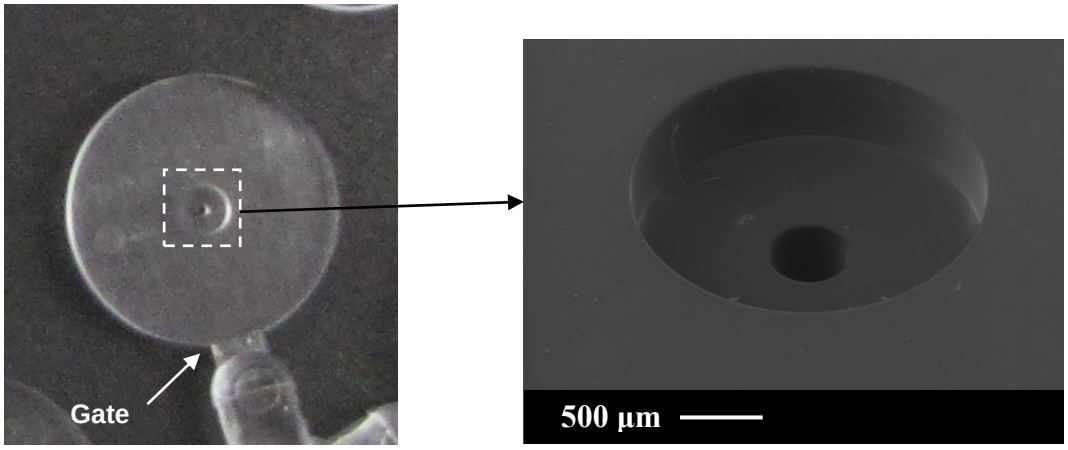

Figure 9-1 A photograph of the tested substrate and an SEM micrograph of the micro-features on the patterned side of the substrate

Melt T. [°C]	250
Mould T. [°C]	81
Holding P. [bar]	416
Injection V. [mm/s]	200
t_c [s]	4
V_e [mm/s]	300
F_e [kN]	0.8

Table 9-1 Initial process conditions. The first five factors were optimised for part filling in prior experiments

9.2.2 Experimental design

Table 9-2 shows the two levels of the variable factors and fixed processing conditions for the experimental design to investigate effects on part flatness.

Variable Factors		
Levels	**(-)**	**(+)**
V_e [mm/s]	150	300
F_e [kN]	0.4	0.8
t_c [s]	4	8
Fixed process conditions		
Melt T. [°C]	250	
Mould T. [°C]	81	
Holding P. [bar]	416	
Injection V. [mm/s]	200	

Table 9-2 Levels of variable factors and fixed process conditions

The levels of the ejection velocity and ejection force were selected to be the minimum and maximum allowable values in the machine.

For the cooling time, the low level was selected as the minimum time necessary to cool the part for ejection to be achieved (based on previous experiments [279]). The high level was selected as twice the low level. As before, the fixed process conditions were selected as the optimised process conditions for completely filling the part cavity, as obtained from previous experiments [279].

A DOE plan was used to investigate the effect of three post-filling parameters: cooling time (t_c), ejection force (F_e) and ejection velocity (V_e). A two-level, full factorial design (2^3) was selected for this purpose. Table 9-3 lists the standard order of the experiment plan. The sequence of runs was conducted in a random order. 3 parts

were produced for each experimental run. The flatness measurement protocol was undertaken for each part 3 times, yielding a total of 9 flatness measurements for each run. The average of these values was taken as the experimental response.

Standard Order	V_e [mm/s]	F_e [kN]	t_c [s]
1	-	-	-
2	+	-	-
3	-	+	-
4	+	+	-
5	-	-	+
6	+	-	+
7	-	+	+
8	+	+	+

Table 9-3 A two-level full factorial experimentation design

Experimental data were processed and analysed using Minitab® 15 [270].

9.2.3 Flatness measurement protocol

Flatness measurements were recorded using a micro-coordinate measurement machine (μ-CMM) of type F25 from Zeiss, based at the National Physical Laboratory (NPL). The machine uses a tactile scanning probe of diameter 300 μm, which is coupled with a visual inspection system, and the measurement uncertainty is 250 nm.

Flatness measurements were taken at different points across the "welding surface" of the substrate (approximately 100 points for each disc). A software package (CALYPSO) was used to interpolate between the measured points, and a visual representation of the surface shape was produced.

The following protocol was used to measure the samples' "flatness":

1. The polymer discs were detached from the gate, cleaned and located on a ceramic reference platen (flatness < 50 nm). The sample was fixed in position using double-sided carbon tape. The platen with the fixed sample was them placed in the μ-CMM. Figure 9-2 illustrates the measurement setup.
2. The platen was probed to generate the z-datum plane. The sample was then further probed in a point pattern of concentric circles ranging from 6 to 9 mm in

diameter. The circles covered the area that was allocated for welding to take place. Figure 9-3 shows a snapshot of the measurement software with the measurement locations highlighted close to the sample circumference.

3. Height measurements were collected at designated points, and a graphical representation is generated for the surface shape.
4. A simple measurement of "sample flatness" was obtained by calculating the difference between the highest and lowest points on the part surface relative to the Z datum plane.

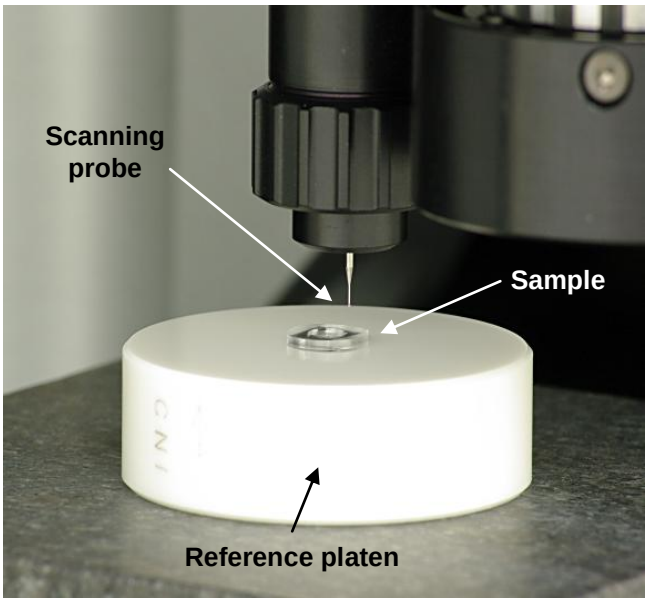

Figure 9-2 Measurement setup for part flatness (Image courtesy of Alan Wilson, NPL)

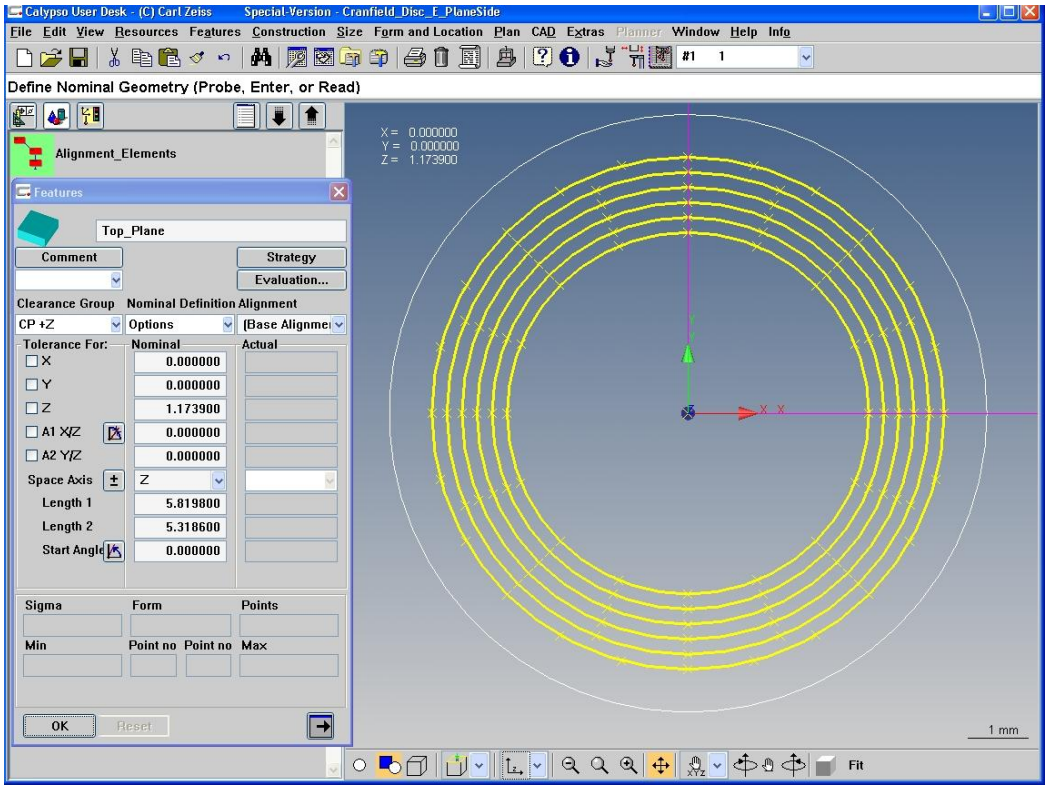

Figure 9-3 A snapshot from the measurement software, CALYPSO. The sample circumference is shown in white, whilst the X-marks along the yellow circles designate the measurement points (Image courtesy of Alan Wilson, NPL)

9.3 Results

Figure 9-4 shows a graphical representation of flatness of the mould insert used to mould the polymer substrate. The flat grey concentric circles are the measurement locations, and the superimposed blue circles represent the measured shape of the surface. Whilst the X and Y directions are to scale, the Z-scale is magnified relative to X and Y in order to clarify the general shape of the part surface. The measured flatness was of the order of 1 μm.

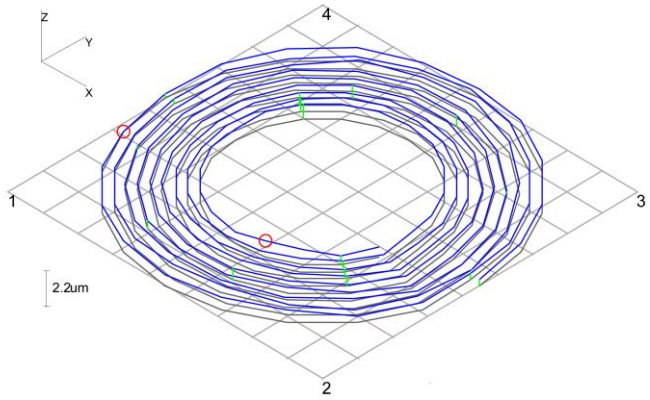

Figure 9-4 A graphical representation of the flatness of the mould insert (Image courtesy of Alan Wilson, NPL)

Figure 9-5 illustrates a typical graphical representation of part flatness for parts moulded at the conditions shown in Table 9-1. For reference, the figure also shows the location of the gate, where the material enters the mould cavity.

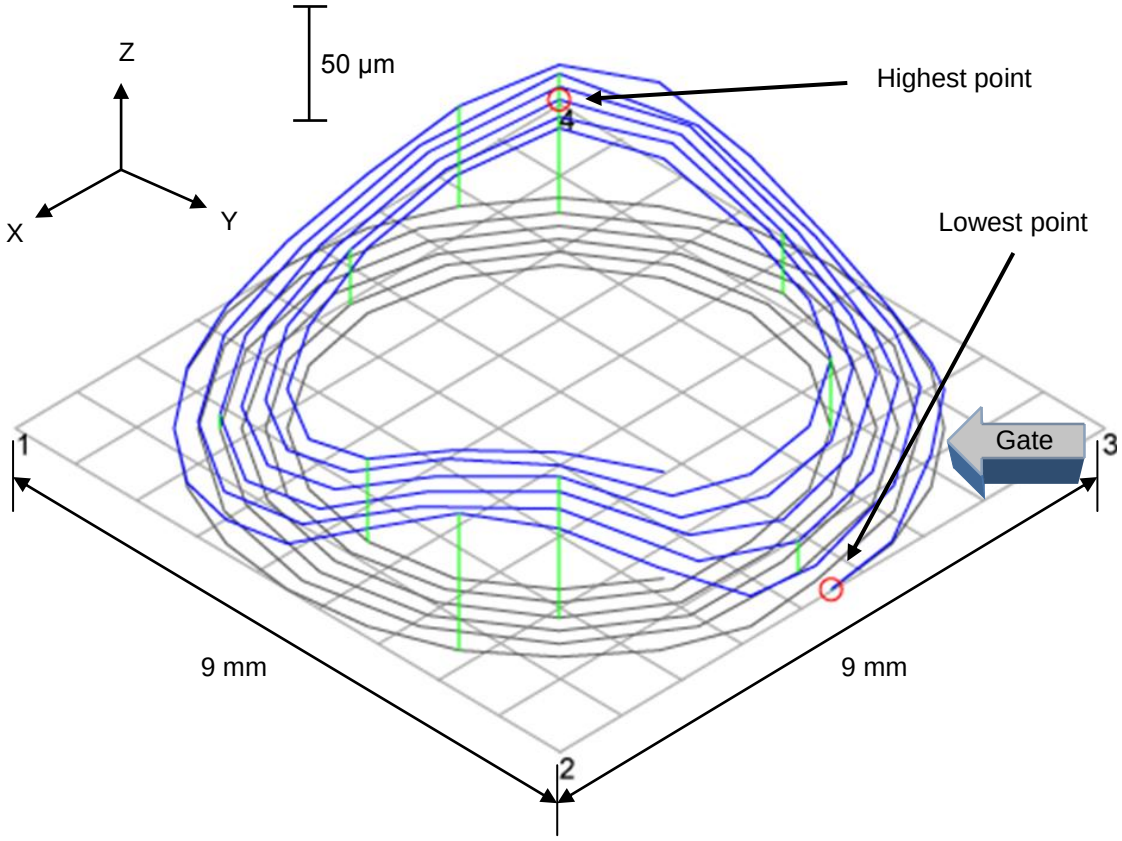

Figure 9-5 A graphical representation of the part surface flatness (Image courtesy of Alan Wilson, NPL)

Table 9-4 shows the flatness measurements and their averages on the patterned and plain sides of the substrate.

	Substrate side	
Flatness [μm]	Patterned	Plain
Measurement A	47	55
Measurement B	50	59
Average	48	57

Table 9-4 Initial measurements of surface flatness

Figure 9-6 presents the measurement locations where the minimum and maximum flatness levels were located. Locations of ejector pins are highlighted in red circles. The moulded substrate is struck on its plain side by the ejector pin.

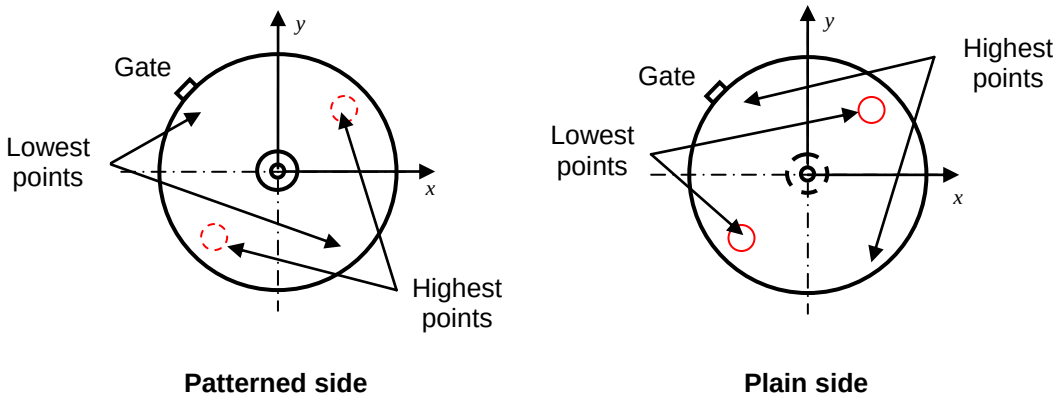

Figure 9-6 Locations of highest and lowest deviation from flatness on the patterned and plain sides of the sample

Figure 9-6 shows that the locations of the highest and lowest points, as measured on both sides of the substrate, corresponded, but were opposite, i.e. the lowest point on the patterned side corresponded to the highest point on the plain side, and vice versa. This indicated that the substrate as a whole was skewed into a "saddle" shape.

The correspondence of the locations of the highest points of the patterned side to the location where the part would be struck by the ejector pins on ejection, indicates that post-filling process conditions affected part-flatness. The design shown in Table 9-3

was implemented to investigate such possible post-filling effects. Table 9-5 tabulates the chosen experimentation response, the average flatness

Standard Order	V_e [mm/s]	F_e [kN]	t_c [s]	Flatness [µm]
1	-	-	-	100
2	+	-	-	98
3	-	+	-	101
4	+	+	-	89
5	-	-	+	47
6	+	-	+	46
7	-	+	+	46
8	+	+	+	45

Table 9-5 Flatness measurements for the DOE runs

Figures 9-7 and 9-8 shows the main effect plot and the Pareto chart, respectively.

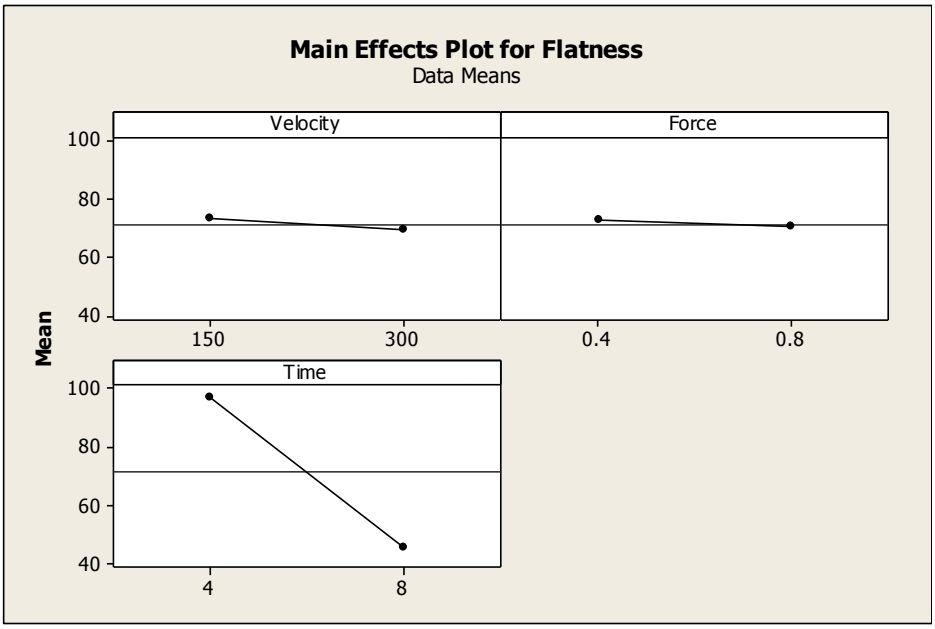

Figure 9-7 Main effects plot of surface flatness

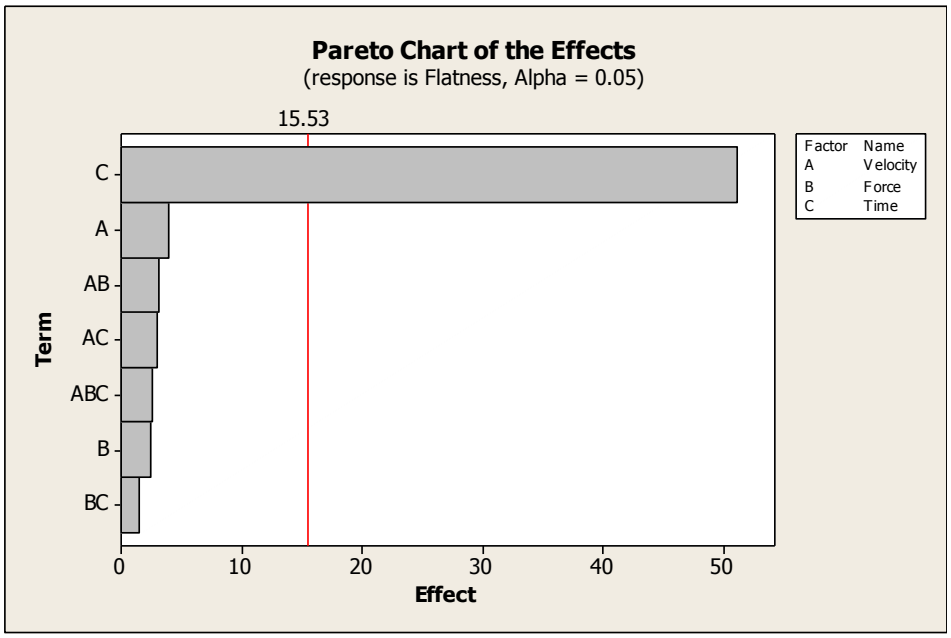

Figure 9-8 Pareto chart of surface flatness

The DOE analysis indicated a significant effect of cooling time on this measurement of surface flatness, where flatness decreases as cooling time increases.

To further test this effect, parts were produced at different cooling times ranging from 8 seconds to 40 seconds. Figure 9-9 plots surface flatness versus cooling time.

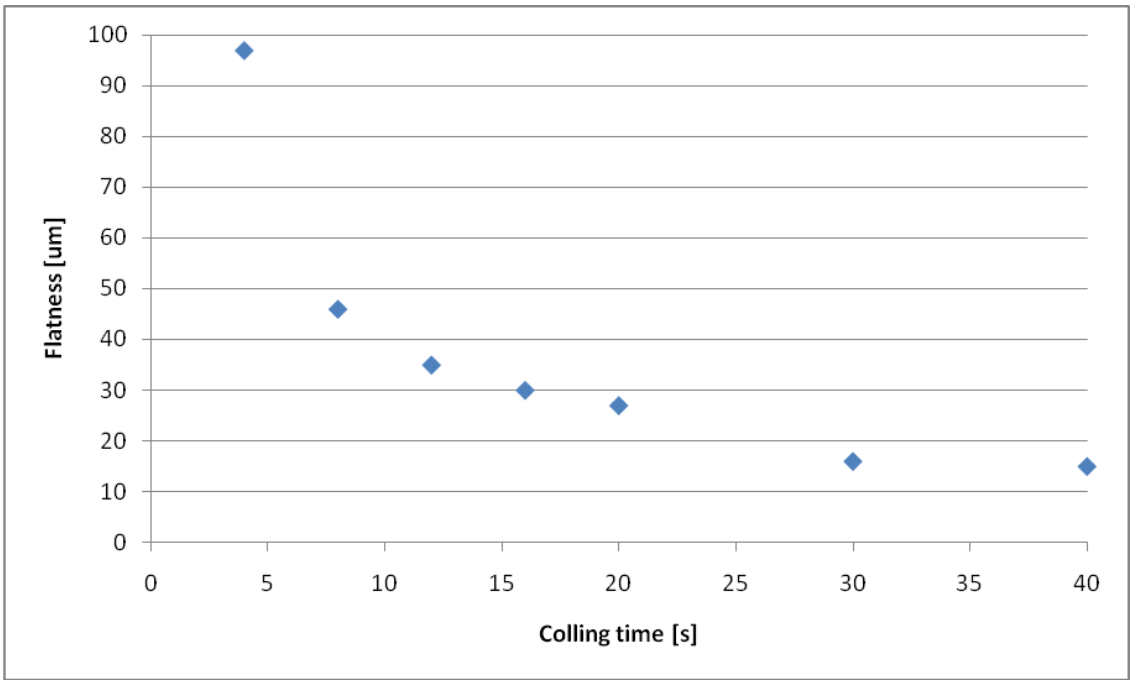

Figure 9-9 Surface flatness versus cooling time

9.4 Discussion

9.4.1 Initial measurements

Flatness measurements of the mould insert shown in Figure 9-4 confirmed that deviation in sample flatness was not because of the mould geometry.

Figure 9-6 shows a correspondence between the points where the deviation from flatness was the greatest at the locations of ejector pins. Hence, these deviations from flatness, of approximately 5-6% of the part thickness, were likely to be related to the post-filling ejection process.

During original optimisation of processing conditions, complete filling of the part was the measured response. To achieve complete filling, a mould temperature of 81°C was assigned. However, this lies close to the glass transition temperature (T_g) of the polymer. As the cooling time was relatively short (4 seconds), after the elapse of the cooling time, the part was ejected at a temperature still relatively close to the T_g. It is likely therefore, that the temperature of the part was close enough to T_g for the part to be deformable by the stresses associated with ejection.

As the moulding temperature could not be changed without compromising the optimised filling, this suggested that improved control of the ejection system (force and speed) and the cooling time might improve the flatness of the part.

Figures 9-7 and 9-8 showed that cooling temperature was the only statistically significant parameter to affect part flatness. The main-effects plot showed that the flatness decreased by more than 50% with increasing the cooling time from 4 to 8 seconds. This result confirms the effect of part temperature during ejection, as discussed above.

Figure 9-8 shows the relationship between the cooling time and substrate flatness. They are inversely related, as suggested by the main-effect plot, but do not have a linear correspondence. The figure shows that a substantial increase in cooling time would decrease the deviation from flatness down to a plateau level. For this particular substrate moulding, this flatness was approximately 15 μm, with an improvement in flatness of more than 80%.

However, in an industrial environment it would probably be impractical to increase the cooling time to such high values, as this would considerably increase the cycle time. One alternative would be to select a shorter cycle time and constrain the ejected part in a flat jig while still warm until it reaches the room temperature. Changing the number, size and distribution of the ejector pins, to reduce ejection stresses, also has the potential to improve the flatness of the part.

9.5 Conclusions

Flatness of micro-moulded substrates is rarely investigated in the literature, though it can be of key importance to post-moulding sealing and lamination processes. Here, a PMMA substrate of a microfluidic device was used as a case study to investigate the effect of three post-filling processes on sample flatness.

- Flatness deviation in a substrate for which optimisation of mould filling had been undertaken was measured to be approximately between 50-60% of the part thickness. This was attributed to the ejection impact from the pins.
- A DOE analysis showed that flatness was exclusively affected by cooling time. It is likely that at short cooling times the temperature of the part was close enough to the T_g of the polymer for the part to be deformable by ejection stresses.
- Increasing the cooling time significantly improved the flatness up to a plateau value. For this substrate, flatness was improved by more than 80%.

10 A process chain for integrating functional elements by micro-overmoulding of thermoplastic elastomers

Abstract

This paper presents a process chain for integrating functional elements by a variant of micro-injection moulding (μIM). A SEBS-based thermoplastic elastomer (TPE) was moulded over polymethylmethacrylate (PMMA) to produce a hybrid microfluidic structure. The process chain implemented micromilling for fabricating micro-structured tool inserts, and μIM and micro-overmoulding was used for replication. A two-plate mould was used for moulding the substrate, whilst a three-plate mould with a replaceable insert was used for TPE overmoulding. The presented application was an interconnect system for a microfluidic device.

10.1 Introduction

Micro-injection moulding (μIM) has evolved during the past decade to be one of the most important processes for high-volume fabrication of micro-components. Advantages of the process include replication fidelity, dimensional accuracy and wide variety of processable materials. Due to the increasing demand for micro-components with relatively complex structures or integrated functionalities, process variants are being developed.

A developing variant of μIM is micro-assembly injection moulding (μAIM), which is a process that allows for the assembly of hybrid micro-structures [80]. Similar to conventional moulding, μAIM combines different processing aspects, such as movable elements, hard/soft combinations and hollow structures [79]. The process can involve a combination of different polymers or polymers with other materials [209,280].

Combining polymers with elastomers is a well established process in macro-scale injection moulding, where the mechanical properties of elastomers (e.g. low tensile

strength, high elongation at break and range of hardness values) make them suitable for applications such as gripping elements, gaskets, insulations and part aesthetics.

Unlike the case with macro-scale moulding, very little is available in the literature about μIM of elastomers. A single experiment has been reported were thermoplastic polyurethanes were micromoulded as non-hybrid into high-aspect ratio structures [96]. In another paper, TPE was used for packaging an injection-moulded microfluidic device [281]. Here, a TPE foil was welded to Polypropylene (PP) substrates by post-processing. In these two cases, TPE was either micromoulded alone or assembled by post processing, but no prior work exists where micro-overmoulding was done with a TPE.

The presented process chain involves the use of a 3-plate mould for overmoulding. Micro-moulding by a 3-plate mould has been reported in one experiment [44,115] to fabricate a polyoxymethylene (POM) micro-gear and a polycarbonate (PC) lens array. The micro-gear mould had a gate diameter of 0.6 mm, whilst the lens component had a gate diameter of 0.3 mm. No prior work exists where 3-plate moulds with replaceable inserts where used for micro-over moulding.

This paper assesses the feasibility of a process chain for integrating functional structural elements in μIM. A micro-overmoulding process was used to micromould a TPE over a PMMA substrate using a 3-plate mould with replaceable inserts. The case study used to assess the process chain regards an interconnection system for attaching tubes into a 3-D microfluidic system.

Interconnection systems are usually produced by post-processing techniques, such as using adhesives or commercially available, usually expensive, ports. The selected case study is an example of how direct integration within micromoulding could decrease the time and cost of post-processing step, which can sometimes make up to 80% of the device manufacturing cost [160]. A review is available in the literature about current integration methods of interconnection elements by high-volume polymer replication methods [282].

10.2 Experiments

10.2.1 Case study

The case study presented in this paper is a building block in a laminated 3-D microfluidic device for blood/plasma separation. It consists of a substrate that has two outlets, one for a cell-rich phase and the other for the plasma-rich phase. A detailed description of the device functionality is available in the literature [271].

The original substrate was designed such that tubes are interconnected into outlets by adhesives in post-processing steps. A modified design, presented here, integrates an interconnection element by μIM, into which tubes would be directly press-fitted. Figure 10-1 shows the original and modified designs.

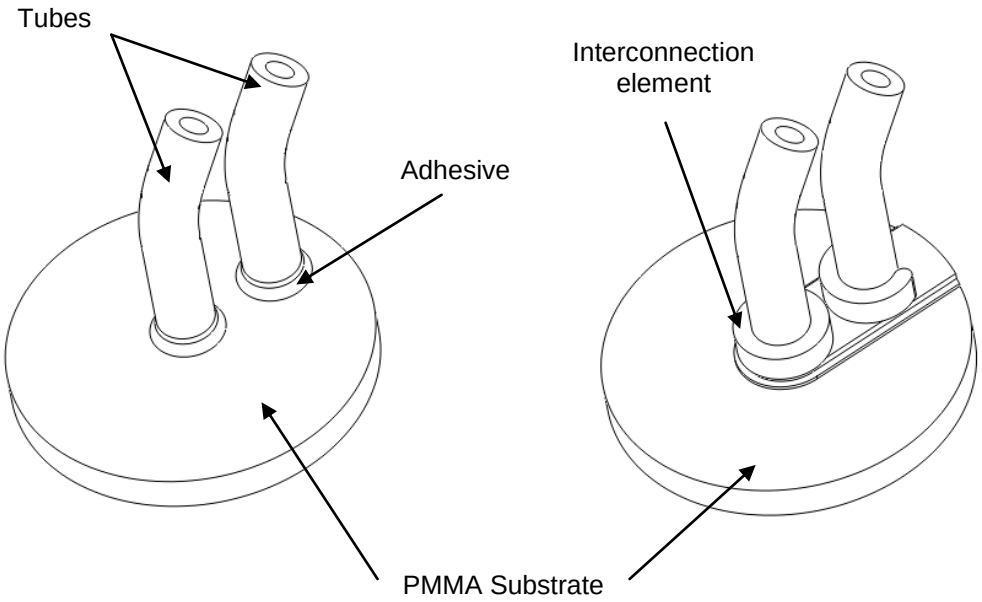

Figure 10-1 Two substrates with post-processed and integrated interconnection systems

10.2.2 Part design

The interconnection element was fabricated by micro-overmoulding, where TPE was moulded over a substrate made of PMMA. Figure 10-2 shows a half cross-section of the sample. The substrate had outer dimensions of 10 mm in diameter and 1 mm in thickness. One interconnect port is fully cylindrical along the thickness of the TPE

element, whilst the other port is partially cylindrical along half the thickness. This was done to avoid interference between the mould cavity of partially-cylindrical port with the gate cavity which is adjacent to the port.

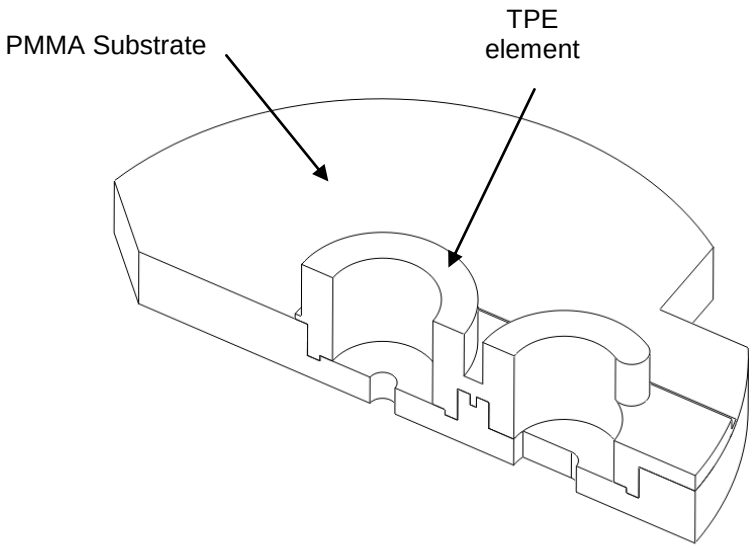

Figure 10-2 Half cross section of the interconnection system

Each port has a thickness of 500 μm and a depth of 1.3 mm, which makes the aspect ratio (AR) of the corresponding cavity in the mould equals to 2.6.

Figure 10-3 presents a CAD image of the PMMA substrate alone. The part was designed to receive the fluidic sample from the other layers of the device through 400-μm-diameter channels, which delivered the fluidic samples to the ports, where tubes were connected.

Some features have been introduced to the surface of the part to allow mechanical interlocking with the overmoulded TPE. They consist of channels of dimensions of 100 μm width x 200 μm depth (AR = 2). Also, positioning marks were introduced to accurately position the substrate during overmoulding and restrict possible motion in the mould.

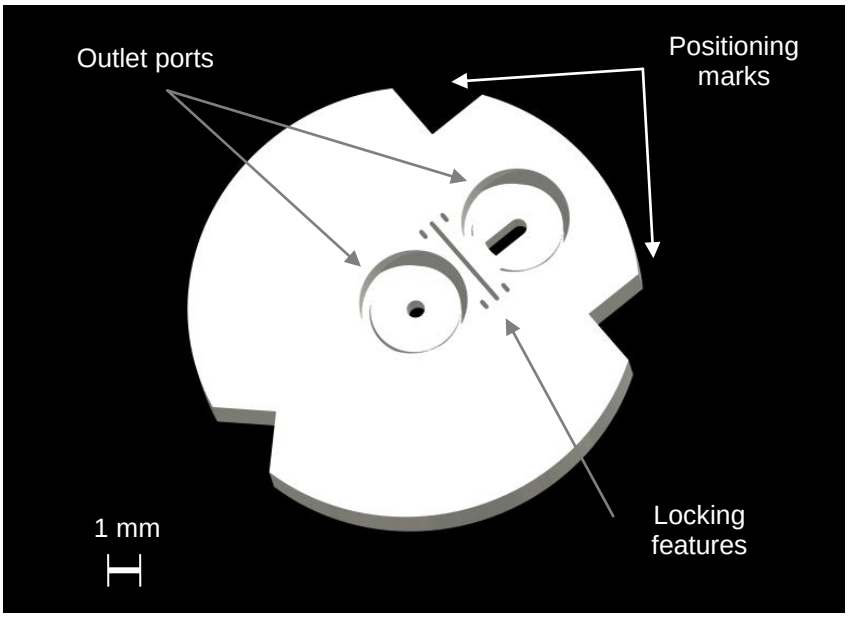

Figure 10-3 A CAD drawing of the PMMA substrate

10.2.3 Mould design

The moulding process took place in two stages, the first of which was the moulding of the PMMA substrate, whilst the second was the overmoulding of the TPE interconnection element. The first stage was done with a 2-plate mould, while the second stage was done with a 3-plate mould as detailed in the following sections.

10.2.3.1 Substrate mould design

The substrate mould consisted of a reconfigurable system, where micro-features were micro-milled in an aluminium insert, whilst the mould body was made of steel. This allowed for more flexibility in mould design and reduced micro-milling time and cost. The other side of the 2-plate mould was a flat steel plate. Figure 10-4 shows a diagram of the insert and Figure 10-5 shows an SEM image of the micro-milled insert.

The micromilling sequence consisted of a roughening and finishing steps. Cutting tools of different diameters were used, the least of which was 100 μm. All cutting tools were tungsten-carbide, flat-end milling cutters.

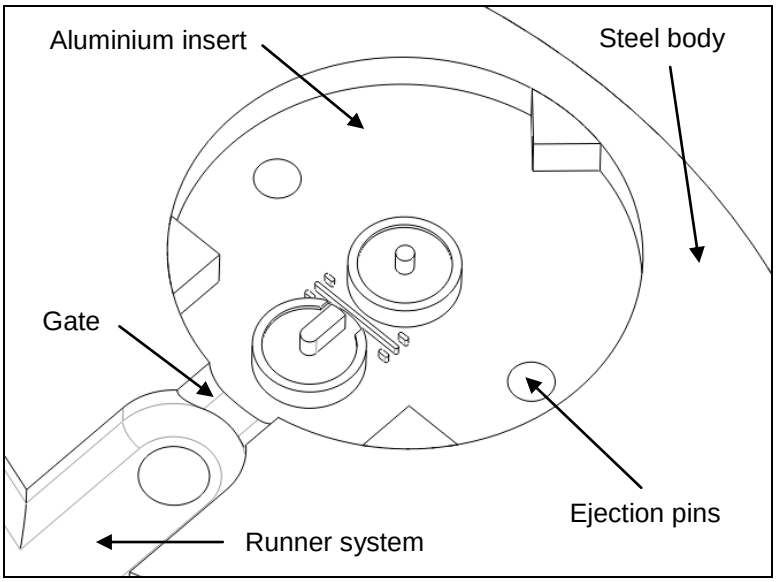

Figure 10-4 A CAD diagram of the reconfigurable mould

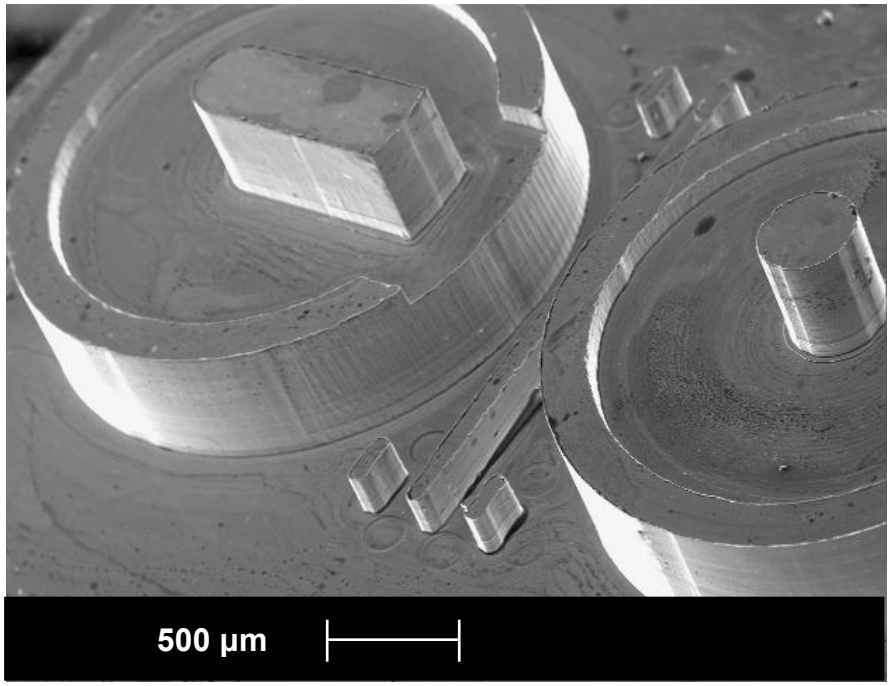

Figure 10-5 An SEM micrograph of the aluminium insert

10.2.3.2 TPE mould design

The overmoulding design was relatively more complex in that the substrate and required features on both sides of the parting surface. A 3-plate mould with a replaceable insert was therefore implemented, where the PMMA substrate was

positioned on the moving half of the mould, whilst the overmoulding took place on the middle (third) plate. The mould was designed with two cavities. Figure 10-6 presents a schematic diagram of the system, where, due to size limitations, only the reconfigurable parts are shown without the surrounding mould body (ejector pins were eliminated from the figure for simplicity). Detailed dimensioned drawings are available in the Appendix A3.

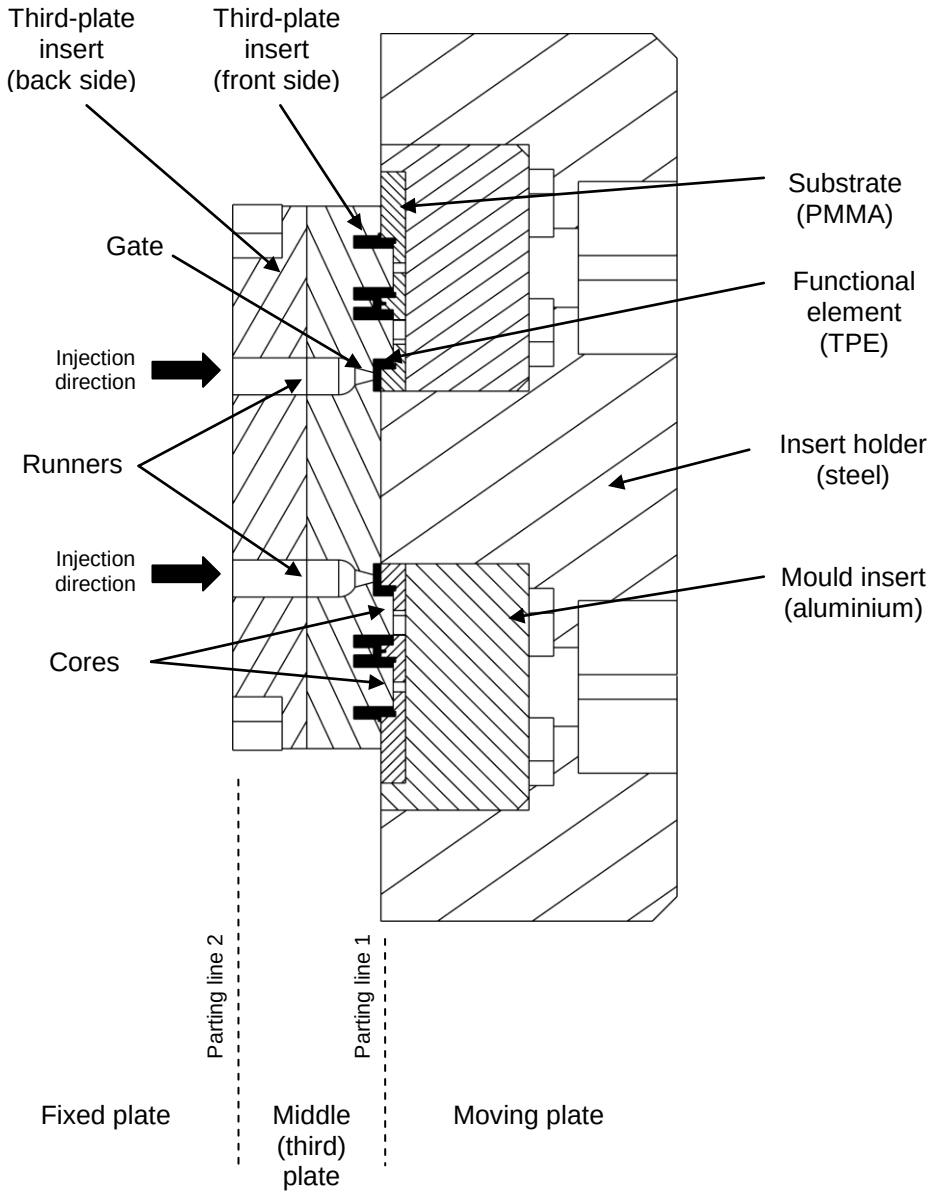

Figure 10-6 Cross-section of the 3-plate micromould

In Figure 10-6, two parting lines define the 3 plates of the mould, namely a moving plate, a fixed plate and a middle, third plate. All parts were made from hardened tool steel except for the replaceable aluminium inserts. The third and moving plates were both two-cavity moulds.

The third plate was also designed with a replaceable steel insert, where features were produced by micro-milling. Due to the required geometry of the interconnection system, two cores were required for each part to form the cylindrical cavities, where interconnection tubes would be fitted into the port. As shown in Figure 10-6, the four cores protruded beyond parting line 1 into the PMMA substrate. The standard steel inserts of the third plate had a thickness that made them flush with the parting surface (parting line 1). Therefore, the insert was redesigned into two halves, where the front half is thicker than the rest of the third plate, allowing for the milling of the protruding cores, as shown in the figure.

Figures 10-7 and 10-8 show the moving side and the third plate side of the 3-plate mould, respectively.

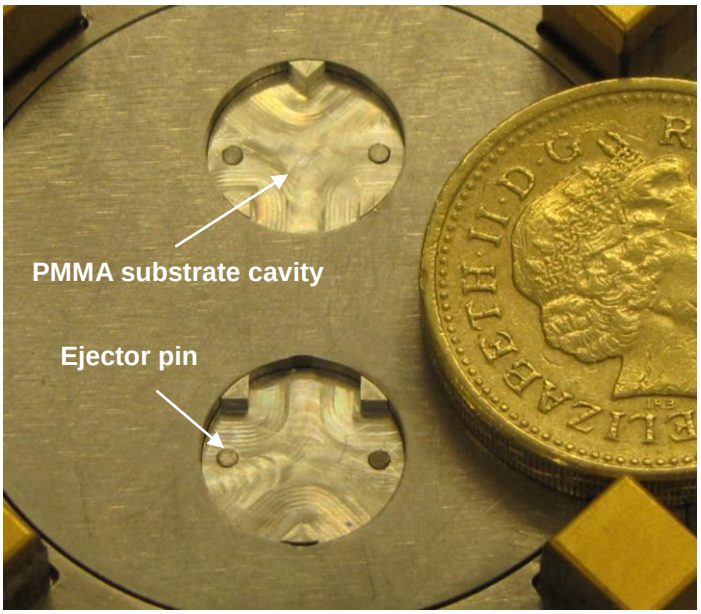

Figure 10-7 Moving-plate side of a 3-plate mould: cavities for holding PMMA substrates.

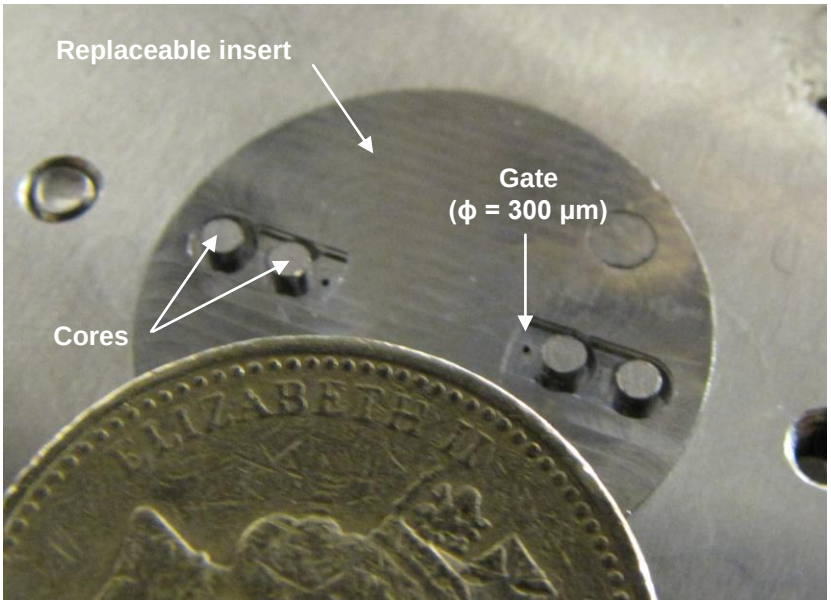

Figure 10-8 Third plate side of a 3-plate mould

Some features in Figure 10-8 had to be redesigned in terms of their aspect ratios to be machinable by standard cutters. The gate holes shown in the figure were done by bespoke cutters with extended lengths to reach the required depth of cut.

10.2.4 Micromoulding of hybrid components

The micro-moulding process was undertaken as two stages. The first was the moulding of the PMMA substrates, and the second was the overmoulding of TPE to form the interconnection element. A high-flow PMMA grade was used in this experiment (VS-UVT from Altuglas). The TPE was a Styrene-Ethylene-Butylene-Styrene (SEBS) copolymer. The grade used (MEGOL SV/P from API) was selected for its adhesion compatibility with polar polymers, such as PMMA. This particular TPE grade has a tensile strength of 0.015 GPa and elongation at break of 450%. The micro-injection moulding machine was a Battenfeld Microsystems 50 and the micromilling machine was a KERN Evo. The following sections present the two stages of the process.

Table 10-1 shows the process conditions for the two stages: polymer-melt temperature (T_p), mould temperature (T_m), injection speed (V_i), holding pressure (P_h) and cooling time (t_c).

	T_p [°C]	T_m [°C]	V_i [mm/s]	P_h [bar]	t_c [s]
Micro-moulding of PMMA	260	84	200	300	4
Micro-overmoulding of TPE	200	65	200	400	10

Table 10-1 Processing conditions for PMMA and TPE

The cycle times for µIM of PMMA and micro-overmoulding of the TPE were approximately 5 and 12 seconds, respectively.

10.3 Results

Figure 10-9 shows an SEM image of the replicated PMMA substrate.

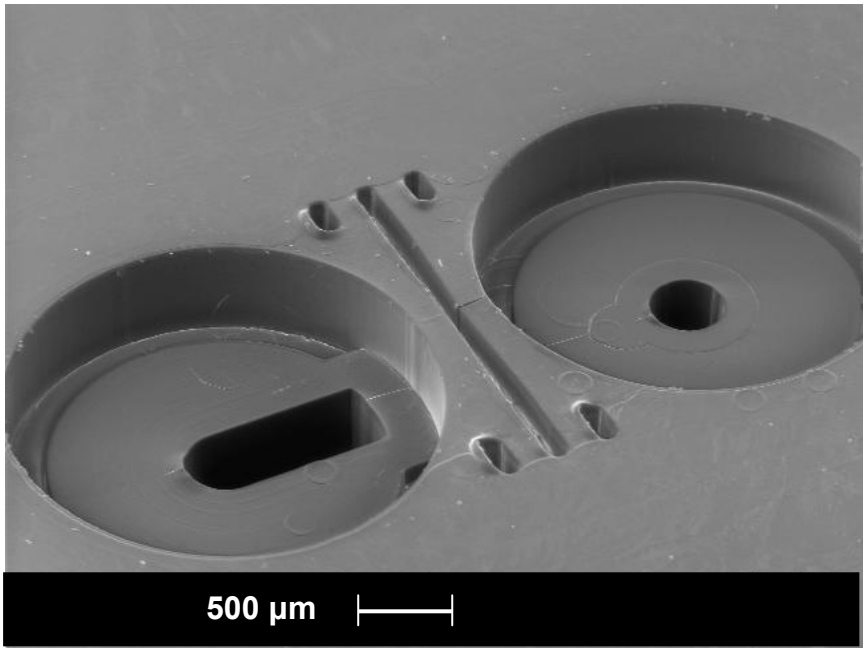

Figure 10-9 An SEM micrograph of the PMMA substrate

Figures 10-10 and 10-11 show images of the top view of the hybrid component and the tube connections, respectively.

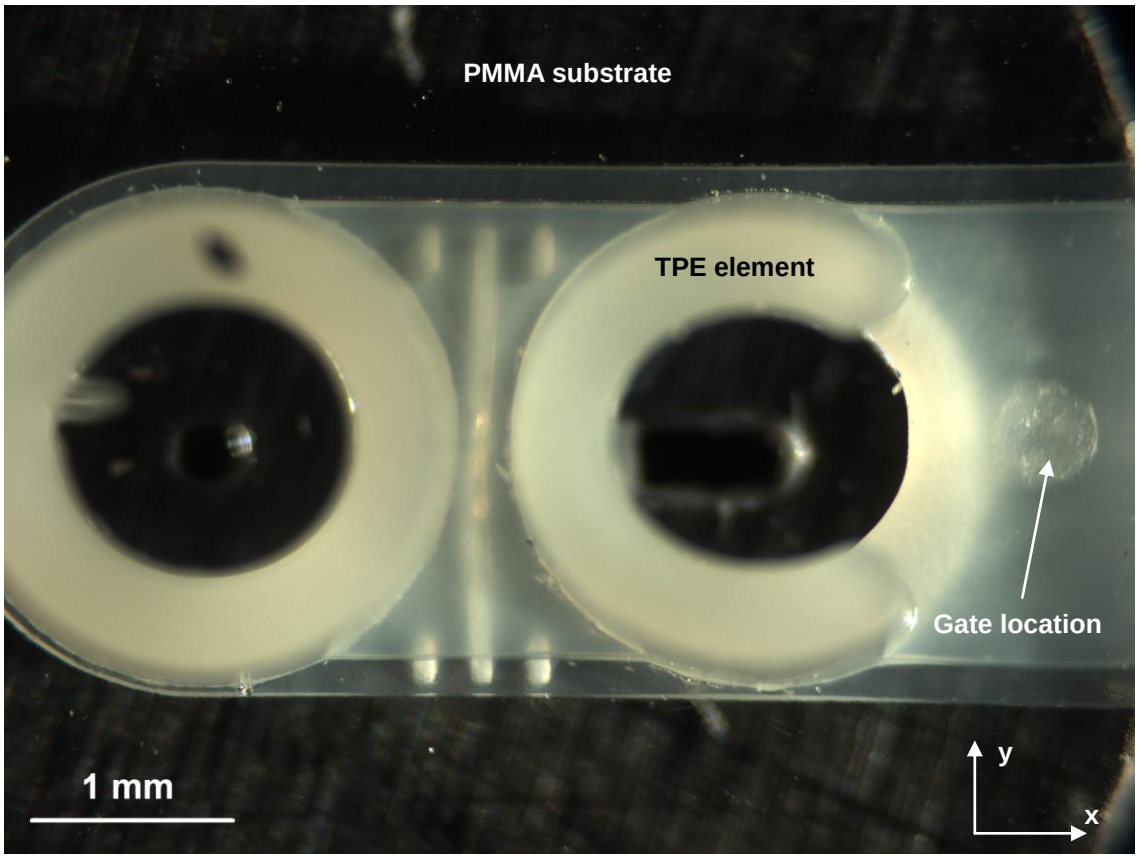

Figure 10-10 A top view of the PMMA-TPE hybrid component

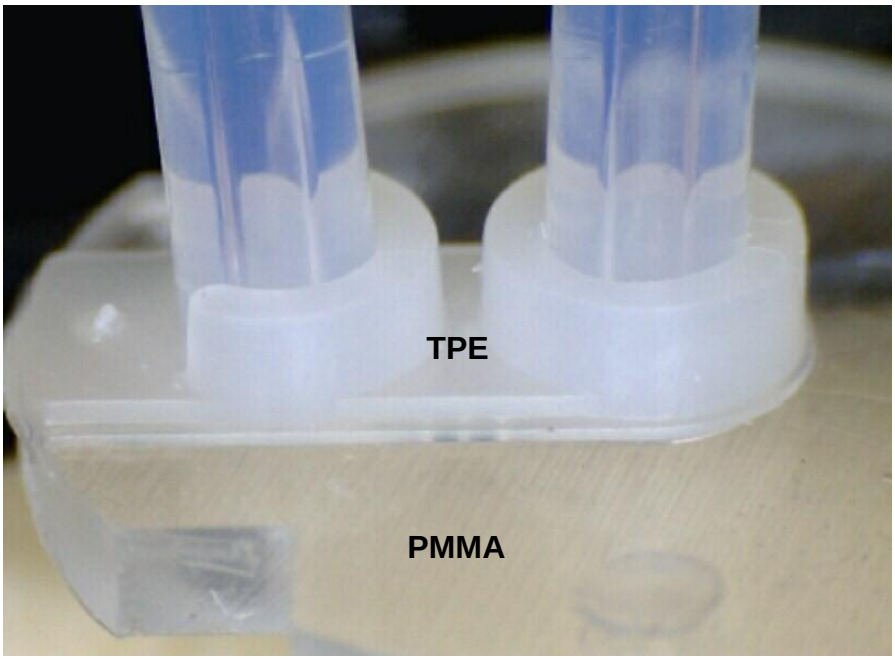

Figure 10-11 A view of the outlet tubes fitted inside the interconnection element

It is noted from Figure 10-10 that there is a misalignment in the *y*-direction by approximately 200 μm. Figure 10-11 show that standard 1.6-mm tubes fits well in the interconnection element.

As a preliminary leakage test, the hybrid component was joined to a PMMA substrate with a single microfluidic channel. The system was tested with water-diluted ink at a number of flow rates starting with 0.32 ml/min (the flow rate at which plasma separation takes place with diluted blood) up to double this value. No leakage was observed in this range. Figure 10-12 shows the testing setup.

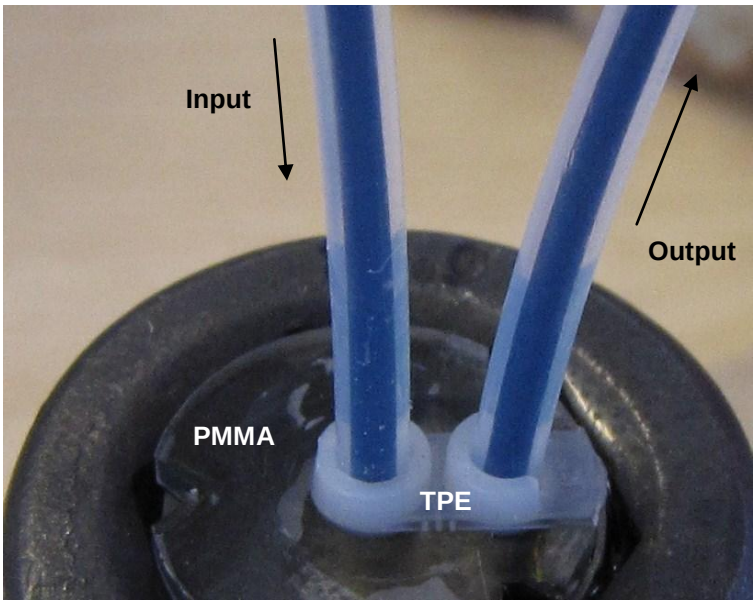

Figure 10-12 A leakage test with water-diluted black ink

10.4 Discussion

This paper presented a novel process chain for functional integration in μIM. The approach was based on micro-overmoulding of TPE using a 3-plate mould with a replaceable insert. The approach used depended on developing a hybrid structure that benefited from different polymer properties. PMMA was used as a low-shrinkage, rigid and transparent polymer for the microfluidic substrate, whilst TPE was used as a low-tensile-modulus polymer for interconnect fittings. The process chain involved two main

steps: mould manufacturing and replication, where the latter was done through two moulding stages.

10.4.1 Mould microfabrication

Concerning mould manufacturing, micro-milling was used to machine the features of the reconfigurable moulds: 2-plate and 3-plate moulds. For the 2-plate mould, Figures 10-5, 10-7 and 10-8 showed that micromilling was suitable for producing the required features within specified tolerances using roughening and subsequent finishing stages. The micro-milling process used Tungsten-carbide cutters with diameters down to 100 μm.

However, the figures also show some of the micro-milling limitations, such as irregular surface finishes and burrs, for example figure 10-5. In addition, micro-milling cutters have limitations in terms of their cutting length relative to their diameter. Bespoke cutters were used to machine some features to the required depth.

10.4.2 Replication by μIM

With regard to replicating the PMMA substrate, Figures 10-9 showed a complete replication of all the substrate features, including the channels that had an aspect ratio of 2. A weld-line could also be observed along the centreline of the features.

Concerning the micromoulding of TPE, Figure 10-10 shows that TPE completely filled the cavities around the cores, leaving the required space for tubes to be fitted as shown in Figure 10-11. This shows the feasibility of using TPEs in micromolding of relatively high-aspect ratio applications. The use of the 3-plate mould offered the advantages of automatic separation of gates and the existence of features on both sides of the mould cavity.

A unidirectional shift of approximately 200 μm was, however, observed between the PMMA and the TPE layer. This unidirectional shift indicates the existence of a misalignment between the moving plate and the third plate. The misalignment did not affect the functionality in this particular case, since it did not block the microfluidic channels. However, for application with tighter tolerances, further positioning calibration would be required.

In addition to mould positioning, two areas of improvement would be useful to achieve a well established process. Firstly, the runner system should be redesigned to

decrease its volume relative to the parts. Figure 10-13 shows the relative size of the runner system with respect to the replicated parts. This is a typical challenge in μIM, where runners consume a large volume fraction of processed material per shot. Another alternative would be to increase the number of cavities in the mould to produce more parts per shot.

Figure 10-13 A runner system compared to replicated parts.

Initial leakage tests were conducted using water-diluted ink, where no leakage was observed in the flow rate range between 0.32 and 0.62 ml/min. This indicated that the TPE ports were efficiently gripping the tubes.

A mass-manufacturing consideration of the presented process chain is the ability to automate the process, such that 2-component integration is done in a single stage. One approach to automation is the use of two-component machines, commonly used in conventional moulding. Two-component micro-injection moulding machines have been recently introduced into the market, such as FormicaPlast 2K from DESMA [283].

10.5 Conclusion

This paper presented a process chain for integrating functional elements by micro-overmoulding. A hybrid structure was produced by micro-moulding TPE over PMMA to produce integrated interconnection ports. The process chain was based on using

micromilling for producing micro-structured replaceable moulds, followed by replication with μIM. A 2-plate mould was used for producing the PMMA substrate using a reconfigurable aluminium insert. A 3-plate mould with a replaceable insert was used to mould TPE over the PMMA substrate. The required cavities (AR of 2.6) for tube fittings were successfully produced. A shift of about 200 μm was detected due to mould-halves misalignment. This did not affect the functionality of the system since it was within acceptable tolerance. A leakage test showed that the system was leak-proof within a range of flow rates between 0.32 and 0.62 ml/min.

11 General Discussion

The work presented throughout this thesis aimed at addressing the research gaps identified from the literature review (Chapters 1 to 3).

Chapter 1 highlighted the main developments that have been achieved in different aspects of μIM of microfluidic devices. Areas covered included device design, mould manufacturing, material selection, process parameters, numerical simulation and post processing. The main outcome of this chapter was to identify key areas of improvement that would lead μIM to be an established high-volume technology in microsystem applications, especially microfluidics. A major research gap was to develop methodologies to control the process parameters and optimise process conditions in μIM for particular quality requirements.

Chapter 2 focused on functional integration in high-volume replication methods. Functional elements were classified according to their transformation functions defined relative to their physical inputs and outputs (mass, energy and information). Functions were categorised according to their degree of integration, i.e. in-line, post-processed or not-integrated. This taxonomy gave an overall picture of the state of the art in integration by high-volume micromoulding. It was clearly shown that direct, in-line integration is usually associated with mass manipulation, whilst post-processing or non-integration was likely to occur when energy or information were involved. The chapter highlighted the importance of developing in-line integration methods in order to advance high-volume micromoulding techniques for fabricating relatively complex microfluidics.

Chapter 3 aimed at assessing μIM as a technique for producing 3-D components. In spite of the major advantages of μIM as a mass-fabrication method, its capabilities could be limited by relatively complex geometries. The chapter discussed the main elements to be considered when designing for μIM, namely demouldability and replicability by μIM. Based on these criteria, a flow chart was proposed as a general guideline on how to evaluate a particular 3-D component for manufacturability by μIM.

Based on the work presented in Chapters 1, 2 and 3, three research gaps were identified, namely (1) micro-injection moulding of three-dimensional microfluidics, (2) quality control and process optimisation and (3) In-line functional integration. The

three issues were tackled as follows: A process chain for producing three-dimensional microfluidic devices produced by μIM for medical applications was developed and assessed. Statistical quality control was used to identify influential process parameters and optimise the micro-moulding process for filling quality, process stability and part flatness. The process was then adapted to enable functionality integration within the high-volume process chain. This was achieved by micro-assembly injection moulding (μAIM) and a three-plate micromould design. Figure 11-1 shows a schematic diagram of the main outcomes of the thesis. The following sections present a general discussion of the thesis outcomes.

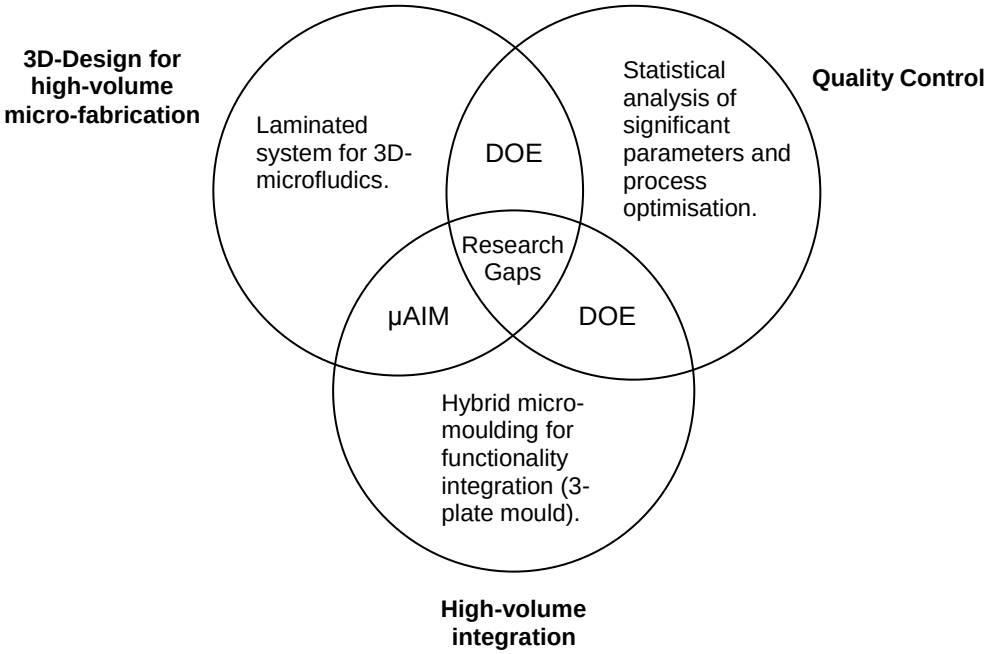

Figure 11-1 A schematic diagram of the basic research outcomes

11.1 Assessment of the process chain

The process chain presented in Chapter 5 illustrated the feasibility of producing 3-D microfluidic structures using high-volume processes. The assessed route was based on combining micromilling with micro-injection moulding (μIM) to produce a laminated 3-D blood-separator.

The lamination approach was shown to be successful in producing 3-D microfluidics. Similar in principle to rapid prototyping, the 3-D lamination approach offers a relatively higher level of design flexibility within a defined space. For example, the blood-separator case study consisted of a system that occupied a total volume of less than 400 mm^3, including spaces for welding and tube interconnections. For demonstration purposes, the system contained a single fluid-manipulation task, namely flow separation. However, future iterations of the design could include more functionalities, e.g. dosing or mixing, within the unused spaces of the same volume by redesigning the individual layers.

The process chain was also used for functionality integration. Tube interconnection and sealing were designed to be part of the device structure. The reconfigurable design of the mould proved to be an efficient approach to produce micro-featured inserts economically and with considerable flexibility in geometrical structure. It is recommended, however, to limit this approach to prototyping stages in which the desired shape is being iterated. For mass-manufacturing purposes, it is advisable to machine the required features directly into a monolithic mould. This would eliminate the potential errors of fitting tolerances and simplifies the mould-assembly process.

It was possible using this process chain to produce a 3-D microfluidic-based blood/plasma separator for medical analysis. Initial experiments using diluted horse blood, resulted in separation efficiency of 80%.

In addition to design flexibility and integration, the process chain provided high-volume capabilities in terms of time and cost. Machining a single mould insert takes less than one hour by micromilling. Once the mould inserts are produced, thousands of plastic parts could be replicated in a single shift. For the blood-separator case study, the five building elements of a complete device could be replicated every 10-12 seconds. This shows the great potential of the process chain in an industry environment.

On the other hand, the process chain had a number of limitations in terms of design and manufacturing. Considering the design process, μIM limits the design of the replicated parts to demouldable shapes, as reviewed in Chapter 3. This requires careful consideration from the designer on how a complex 3-D structure should be "sliced" into demouldable layers. For the blood-separator case, five layers were required for separation. If more functionalities are to be included, extra partitioning

might be required, and hence, a longer process chain. The type of the mould, 2-plate or 3-plate, is another consideration when designing the individual layers.

Another design limitation is related to layer alignment, since accurate alignment of the layers is crucial for the functionality of the device. In the case study, alignment was achieved based on the outer circumference of the layers, which was a suitable approach for the dimensional tolerances. In other applications, where dimensional tolerances might be tighter, registration marks might be necessary to secure accurate alignment.

Considering manufacturing aspects, micromilling is limited in terms of feature size and surface quality it can produce. Commercially available micromilling tools have minimum diameters in the order of tens of microns. Feature sizes of a few microns or less would be unsuitable for micromilling. The tool diameter also affects the cutting length of the tool and, hence, the maximum aspect ratio of the machined feature.

Surface quality is governed by the cutting parameters and is usually irregular across the machining surface. Controlling the surface roughness (e.g. to achieve a required hydrophobicity) would require an extra finishing process.

Automation is an important aspect of the process chain, since post-processing assembly is required. Both micromilling and μIM are automated processes, but additional automation, by robotics for example, would be necessary for post-ejection processes, such as sample handling, sprue and runner separation, alignment and joining. This is likely to increase the efficiency of the process chain but will add to its cost.

11.2 Effect of process parameters and part geometry on part filling

The experiments presented in Chapter 6 aimed at identifying and controlling the process parameters to achieve complete filling in μIM. A three-stage DOE approach was applied comprising familiarisation, screening and optimisation, where part mass was used as a representation of part filling.

Familiarisation was useful in determining the levels of the investigated parameters between which it was possible to detect statistically significant changes.

This stage was also used to investigate the change in part mass during the process cycles, which sets the process-stability conditions of the experiment.

The five PMMA layers presented in Chapter 5 were used as case studies for quality control. Results obtained illustrated the significance of holding pressure on part mass. The measured masses of the five tested samples were all dependent on holding pressure as the primary, and in most cases the only, significant process parameter. These results highlighted the important role of holding pressure in overcoming premature freezing, which is typical in μIM, at the final stages of the injection process.

In agreement with previous work, cooling time and melt temperature were both found insignificant to part mass. This is because the cooling process tends to affect the shape of the part rather than its mass. Melt temperature was insignificant, because all the experiments took place at a mould temperature below T_g, which practically causes the melt temperature to decrease instantly once the polymer comes into contact with the mould walls.

The injection velocity was insignificant because the two levels of the experiment were high enough to make any change in polymer viscosity insignificant.

In the optimisation stage, desirability functions were used to control the process, such that a set of process parameters is calculated to achieve preset target masses. The technique was validated for all the five tested samples, where the maximum and minimum masses where within 0.5% of the target masses.

The desirability function technique proved to be useful in optimising the process, and the filling process was improved based on its suggested values. It was also possible to use the optimised results to obtain a set of compromise conditions for filling all the five parts in one single shot.

The effect of part geometry was investigated in this set of experiments. All the parts had the same outer dimensions but different micro-features, which offered an opportunity to investigate the effect of geometry by comparing the significant parameters identified for all the parts.

Unlike the rest of the parts, Part *d* showed a significant effect of mould temperature and injection velocity, in addition of holding pressure. This combination of parameters was due to the relatively complex geometry of the part. Complexity was represented here by the minimum thickness along the flow path, which was significantly smaller in part *d* that the other four parts.

Experiments with short shots showed that the flow path of the polymer inside Part *d*, as compared for example to Part *a*, was affected by premature freezing occurring at the small-thickness areas. The last-filled point was located at the middle of the part, rather than the far edge from the gate due to hesitation effect caused by the small-thickness areas. As the thickness decreases, the effect of injection speed and mould temperature becomes more significant in affecting the injection pressure required to fill the cavity.

11.3 Process variability in µIM

Chapter 7 focused on another quality aspect of µIM, which is process variability. This aspect is particularly important for high-volume production environments, where changes in, for example, material batches, production shifts or operators might affect the stability of the process. In this set of experiments, variability was assessed by replicating experiments for two different parts, namely Parts *a* and *d*. Variability was measured by the standard deviation of part masses measured for three identical experiments performed at different times and in different run orders.

The results showed that for Part *a*, similar to the original DOE results of Chapter 6, holding pressure was the only significant parameter for the three sets of designed experiments. Some discrepancies were observed for the non-significant parameters, which were due to the process noise. The DOE was unable to detect a particular parameter for variation, which indicates that the process was only affected by noise due to cycle repeatability.

Unlike the case for Part *a*, Part *d* showed different analysis results for the three replications. Holding pressure and injection velocity were significant parameters for all experiments, but mould temperature for only one of them. The analysis for standard deviation showed that injection velocity was the source of variability for this particular part.

Surface plots and desirability functions were used to decrease variability by controlling the melt temperature. This approach resulted in a decrease in variability by approximately 40%.

The main outcome of these experiments is that process variability plays a role in the filling quality in μIM. Previous work with DOE has assumed the process to be invariant, which is not necessarily the case. Another important aspect is that the factor that affects variability of a particular quality parameter is not necessarily the same factor that affects the parameter itself. Once a source of variability is detected, it is possible to decrease it using statistical optimisation tools such as surface plots and desirability functions.

11.4 Optimising process conditions for multiple quality criteria

Optimising more than one quality parameter is a common requirement in industry, where functionality specifications require a combination of outputs to be optimised. Chapter 8 discussed the issue of multiple-criteria optimisation in μIM, where targeting a specific part mass and minimising variability were required.

Part *b* was investigated as a case study, where significant parameters affecting part mass were found to be holding pressure, melt temperature and injection velocity. These results were based on the average of three replicated DOE experiments. Earlier DOE experiment for Part *b* (presented in Chapter 6) revealed that its mass was only affected by holding pressure. The inclusion of melt temperature and injection velocity in the *averaged* data of three replications indicated the influential presence of process variability.

A DOE to test variability, as represented by the standard deviation of part mass, showed that injection velocity was the source of variability. The quality requirements to be met were to meet a specific target mass and to minimise variability. Desirability functions were used for this purpose.

Due to the different effect of injection velocity on both requirements, it was necessary to reach a compromise value. Therefore, the overall desirability *D* was 0.83, less than the ideal value of 1.

The parameters suggested by the function were validated, and the measured mass lay within the preset tolerance of ±0.4 mg. The variability was decreased to within the lowest quarter of the original data set.

11.5 Evaluating part flatness

Part flatness of micro-moulded samples was evaluated using a micro-coordinate measurement machine (μ-CMM). Chapter 9 presented a DOE approach, which was used to investigate post-filling process parameters. It was shown that cooling temperature significantly affected part flatness.

By increasing the cooling time, it was possible to decrease deviation in flatness by more than 80%, which came at the expense of the cycle time. In an industrial environment, it would be required to optimise all process conditions to reach both complete filling and part flatness.

11.6 Integration of functional elements

The process chain assessed in Chapter 10 offered a new approach for integrating functional elements within μIM. Micro-overmoulding was used to mould TPE over PMMA to produce a press-fit interconnection element. The process was done by firstly moulding the PMMA substrate using a 2-plate mould, and then overmoulding it with TPE using a 3-plate mould with a replaceable insert.

The interlocking features at the top of the PMMA had an aspect ratio of 2, and the cylindrical ports had an aspect ratio of 2.6. Both were fully filled with TPE.

The process chain was shown to be feasible for integration of interconnection elements. A leakage test was performed using water-diluted ink, and the system was shown to be leak-proof up to 0.62 ml/min.

12 Conclusions and future work

The research presented in this thesis aimed at assessing the feasibility of micro-injection moulding (μIM) as a mass-production technique for producing 3-D integrated microfluidic devices. Three research gaps were identified from the literature review: designing 3-D microfluidics within the limitations of μIM, quality control and process optimisation in high-volume micro-moulding and the process integration of functional elements.

In order to address these research questions, the research activities passed through three main stages. The first stage was to design and fabricate a three-dimensional microfluidic system using a process chain involving μIM. This stage required an understanding of the capabilities and limitations of μIM (Chapter 3). The developed design guidelines were implemented in the case study of a 3-D blood/plasma separator (Chapter 5), where a lamination approach was implemented to overcome design and fabrication limitations of μIM.

The second stage was to develop quality control techniques suitable for high volume manufacturing in μIM as a microsystem technology. These techniques were investigated as an alternative assessment method to commercial simulation packages that were reported to be inaccurate on the micro-scale (Chapter 1). This stage involved the implementation of design-of-experiments (DOE) to investigate the effect of process parameters on certain quality criteria (Chapters 6 to 9). A systematic approach consisting of familiarisation, screening and optimisation was implemented to control cavity filling, process variability and part flatness.

The third stage focused on process integration of functional elements in microfluidic systems. As reviewed in Chapter 2, microfluidic functional elements are mostly integrated by post processing or used as non-disposable elements, which implied considerable investments in cost and time. Chapter 10 presented a process chain for functional integration by micro-assembly injection moulding of thermoplastic elastomers (TPEs). A 3-plate mould was used to integrate TPE with PMMA to form interconnect elements for a microfluidic system.

The following items indentify the contribution to knowledge achieved through the three research stages:

1) **3-D design for μIM:**
   a. A flow chart was developed for evaluating 3-D micro-components for manufacture based on the capabilities and limitations of μIM.
   b. A high-volume process chain was developed and assessed to produce 3-D microfluidics by lamination of micro-moulded substrates produced by reconfigurable moulds.
   c. A three-dimensional blood/plasma separator was designed, fabricated and tested using the developed process chain.

2) **Quality control and process optimisation:**
   a. The literature review evaluated the state-of-the-art advances in μIM of microfluidics. It highlighted key areas of improvement for μIM to be an established technology in the microfluidics industry. Special emphasis was directed to statistical quality control and process optimisation in high-volume micromoulding as an alternative approach for simulation methods.
   b. A systematic DOE approach based on familiarisation, screening and optimisation was implemented for quality control in μIM. Part mass was shown to be a reliable representation for part filling to an accuracy of 0.2 mg.
   c. The relation between process parameters and part geometry was investigated using multiple-geometry inserts.
   d. Process variability was assessed, and was shown to be related to process parameters. Desirability functions were used to minimise variability.
   e. Desirability functions were used to optimise multiple quality criteria in μIM by reaching compromise conditions.
   f. A DOE approach was implemented to investigate part flatness measured by μ-CMM and to highlight the relation between flatness and post-filling process parameters. Sample flatness was improved down to 15 μm.

3) **Functional integration:**
   a. A taxonomy of process integration in μIM was developed based on functionality (mass, energy and information) in relation with integration level (in-line, post-processed or not-integrated).
   b. A novel process chain was developed and tested for integrating press-fit interconnection elements by micro-assembly injection moulding.
   c. A SEBS-based TPE was successfully micro-overmoulded with PMMA to form interconnect elements.
   d. Reconfigurable inserts were designed, fabricated and tested in a 3-plate mould for functional integration in μIM.

Future work

A number of research aspects presented in this project could be explored further:

- New three-dimensional design concepts could be implemented to overcome the design limitations of μIM and maintain high-volume production. One approach is to use "origami" concept, where all the layers could be produced as modules connected by flexible hinges to ensure alignment between layers (Figure 12-1). Another 3-D approach would be to use micro-scaled sacrificial "lost cores" made of a material with a lower T_g than the device polymer.

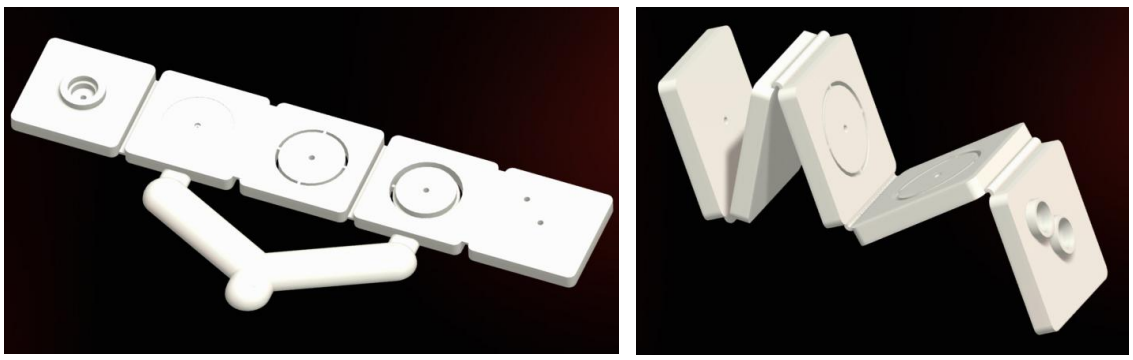

Figure 12-1 A CAD image of a 3-D design concept for μIM where micro-hinges are implemented

- The designed 3-D blood/plasma separator could be further developed to reach separation efficiency higher than the measured 80%. This could be done by investigating the relation between the number of separation layers, input flow rate and dilution percent.
- Recent simulation results from project partners at the University of Greenwich (private communication) showed that higher separation efficiency is achieved when the separation layers are formed into channels rather than open-space discs. Figure 12-2 presents a CAD image of this change could be implemented to the current design.

Figure 12-2 A CAD image showing how separation layers could be modified for higher efficiency

- With regard to quality control and process optimisation, designed experiments could be conducted to give a more detailed understanding of the processing parameters that were investigated in this thesis. This could include, for example, the effect of modifying the three heating zones of melt temperature, the effect of holding pressure time or the effect of changing injection speed over a profile.
- The effect of material type is another factor that could compliment the geometry effect presented in this thesis. The performance of semicrystalline polymers versus amorphous polymers is one example. The behaviour of filled polymers would also be of interest.
- For a better understanding of the relationship between factors and responses, a three-level DOE would be useful to explore possible nonlinearity.
- With regard to process integration, modified designs could better utilise the use of TPE in micro-assembly injection moulding. One common challenge in microfluidics design is to produce a leak-proof system, and TPE could be used to

injection mould micro-gaskets. Figure 12-3 presents a half cross section of a substrate, where TPE is used as both an interconnect element (from top) and a sealing gasket (from below).

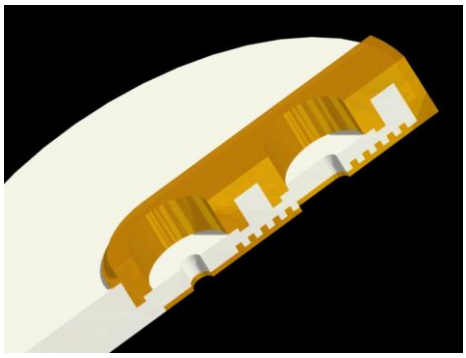

Figure 12-3 A CAD image of a PMMA substrate with TPE moulding for interconnect and sealing

- Another area of improvement with regard to elastomeric interconnections is to test the bonding between the TPE and PMMA using, for example, peel or pressure tests. In addition, leakage tests should be performed to test the efficiency of the interconnection beyond at higher flow rates and with different fluids.

REFERENCES

[1] Becker H. Microfluidics: A Technology coming of age. *Medical Device Technology* 2008; 19: 21-24.

[2] Bourdon R, Schneider W. A systematic approach to microinjection moulding. *Business Briefing: Medical Device Manufacturing & Technology* 2002: 1-3.

[3] Heckele M, Schomburg W. Review on micro molding of thermoplastic polymers. *J. Micromech. Microengineering* 2004; 14(3).

[4] Giboz J , Copponnex T , Mélé P . Microinjection molding of thermoplastic polymers: A Review. *J. Micromech. Microengineering* 2007; 17(6).

[5] Becker H , Gärtner C . Polymer microfabrication methods for microfluidic analytical applications. *Electrophoresis* 2000; 21(1): 12-26.

[6] Reyes D, Iossifidis D, Auroux P, Manz A. Micro total analysis systems. 1. Introduction, theory, and technology. *Anal. Chem.* 2002; 74(1): 2623-2636.

[7] Zhang C, Xu J, Ma W, Zheng W. PCR Microfluidic devices for DNA amplification. *Biotechnol. Adv.* 2006; 24: 243-284.

[8] Fiorini GS, Chiu DT. Disposable microfluidic devices: fabrication, function, and application. *BioTechniques* 2005; 38: 429-446.

[9] Weber L, Ehrfeld W. Molding of microstructures for high-tech applications. *Proceedings of the 56th Annual Technical Conference (ANTEC 1998)*. Part 3 (of 3); 26-30 April 1998; Atlanta, GA, USA.

[10] Niggemann M, Ehrfeld W, Weber L. Fabrication of miniaturized biotechnical devices. *Proceedings of SPIE - The International Society for Optical Engineering*; 21 September 1998 through 22 September 1998; Santa Clara, CA.

[11] Hanemann T, Pfleging W, Haußelt J, Zum K. Laser micromaching and light induced reaction injection molding as suitable process sequence for the rapid fabrication of microcomponents. *Microsys. Technol.* 2002 01/22; 7(5): 209-214.

[12] Becker H, Heim U. Hot embossing as a method for the fabrication of polymer high aspect ratio structures. *Sens. Actuators A Phys. 2000*; 7-10 June 1999; 83(1): 130-135.

[13] Grande JA. Micro-thermoforming makes its debut. *Plastics Technology;* 2006; 52(11): 37-41.

[14] Kukla C, Loibl H, Detter H, Hannenheim W. Micro-injection moulding - The aims of a project partnership. *Kunsts. Plast Eur.* 1998; 88(9): 6-7.

[15] Angelov A, Coulter, J. Micromolding product manufacture - A progress report. *Proceedings of the Annual Technical Conference, (ANTEC 2004)*; 16 May 2004 through 20 May 2004; Chicago, IL.

[16] Whiteside B, Martyn M, Coates P, Allan P, Hornsby P, Greenway G. Micromoulding: Process characteristics and product properties. *Plast. Rubber Compos*. 2003; 32(6): 231-239.

[17] Martyn M, Whiteside B, Coates, P, Allan P, Greenway G, Hornsby, P. Aspects of micromoulding polymers for medical applications. *Proceedings of the Annual Technical Conference, (ANTEC 2004)*; 16 May 2004 through 20 May 2004; Chicago, IL.

[18] Bibber D. Advanced micromolding applications. *Proceedings of the Annual Technical Conference, (ANTEC 2005)*; 1 May 2005 through 5 May 2005; Boston, MA.

[19] Tom A, Layser G, Coulter J. Mechanical property determination of micro injection molded tensile test specimens. *Proceedings of the Annual Technical Conference, (ANTEC 2006)*; 7 May 2006 through 11 May 2006; Charlotte, NC; 2006.

[20] Yao D, Kim B. Injection molding high aspect ratio microfeatures. *J. Inject. Molding Technol.* 2002; 6(1): 11-17.

[21] De Mello A. Plastic fantastic? *Lab Chip*; 2002; 2(2).

[22] Wimberger-Friedl R. Injection molding of sub-μm grating optical elements. *J. Inject. Molding Technol.* 2000; 4(2): 78-83.

[23] Piotter V, Guber AE, Heckele M, Gerlach A. Micro moulding of medical device components. *Business Briefing: Medical Device Manufacturing & Technology*, 2004; Avaialble at: http://www.touchbriefings.com/pdf/954/piotter.pdf. Accessed February 2007.

[24] Pirskanen J, Immonen J, Kalima V, Pietarinen J, Siitonen S, Kuittinen M, Kuittinen M, Mönkkönen K , Pakkanen T, Suvanto M, Pääkkönen EJ . Replication of sub-micrometre features using microsystems technology. *Plast. Rubber Compos*. 2005; 34(5-6): 222-226.

[25] Mazzeo A, Dirckx M, Hardt, D. Process selection for microfluidic device Manufacturing. *Proceedings of the Annual Technical Conference, (ANTEC 2007)*; 6 May 2007 through 11 May 2007.

[26] Weber L, Ehrfeld W, Freimuth H, Lacher M, Lehr H, Pech B. Micromolding: A Powerful tool for large-scale production of precise microstructures. *Proceedings of SPIE - The International Society for Optical Engineering*; 14-15 October 1996; Austin, TX, USA.

[27] Weber L, Ehrfeld W. Micro-moulding - Processes, moulds, applications. *Kunsts. Plast. Eur.* 1998; 88 : 60-63.

[28] Ruprecht R, Hanemann T, Piotter V, Haußelt J. Polymer materials for microsystem technologies. *Microsys. Technol*. 1998; 5(1): 44-48.

[29] Bartels Mikrotechnik GmbH. Available at: www.bartels-mikrotechnik.de Accessed 2009.

[30] Becker H, Locascio L. Polymer microfluidic devices. *Talanta*; 2002; 56(2): 267-287.

[31] ThinXXS Microtechnology AG. Available at: www.thinxxs.com Accessed 2009.

[32] Piotter V, Hanemann T, Ruprecht R, Haußelt J. Microinjection moulding of medical device components. *Business Briefing: Medical Device Manufacturing & Technology*; 2002: 63-66.

[33] Kim D, Lee S, Ahn C, Lee J, Kwon T. Disposable integrated microfluidic biochip for blood typing by plastic microinjection moulding. *Lab Chip Miniaturisation Chem. Biol.* 2006; 6(6): 794-802.

[34] Micralyne Inc. Available at: http://www.micralyne.com Accessed 2009.

[35] Abbott Laboratories. i-STAT. Available at: http://www.abbottpointofcare.com/istat Accessed 2009.

[36] Microfluidic ChipShop GmbH. Lab-on-a-Chip Catalogue 01/2009. Available at: http://www.microfluidic-chipshop.com Accessed 2009.

[37] Gottschlich N. Production of plastic components for microfluidic applications. *Business Briefing: Future Drug Discovery*, 2004; Available at: http://www.touchbriefings.com/pdf/855/fdd041_greiner_tech.pdf. Accessed 2007.

[38] Boone T, HughFan Z, Hooper H, Ricco A, Tan H, Williams S. Plastic advances microfluidic devices. *Anal. Chem.* 2002; 74(3).

[39] Yu L, Koh C, Lee L, Koelling K, Madou M. Experimental investigation and numerical simulation of injection molding with micro-features. *Polym. Eng. Sci.* 2002; 42(5): 871-888.

[40] Bourdon R. Short cycles for injection moulded microfluidics parts. *Kunsts. Plast. Eur.* 2003; 93(9): 9,11+33.

[41] Xu G, Kim D, Koelling K, Lee L. Flow dynamics in injection molding with microfeatures. *Proceedings of the Annual Technical Conference, (ANTEC 2005)*; 1-5 May 2005; Boston, MA.

[42] Schneider C, Maier G. Small, but potent: special plastics for injection moulding microparts. *Kunsts. Plast. Eur.* 2001; 91(3): 27-28.

[43] Gerlach A, Knebel G, Guber AE, Heckele M, Herrmann D, Muslija A, et al. Microfabrication of single-use plastic microfluidic devices for high-throughput screening and DNA analysis. *Microsys. Technol.* 2002; 7(5-6): 265-268.

[44] Zhao J, Mayes R, Chen G, Chan PS, Xiong ZJ. Polymer micromould design and micromoulding process. *Plast. Rubber Compos.* 2003; 32(6): 240-247.

[45] Song S, Lee KY. Polymers for microfluidic chips. *Macromol. Res.* 2006; 14(2): 121-128.

[46] Stange T. Development and production of microfluidic chips made of polymers. *Am. Biotechnol. Lab.* 2002; 20(8): 8-10.

[47] Mönkkönen K, Hietala J, Pääkkönen P, Pääkkönen E, Kaikuranta T, Pakkanen T, Jääskeläinen T. replication of sub-micron features using amorphous thermoplastics. *Polym. Eng. Sci*. 2002; 42(7): 1600-1608.

[48] Liou A, Chen R. injection molding of polymer micro- and sub-micron structures with high-aspect ratios. *Int. J. Adv. Manuf. Technol.* 2006; 28(11-12): 1097-1103.

[49] Angelov A, Coulter J. The development and characterization of polymer microinjection molded gratings. *Polym. Eng. Sci.* 2008; 48(11): 2169-2177.

[50] Macintyre D, Thoms S. The fabrication of high resolution features by mould injection. *Microelectron Eng.* 1998; 41-42: 211-214.

[51] Pranov H, Rasmussen H, Larsen N, Gadegaard N. On the injection molding of nanostructured polymer surfaces. *Polym. Eng. Sci*. 2006; 46(2): 160-171.

[52] Angelov A, Coulter J. A feasibility study for sub-100 nm polymer injection molding. *Proceedings of the Annual Technical Conference, (ANTEC 2007)*; 6-11 May 2007.

[53] Gadegaard N, Mosler S, Larsen NB. Biomimetic polymer nanostructures by injection molding. *Macromol. Mater. Eng*. 2003; 288(1): 76-83.

[54] Erickson D, Li D. Integrated microfluidic devices. *Anal. Chim. Acta* 2004; 507(1): 11-26.

[55] Soper S, Henry A, Vaidya B, Galloway M, Wabuyele M, McCarley R. surface modification of polymer-based microfluidic devices. *Analytica Chimica Acta* 2002 10/11; 470(1): 87-99.

[56] Whitesides G. The Origins and the future of microfluidics. *Nature* 2006; 442(7101): 368-373.

[57] Soper SA, Ford S, Qi S, McCarley R, Kelly K, Murphy M. polymeric microelectromechanical systems. *Anal. Chem*. 2000; 72(19).

[58] Raviwongse R, Allada V. Artificial neural network based model for computation of injection mould complexity. *Int. J. Adv. Manuf. Technol*. 1997; 13(8): 577-586.

[59] Little G, Tuttle R, Clark D, Corney J. A feature complexity index. *Proc. Inst. Mech. Eng. Part C J. Mech. Eng. Sci*. 1998; 212(5): 405-412.

[60] Rosen D, Dixon J, Poli C, Dong X. Features and algorithms for tooling cost evaluation in injection molding and die casting. *Proceedings of the ASME International Computers in Engineering Conference and Exposition*; 2-6 August 1992; New York, NY, United States: Publ by ASME; 1992.

[61] Greener J, Wimberger-Friedl R. Precision Injection Molding: Process, Materials, and Applications. Cincinnati: Hanser Gardner Publications; 2006.

[62] Rötting O, Röpke W, Becker H, Gärtner C. Polymer microfabrication technologies. *Microsyst. Technol.* 2002; 8(1): 32-36.

[63] Madou M, Lee L, Koelling K, Lai S, Koh C, Juang Y, Yu L, Lu Y. Design and fabrication of polymer microfluidic platforms for biomedical applications. *Proceedings of the Annual Technical Conference, (ANTEC 2001)*; 3: 2534-2538.

[64] Derdouri A, Ilinca F, Hétu J. Microinjection molding of microstructures - Experimental and numerical simulation. *AIChE Annual* Meeting, Conference Proceedings; 30 October - 4 November 2005; Cincinnati, OH.

[65] Wimberger-Friedl R, Balemans W, Van Iersel B. Molding of microstructures and high aspect ratio features. *Proceedings of the Annual Technical Conference, (ANTEC 2003)*; 4-8 May 2003; Nashville, TN.

[66] Piotter V, Mueller K, Plewa K, Ruprecht R, Haußelt J. Performance and simulation of thermoplastic micro injection molding. *Microsys. Technol.* 2002; 8(6): 387-390.

[67] Sha B, Dimov S, Griffiths C, Packianather M. Micro-injection moulding: factors affecting the achievable aspect ratios. *Int. J. Adv. Manuf. Technol*. 2006.

[68] Ong N, Zhang H, Woo W. Plastic injection molding of high-aspect ratio micro-rods. *Mater. Manuf. Process*. 2006; 21(8): 824-831.

[69] Despa M, Kelly K, Collier J. Injection molding using high aspect ratio microstructures mold inserts produced by LIGA technique. *Proceedings of SPIE - The International Society for Optical Engineering*; 21-22 September 1998; Santa Clara, CA, USA.

[70] Kemmann O, Schaumburg C, Weber L. Micro moulding behaviour of engineering plastics. *Proceedings of SPIE - The International Society for Optical Engineering*; 30 March - 1 April 1999; Bellingham, WA, United States: 464-471.

[71] Hörr, M. Grundlagenuntersuchungen durch strukturdefinition beim mikrospritzgießen im rahmen des LIGA-prozesses. Darmstadt: Fachhochschule Darmstadt; 1997.

[72] Michaeli W, Gärtner R. New demolding concepts for the injection molding of microstructures. *J. Polym. Eng*. 2006; 26(2-4): 161-177.

[73] SMS Group. Battenfeld Service Manual, Version MB4GBV20 10/03. 2006.

[74] Kistler Instrument Corporation. Available at: http://www.kistler.com. Accessed: 2007.

[75] Griffiths C, Dimov S, Brousseau E, Chouquet C, Gavillet J, Bigot S. Micro-injection moulding: surface treatment effects on part demoulding. *4M2008 Proceedings*; 9th - 11th September; UK: Whittles Publishing; 2008.

[76] Bissacco G, Hansen H, Tang T, Fugl J. Precision manufacturing methods of inserts for injection molding of microfluidic systems. *ASPE Spring Topical Meeting on Precision Micro/Nano Scale Polymer Based Component & Device Fabrication*; April 2005.

[77] Yao D, Kim B. Simulation of the filling process in micro channels for polymeric materials. *J. Micromech. Microengineering* 2002; 12(5): 604-610.

[78] Tosello G, Fillon B, Azcarate S, Schoth A, Mattsson L, Griffiths C, Staemmler L, Bolt P. Hybrid tooling technologies and standardization for the manufacturing of inserts for micro injection molding. *Proceedings of the Annual Technical Conference, (ANTEC 2007)*; 6-11 May 2007.

[79] Michaeli W, Rogalla A, Ziegmann C. Processing technologies for the injection moulding of hybrid microstructures. *Macromol. Mater. Eng.* 2000; 279: 42-45.

[80] Michaeli W, Ziegmann C. Micro assembly injection moulding for the generation of hybrid microstructures. *Microsyst. Technol.* 2003; 9(6-7): 427-430.

[81] Michaeli W, Opfermann D. Bonding strength in micro injection assembly moulding. *Proceedings of the Annual Technical Conference, (ANTEC 2005)*; 1 May 2005 through 5 May 2005; Boston, MA.

[82] Michaeli W, Opfermann D. Micro assembly injection moulding. *Microsyst. Technol.* 2006; 12(7): 616-619.

[83] Michaeli W, Opfermann D. Increasing the feasible bonding strength in micro assembly injection molding using surface modifications. *Proceedings of the Annual Technical Conference, (ANTEC 2006)*; 7-11 May 2006; Charlotte, NC; 2006.

[84] Weber L, Ehrfeld W. Micromoulding: Market position and development potential. *Kunststoffe* 1999; 89(10): 192-202.

[85] Clay J, Heggs R. Material challenges in medical micromolding applications. *Proceedings of the Annual Technical Conference, (ANTEC 2002)*; 5-9 May 2002

[86] Martyn M, Whiteside B, Coates P, Allan P, Greenway G, Hornsby P. Micromoulding: Consideration of processing effects on medical materials. *Proceedings of the Annual Technical Conference, (ANTEC 2003)*; 4-8 May 2003; Nashville, TN.

[87] Tolinski M. Macro challenges in micromolding. *Plast. Eng*. 2005; 61(9): 14-16.

[88] Yoon S-H; Alabran M, Lee J, Mead J, Barry C, Carter D. Micro-injection molding of high aspect ratio features with thermoplastic polyurethanes. *Proceedings of the Annual Technical Conference, (ANTEC 2007)*; 6-11 May 2007.

[89] Ruprecht R, Bacher W, Haußelt J, Piotter V. Injection molding of liga and liga-similar microstructures using filled and unfilled thermoplastics. *Proceedings of SPIE - The International Society for Optical Engineering*; 23-24 October 1995; Austin, TX.

[90] Kim S, Trichur R, Beaucage G, Ahn C, Kim B. New plastic microinjection molding technique for extremely tall plastic structures using remote infrared radiation heating method. *Proceedings of the 10th Solid-State Sensor, Actuator and Microsystems Workshop*; June 2-6, 2002.

[91] Chen S, Chang J, Chang Y, Chau S. Micro injection molding of micro fluidic platform. *Proceedings of the Annual Technical Conference, (ANTEC 2005)*; 1-5 May 2005.

[92] Griffiths C, Dimov S, Brousseau E, Hoyle R. The effects of tool surface quality in micro-injection moulding. *J. Mater. Process. Technol.* 2007; 189(1-3): 418-427.

[93] Miller T, Fontaine J. Performance and materials for high performing injection molded optical elements. *Proc. Conf. Plast. Portable Wireless Electron*; 25-26 January 1999 (Brookfield, CT, United States): 37-42.

[94] Kalima V, Pietarinen J, Siitonen S, Immonen J, Suvanto M, Kuittinen M, Mönkkönen K , Pakkanen TT. Transparent thermoplastics: Replication of diffractive optical elements using micro-injection molding. *Opt. Mater.* 2007; 30(2): 285-291.

[95] Sha B, Dimov S, Griffiths C, Packianather M. Investigation of micro-injection moulding: factors affecting the replication quality. *J. Mater. Process. Technol.* 2007; 183(2-3): 284-296.

[96] Zhang K, Lu Z. Analysis of morphology and performance of PP microstructures manufactured by micro injection molding. *Microsyst. Technol.* 2008; 14(2): 209-214.

[97] Stewart R. Nanomaterials: Still climbing the steep curve of material development. *Plastics Engineering* April 2006;:12-20.

[98] Piotter V, Finnah G, Oerlygsson G, Ruprecht R, Haußelt J. Special variants and simulation of micro injection moulding. *Injection Moulding 2005: Collected Papers of the 5th International Conference,* Copenhagen, Denmark; March 1-2, 2005.

[99] Fassett J. Thin wall molding: differences in processing over standard injection molding. *Proceedings of the Annual Technical Conference, (ANTEC 1995)*; 7 May 1995 through 11 October 1995; Boston, MA, USA.

[100] Spennemann A, Michaeli W. Process analysis and machine technology for the injection molding of microstructures. *Proceedings of the Annual Technical Conference, (ANTEC 1999)*; May 2-6, 1999.

[101] Shepard T, Dunn D. Micro-injection molding of medical products: Machine specification and process simulation. *Proceedings of the Annual Technical Conference, (ANTEC 1995)*; 1995.

[102] Catanzaro J, Kadykowski B. Micro molding - "A new way". *Proceedings of the Annual Technical Conference, (ANTEC 2002)*; 3:2627-2633.

[103] Tipler P, Manser P. Developments in micromoulding. *Proceedings of Polymer Processing Engineering 01*; Bradford; UK; June 2001 UK; 2001.

[104] Michaeli W, Spennemann A. A New injection molding technology for micro parts. *J. Polym. Eng.* 2001; 21(2-3): 87-98.

[105] Michaeli W, Spennemann A, Gärtner R. New Plastification concepts for micro injection moulding. *Microsyst. Technol.* 2002; 8(1): 55-57.

[106] Liu M-K, Huang K-S, Chang J-Y, Wu C-H, Lin Y-C. Using a CD-like microfluidic platform for uniform calcium alginate drug carrier generation. *Proceedings of SPIE - The International Society for Optical Engineering*; 22-24 January 2007; San Jose, CA; 2007.

[107] Yu L, Lee L, Koelling K. Flow and heat transfer simulation of injection molding with microstructures. *Polym. Eng. Sci.* 2004; 44(10): 1866-1876.

[108] Chang P, Hwang S, Lee H, Huang D. Development of an external-type microinjection molding module for thermoplastic polymer. *Journal of Materials Processing Technology* 2007 4/12; 184(1-3): 163-172.

[109] Strassner J. Precision as a competitive edge. *Demagpress* 2004:3-4.

[110] Wang Y-D, Chang P-Q, Wu Y-F, Hwang S-J, Hwang, D-Y, Cheng, R-W. Design and fabrication of an all-electric tiebarless injection molding machine. *IEEE International Conference on Mechatronics, ICM '05*; 10-12 July 2005.

[111] Kelly A, Woodhead M, Coates P. Comparison of injection molding machine performance. *Polymer Engineering & Science* 2005; 45(6): 857-865.

[112] Bibber D. Micro molding challenges. Proceedings of *the Annual Technical Conference, (ANTEC 2004)*; 16-20 May 2004; Chicago, IL.

[113] Murakami O, Yamada K, Kotaki M. Replication and optical properties of injection moldings with microstructures. *Proceedings of the Annual Technical Conference, (ANTEC 2007)*; 6 May 2007 through 11 May 2007.

[114] Shen YK, Yeh SL, Chen SH. Three-dimensional non-Newtonian computations of micro-injection molding with the finite element method. *Int. Commun. Heat Mass Transf.* 2002; 29(5): 643-652.

[115] Zhao J, Mayes R, Chen G, Xie H, Chan P. Effects of process parameters on the micro molding process. *Polym. Eng. Sci.* 2003; 43(9): 1542-1554.

[116] Aufiero R. The effect of process conditions on part quality in microinjection molding. *Proceedings of the Annual Technical Conference, (ANTEC 2005)*; 1-5 May 2005; Boston, MA.

[117] Sha B, Dimov S, Griffiths C, Packianather MS. Micro-injection moulding: Factors affecting the achievable aspect ratios. *Int. J. Adv. Manuf. Technol.* 2007; 33(1-2): 147-156.

[118] Tosello G, Gava A, Hansen H, Lucchetta G. Influence of process parameters on the weld lines of a micro injection molded component. *Proceedings of the Annual Technical Conference, (ANTEC 2007)*; 6-11 May 2007.

[119] Jung W-C, Heo Y-M, Shin K-H, Yoon G-S, Chang S-H. An experimatal study on micro injection paramaters. *Proceedings of the Annual Technical Conference, (ANTEC 2007)*; 6-11 May 2007: 638-642.

[120] Lee B-, Hwang CJ, Kim DS, Kwon TH. Replication quality of flow-through microfilters in microfluidic lab-on-a-chip for blood typing by microinjection molding. *J. Manuf. Sci. Eng. Trans. ASME* 2008; 130(2): 0210101-0210108.

[121] Zhao J, Chen G, Juay Y. Development of process monitoring technologies for polymer micro moulding process. Available at: http://www.simtech.a-star.edu.sg/Research/TechnicalReports/TR0321.pdf. Accessed 2007.

[122] Whiteside B, Martyn M, Coates P. Micromoulding: Process evaluation. *Proceedings of the Annual Technical Conference, (ANTEC 2004)*; 16 May 2004 through 20 May 2004; Chicago, IL.

[123] Ono Y, Cheng C, Jen C, Tatibouët J, Hétu J. Ultrasonic technique and probes for monitoring surface imperfection of microfluidic plastic devices during injection molding. *Proceedings of the Annual Technical Conference, (ANTEC 2005)*; 1-5 May 2005; Boston, MA.

[124] Whiteside B, Brown E, Ono Y, Jen C, Coates P. Polymer degradation and filling incompletion monitoring for micromolding using ultrasound. *Proceedings of the Annual Technical Conference, (ANTEC 2005)*; 1-5 May 2005; Boston, MA.

[125] Ilinca F, Hétu J-F, Derdouri A. Numerical simulation of the filling stage in the micro-injection molding process. *Proceedings of the Annual Technical Conference, (ANTEC 2004)*; 16-20 May 2004; Chicago, IL.

[126] Kemmann O, Weber L, Jeggy C, Magotte O. Simulation of the micro injection molding process. *Proceedings of the Annual Technical Conference, (ANTEC 2000)*: 576-580.

[127] Hill S, Kämper K, Dasbach U, Döpper J, Ehrfeld W, Kaupert M. An investigation of computer modelling for micro-injection moulding. *Proceedings of Microsym'95*; September 1995.

[128] Norajitra P, Muller K, Ruprecht R, Haußelt J. computersimulation zur verbesserung der wirtschaftlichkeit beim spritzgießen von kunststoffmikrostrukturen. *Proceedings of Werkstoffwoche 1996, Symposium 8*; DGM-Informationsgesellschaft Verlag; 1996.

[129] Shen YK, Wu WY. An analysis of the three-dimensional micro-injection molding. *Int.Commun.Heat Mass Transf*. 2002; 29(3): 423-431.

[130] Young W. Simulation of the filling process in molding components with micro channels. *Microsyst. Technol*. 2005; 11(6): 410-415.

[131] Mehta N, Barry C, Bibber D, Tully D. Validation of flow simulation for micromolded parts. *Proceedings of the Annual Technical Conference, (ANTEC 2003)*; 4-8 May 2003; Nashville, TN; 2003.

[132] Shen Y, Chien H, Lin Y. Optimization of the micro-injection molding process using grey relational analysis and MoldFlow analysis. *J. Reinf. Plast.* Compos. 2004;23(17):1799-814.

[133] Majmundar R, Asthana A, Ghumman B, Barry C. Comparison of predicted and experimental filling of micromolded parts. *Proceedings of the Annual Technical Conference, (ANTEC 2005)*; 1-5 May 2005; Boston, MA.

[134] Sammoura F, Kang J, Heo Y, Jung T, Lin L. Polymeric microneedle fabrication using a microinjection molding technique. *Microsyst. Technol*. 2007; 13(5-6): 517-522.

[135] Kirkland C. A first in micromold flow analysis. *Injection Molding Mag*. May 2003.

[136] Whiteside B, Martyn M, Coates P, Greenway G, Allen P, Hornsby P. Micromoulding: Process measurements, product morphology and properties. *Plast. Rubber Compos*. 2004; 33(1): 11-17.

[137] Martyn M, Whiteside B, Coates P, Allan P, Hornsby P. Studies of the process-property interaction of the micromoulding process. *Proceedings of the Annual Technical Conference, (ANTEC 2001)*; 5-9 May 2001. Brookfield Center, CT, USA.

[138] Greenway G, Allan P, Bevis M, Hornsby P. The mechanical testing of micro injection mouldings. *Proceedings of the Annual Technical Conference, (ANTEC 2001)*; 5-9 May 2001.

[139] Greenway G, Allan P, Hornsby P. The characterisation and physical testing of micro-mouldings. *Proceedings of the Annual Technical Conference, (ANTEC 2003)*; 4 May 2003 through 8 May 2003; Nashville, TN.

[140] Morales A, Simmons B, Wallow T, Campbell K., Mani S, Mittal B, Crocker RW, Cummings EB, Davalos RV, Domeier LA, Hunter MC, Krafcik KL, McGraw GJ, Mosier BP, Sickafoose SM. Injection Molded Microfluidic Devices for Biological Sample Separation and Detection. Proceedings of SPIE - *The International Society for Optical Engineering*; 25-25 January 2006; San Jose, CA.

[141] Mair D, Geiger E, Pisano A, Fréchet J, Svec F. Injection molded microfluidic chips featuring integrated interconnects. *Lab Chip Miniaturisation Chem. Biol.* 2006; 6(10): 1346-1354.

[142] Heckele M, Guber A, Truckenmüller R. Replication and bonding techniques for integrated microfluidic systems. *Microsyst. Technol.* 2006; 12(10-11): 1031-1035.

[143] Sung W, Lee G, Tzeng C, Chen S. Plastic microchip electrophoresis for genetic screening: The analysis of polymerase chain reactions products of fragile X (CGG)n alleles. *Electrophoresis 2001*; 22: 1188-1193.

[144] Lee S, Kim S, Kang J, Ahn C. A polymer lab-on-a-chip for reverse transcription (RT)-PCR based point-of-care clinical diagnostics. *Lab Chip Miniaturisation Chem. Biol.* 2008; 8(12): 2121-2127.

[145] Yussuf A, Sbarski I, Hayes J, Solomon M. Sealing and bonding techniques for polymer-based microfluidic devices. Swinburne University of Technology; Available at: http://www.swin.edu.au/iris/pdf/profiles/AbdirahmanYussuf.pdf. Accessed: March 2007.

[146] Noerholm M, Bruus H, Jakobsen MH, Telleman P, Ramsing NB. Polymer microfluidic chip for online monitoring of microarray hybridizations. *Lab Chip Miniaturisation Chem. Biol.* 2004; 4(1): 28-37.

[147] Blattert C, Jurischka R, Schoth A, Kerth P Menz W. Fabrication and testing of novel blood separation devices based on microchannel bend structures. *Progress in Biomedical Optics and Imaging - Proceedings of SPIE*; 13-15 December 2004; Sydney, NSW.

[148] Klepárník K, Horký M. Detection of DNA fragmentation in a single apoptotic cardiomyocyte by electrophoresis on a microfluidic device. *Electrophoresis* 2003; 24(2): 3778-3783.

[149] Tahhan I, Blattert C, Jurischka R, Schoth A, Kerth P, Reinecke H. Improved and simple sealing of microfluidic structures. *3rd IEEE/EMBS Special Topic Conference on Microtechnology in Medicine and Biology*; 12-15 May 2005.

[150] Tan W, Fan ZH, Qiu CX, Ricco AJ, Gibbons I. Miniaturized capillary isoelectric focusing in plastic microfluidic devices. *Electrophoresis* 2002; 23(2): 3638-3645.

[151] Weigl B, Domingo G, LaBarre P, Gerlach J. Towards non- and minimally instrumented, microfluidics-based diagnostic devices. *Lab Chip Miniaturisation Chem. Biol*. 2008; 8(12): 1999-2014.

[152] Qi S, Liu X, Ford S, Barrows J, Thomas G, Kelly K, McCandless A, Lian K, Goettert J, Soper SA. Microfluidic devices fabricated in poly(methyl methacrylate) using hot-embossing with integrated sampling capillary and fiber optics for fluorescence detection. Lab Chip Minituarisation Chem. Biol. 2002; 2: 88-95.

[153] Sassi AP, Paulus A, Cruzado ID, Bjornson T, Hooper HH. Rapid, parallel separations of D1S80 alleles in a plastic microchannel chip. *J. Chromatogr. A* 2000; 894(1): 203-217.

[154] Zhou X-M, Shao S-J, Xu G-D, Zhong R-T, Liu D-Y, Tang J-W, Gao Y-N, Cheng S-J, Lin B-C. Highly sensitive determination of the methylated *p16* gene in cancer patients by microchip electrophoresis. *J. Chromatogr. B Anal. Technol. Biomed. Life Sci.* 2005; 816(1): 145-151.

[155] Madou MJ, Lee LJ, Daunert S, Lai S, Shih C-H. Design and fabrication of CD-like microfluidic platforms for diagnostic: Mircrofluidic functions. *Biomed. Microdevices* 2001; 3(3): 245-254.

[156] Webb DP, Hutt DA, Hopkinson N, Palmer PJ, Conway PP. Integration and packaging of microsystems by polymer overmoulding. *Proc. ESTC 2006 - 1st Electronics Systemintegration Technology Conference* (5-7 September 2006): 567-574.

[157] Tosello G, Hansen HN. In-process assembly of micro metal inserts in a polymer matrix. *Proc. 4M2006*; 2006: 83-86.

[158] Gravesen P, Branebjerg J, Jensen OS. Microfluidics - a review. *J. Micromech. Microengineering* 1993; 3: 168-82.

[159] Vilkner T, Janasek D, Manz A. Micro total analysis systems. Recent developments. *Anal. Chem.* 2004; 76(12): 3373-3386.

[160] Becker H , Gärtner C . Polymer microfabrication technologies for microfluidic systems. *Anal. Bioanal. Chem*. 2008; 390(1): 89-111.

[161] Attia UM, Marson S, Alcock JR. Micro-injection moulding of polymer microfluidic devices. *Microfluid. Nanofluid*. 2009; 7(1): 1-28.

[162] Auroux P-A, Iossifidis D, Reyes DR, Manz A. Micro total analysis systems. 2. Analytical standard operations and applications. *Anal. Chem.* 2002; 74(1): 2637-2652.

[163] Abgrall P, Gué A-M. Lab-on-chip technologies: Making a microfluidic network and coupling it into a complete microsystem - A review. *J. Micromech. Microengineering* 2007; 17(5).

[164] Li S, Xu Z, Mazzeo A, Burns DJ, Fu G, Dirckx M, Shilpiekandula V, Chen X, Nayak NC, Wong E, Yoon SF, Fang ZP, Youeef-Toumi K, Hardt D, Tor SB, Yue CY, Chun J-H. Review of production of microfluidic devices: Material, manufacturing and metrology. *Proc. of SPIE* 6993; 2008. Article number 69930F.

[165] Sun Y, Kwok YC. Polymeric microfluidic system for DNA analysis. *Anal. Chim. Acta* 2006; 556: 80-96.

[166] Brüning H, Stange T. Towards lab-on-a-chip devices for personalised medication and diagnostics. *Med. Device Technol*. 2004; 15(10): 40-41.

[167] Soper SA, Stryjewski W, Zhu L, Xu Y, Wabuyele M, Chen H, Galloway M, McCarley RL. Polymer-based modular microsystems for DNA sequencing. *7th International Conference on Miniaturized Chemical and Biochemical Analysis Systems*; October 5-9; 2003: 717-720.

[168] McCormick RM, Nelson RJ, Alonso-Amigo MG, Benvegnu DJ, Hooper HH. Microchannel electrophoretic separations of DNA in injection-molded plastic substrates. *Anal. Chem.* 1997; 69(1): 2626-2630.

[169] Gärtner C, Becker H, Anton B, Rötting O. The microfluidic toolbox - Tools and standardization solutions for microfluidic devices for life sciences applications. *Proc. SPIE Int. Soc. Opt. Eng.* 2004; 5345: 159-162.

[170] Datta P, Hammacher J, Pease M, Gurung S, Goettert J. Development of an integrated polymer microfluidic stack. *J. Phys. Conf. Ser*. 2006; 34(1): 853-858.

[171] Ahn CH, Choi J-W, Beaucage G, Nevin JH, Lee J-B, Puntambekar A, Lee JY. Disposable smart lab on a chip for point-of-care clinical diagnostics. *Proc. IEEE 2004*; 92(1): 154-173.

[172] Grodzinski P, Liu RH, Chen B, Blackwell J, Liu Y, Rhine D, Smekal T, Ganser D, Romero C, Yu H, Chan T, Kroutchinina N. Development of plastic microfluidic devices for sample preparation. Biomed. *Microdevices* 2001; 3(4): 275-283.

[173] Singh V, Desta Y, Datta P, Guy J, Clarke M, Feedback DL, Weimert J, Goettert J. A hybrid approach for fabrication of polymeric BIOMEMS devices. *Microsyst. Technol.* 2007; 13(3-4): 369-377.

[174] Koh CG, Tan W, Zhao M-Q, Ricco AJ, Fan ZH. Integrating polymerase chain reaction, valving, and electrophoresis in a plastic device for bacterial detection. *Anal. Chem.* 2003; 75(1): 4591-4598.

[175] Biehl M, Velten T. Gaps and challenges of point-of-care technology. *IEEE Sensors J.* 2008; 8(5): 593-600.

[176] Bo Y, Salustri FA. Function Modeling Based on Interactions of Mass, Energy and Information. Function modeling based on interactions of mass, energy and information. *Proc. of the Twelfth International Florida Artificial Intelligence Research Society Conference*; 1999: 384-388.

[177] Salustri FA. Function modeling for an integrated framework: A progress report. *Proc. of the Eleventh International Florida Artificial Intelligence Research Symposium Conference (FLAIRS '98)*, (May 27, Menlo Park, California: The AAAI Press); 1998: 339-343.

[178] Huang F-C, Chen Y-F, Lee G-B. CE chips fabricated by injection molding and polyethylene/thermoplastic elastomer film packaging methods. *Electrophoresis* 2007; 28(7): 1130-1137.

[179] Upchurch Scientific. Upchurch Scientific: Micro Fluidic Connectors. Available at: http://www.upchurch.com/PDF/Lit/micro_singles.pdf. Accessed 2007.

[180] Puntambekar A, Ahn CH. Self-aligning microfluidic interconnects for glass- and plastic-based microfluidic systems. *J. Micromech. Microengineering* 2002; 12(1): 35-40.

[181] Lee Lee D-S, Park SH, Yang H, Chung K-H, Yoon TH, Kim S-J, Kim K, Kim YT. Bulk-micromachined submicroliter-volume pcr chip with very rapid thermal response and low power consumption. *Lab Chip Miniaturisation Chem. Biol.* 2004; 4: 401-407.

[182] Webb DP, Hsu CC, Hutt DA, Hopkinson N, Conway PP, Palmer PJ. Polymer overmoulding for microfluidic device packaging and system integration. Polytronic 2005, *5th Int. Conf. Polym. Adhes. in Microelectr. Photonics Proc.* 2005:134-139.

[183] Lee LJ, Madou MJ, Koelling KW, Daunert S, Lai S, Koh CG, Juang Y-J, Lu,Y, Yu L. Design and fabrication of CD-like microfluidic platforms for diagnostics: Polymer-based microfabrication. *Biomed. Microdevices* 2001; 3(4): 339-351.

[184] Choi SH, Kim DS, Kwon TH. microinjection molded disposable microfluidic lab-on-a-chip for efficient detection of agglutination. *Microsyst. Technol.* 2009; 15(2): 309-316.

[185] De Mello A. Research highlights - Phase change microvalves. *Lab Chip* 2004; 4: 3rd of May 2007.

[186] Geschke O, Klank H, Tellemann P. Microsystem Engineering of Lab-on-a-chip Devices. Weinheim: Wiley-VCH; 2004.

[187] Oh KW, Ahn CH. A review of microvalves. *J. Micromech. Microengineering* 2006; 16: R13-R39.

[188] Ahn CH, Puntambekar A, Lee SM, Cho HJ, Hong C-C. Structurally programmable microfluidic systems. *Proc. microTAS*; 2000: 205-208.

[189] Worgull M, Heckele M, Mappes T, Matthis B, Tosello G, Metz T, Gavillet J, Koltay P, Hansen HN. Sub-μm structured lotus surfaces manufacturing. *Microsyst. Technol.* 2008:1-7.

[190] Choi J-W, Puntambekar A, Hong C-C, Gao C Zhu X, Trichur R, Han J, Chilukuru S, Dutta M, Murugesan S, Kim S, Sohn Y-S, Nevin JH, Beaucage G, Lee J-B, Lee JY, Bissell MG, Ahn CH. A disposable plastic biochip cartridge with on-chip power sources for blood analysis. *Proc. IEEE Micro Electro Mech. Syst. MEMS*; 2003:447-450.

[191] Choi J-W, Kim S, Trichur R, Cho HJ, Puntambekar A, Cole RL, Simkins JR, Murugesan S, Kim K, Lee J-B, Beaucage G, Nevin JH, Ahn CH. A plastic micro injection molding technique using replaceable mold-disks for disposable microfluidic systems and biochips. *Proc. micro-TAS 2001*; 2001: 411-412.

[192] Do J, Ahn CH. A polymer lab-on-a-chip for magnetic immunoassay with on-chip sampling and detection capabilities. *Lab Chip Miniaturisation Chem. Biol*. 2008; 8(4): 542-549.

[193] Schuenemann M, Thomson D, Atkins M, Garst S, Yussuf A, Solomon M, Hayes J, Harvey E. Packaging of disposable chips for bioanalytical applications. *Proc. Electron Compon. Technol. Conf*. 2004; 1: 853-861.

[194] Gärtner C, Klemm R, Becker H. Methods and instruments for continuous-flow PCR on a chip. *Proc. SPIE Int. Soc. Opt. Eng.* 6465; 2007; Article no. 646502.

[195] Li C, Wu P-M, Browne A, Lee S, Ahn CH. Hot-embossed piezoelectric polymer micro-diaphragm arrays integrated with lab-on-a-chip for protein analysis. *Proc. IEEE Sens*. 2007: 462-465.

[196] Do J, Lee S, Han J, Kai J, Hong C-C, Gao C, et al. Development of functional lab-on-a-chip on polymer for point-of-care testing of metabolic parameters. *Lab Chip Miniaturisation Chem.Biol.* 2008; 8(12): 2113-2120.

[197] Nugen SR, Asiello PJ, Baeumner AJ. Design and fabrication of a microfluidic device for near-single cell mRNA isolation using a copper hot embossing master. *Microsyst. Technol.* 2009; 15(3): 477-483.

[198] Guber AE, Heckele M, Herrmann D, Muslija A, Saile V, Eichhorn L, Gietzelt T, Hoffmann W, Hauser PC, Tanyanyiwa J, Gerlach A, Gottschlich N, Knebel G. Microfluidic lab-on-a-chip systems based on polymers - Fabrication and application. *Chem. Eng. J.* 2004; 101(1): 447-453.

[199] Garst S, Schuenemann M, Solomon M, Atkin M, Harvey E. Fabrication of multilayered microfluidic 3D polymer packages. *Proc. Electron. Compon. Technol. Conf. 2005*; 1:603-610.

[200] Tsao C-W, DeVoe DL. Bonding of thermoplastic polymer microfluidics. *Microfluid. Nanofluid*. 2009; 6(1): 1-16.

[201] Yoo J-C, Moon M-C, Choi YJ, Kang CJ, Kim Y-S. A high performance microfluidic system integrated with the micropump and microvalve on the same substrate. *Microelectron*. Eng. 2006; 83:1684-1687.

[202] Erickson D, Sinton D, Li D. A miniaturized high-voltage integrated power supply for portable microfluidic applications. *Lab Chip*; 2004; 4: 87-90.

[203] Hong C-C, Choi J-W, Ahn CH. An on-chip air-bursting detonator for driving fluids on disposable lab-on-a-chip systems. *J. Micromech. Microengineering*; 2007; 17: 410-417.

[204] Ellis M. Plastic diagnostic lab-on-a-chip. *Materials World 2009*; 17: 12-13.

[205] Datta P, George G, Tiwari S, Goettert J. Monolithic fabrication of electro-fluidic polymer microchips. *Microsyst. Technol*. 2009; 15: 463-469.

[206] Gharib Naseri N, Baldock SJ, Economou A, Goddard NJ, Fielden PR. Disposable injection-moulded cell-on-a-chip microfluidic devices with integrated conducting polymer electrodes for on-line voltammetric and electrochemiluminescence detection. *Electroanalysis* 2008; 20(4): 448-454.

[207] Chen C, Chang G, Lin C. Performance evaluation of a capillary electrophoresis electrochemical chip integrated with gold nanoelectrode ensemble working and decoupler electrodes. *Journal of Chromatography A* 2008 6/20; 1194(2): 231-236.

[208] Michaeli W, Opfermann D, Kamps T. Advances in micro assembly injection moulding for use in medical systems. *Int. J. Adv. Manuf. Technol*. 2007; 33(1-2): 206-211.

[209] Michaeli W, Kamps T. Micro assembly injection moulding with plasma treated inserts. *Microsyst. Technol*. 2008; 14(12): 1903-1907.

[210] Becker H, Mühlberger H, Hoffmann W, Clemens T, Klemm R, Gärtner C. Portable CE-system with contactless conductivity detection in an injection molded polymer chip for on-site food analysis. *Proc. SPIE Int. Soc. Opt. Eng.* 6886; 2008; Article no. 68860C.

[211] Heller MJ, Guttman A. Integrated Microfabricated Biodevices: Advanced Technology for Genomics, Drug Discovery, Bioanalysis, and Clinical Diagnostics. New York: Marcel Dekker, Inc. 2002.

[212] Gärtner C, Kirsch S, Anton B, Becker H. Hybrid microfluidic systems - combining a polymer microfluidic toolbox with biosensors. *Proc. SPIE Int. Soc. Opt. Eng*. 6465; 2007; Article no. 64650F.

[213] Nguyen N-N, Wereley S. Fundamentals and Applications of Microfluidics. 2nd ed. Boston: Artech House; 2006.

[214] Hashimoto M, Chen P-C, Mitchell MW, Nikitopoulos DE, Soper SA, Murphy MC. Rapid PCR in a continuous flow device. *Lab Chip Miniaturisation Chem. Biol.* 2004; 4: 638-645.

[215] Do J, Choi J-W, Ahn CH. Low-cost magnetic interdigitated array on a plastic wafer. *IEEE Trans. Magn.* 2004; 40 (4 II): 3009-3011.

[216] Hsiung S-K, Lin C-H, Lee G-B. A microfabricated capillary electrophoresis chip with multiple buried optical fibers and microfocusing lens for multiwavelength detection. *Electrophoresis* 2005; 26(6): 1122-1129.

[217] Lin C-H, Hsiung S-K, Lee GB. High-throughput micro capillary electrophoresis chip for bio-analytical application utilizing multi-wavelength detection. *Proc. IEEE Int. Conf. Micro Electro Mech. Syst. MEMS*; 2004: 304-307.

[218] Lee G-B, Chen S-H, Huang G-R, Sung W-C, Lin Y-H. Microfabricated plastic chips by hot embossing methods and their applications for DNA separation and detection. *Sens. Actuators, B Chem*. 2001; 75(1-2): 142-148.

[219] Wainright A, Nguyen UT, Bjornson T, Boone TD. Preconcentration and separation of double-stranded DNA fragments by electrophoresis in plastic microfluidic devices. *Electrophoresis* 2003; 24(2): 3784-3792.

[220] Sun Y, Lim CS, Liu AQ, Ayi TC, Yap PH. Design, simulation and experiment of electroosmotic microfluidic chip for cell sorting. *Sens. Actuators A Phys*. 2007; 133(2 SPEC. ISS.): 340-348.

[221] Sabur R, Matin MA. Study of electro-osmotic flow in microfluidic devices. Proc. IEEE-EMBS *Int. Summer Sch. Symp. Med. Devices Biosens*. 2006: 126-129.

[222] Wang Y, Vaidya B, Farquar HD, Stryjewski W, Hammer RP, McCarley RL, Soper SA, Cheng Y-W, Barany F. Microarrays assembled in microfluidic chips fabricated from poly(methyl methacrylate) for the detection of low-abundant DNA mutations. *Anal. Chem.* 2003; 75:1130-1140.

[223] Anonymous. Integrating functions in the injection moulding process. *Today, the ARBURG magazine*, Issue 36, pp. 10-11. Available at: http://www.arburg.com/com/common/download/today/today36_2007_EN_GB.pdf. Accessed 2009

[224] Myers FB, Lee LP. Innovations in optical microfluidic technologies for point-of-care diagnostics. *Lab Chip Miniaturisation Chem. Biol.* 2008; 8(12): 2015-2031.

[225] Meagher RJ, Hatch AV, Renzi RF, Singh AK. An integrated microfluidic platform for sensitive and rapid detection of biological toxins. *Lab Chip Miniaturisation Chem. Biol.* 2008; 8(12): 2046-2053.

[226] Topham D, Harrison D. The conceptual design of products benefiting from integrated micro-features. *2nd Electronics Systemintegration Technology Conference, ESTC*; 1 September 2008 through 4 September 2008.

[227] Shah JJ, Mantyla M. Parametric and Feature-Based CAD/CAM. New York; Chichester: Wiley; 1995.

[228] Boothroyd G, Dewhurst P, Knight WA. Product Design for Manufacture and Assembly. 2nd , rev. and expand ed. New York: M. Dekker; 2002.

[229] McMahon C. CADCAM: Principles, Practice, and Manufacturing Management. 2nd ed. Harlow: Addison-Wesley; 1998.

[230] Pearson Education Limited. The Longman Dictionary of Contemporary English Online. 2009; Available at: www.ldoceonline.com. Accessed 2009.

[231] Merriam-Webster I. Merriam-Webster Online. 2009; Available at: www.merriam-webster.com. Accessed 2009.

[232] Verma AK, Rajotia S. Automatic identification of aspect vectors and geometrical validation of 2.5D parts. *Int. J. Prod. Res.* 2006; 44(5): 999-1013.

[233] Corney J, Clark DER, Murray JL, Yue Y. Automatic classification of 2 1/2 D components. *ASME Prod. Eng. Div. Publ. PED*; 8 November 1992 through 13 November 1992; Anaheim, CA, USA: Publ by ASME; 1992.

[234] Willis D, Donaldson IA, Ramage AD, Murray JL, Williams MH. A knowledge-based system for process planning based on a solid modeller. *Comput. Aided Eng. J.* 1989; 6(1): 21-6.

[235] Yue Y, Murray JL. Validation, workpiece selection and clamping of complex 2.5D components. *Advances in Feature Based Manufacturing*; 1994:185-213.

[236] Alting L, Kimura F, Hansen HN, Bissacco G. Micro engineering. *CIRP Annals* 2003; 52/2/2003: 635-58.

[237] Liu X, DeVor RE, Kapoor SG, Ehmann KF. The mechanics of machining at the microscale: Assessment of the current state of the science. *J. Manuf. Sci. Eng. Trans. ASME* 2004; 126(4): 666-678.

[238] Hansen HN, Carneiro K, Haitjema H, De Chiffre L. Dimensional micro and nano metrology. *CIRP Ann. Manuf. Technol.* 2006; 55(2): 721-743.

[239] Madou MJ. Fundamentals of Microfabrication: The Science of Miniaturization. 2nd ed. Boca Raton, FL: CRC Press; 2001.

[240] Bissacco G. Tooling process chains. *Summer School 2007, Micro Mechanical Systems Design and Manufacturing*; Technical University of Denmark (DTU) 2007.

[241] De Grave A, Brissaud D. Collaboration and integration in the design of microelectromechanical systems (MEMS). *CIRP Design Conf.* 2005.

[242] Stokes C, Palmer, PJ. 3D micro-fabrication processes: A review. *Institution of Engineering and Technology Seminar on MEMS Sensors and Actuators, ICEPT*; 27-28 April 2006.

[243] Yeh H-M, Chen K-S. Development of a digital-convolution-based process emulator for three-dimensional microstructure fabrication using electron-beam lithography. *IEEE Trans.Ind.Electron.* 2009; 56(4): 926-936.

[244] Uriarte L, Ivanov A, Oosterling H, Staemmler L, Tang PT, Allen D. A comparison between microfabrication technologies for metal tooling. *Proc. 1st Int. Conf. 4M 2005*; 2005: 351-354.

[245] Osswald TA, Turng LS, Gramann PJ (Editors). Injection Molding Handbook. Cincinnti, OH: Hanser/Gardner Publications; 2001.

[246] Campo EA. The Complete Part Design Handbook for Injection Molding of Thermoplastics. Munich; Cincinnati: Hanser Gardner Publications; 2006.

[247] Rees H. Understanding Injection Mold Design. Cincinnati, OH: Hanser Gardner Publications; 2001.

[248] Anonymous. Ejector for micro structured and micro optical parts without surface defects announced by KuZ. *The International Magazine for Micro, Precision and Nano Technologies* 2009; Rapid News Publications plc Avaialble at: http://www.micromanu.com/x/guideArchiveArticle.html?id=588. Accessed 2009.

[249] Michaeli W, Gärtner R. Injection molding of micro-structured surfaces. *Proceedings of the Annual Technical Conference*, (ANTEC 2004); 16-20 May 2004. Chicago, IL.

[250] Zhang HL, Ong NS, Lam YC. Mold surface roughness effects on cavity filling of polymer melt in micro injection molding. *Int. J. Adv. Manuf. Technol.* 2008; 37(11-12): 1105-1112.

[251] Ong NG, Zhang HL, Lam YC. Numerical simulation of cavity roughness effects on melt filling in microinjection molding. *Adv. Polym. Technol*. 2008; 27(2): 89-97.

[252] Kim DS, Lee K-, Kwon TH, Lee SS. Micro-channel filling flow considering surface tension effect. *J. Micromech. Microengineering* 2002; 12(3): 236-246.

[253] Hung, WNP; Ali, MY, Agnihotri MM, Yuan S. Molding of three-dimensional microcomponents. *Proc. Int. Conf. Manufac. Sci. Eng*. 8-11 October 2006; Ypsilanti, MI; 2006.

[254] Yao D, Kim B. Scaling issues in miniaturization of injection molded parts. *J. Manuf. Sci. Eng. Trans. ASME* 2004; 126(4): 733-739.

[255] Giboz J, Copponnex T, Mélé P. Microinjection molding of thermoplastic polymers: Morphological comparison with conventional injection molding. *J. Micromech. Microengineering* 2009; 19(2).

[256] Martinez AW, Phillips ST, Whitesides GM. Three-dimensional microfluidic devices fabricated in layered paper and tape. *Proceedings of the National Academy of Sciences*; December 2008; 16; 105(50):19606-19611.

[257] Weigl BH, Bardell R, Schulte T, Battrell F, Hayenga J. Design and rapid prototyping of thin-film laminate-based microfluidic devices. *Biomed. Microdevices* 2001; 3(4): 267-274.

[258] Unger MA, Chou H-P, Thorsen T, Scherer A, Quake SR. Monolithic microfabricated valves and pumps by multilayer soft lithography. *Science* 2000; 288(5463): 113-116.

[259] Yang JM, Bell J, Huang Y, Tirado M, Thomas D, Forster AH, Haigis RW, Swanson PD, Wallace RB, Martinsons B Krihak M. An integrated, stacked microlaboratory for biological agent detection with DNA and immunoassays. *Biosens. Bioelectron*. 2002; 17(6-7): 605-618.

[260] King Jr. CR, Sekar D, Bakir MS, Dang B, Pikarsky J, Meindl JD. 3D stacking of chips with electrical and microfluidic I/O interconnects. Proc. Electron. *Compon. Technol. Conf.* 2008, 1-7, Lake Buena Vista, FL

[261] Harrison DJ, Fluri K, Seiler K, Fan Z, Effenhauser CS, Manz A. Micromachining a miniaturized capillary electrophoresis-based chemical analysis system on a chip. *Science* 1993; 261(5123): 895-897.

[262] 3D-MINTEGRATION: The design and manufacture of 3D miniaturised integrated products. 2007; Available at: www.3d-mintegration.com. Accessed 2007.

[263] Cohn G.E., Katzir A., editors. The LabCD™: A centrifuge-based microfluidic platform for diagnostics. *Systems and Technologies for Clinical Diagnostics and Drug Discovery*; 26-27 January 1998.

[264] Fung YC. Biomechanics: Mechanical Properties of Living Tissues. 2nd ed. New York ; London: Springer-Verlag; 1993.

[265] Yang S, Ündar A, Zahn JD. A microfluidic device for continuous, real time blood plasma separation. *Lab Chip Miniaturisation Chem. Biol.* 2006; 6(7): 871-880.

[266] Faivre M, Abkarian M, Bickraj K, Stone HA. Geometrical focusing of cells in a microfluidic device: An approach to separate blood plasma. *Biorheology* 2006; 43(2): 147-159.

[267] Kersaudy-Kerhoas M, Amalou F, Kavanagh D, Marson S, Attia UM, Summersgill P, Ryan T, Desmulliez MPY. Design, Manufacturing and Test of Disposable Microfluidic System for Blood-Plasma Separation. 2008; Available at: www.eposters.net.

[268] Whiteside B, Manser P. Reinventing Micro- and Nanomoulding. March 2007; Available at: http://www.devicelink.com/mdt/archive/07/03/002.html. Accessed 2009.

[269] Eriksson L, Johansson N, Kettaneh-Wold N, Wikstrom C, Wold S. Design of Experiments: Principles and Applications. 3rd Edition ed. Umea: Umetrics; 2008.

[270] Minitab Inc. Available at: www.minitab.com. Accessed 2008.

[271] Marson S, Attia UM, Allen DM, Tipler P, Jin T, Hedge J and Alcock JR. Reconfigurable micro-mould for the manufacture of truly 3D polymer microfluidic devices. *Proc CIRP Design Conf*. Cranfield, UK, 30-31 March 2009: 343-346

[272] Lahey JP, Launsby RG. Experimental Design for Injection Molding. Colorado Springs, CO: Launsby Consulting; 1998.

[273] Montgomery DC. Design and Analysis of Experiments. 6th ed. Hoboken; Great Britain: Wiley; 2005.

[274] Ong NS, Koh YH. Experimental investigation into micro injection molding of plastic parts. *Mater. Manuf. Process*. 2005; 20(2): 245-253.

[275] Del Vecchio RJ. Understanding Design of Experiments: a Primer for Technologists. Cincinnati, Ohio: Hanser; Hanser/Gardner Publications; 1997.

[276] Antony J. Design of Experiments for Engineers and Scientists. Oxford: Butterworth-Heinemann; 2003.

[277] Shilpiekandula V, Burns DJ, El Rifai K, Youcef-Toumi K, Shiguang L, Reading I, Yoon SF. Metrology of microfluidic devices: A review. *1st International Conference on Micromanufacturing (ICOMM 2006)*; 13-15 September 2006.

[278] Alonso-Amigo MG, Adams T. Development of a plastic microfluidics chip. 2009; Available at: http://www.devicelink.com/ivdt/archive/03/03/003.html. Accessed 2009.

[279] Attia UM, Alcock JR. An evaluation of process-parameter and part-geometry effects on the quality of filling in micro-injection moulding. *Microsyst. Technol.* 2009. DOI: 10.1007/s00542-009-0923-1.

[280] Piotter V, Prokop J, Ritzhaupt-Kleissl H-J, Ruh A, Hausselt J. Multi-component microinjection moulding-trends and developments. *Int. J. Adv. Manuf. Technol.* 2009: 1-9.

[281] Van der Beek M, Mathew A, Andreadaki A, Kieft I, Nellissen T, Weekamp W. Development of integrated microfluidic devices - Packaging and interconnect solutions. *Mstnews* 3/09; June 2009.

[282] Attia UM, Alcock JR. Integration of functionality into polymer-based microfluidic devices produced by high-volume micromoulding techniques. *Int. J. Adv. Manuf. Technol.* 2009. DOI: 10.1007/s00170-009-2345-8.

[283] DESMA TEC. Micro injection moulding machine for smallest shot weights. 2009; Available at: http://www.desma-tec.de/en/machines/micro_injection/micro_injection.html. Accessed 2008.

APPENDICES

APPENDIX A1: Dimensioned drawings of the five layers of the blood/plasma separator

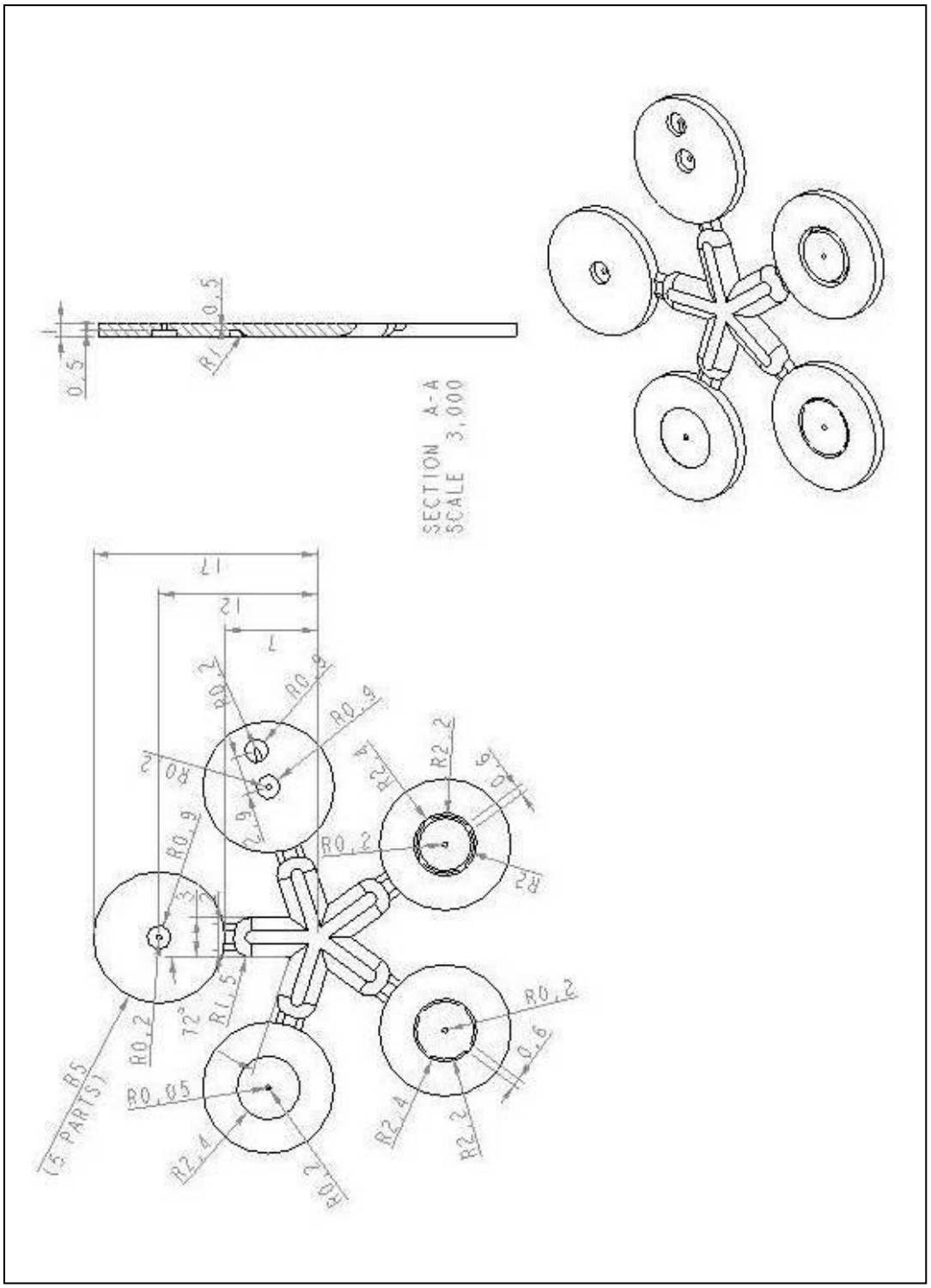

APPENDIX A2: Dimensioned drawings of the blood separator mould and inserts

❒ INSERT HOLDER

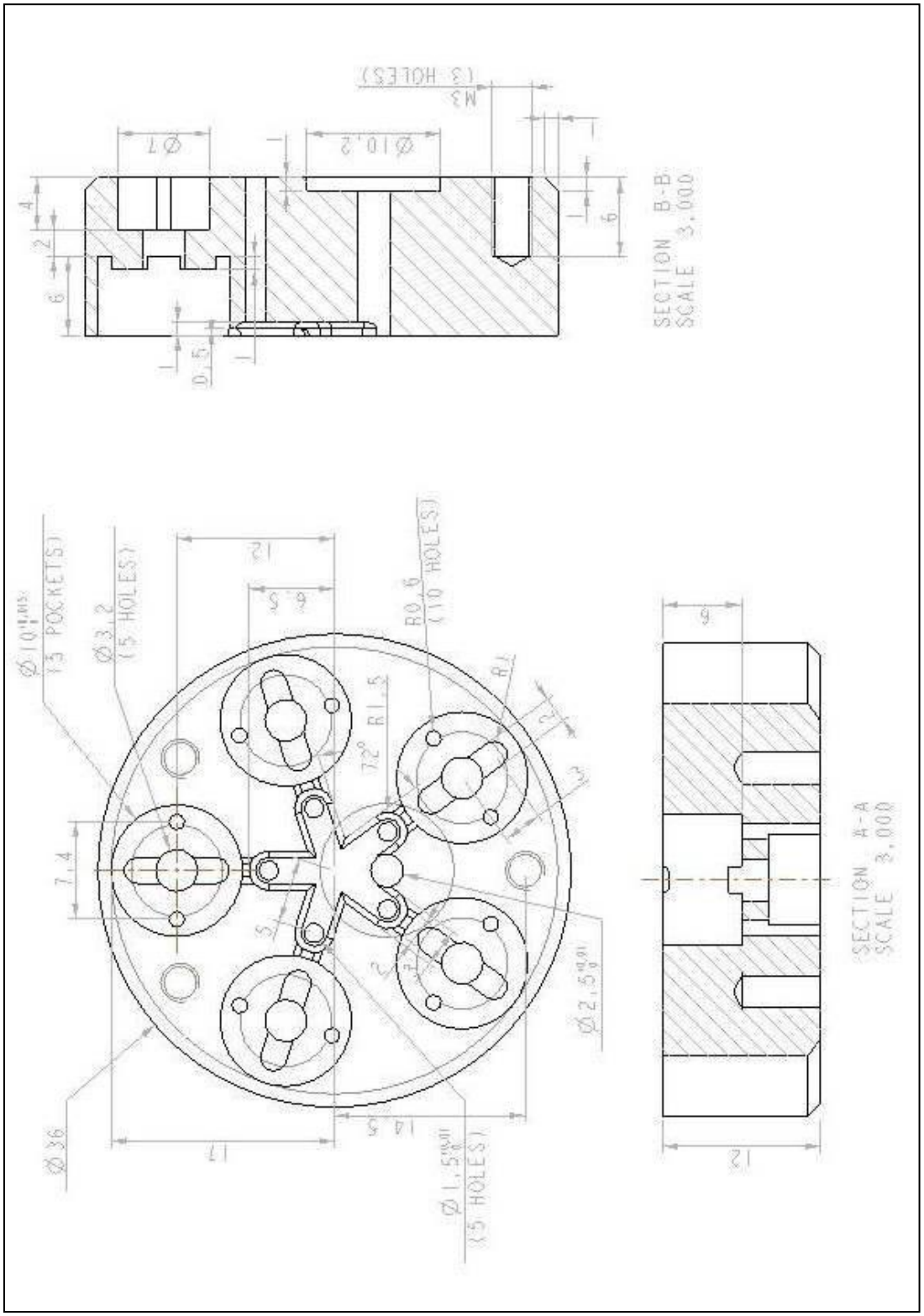

❒ MOULD HOUSING

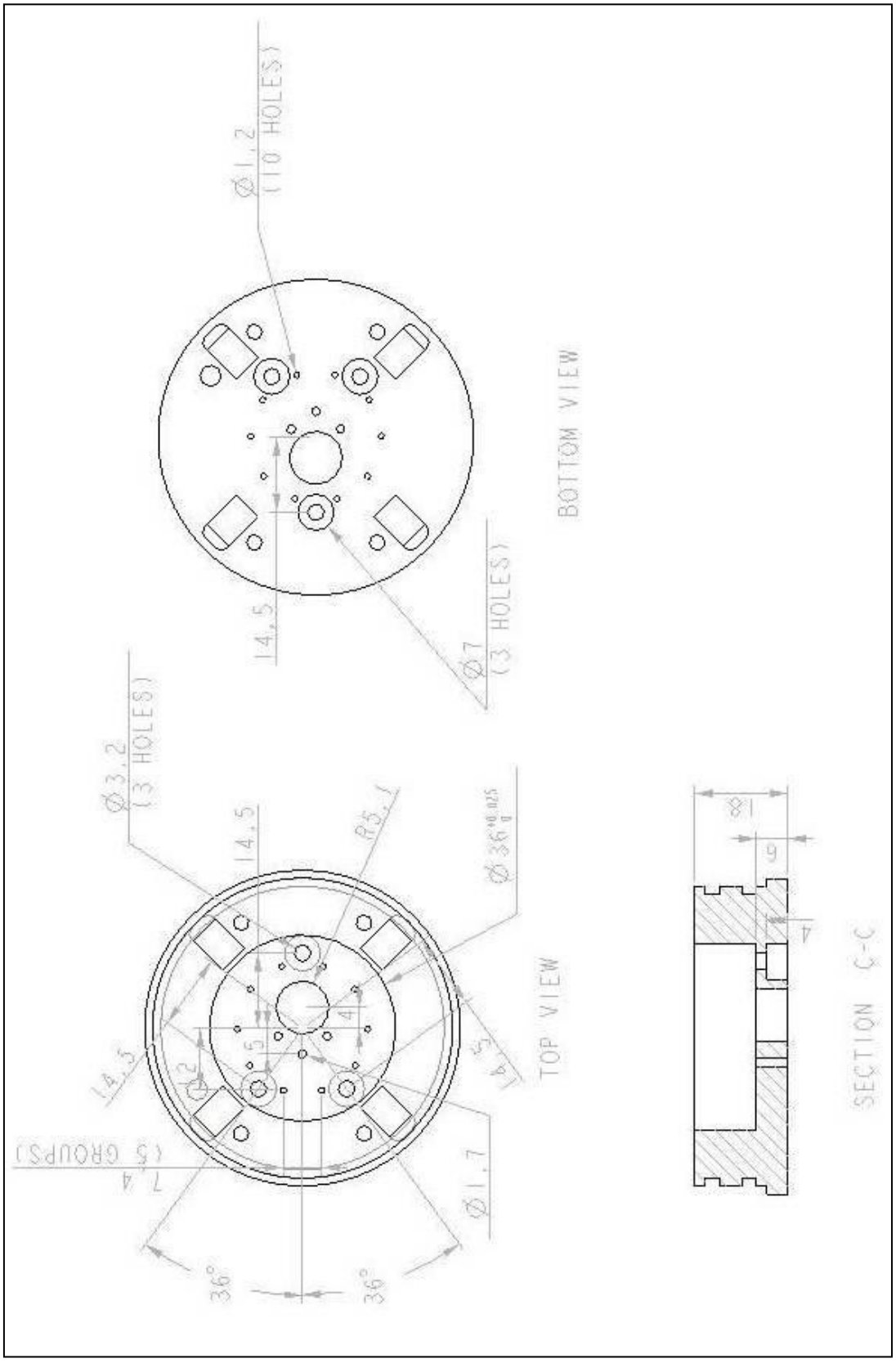

❒ HEATER PLATE

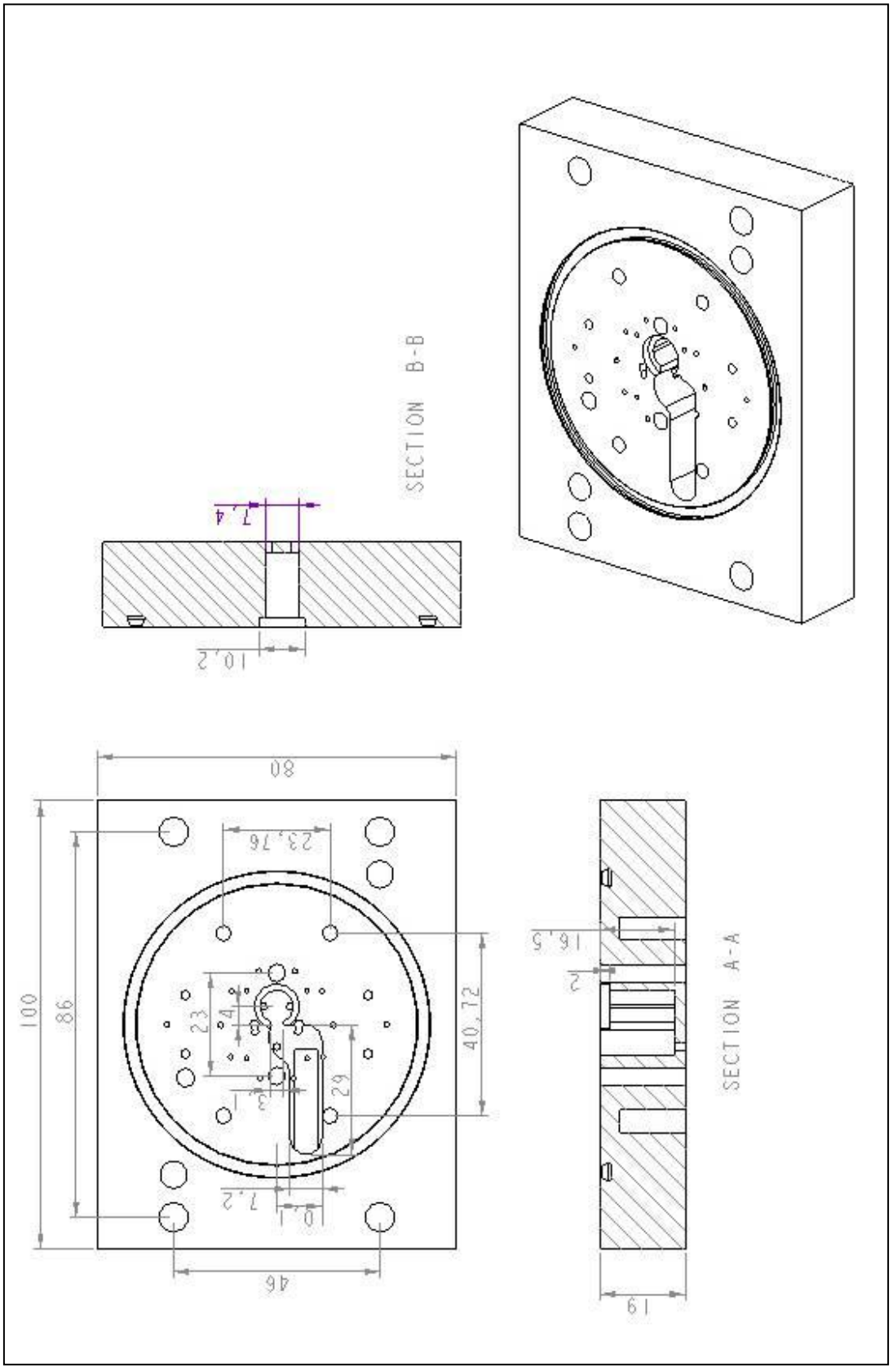

❒ EJECTION PLATE

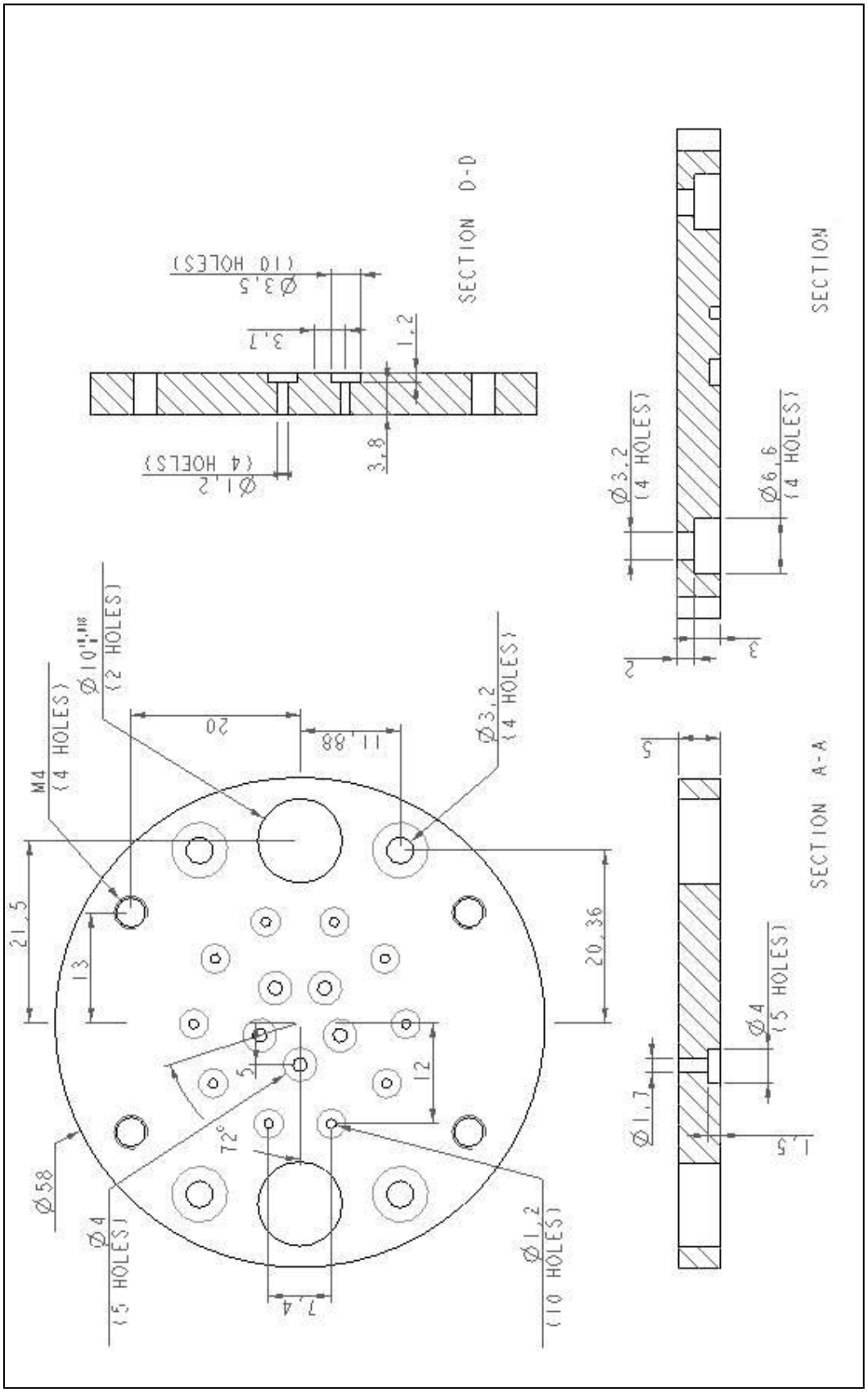

❒ ASSEMBLED MOULD

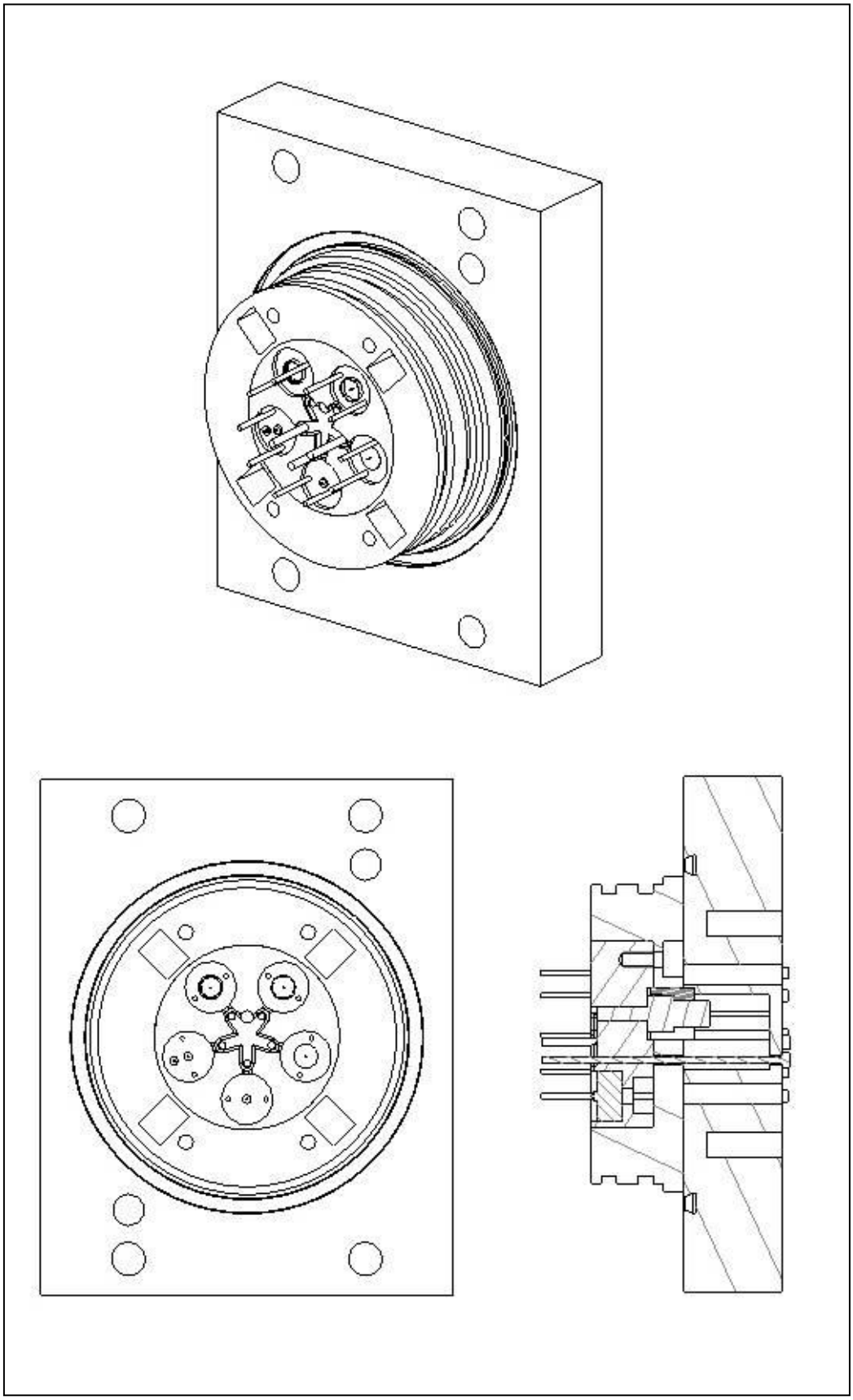

❒ INSERT FOR PART A

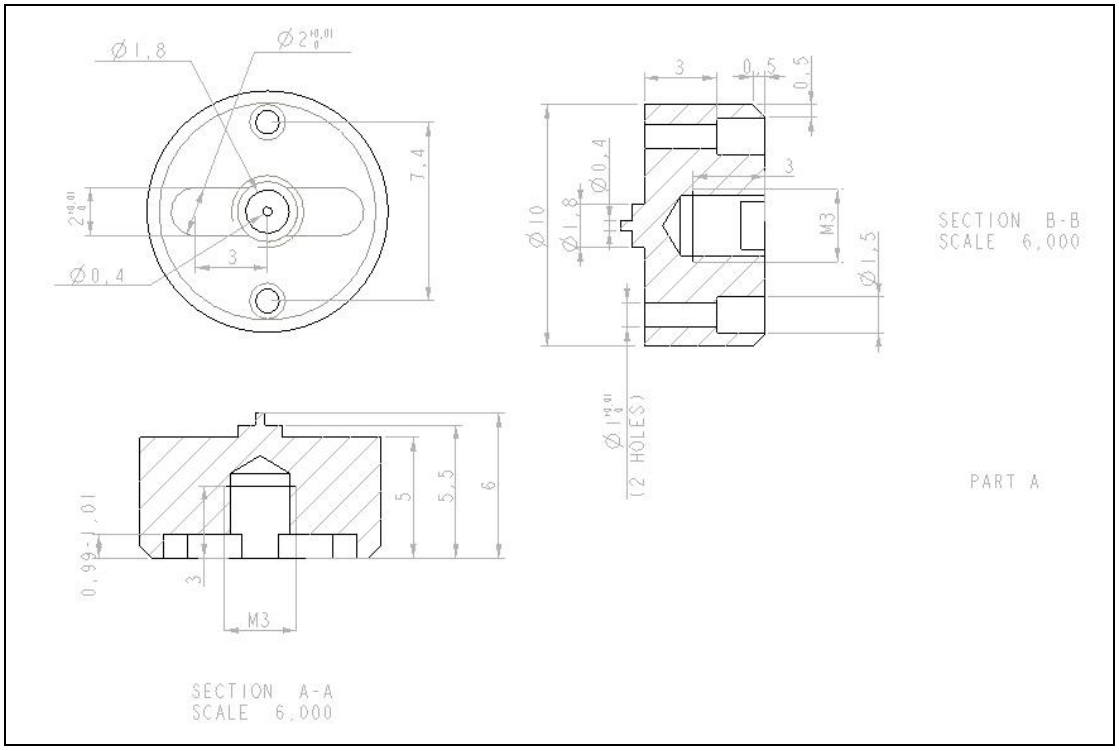

❒ INSERT FOR PART B

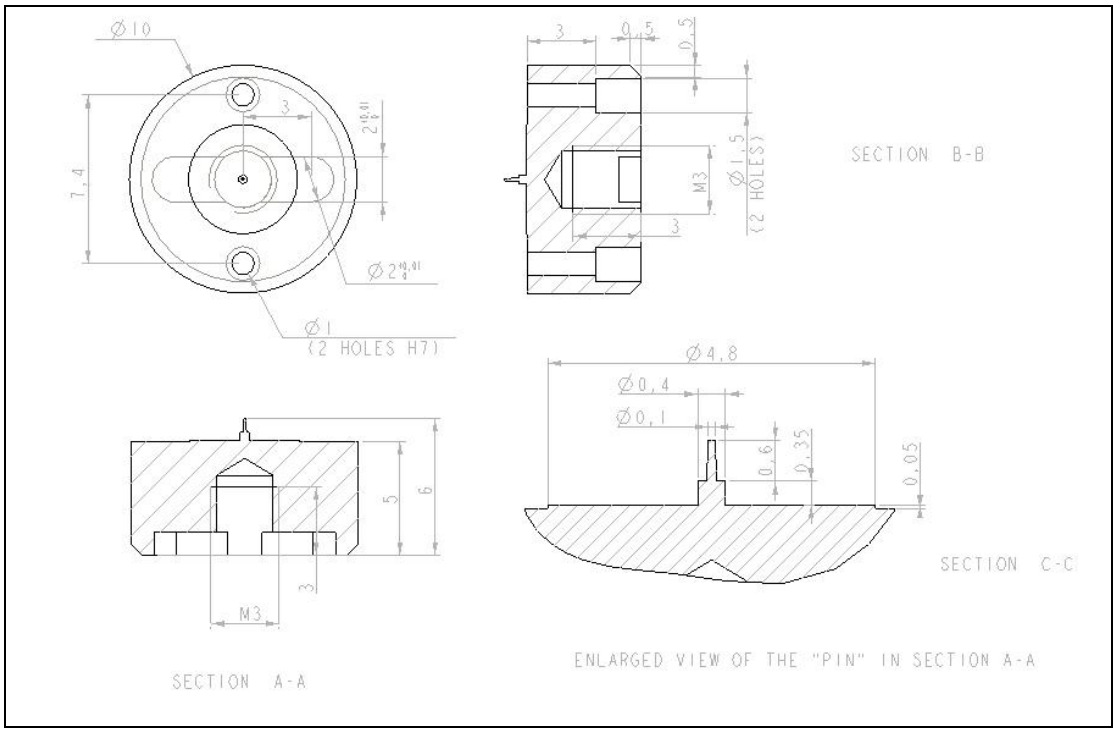

❒ INSERT FOR PART C

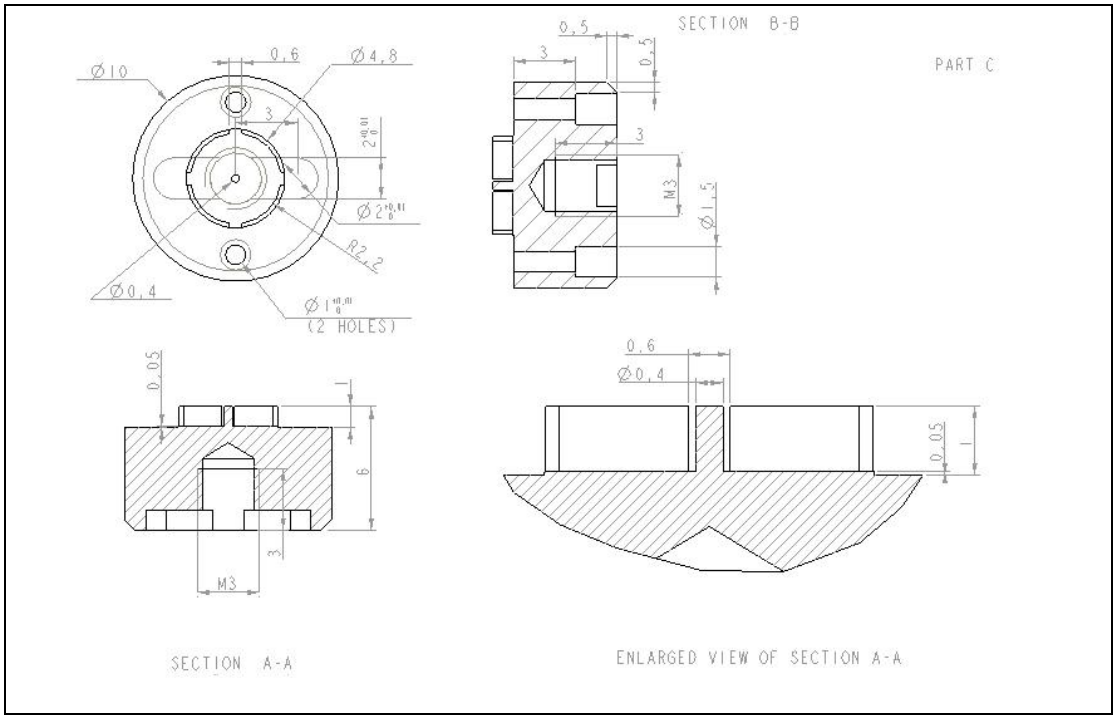

❒ INSERT FOR PART D

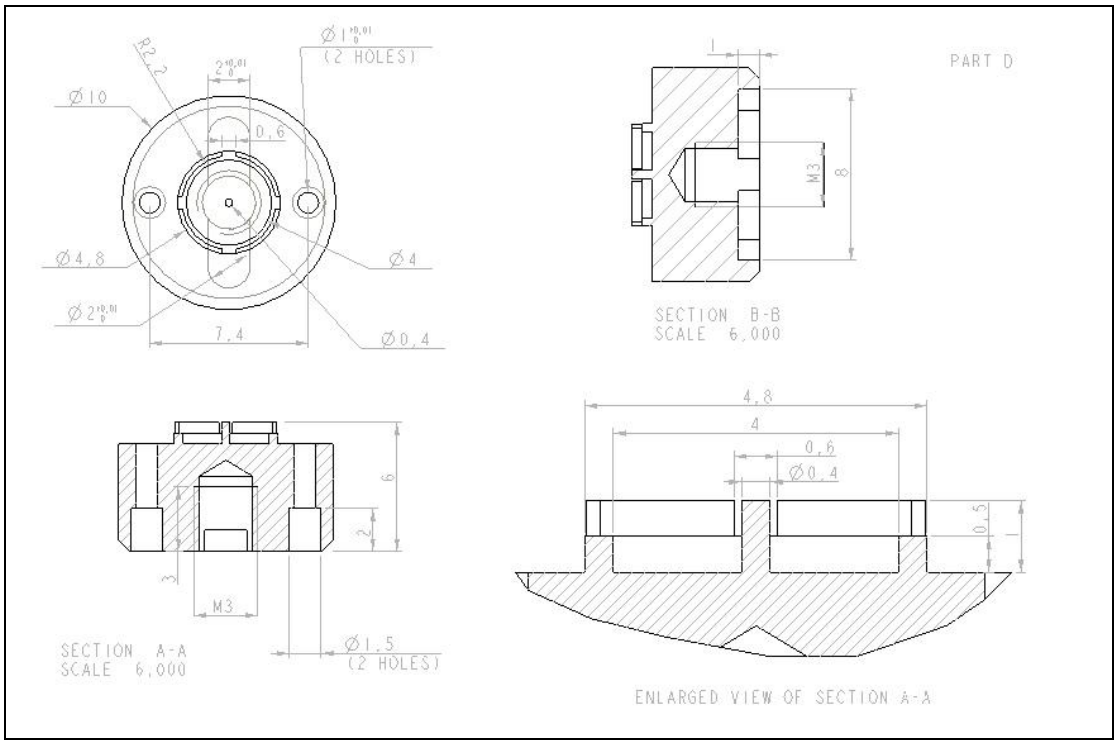

❒ INSERT FOR PART E

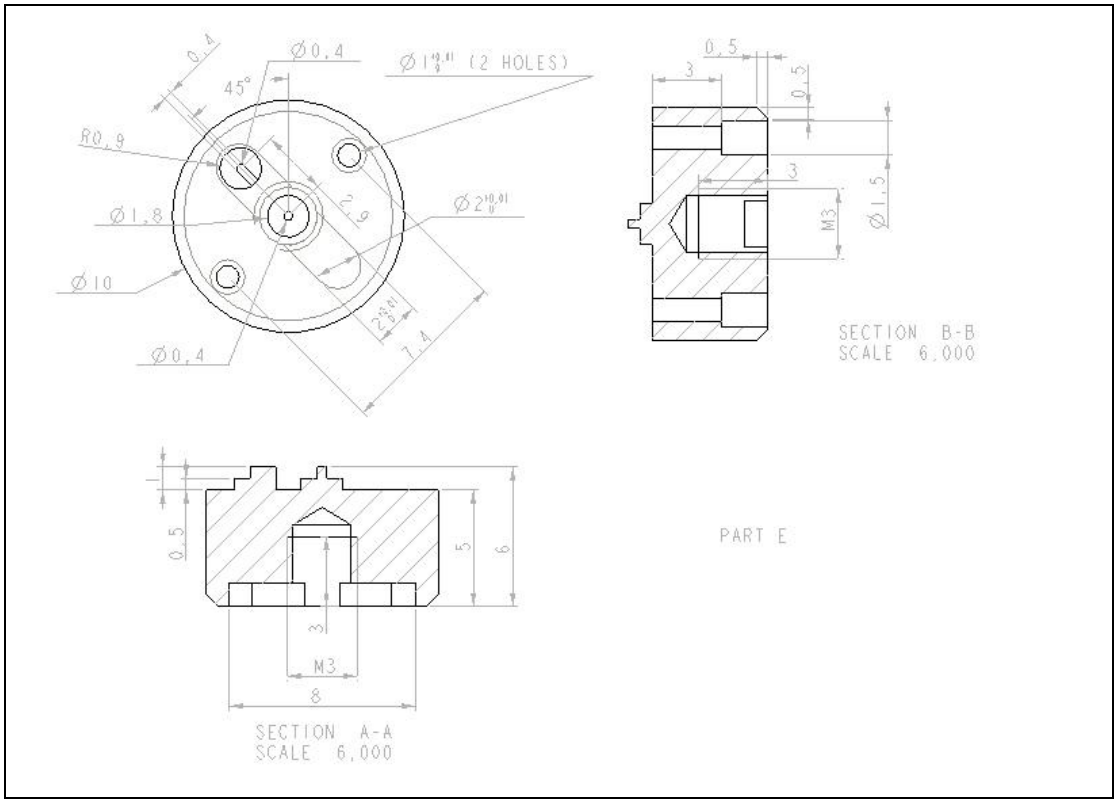

APPENDIX A3: Dimensioned drawings of the 3-plate mould with replaceable insert

❒ INSERT HOLDER FOR PMMA SUBSTRATE

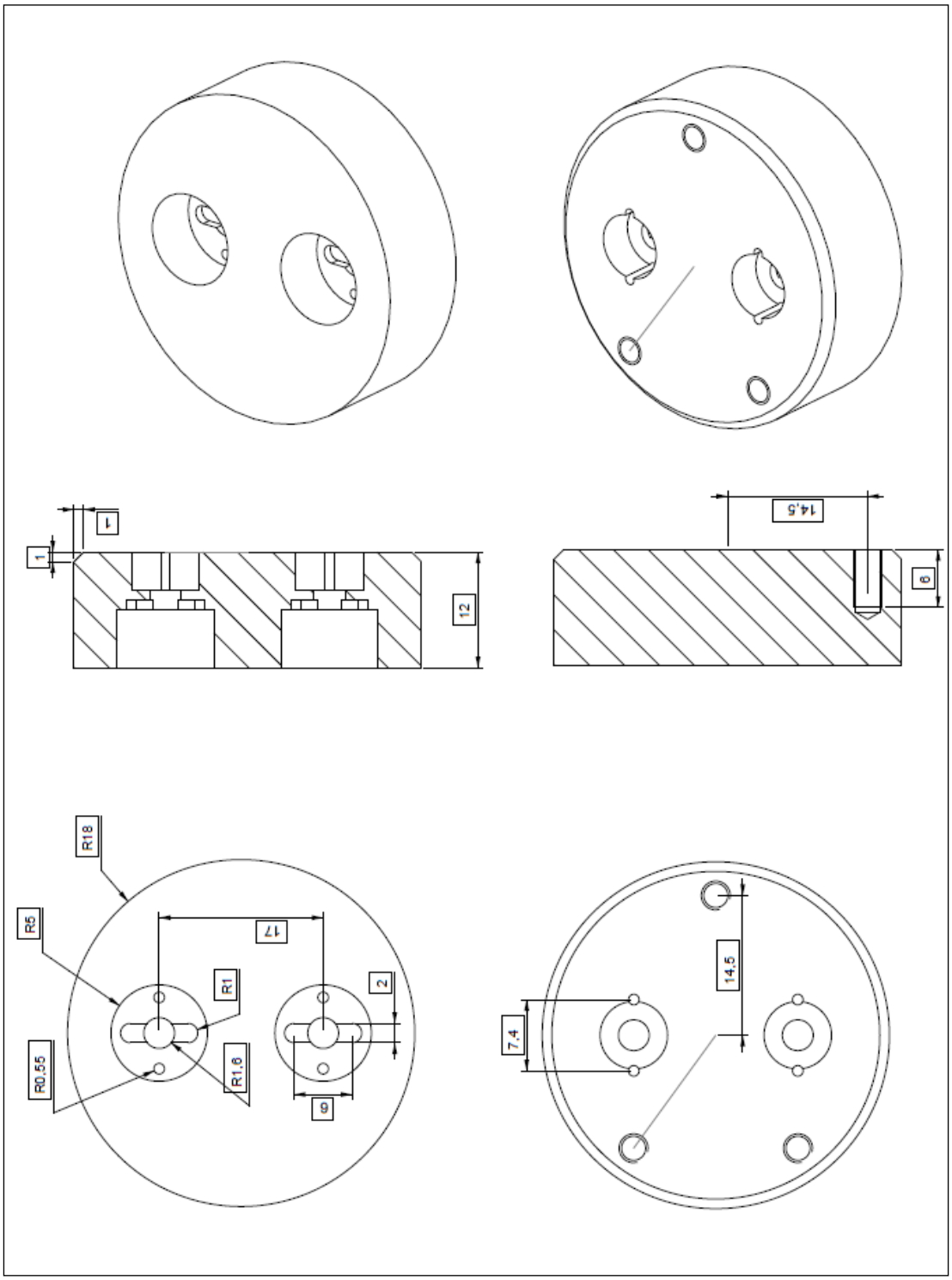

❒ THREE-PLATE MOULD: FRONT HALF OF THE REPLACEABLE INSERT

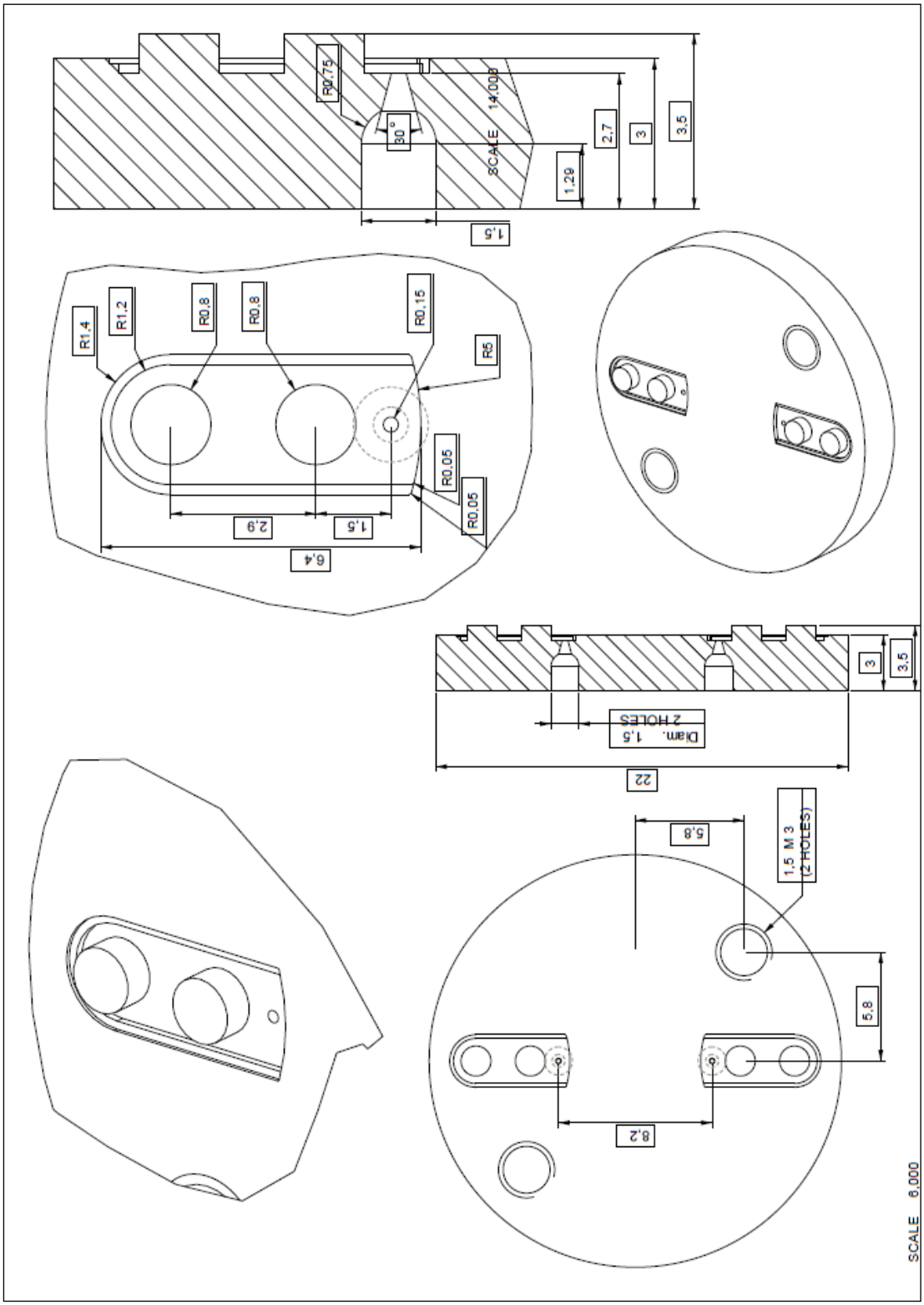

❒ THREE-PLATE MOULD: BACK HALF OF THE REPLACEABLE INSERT

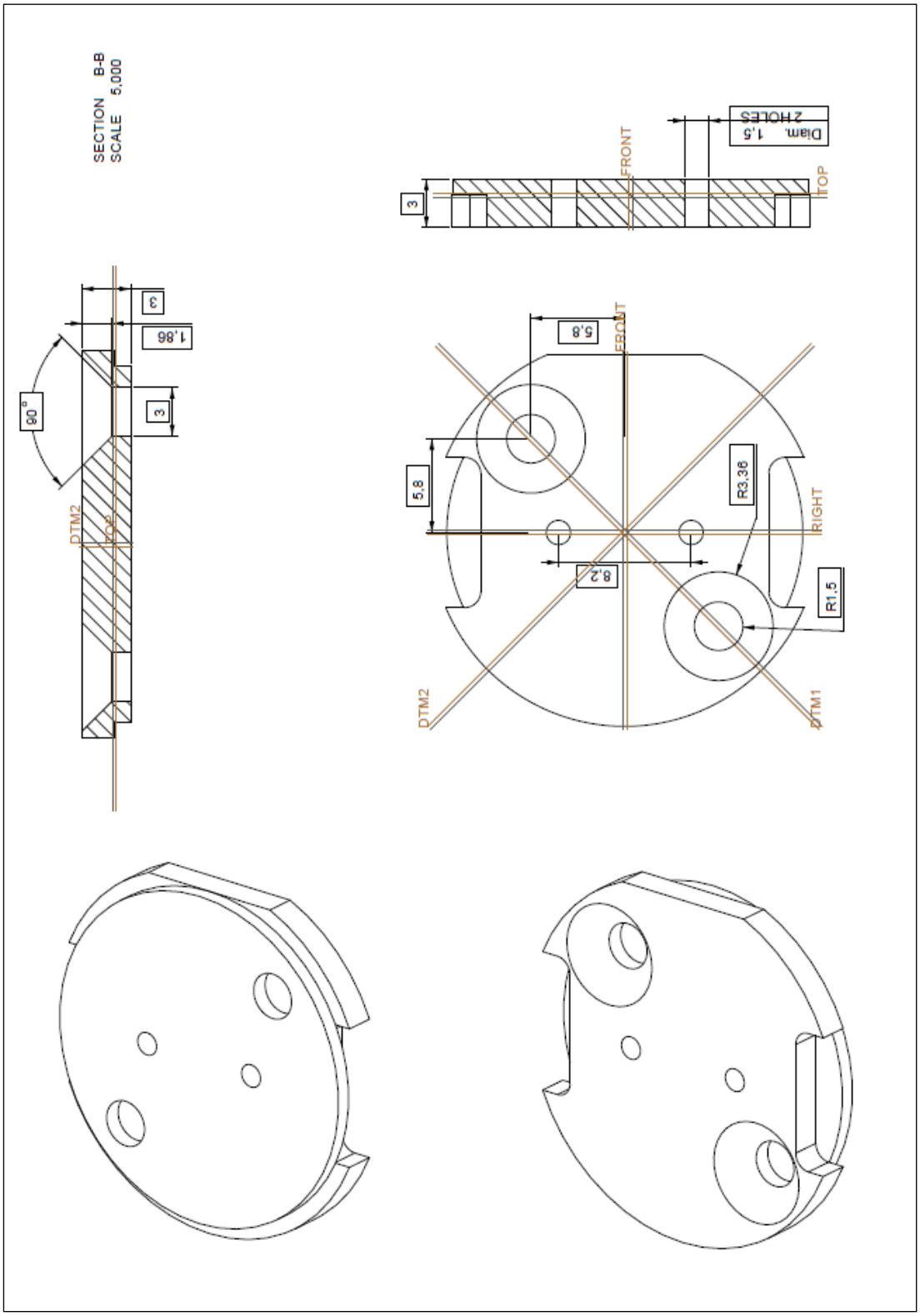

APPENDIX A3: Measuring the mass of micro-injection moulded samples

The masses of the micro-injection moulded samples shown in Figure 5-13 were measured using the following procedure:

1. The moulded samples are manually separated from the common runner system using pliers. Different techniques were tested for separating the samples at their respective gates, such as manual cutters. It was shown that pliers gave the most uniform cut at the gate without causing cracks at the cut sample.
2. After separating the samples, the attached remains of the gates were manually removed using a file. This method was used because it had no significant effect on the sample mass. This was tested by filing 10 randomly selected samples and weighing them before and after filing. The mass change due to filing the gate was in the order of 0.01 mg, which is an order of magnitude below the mass tolerance of 0.2 mg that could be detected by the implemented designed experiments. This meant that variations in mass due to manually removing the remaining of the gates would be statistically insignificant in the analysis of the designed experiments and would, therefore, not affect the final results.
3. When all the gate remains were removed, 10 repeats of each sample were weighed using a sensitive scale with a readability of 0.01 mg. The averages of the measured masses were recorded and analysed using Minitab® 15.